3rd JSPFI & 5th IWPFI

Joint Meeting combining
The 3rd meeting of the Japanese Society of Pulmonary Functional Imaging and
5th International Workshop of Pulmonary Functional Imaging

"The Interaction between Medical Engineering and Clinical Medicine"

Date : January 28 [Fri] - 30 [Sun], 2011

Venue : Awaji Yumebutai International Conference Center, Hyogo, Japan
1 Yumebutai, Awaji City, Hyogo 656-2306 Japan

Phone : +81-799-74-1020 Fax : +81-799-74-1021

President : Yoshiharu Ohno, M.D., Ph.D
(Department of Radiology, Kobe University Graduate School of Medicine)

Secretariat of 3rd JSPFI & 5th IWPFI
c/o Department of Radiology, Kobe University Graduate School of Medicine
7-5-2 Kusunoki-cho, Chuo-ku, Kobe, 650-0017, Japan
Phone : +81-78-382-6104 Fax : +81-78-382-6129
E-mail : jspfi3@med.kobe-u.ac.jp
Secretariat Chair : Daisuke Takenaka M.D.

INDEX

Welcome Message ····· 1

Access & Map ····· 2

Floor Guide ····· 4

Information for Participants ····· 6

Instruction for Speakers and Moderators/Discussers ····· 8

Time Table ····· 10

Program

January 28, 2011[Fri] ····· 17

January 29, 2011[Sat] ····· 29

January 30, 2011[Sun] ····· 39

Abstract

Special Lecture ····· 45

Luncheon Lecture ····· 59

Evening Lecture ····· 75

Core Session (Includes Scientific Presentation) ····· 83

Poster Session ····· 115

Welcome Message from President

Dear Colleagues and Friends,

It is our great pleasure to invite you to a joint meeting, combining the 3rd meeting of the Japanese Society of Pulmonary Functional Imaging and the 5th International Workshop for Pulmonary Functional Imaging, scheduled for January 28-30, 2011. This joint meeting aims to serve emerging clinical needs for improved imaging diagnostics for various lung diseases by bringing together a multidisciplinary group of researchers and clinicians working at the forefront of image-based approaches to lung function analysis. The scientific program offers an attractive combination of invited keynote lectures, selected scientific papers and poster presentations on several specific topics.

The inaugural meeting of the Japanese Society of Pulmonary Functional Imaging in Kyoto in 2009 was followed by a second meeting in Okinawa in 2010, while the inaugural meeting of the International Workshop for Pulmonary Functional Imaging, was started in Philadelphia in 2002 and followed up with meetings in Awaji in 2004, in Heidelberg in 2006 and in Boston in 2009. This time, we plan to hold the 1st joint meeting of the two organizations, one academic and the other concerned with clinical activities in this field, at the Awaji Yumebutai International Conference Center and Westin Hotel, where the 2nd International Workshop for Pulmonary Functional Imaging was held in 2004. As you may know, Awaji Island is located just off the coast of Honshu about 20 kilometers west of Kobe, 40 kilometers west of Osaka and 60 kilometers west of Kyoto.

We cordially invite you to join us on this beautiful island where you can experience warm hospitality as well as both modern and traditional Japanese culture while sharing and adding to your knowledge of Pulmonary Functional Imaging. We are expecting a large number of researchers, physicians and students at this exciting meeting. We look forward to seeing you on Awaji Island in January, 2011.

Yoshiharu Ohno, M.D., Ph.D.
President of the Organizing Committee
Joint Meeting combining
The 3rd meeting of the Japanese Society of Pulmonary Functional Imaging and
5th International Workshop for Pulmonary Functional Imaging

Access & Map

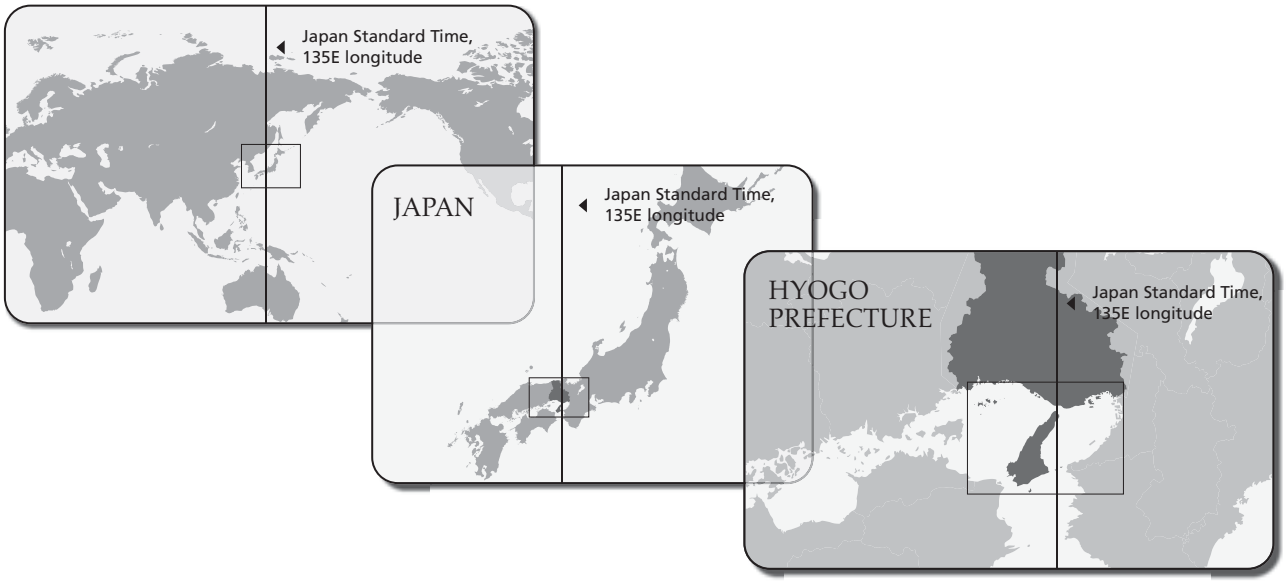
Japan Standard Time,
135E longitude
JAPAN
Japan Standard Time,
135E longitude
HYOGO
PREFECTURE
Japan Standard Time,
135E longitude

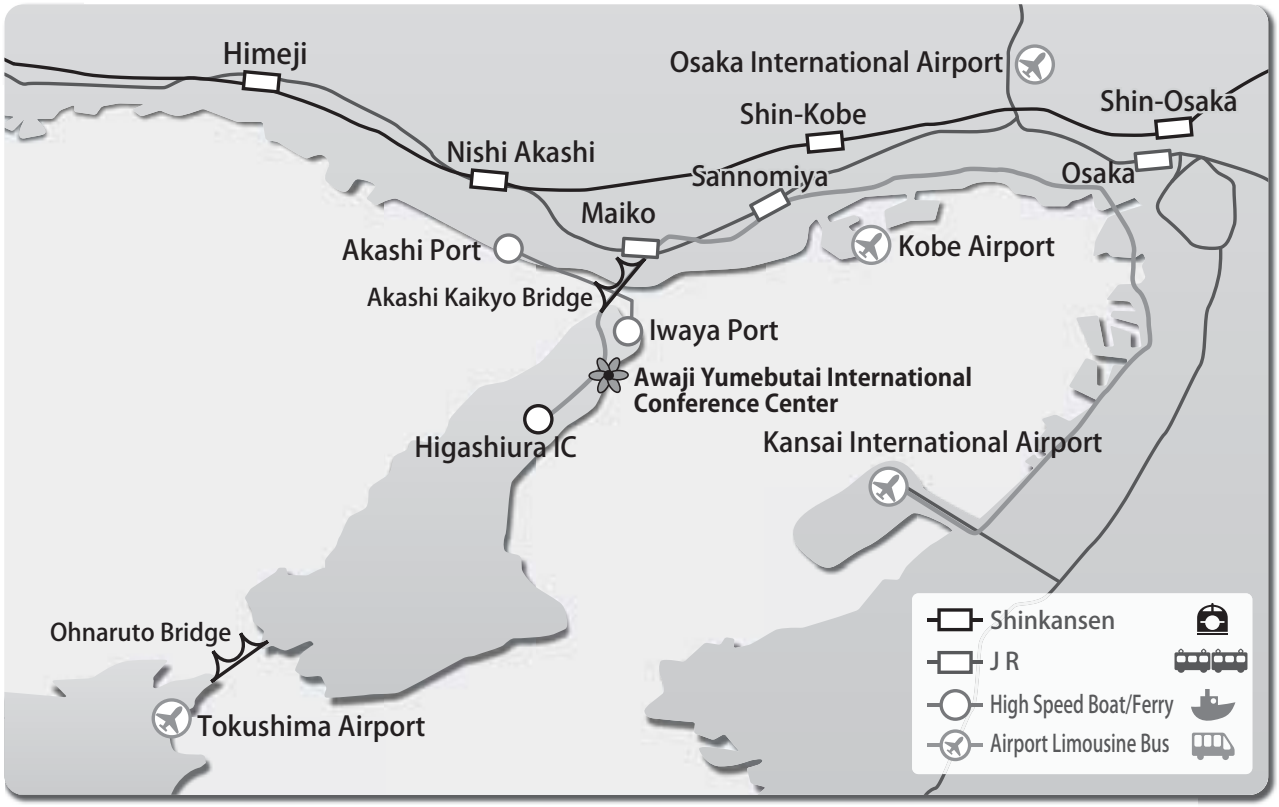
Himeji
Osaka International Airport
Shin-Kobe
Shin-Osaka
Nishi Akashi
Sannomiya
Osaka
Maiko
Akashi Port
Kobe Airport
Akashi Kaikyo Bridge
Iwaya Port
Awaji Yumebutai International
Conference Center
Higashiura IC
Kansai International Airport
Ohnaruto Bridge
Tokushima Airport
Shinkansen
J R
High Speed Boat/Ferry
Airport Limousine Bus

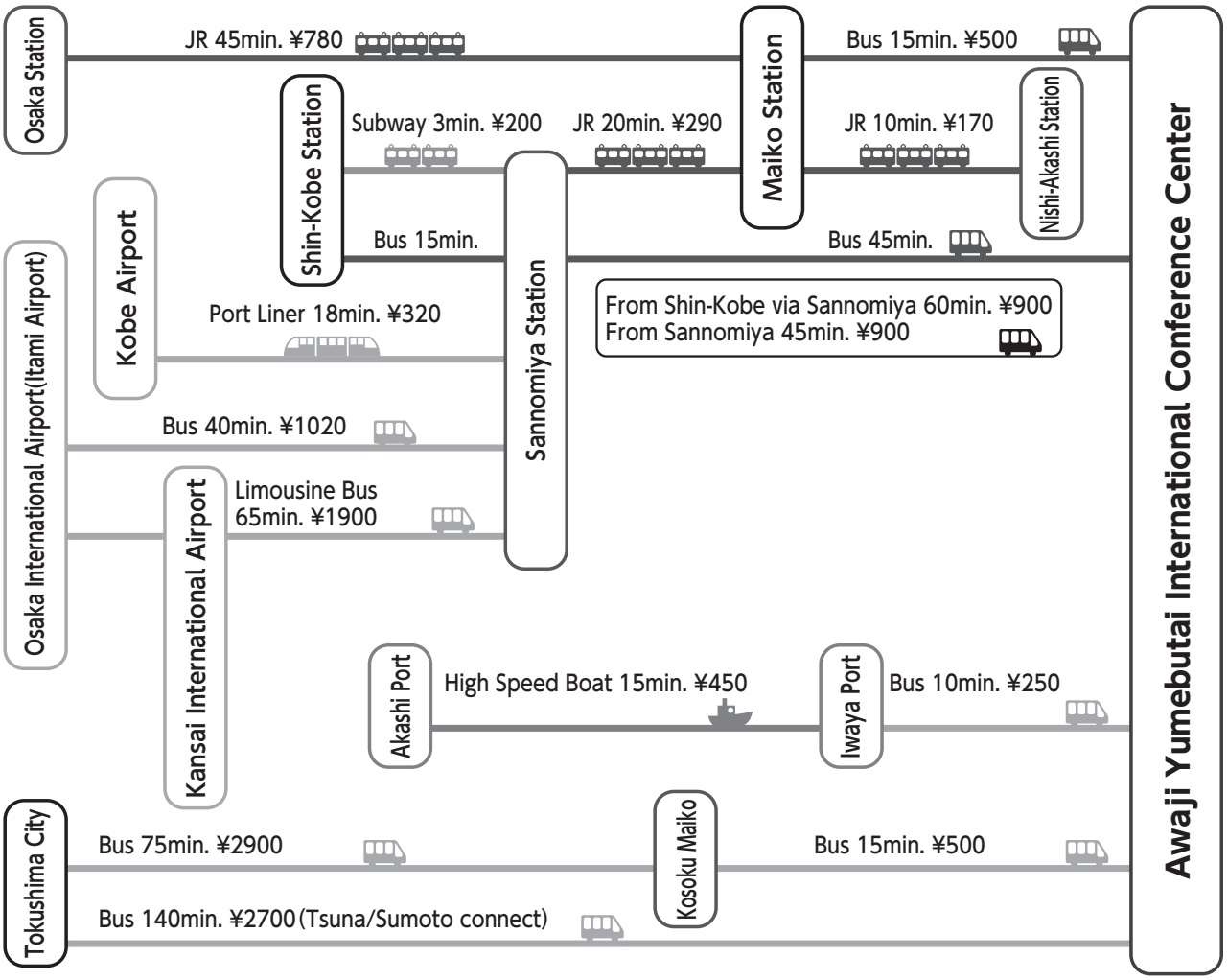

By Car

You can access Awaji Yumebutai in :

- 30 min. from Kobe (Sannomiya) - 30 km
- 60 min. from Osaka (Umeda) - 60 km
- 90 min. from Kansai International Airport (via the Hanshin Highway Wangan Line and Akashi Kaikyou Bridge) - 100 km
- 50 min. from Osaka International Airport (via the Chugoku Expressway, Hanshin Highway Kitakobe Line, and Akashi Kaikyo Bridge) - 75km
- 45 min. from Kobe Airport - 45 km
- 70 min. from Tokushima Airport - 85 km
- 5 min. along Route 28 from Awaji IC exit or Higashiura IC exit on Kobe Awaji Naruto Expressway.

Floor Guide

- Awaji Yumebutai -

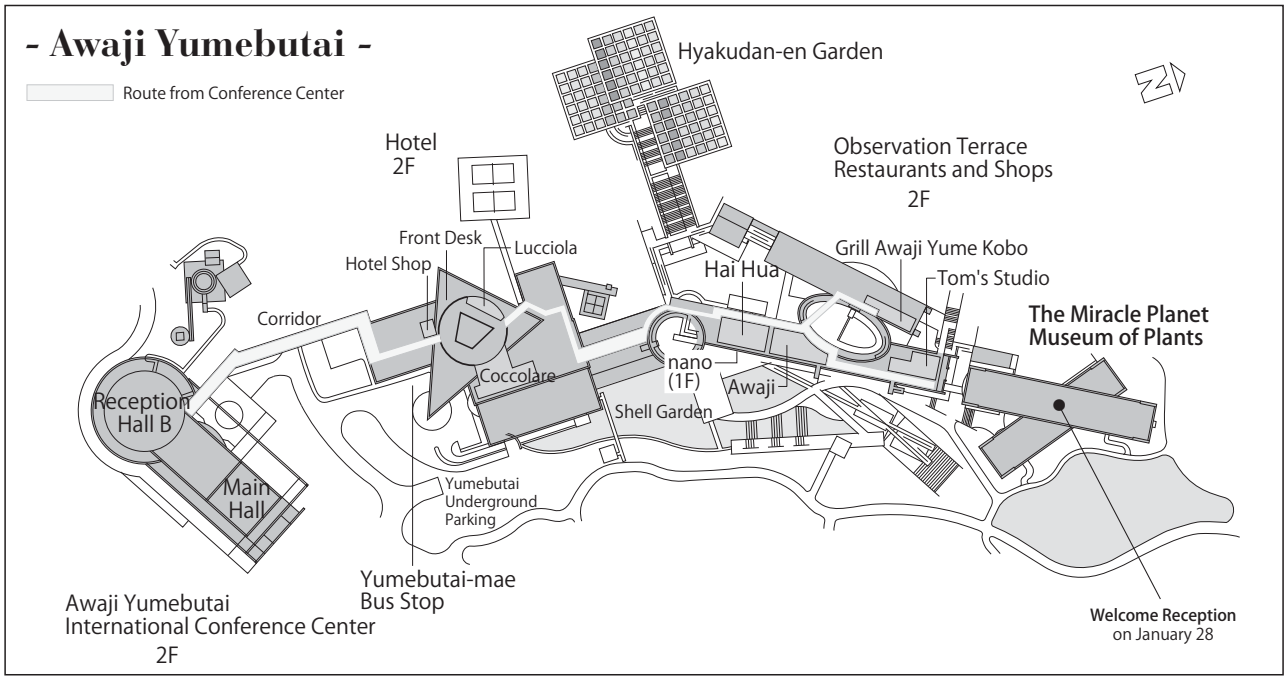

- The Westin Awaji Island -

2F

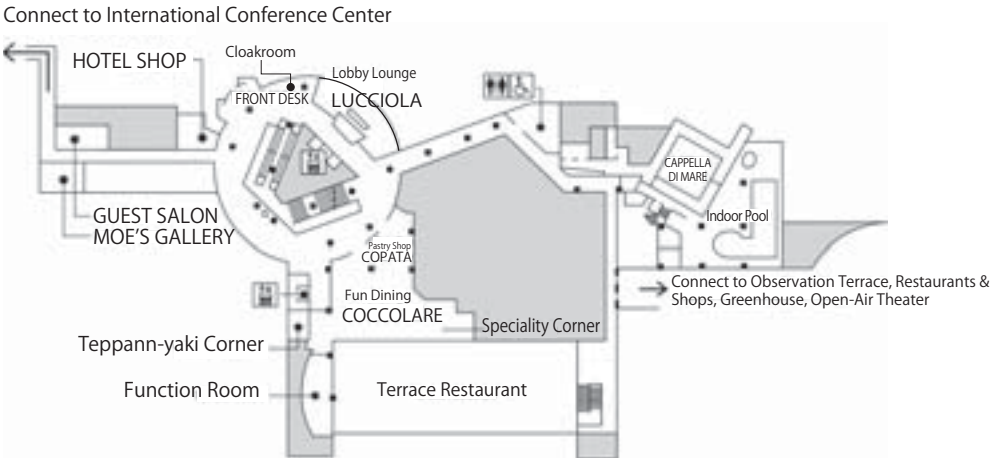

1F

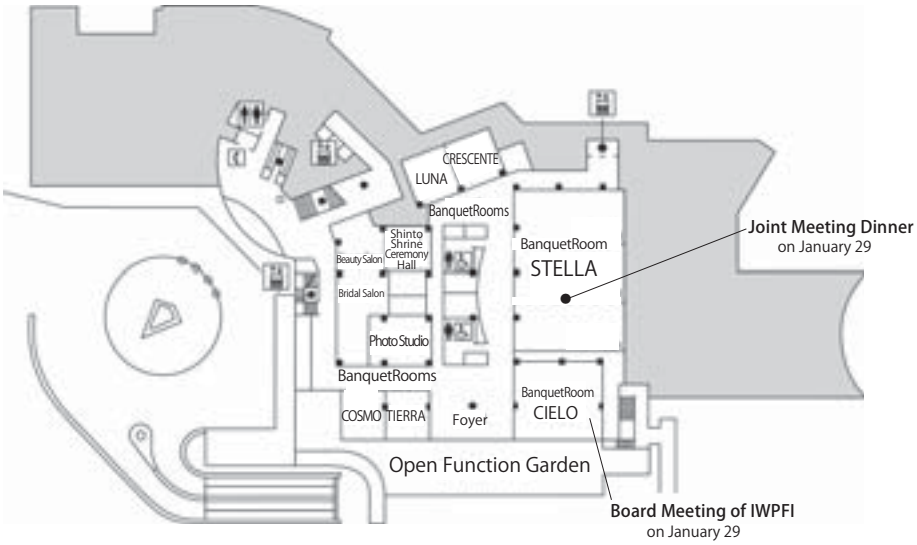

- Awaji Yumebutai International Conference Center -

3F

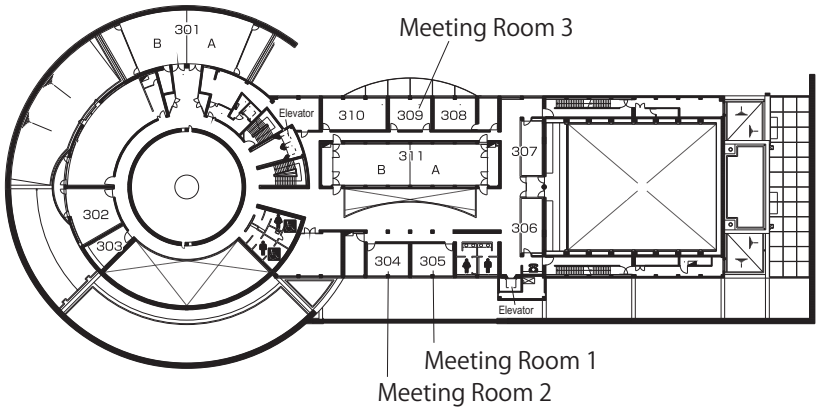

2F

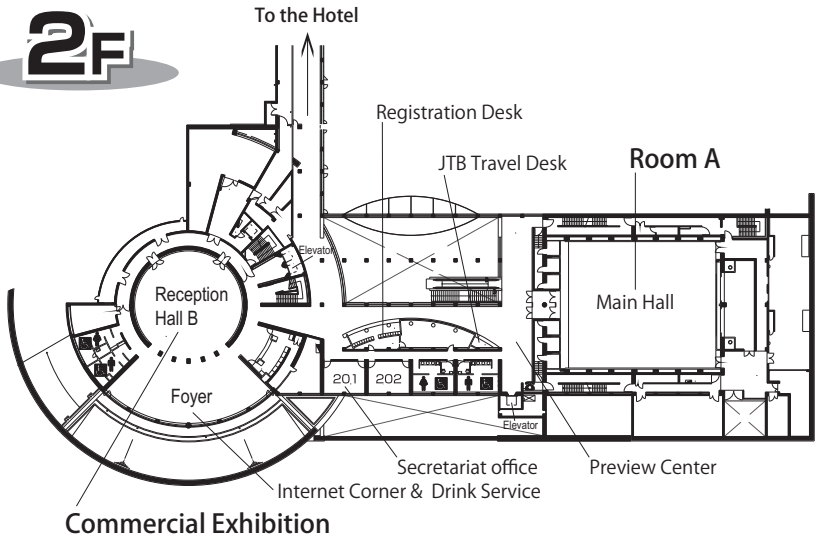

B1

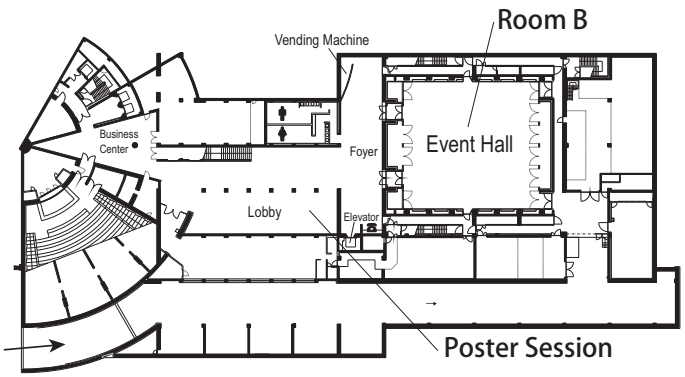

Information for Participants

1. Registration

On-site Registration

Registration Desk

Registration Desk will be opened the following hours at the meeting venue.

---Open Hours---

17:00-18:00 Thursday, January 27, 2011
8:00-18:30 Friday, January 28, 2011
8:00-18:30 Saturday, January 29, 2011
8:00-14:30 Sunday, January 30, 2011

1) Registration fee (Only Japanese Yen)

	On-site Registration	
	JSPFI Member	JSPFI Non-Member
Medical Doctor	¥28,000	¥30,000
Non-Medical Doctor	¥25,000	¥27,000
Student* (Includes Graduate Student)	¥15,000	

JSPFI: Japanese Society for Pulmonary Functional Imaging

※JSPFI member except student must pay the annual membership fee 2,000yen. The annual membership fee is able to pay at the Registration Desk.

*Student(Includes Graduate student) : Student participants are required to present a valid student ID upon the Registration Desk.

The all type of registration fee includes: 1. Admission to scientific programs
2. Admission to the exhibition
3. Documentation including a book of abstracts.
4. Reception on January 28 & 29.

2) Payment Method (Only Japanese Yen)

Payment must be made in Japanese Yen, by cash or with a credit card at Registration Desk. Please note that neither personal checks nor any other currencies will be accepted.

Credit card: American Express, Visa, MasterCard, Diners Club, and JCB are acceptable.

2. Name Badges

Please wear your name badges at all times during the meeting for identification and security purposes. Only registered participants wearing a name badges will be allowed access to the session rooms, exhibition and social programs.

3. Commercial Exhibition

Commercial Exhibition will be held at the "Reception Hall B" during the meeting.
Exhibitors will be eager to demonstrate and explain their latest products, and answer your question.

4. Internet Access Service & Drink Service

Internet access service and drink service are available at the "Reception Hall B Foyer".

5. Travel Desk

Travel Desk will be opened at the venue operated by JTB.

6. Mobile Phone

During the session, you are prohibited from using a mobile phone. Please turn off or switch to the silent mode.

7. Message Board

To prevent from interrupting the sessions, we do not call up anyone in the meeting venue. Please use message board. Leave your message for your friends and colleagues and look for messages left for you.

8. Cloakroom

The Cloakroom is on 2F near by Front Desk of the Westin:

9. Be warned against pickpockets or stolen

Please keep valuables in your possession at all times. The meeting cannot responsible for lost or stolen items.

10. Social Events

The organizing committee takes pleasure in presenting the following social events that offer all participants and accompanying persons.

Welcome Reception
19:30-21:30, Friday, January 28, 2011 at Botanical Gardens, "The Miracle Planet Museum of Plants"

Joint Meeting Dinner at The Westin
19:30-21:30, Saturday, January 29, 2011 at The Westin Awaji Island, "STELLA"

Instruction for Speakers and Moderators / Discussers

Instruction for Speakers

Presentation Time (except Invited Speakers)

Session	Presentation(min.)	Discussion(min.)	Method
Core Session Scientific Presentation	7	3	PC
Poster Session	5	4	–

For Invited Speakers: Please follow the instruction for presentation and discussion time from secretariat and moderators.

Oral Presentation Information

(Special Lecture, Luncheon Lecture, Evening Lecture, Core Session)

Equipment: Computers

OS	Software for Presentation
Windows 7	PowerPoint ver. 2000 to 2010
Mac OSX10.5	PowerPoint ver. 2004 & 2008, Keynote ver. 5

All meeting rooms are equipped with the following audio - visual equipment:
1 - Video Projector, 1 - Screen, 1 - Windows-based PC, 1 - Macintosh-based PC, 1 - Laser Pointer

Preview Center (2F, "Foyer")

---Open Hours---

17:00-18:00 Thursday, January 27, 2011
8:00-18:30 Friday, January 28, 2011
8:00-18:30 Saturday, January 29, 2011
8:00-14:30 Sunday, January 30, 2011

- All Speakers (except Poster Session) are requested to come to the Preview Center at least **30 minutes** in advance of their presentations to verify that the data functions properly on the equipment provided.

※ If you bring your own laptop PC, after checking-in at the Preview Center, please come to the PC operation desk in front of the podium located at the left-front in the session room by **15 minutes prior** to your presentation and hand your PC to the staff. (You can come to the PC operation desk while the previous session in proceeding.)

PowerPoint Presenters

- Bring your presentation in a USB flash Drive or CD-ROM. **In case you use animation, you should to bring your own laptop PC.**
- Make sure that you close or "finalize" your presentation file when create a CD. If you omit this step, you cannot access the CD from any other computers.
- Only the standard font (e.g., Times New Roman, Arial, Century) will be available. Unusual fonts may not be displayed properly on the computers in session rooms.
- Please name the file as:
  "Date of presentation_presenter's name,ppt(x)" e.g., 0128_TaroAWAJI. pptx
- In order to avoid virus infection, please scan your data with updated anti-virus software beforehand.
- Please note that you cannot make any modification at the Preview Center and session room.
- After the meeting, all presentation data will be erased by secretariat.

Laptops

- Speakers using their own laptops must have a **Mini D-sub 15pin female output**. Special video output cable is required for some laptops to use Mini D-sub 15pin to connect to external monitors and data projectors. Please note that we are not equipped with that special cable and you must bring it in case it is necessary.

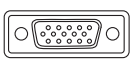
Mini D-sub 15pin

- Please be sure to bring the power adapter.

Poster Presentation Information

Guidelines for Poster Presenters:

Presenters are requested to follow the schedule below in mounting poster on their assigned board. The poster number for your presentation can be found in the program book. Please follow the instructions provided.

・Schedule

Date	Mounting	Poster Viwing	Presentation	Removal
Thursday January 27, 2011	17:00-18:00	/	/	/
Friday January 28, 2011	8:00-11:00	11:00-12:00	17:40-18:52 Last	/
Saturday January 29, 2011	/	11:00-12:00	17:40-18:52 Last	/
Sunday January 30, 2011	/	/	/	8:00-15:00

Poster Board Information

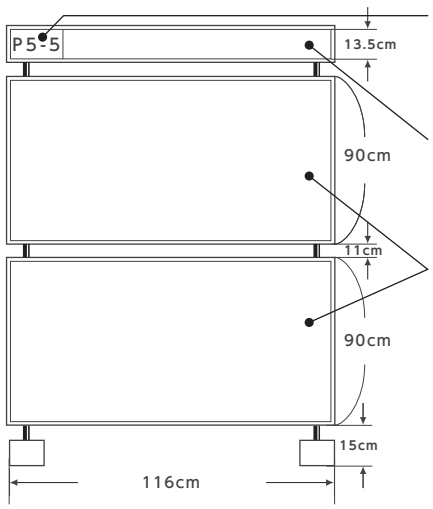

Program Number
(W16.0cm[6.3in] × 13.5cm[5.3in])
※ Prepared by Secretariat

Title/Author's Name/Institution and Country
(W100.0cm[39.4in] × 13.5cm[5.3in])
※ Prepared by Presenter

Presentation Materials
(W90cm[35.4in] × 116cm[45.7in])

- Your poster number will already be on your assigned board.
- Please prepare a label showing the title, institution(includes country) and the auhtor's name. You cannot use pins or adhesive tape.
- Hook - and - loop fastener for mounting will be available from the Poster Reception Desk at the Poster Session Area.
- Poster should be brought by yourself to the meeting and not mailed, as the organizing committee cannot be responsible for loss or mishandling.
- Presenters are responsible for posting and removing their own materials.
- Audio-visual equipment may not be used. Please refer to the poster image for your poster.

The Best Poster Award

This award will be established committee of the meeting to encourage the high performance of the presentation in the poster session. The winner will be selected during the poster presentation time by the moderators.

For the winner

Acommendation ceremony by the president of the meeting during the Joint Meeting Dinner at The Westin, 19:30-, January 28.

Instructions for Moderators and Discussers

All moderators and discussers are asked to ensure that each sessions start on time and finish punctually as scheduled.

Oral Sessions

- Please come to the "Next moderator"'s seat of the session room (the front row on your right side) no later than **15 minutes prior** to the beginning of the session and identify yourself to the staff.

Poster Sessions

- All moderators for poster session are requested to come to the "Poster Reception Desk" near by Poster Session Area no later than **15 minutes prior** to the beginning of the session.
- **Please select the best poster presentation of the session (one person per session), and tell the staff of "Poster Reception Desk".**

Time Table

January 27, 2011 [Thu]

Room A	Room B	Poster Exhibition	Commercial Exhibition	Receptions
Main Hall (2F)	Event Hall (B1)	Lobby (B1)	Reception Hall B (2F)	
16:00				
17:00		17:00-18:00 **Poster Mounting**		
18:00				

January 28, 2011 [Fri]

Room A	Room B	Poster Exhibition	Commercial Exhibition	Receptions
Main Hall (2F)	Event Hall (B1)	Lobby (B1)	Reception Hall B (2F)	
8:00		8:00-11:00 **Poster Mounting**		
8:45-9:00 **Opening Remark**			9:00-18:00	
9:00	9:00-10:50 **Core Session 1** **Pulmonary Hypertension**			
10:00				
11:00	11:00-11:45 **Organizer Meeting of JSPFI**	11:00-12:00 **Poster Viewing**		
12:00	12:00-13:00 **Luncheon Lecture 1** Functional Imaging for Pediatrics			
13:00				
13:20-14:20 **Special Lecture 1** From Morphology to Function and Metabolism			**Commercial Exhibition**	
14:00				
14:30-16:20 **Core Session 2** Thoracic Malignancy: Lung Cancer Treatment				
15:00				
16:00				
16:30-17:30 **Evening Lecture 1** Functional Imaging at High-Field MR System				
17:00				
17:40-18:52 Last **Poster Session 1-8**				
18:00				
19:00				
20:00				19:30-21:30 **Welcome Reception at Botanical Gardens** "The Miracle Planet Museum of Plants"
21:00				

January 29, 2011 [Sat]

	Room A Main Hall (2F)	Room B Event Hall (B1)	Poster Exhibition Lobby (B1)	Commercial Exhibition Reception Hall B (2F)	Receptions
8:00	8:00-8:40 **Board Meeting of IWPFI at The Westin "CIELO",1F**				
9:00	9:00-10:50 **Core Session 3** Chronic Obstructive Pulmonary Diseaes			9:00-18:00	
10:00					
11:00	11:00-11:45 **General Meeting of JSPFI**		11:00-12:00 **Poster Viewing**		
12:00		12:00-13:00 **Luncheon Lecture 2** Imaging for Asthmatics and COPD			
13:00	13:20-14:20 **Special Lecture 2** Basics and Future Direction for Quantitative Functional CT Assessment			**Commercial Exhibition**	
14:00					
15:00	14:30-16:15 **Core Session 4** Interstitial Lung Disease				
16:00					
17:00		16:30-17:30 **Evening Lecture 2** New Techniques for Pulmonary Vascular Disease			
18:00			17:40-18:52 Last **Poster Session 9-15**		
19:00					
20:00					19:30-21:30 **Joint Meeting Dinner at The Westin "STELLA", 1F**
21:00					

January 30, 2011 [Sun]

	Room A Main Hall (2F)	Room B Event Hall (B1)	Poster Exhibition Lobby (B1)	Commercial Exhibition Reception Hall B (2F)
8:00			8:00-15:00	8:00-15:00
9:00	8:30-10:20 **Core Session 5** Asthma and Airway Disease			
10:00				
11:00	10:30-12:15 **Core Session 6** Respiratory Motion Analysis		**Poster Removal**	**Commercial Exhibition**
12:00		12:30-13:30 **Luncheon Lecture 3** Hyperpolarized Noble Gas MRI		
13:00				
14:00	13:50-15:05 **Special Lecture 3** Future Direction for Pulmonary Functional and Molecular Imaging			
15:00	15:05-15:15 **Closing Remark**			

Special Lecture

January 28 [Fri] 13:20-14:20 Sponsored by **Siemens Japan K.K.**

1. From Morphology to Function and Metabolism

Moderator : **Tadashi Abe** Tokai University
Kiyoshi Murata Shiga University of Medical Science
Edwin J.R. van Beek University of Edinburgh

13:20-13:50 Interaction between Functional and Morphological Imaging:
3D Airway Analysis in Chronic Obstructive Pulmonary Disease

Invited Speaker 1 : **Masaharu Nishimura** Hokkaido University

13:50-14:20 Interaction between Metabolic and Morphological Imaging

Invited Speaker 2 : **Kyung Soo Lee** Samsung Medical Center,
Sungkyunkwan University School of Medicine

January 29 [Sat] 13:20-14:20 Sponsored by **PHILIPS**

2. Basics and Future Direction for Quantitative Functional CT Assessment

Moderator : **Michiaki Mishima** Kyoto University
Kenya Murase Osaka University
James P. Butler Harvard Medical School

13:20-13:50 Architecture of Lung Parenchyma
~Basics of Interpretation of HRCT of the Lung~

Invited Speaker 1 : **Harumi Itoh** University of Fukui

13:50-14:20 Current Status and Future Direction of Quantitative Analysis for Functional CT

Invited Speaker 2 : **Eric A. Hoffman** University of Iowa Carver College of Medicine

January 30 [Sun] 13:50-15:05 Sponsored by **TOSHIBA MEDICAL SYSTEMS CORPORATION**

3. Future Direction for Pulmonary Functional and Molecular Imaging

Moderator : **Yasutaka Nakano** Shiga University of Medical Science
Yoshiharu Ohno Kobe University
Hiroto Hatabu Brigham and Women's Hospital, Harvard Medical School

13:50-14:15 From Basic Science Side

Invited Speaker 1 : **Hisataka Kobayashi** National Institute of Health

14:15-14:40 From Radiology Side

Invited Speaker 2 : **Hans-Ulrich Kauczor** Heidelberg University Medical Center

14:40-15:05 From Pulmonology Side -Terminal Air Space of X-ray CT Images in COPD-

Invited Speaker 3 : **Michiaki Mishima** Kyoto University

Luncheon Lecture

January 28 [Fri] 12:00-13:00 Sponsored by **TERUMO**

1. Functional Imaging for Pediatrics

Moderator : **Atsushi Nagai** Tokyo Women's Medical University

12:00-12:30 Functional Thoracic CT for Pediatric Patients

Invited Speaker 1 : **Hyun Woo Goo** Asan Medical Center, University of Ulsan College of Medicine

12:30-13:00 Pediatric Applications of Lung MRI

Invited Speaker 2 : **Talissa A. Altes** (Presented by **Lucia Flors**)
University of Virginia Medical Center

January 29 [Sat] 12:00-13:00 Sponsored by **Astellas Pharma Inc. / AstraZeneca K.K.**

2. Imaging for Asthmatics and COPD

Moderator : **Shoji Kudoh** Double-Barred Cross Hospital

12:00-12:30 CT Assessment of Asthma

Invited Speaker 1 : **Gregory G. King** The Woolcock Institute of Medical Research

12:30-13:00 Hyperpolarized Noble Gas MRI for Asthma and COPD

Invited Speaker 2 : **Mitchell S. Albert** University of Massachusetts Medical School

January 30 [Sun] 12:30-13:30 Sponsored by **DAIICHI SANKYO COMPANY, LIMITED**

3. Hyperpolarized Noble Gas MRI

Moderator : **Toshihiro Nukiwa** Tohoku University

12:30-13:00 Development of Polarizer for Future Clinical Works

Invited Speaker 1 : **F. William Hersman** University of New Hampshire, Xemed LLC

13:00-13:30 Hyperpolarized Noble Gas MRI: Clinical Applications

Invited Speaker 2 : **Hiroto Hatabu** Brigham and Women's Hospital, Harvard Medical School

Evening Lecture

January 28 [Fri] 16:30-17:30 Sponsored by **Bayer Yakuhin, Ltd.**

1. Functional Imaging at High-Field MR System

Moderator : **Yukihiko Sugiyama** Jichi Medical University

16:30-17:00 Animal Studies for Functional Imaging at High-Field System:
Ultra-short TE (UTE) MRI of the Lung

Invited Speaker 1 : **Masaya Takahashi** University of Texas Southwestern Medical Center at Dallas

17:00-17:30 Clinical Functional Imaging at High-Field MRI

Invited Speaker 2 : **Christian Fink** University Medical Center Mannheim

January 29 [Sat] 16:30-17:30 Sponsored by **Eisai Co., Ltd.**

2. New Techniques for Pulmonary Vascular Disease

Moderator : **Kazuro Sugimura** Kobe University

16:30-17:00 Dual-Energy CT Application for Pulmonary Vascular Disease

Invited Speaker 1 : **Joon Beom Seo** University of Ulsan College of Medicine, Asan Medical Center

17:00-17:30 Quantitative MR Assessment for Pulmonary Vascular Disease

Invited Speaker 2 : **David L. Levin** Mayo Clinic

Core Session

January 28 [Fri] 9:00-10:50

1. Pulmonary Hypertension

Moderator : **Hiroshi Kimura** Nara Medical University
Noriyuki Tomiyama Osaka University
Discusser : **Mark L. Schiebler** University of Wisconsin

9:00-9:20 Etiology and Pathophysiology of Pulmonary Hypertension
Invited Speaker 1 : **Koichiro Tatsumi** Chiba University

9:20-9:35 Nuclear Medicine Assessment for Pulmonary Hypertension
Invited Speaker 2 : **Takayuki Shinkai** Nara Medical University

9:35-9:50 CT Assessment of Pulmonary Hypertension
Invited Speaker 3 : **Joon Beom Seo** University of Ulsan College of Medicine, Asan Medical Center

9:50-10:05 MR Assessment for Pulmonary Hypertension
Invited Speaker 4 : **David L. Levin** Mayo Clinic

10:05-10:20 Update of Treatment for Pulmonary Hypertension
Invited Speaker 5 : **David G. Kiely** Royal Hallamshire Hospital

10:20-10:50 Scientific Presentation 1-3

January 28 [Fri] 14:30-16:20

2. Thoracic Malignancy: Lung Cancer Treatment

Moderator : **Michio Kono** Kobe University
Yoichi Nakanishi Kyushu University
Discusser : **Sadayuki Murayama** University of the Ryukyus

14:30-14:50 Newest Evidences of Drug Therapy for Lung Cancer
Invited Speaker 1 : **Yoichi Nakanishi** Kyushu University

14:50-15:05 Update for New Molecular Targeted Therapy for Lung Cancer
Invited Speaker 2 : **Kazuhisa Takahashi** Juntendo University School of Medicine

15:05-15:20 Molecular Imaging for Lung Cancer Treatment
Invited Speaker 3 : **Koji Murakami** Keio University

15:20-15:35 MR Imaging for Lung Cancer Treatment
Invited Speaker 4 : **Juergen Biederer** University Hospital Schleswig-Holstein, Campus Kiel

15:35-15:50 CAD for Lung Cancer Treatment -Evaluation of Tumor Response to Treatment
Invited Speaker 5 : **Jin Mo Goo** Seoul National University Hospital

15:50-16:20 Scientific Presentation 1-3

January 29 [Sat] 9:00-10:50

3. Chronic Obstructive Pulmonary Disease

Moderator : **Toyohiro Hirai** Kyoto University
Kiminori Fujimoto Kurume University School of Medicine
Discusser : **Hans-Ulrich Kauczor** Heidelberg University

9:00-9:20 Etiology and Pathophysiology of COPD
Invited Speaker 1 : **Kazutetsu Aoshiba** Tokyo Women's Medical University

9:20-9:35 PET Assessment for COPD: Changes in Pulmonary Perfusion Distribution
Invited Speaker 2 : **José G. Venegas** Harvard Medical School, Massachusetts General Hospital

9:35-9:50 CT Assessment for COPD-Phenotype on CT in COPD
Invited Speaker 3 : **Keisaku Fujimoto** Shinshu University School of Health Sciences

9:50-10:05 Proton MR Assessment of COPD
Invited Speaker 4 : **Yoshiharu Ohno** Kobe University

10:05-10:20 Hyperpolarized Noble Gas MRI for COPD
Invited Speaker 5 : **Edwin J.R. van Beek** University of Edinburgh

10:20-10:50 Scientific Presentation 1-3

January 29 [Sat] 14:30-16:15

4. Interstitial Lung Disease

Moderator : **Yukihiko Sugiyama** Jichi Medical University
Masashi Takahashi Shiga University of Medical Science
Discusser : **Kyung Soo Lee** Samsung Medical Center,
Sungkyunkwan University School of Medicine

14:30-14:55 Update for Diagnosis of IIP
Invited Speaker 1 : **Takeshi Johkoh** Kinki Central Hospital of Mutual Aid Association of Public School Teachers

14:55-15:15 Update for Treatment of Idiopathic Interstitial Pneumonias (IIPs)
Invited Speaker 2 : **Kingo Chida** Hamamatsu University School of Medicine

15:15-15:30 Smoking-related Interstitial Pneumonia Associated with Emphysema
Invited Speaker 3 : **Minoru Kanazawa** Saitama Medical University

15:30-15:45 Hyperpolarlized Noble Gas MRI for ILD
Invited Speaker 4 : **Hiroto Hatabu** Brigham and Women's Hospital, Harvard Medical School

15:45-16:15 Scientific Presentation 1-3

January 30 [Sun] 8:30-10:20

5. Asthma and Airway Disease

Moderator : **Yuji Tohda** Kinki University
Shigeru Kosuda National Defense Medical College
Discusser : **Shu Hashimoto** Nihon University

8:30-8:50 Pathophysiology of Asthma
Invited Speaker 1 : **Hiromasa Inoue** Kagoshima University

8:50-9:05 Evaluation of Airway Obstruction and Altered Pulmonary Permeability with Lung Scintigraphy in Young Patients
Invited Speaker 2 : **Mayuki Uchiyama** The Jikei University School of Medicine

9:05-9:20 CT Assessment for Asthma
Invited Speaker 3 : **Hiroshi Tanaka** Sapporo Medical University School of Medicine

9:20-9:35 MR Assessment of Asthma; Hyperpolarized ^{3}He Magnetic Resonance Imaging to Probe Temporal and Spatial Airway Functional Changes
Invited Speaker 4 : **Grace Parraga** The University of Western Ontario

9:35-9:50 Update for Treatment of Asthma
Invited Speaker 5 : **Kazuto Hirata** Osaka City University

9:50-10:20 Scientific Presentation 1-3

January 30 [Sun] 10:30-12:15

6. Respiratory Motion Analysis

Moderator : **Ichiro Kuwahira** Tokai University Tokyo Hospital
Shuji Sakai Tokyo Women's Medical University
Discusser : **James Gee** University of Pennsylvania

10:30-10:45 Aims of Respiratory Motion Assessment for Anesthesiology
Invited Speaker 1 : **Klaus Markstaller** Medical University of Vienna

10:45-11:00 MR Assessment of Respiratory Motion
Invited Speaker 2 : **Tae Iwasawa** Kanagawa Cardiovascular and Respiratory Center

11:00-11:15 Nuclear Medicine Assessment for Respiratory Lung Motion
Invited Speaker 3 : **Kazuyoshi Suga** Yamaguchi University School of Medicine

11:15-11:30 Dynamic Volume Scan Using 320-row ADCT for the Assessment of Respiratory Motion
Invited Speaker 4 : **Hiroshi Moriya** Sendai Kousei Hospital

11:30-11:45 Respiratory Motion Assessment to Increase the Accuracy of Non-contact Screening System to Prevent the Spread of Infectious Diseases
Invited Speaker 5 : **Takemi Matsui** Tokyo Metropolitan University

11:45-12:15 Scientific Presentation 1-3

Program

January 28, 2011[Fri]

Room A
Main Hall (2F)

8:45-9:00 **Opening Remark**

9:00-10:50 **Core session 1**

Pulmonary Hypertension

Moderator **Hiroshi Kimura** Nara Medical University
Noriyuki Tomiyama Osaka University
Discusser **Mark L. Schiebler** University of Wisconsin

Invited Speaker

9:00-9:20
1. Etiology and Pathophysiology of Pulmonary Hypertension

Koichiro Tatsumi
Chiba University

9:20-9:35
2. Nuclear Medicine Assessment for Pulmonary Hypertension

Takayuki Shinkai
Nara Medical University

9:35-9:50
3. CT Assessment of Pulmonary Hypertension

Joon Beom Seo
University of Ulsan College of Medicine, Asan Medical Center

9:50-10:05
4. MR Assessment for Pulmonary Hypertension

David L. Levin
Mayo Clinic

10:05-10:20
5. Update of Treatment for Pulmonary Hypertension

David G. Kiely
Royal Hallamshire Hospital

Scientific Presentation

10:20-10:30
1. Optimized Flowchart of Multi-technical MR Protocol for Pulmonary Circulation and Right Heart Function on the Busy Clinical Schedule

Shu-Hui Peng
Chung Shan Medical University Hospital

10:30-10:40
2. V-Q Imbalance in Primary/Passive Pulmonary Hypertension on V/Q SPECT

Kazuyoshi Suga
St. Hill Hospital

10:40-10:50
3. Estimation of Pulmonary Vascular Resistance by the Calculation of Contrast Transit Time from Gadolinium Contrast Enhanced Pulmonary MRI

Adam G Telfer
University of Sheffield

13:20-14:20 **Special Lecture 1** Sponsored by **Siemens Japan K.K.**

From Morphology to Function and Metabolism

Moderator **Tadashi Abe** Tokai University
Kiyoshi Murata Shiga University of Medical Science
Edwin J.R. van Beek University of Edinburgh

13:20-13:50
1. Interaction between Functional and Morphological Imaging:
3D Airway Analysis in Chronic Obstructive Pulmonary Disease

Masaharu Nishimura
Hokkaido University

13:50-14:20
2. Interaction between Metabolic and Morphological Imaging

Kyung Soo Lee
Samsung Medical Center, Sungkyunkwan University School of Medicine

14:30-16:20 **Core session 2**

Thoracic Malignancy: Lung Cancer Treatment

Moderator **Michio Kono** Kobe University
Yoichi Nakanishi Kyushu University
Discusser **Sadayuki Murayama** University of the Ryukyus

Invited Speaker

14:30-14:50
1. Newest Evidences of Drug Therapy for Lung Cancer

Yoichi Nakanishi
Kyushu University

14:50-15:05
2. Update for New Molecular Targeted Therapy for Lung Cancer

Kazuhisa Takahashi
Juntendo University School of Medicine

15:05-15:20
3. Molecular Imaging for Lung Cancer Treatment

Koji Murakami
Keio University

15:20-15:35
4. MR Imaging for Lung Cancer Treatment

Juergen Biederer
University Hospital Schleswig-Holstein, Campus Kiel

15:35-15:50
5. CAD for Lung Cancer Treatment -Evaluation of Tumor Response to Treatment

Jin Mo Goo
Seoul National University Hospital

Scientific Presentation

15:50-16:00
1. Comparative Reading System for Lung Cancer CT Screening

Hidenobu Suzuki
The University of Tokushima

16:00-16:10
2. The Evaluation of Lung Perfusion in a Radiation Field Through the Radiation Therapy for Lung Cancer - Using Lung Perfused Blood Volume Imaging with Dual Energy CT-

Sachiko Miura
Nara Medical University

16:10-16:20
3. Therapy Response Assessment in Neoadjuvant Chemotherapy for Esophageal Cancer: Comparison of PET Response Criteria in Solid Tumors (PERCIST) and Response Evaluation Criteria in Solid Tumors (RECIST)

Masahiro Yanagawa
Osaka University

Room B
Event Hall (B1)

12:00-13:00 **Luncheon Lecture 1** Sponsored by **TERUMO**

Functional Imaging for Pediatrics

Moderator **Atsushi Nagai** Tokyo Women's Medical University

12:00-12:30
1. Functional Thoracic CT for Pediatric Patients

Hyun Woo Goo
Asan Medical Center, University of Ulsan College of Medicine

12:30-13:00
2. Pediatric Applications of Lung MRI

Talissa A. Altes
(Presented by **Lucia Flors**)
University of Virginia Medical Center

16:30-17:30 **Evening Lecture 1** Sponsored by **Bayer Yakuhin, Ltd.**

Functional Imaging at High-Field MR System

Moderator **Yukihiko Sugiyama** Jichi Medical University

16:30-17:00
1. Animal Studies for Functional Imaging at High-Field System:
Ultra-short TE (UTE) MRI of the Lung

Masaya Takahashi
University of Texas Southwestern Medical Center at Dallas

17:00-17:30
2. Clinical Functional Imaging at High-Field MRI

Christian Fink
University Medical Center Mannheim

Poster Session

Event Hall Lobby (B1)

17:40-18:25 Poster Session 1

Pulmonary Circulation 1

Moderator **Toshiko Hoshi** Saitama Cardiovascular and Respiratory Center
Nobuhiro Tanabe Chiba University

P1-1. Follow-up Cases with Perfusion Scintigraphy in Patients with Pulmonary Thromboembolism
Shigeru Tominaga
Juntendo University Urayasu Hospital

P1-2. Most Optimum Display Condition(Width,Center) of Dual Energy Perfusion CT for Diagnosing Pulmonary Embolism
Tomohiro Suzuki
Nagoya City University

P1-3. Pulmonary CT Perfusion Imaging in Assessment of Pulmonary Vascular Disease -First Experience Using 320-MDCT.
Edwin J.R. van Beek
University of Edinburgh

P1-4. Reevaluation of the Tc-99m MAA Whole Body Imaging for Detecting Right-to-left Shunt
Takayuki Shinkai
Nara Medical University School of Medicine

P1-5. Nonembolic Causes of Perfusion Defect on Contrast-enhanced Dual-Energy CT: Review of 85 Consecutive Cases
Chae-Hun Lim
University of Ulsan College of Medicine, Asan Medical Center

17:40-18:52 Poster Session 2

Chronic Obstructive Pulmonary Disease

Moderator **Shin Matsuoka** St. Marianna University School of Medicine
Hiroshi Kimura Nara Medical University

P2-1. Correlation between Airwary Dimensions and Emphysema Scores in Patients with Chronic Obstructive Pulmonary Disease: Patient-based versus Lobe-based Analysus
Ji-Young Ko
Seoul National University Hospital

P2-2. Comparison of Airway Remodelling Assessed by Three-dimensional Computed Tomography between Bronchial Asthma and Chronic Obstructive Pulmonary Disease
Kaoruko Shimizu
Hokkaido University School of Medicine

P2-3. Airway Wall Remodeling in Different Anatomic Locations Assessed by Computed Tomography in Patients with Stable Asthma and COPD
Tsuyoshi Oguma
Kyoto University

P2-4. Quantitative Assessment of Chronic Obstructive Pulmonary Disease (COPD) with Multi-detector row CT (MDCT): Comparison with Lung Structure and Pulmonary Function Test

Jun Sato
Iwata City Hospital

P2-5. Quantitative Assessment of Low Attenuation Volume Percentage(LAV%) and Mean Lung Density(MLD) in Chronic Obstructive Pulmonary Disease Using Inspiratory and Expiratory MDCT

Naoko Kawata
Chiba University

P2-6. Relationship between Low Attenuation Areas Evaluated by Thurlbeck Panel Method and Body Weight in Patients with Stable COPD

Takanobu Shioya
Akita University

P2-7. Effects of Chronic Obstructive Pulmonary Disease on Thoracic Vascular Calcifications

Bertram J Jobst
University of Heidelberg

P2-8. Analysis of Ventilation Abnormalities in Patients with Obstructive Lung Diseases on Xenon-enhanced CT According to Lung Lesion Patterns: Multicenter Study

Eun Jin Chae
Ulsan College of Medicine, Asan Medical Center

17:40-18:43 Poster Session 3

Diffuse Lung Disease

Moderator **Nobuyuki Tanaka** Yamaguchi University School of Medicine
Takashi Hajiro Tenri Hospital

P3-1. Evaluation of the Extent of Ground-glass Opacity on High-Resolution CT in Patients with Interstitial Pneumonia: Comparison between Quantitative and Qualitative Analysis

Hidetake Yabuuchi
Kyushu University

P3-2. Correlation between Pirfenidone Effect and the Initial CT Findings in the Patients with Idiopathic Pulmonary Fibrosis

Tae Iwasawa
Kanagawa Cardiovascular and Respiratory Center

P3-3. Relation between Radiological Abnormalities and Functional Impairment Assessed from Distributional Analysis on Ventilation and Diffusing Capacity to Perfusion in Idiopathic Interstitial Pneumonias

Kazuhiro Yamaguchi
Tokyo Women's Medical University Medical Center East

P3-4. Clinical Considerations of Postoperative Acute Exacerbation in Patients with Interstitial Pneumonia Combined with Lung Cancer

Takahiro Omori
Kanagawa Cardiovascular and Respiratory Center

P3-5. Thoracic and Abdomino-pelvic Radiologic Findings of Japanese Patients with Lymphangioleiomyomatosis

Kuniaki Seyama
Juntendo University School of Medicine

P3-6. Clinical and Radiographic Features of Pulmonary Aspergillosis in Patients with Chronic Fibrosing Interstitial Pneumonia

Akiko Kaga
Saitama Medical University

P3-7. Clinical and Radiographic Features of Pneumothorax and Pneumomediastinum in Patients with Chronic Fibrosing Interstitial Pneumonia

Ayako Shiono
Saitama Medical University

17:40-18:34 **Poster Session 4**

Respiratory Motion 1

Moderator **Masaki Hara** Nagoya City University
Keisaku Fujimoto Shinshu University

P4-1. Effect of Pulmonary Rehabilitation on Parenchymal Lung Motion Evaluated with Dynamic MRI in COPD Patients

Takeshi Shinohara
Kanagawa Cardiovascular and Respiratory Center

P4-2. Diaphragmatic Motion before and after Plication of Central Tendon in Patients with Diaphragmatic Eventration

Koji Chihara
Shizuoka City Shizuoka Hospital

P4-3. Dynamic MRI Measured Respiratory Motion of the Internal Structures of the Lung. Differences between Healthy Subjects and COPD Patients.

Hirofumi Shibata
Yokohama City University School of Medicine

P4-4. Respiratory Motion Analysis with Correlation Function and Frequency Decomposition from MR Image Sequences of COPD Patients and Normal Subjects

Yew Kurabayashi
Takasaki University of Commerce

P4-5. Evaluation of Airway Dimension During Respiration

Hiroshi Wada
Shiga University of Medical Science

P4-6. New Method for Ventilation Function Using Dynamic Chest x-ray Examination: Evaluation of Regional Changes in Inspiratory / Expiratory Flow Rate Ratio

Norihisa Motohashi
Fukujuji Hospital, JATA

17:40-18:34 Poster Session 5

New MR Technique

Moderato **Mitchell S. Albert** University of Massachusetts Medical School
Atsuomi Kimura Osaka University

P5-1. Hyperpolarized 3He Magnetic Resonance Imaging Biomarkers of Bronchoscopic Airway Bypass in COPD

Lindsay Mathew
Robarts Research Institute

P5-2. Line-Narrowed Diode Lasers for High-Efficiency Continuous Production of Hyperpolarized Xe-129 using Optimized Cell for High Concentration of Optically Pumped Rubidum

Mineyuki Hattori
Photonics Research Institute, National Institute of Advanced Industrial Science and Technology

P5-3. Development of a Novel Method for Evaluating Pulmonary Disease Using Hyperpolarized Xe-129 Ultrashort Echo-time MRI

Hirohiko Imai
Osaka University

P5-4. Non-contrast Enhanced MR Angiography Using Volumetric T2-weighted Imaging Technique on 3T

Mitsutomi Ishiyama
St.Luke's International hospital

P5-5. Non-Contrast-Enhanced Pulmonary MR Angiography Using Electrocardiography-triggered Three-Dimensional Half-Fourier FSE with a Swap Phase Encode Extended Data (SPEED) Acquisition and Image Processing

Norio Yoshizaki
Kousei Hospital

P5-6. Quantitative Analysis of the Lung using Hyperpolarized Helium-3 Imaging

James C. Gee
University of Pennsylvania

17:40-18:43 Poster Session 6

Basic Study 1

Moderator **Sumiaki Matsumoto** Kobe University
Toyohiro Hirai Kyoto University

P6-1. The Phantom Study for Analyzing the Small Airway Disease

Noriyuki Yanagawa
Chiba University

P6-2. Integral-based Half-Band Method in Measuring Airway Wall Thickness on CT: Comparison with Conventional Full-Width Half Maximum Method in Actual and Simulated Phantoms

Kim, Namkug
Ulsan University College of Medicine, Asan Medical Center

P6-3. Enhancement of Computerized Differentiation Accuracy of Region Pattern of Diffuse Infiltrative Lung Disease Using Local Context Sensitive SVM Classifier

Kim, Namkug
Ulsan University College of Medicine, Asan Medical Center

P6-4. Newly Developed Denoising Technique:
Utility for Quantitative Assessment of Pulmonary Emphysema on Low-Dose CT Examination

Mizuho Nishio
Kobe University

P6-5. Comparative Study of Respiratory Function for Pulmonary Lobectomy Based on Computer Simulation

Yasushi Hirano
Yamaguchi University

P6-6. Lung CT Image Registration Using Diffeomorphic Transformation Models

Gang Song
University of Pennsylvania School of Medicine

P6-7. Airway Tree Segmentation by Removing Paths of Leakage

Gang Song
University of Pennsylvania School of Medicine

17:40-18:43 Poster Session 7

Clinical Study

Moderator **Koji Takahashi** Asahikawa Medical University
Keisuke Tomii Kobe City Medical Center General Hospital

P7-1. A Low Dose CT Lung Screening Method for Smoking-related Thoracic Abnormalities Using 3D Automatic Exposure Control: Diagnostic Capability and Effectiveness in Radiation Dose Reduction (iLEAD Study)

Takeshi Kubo
Kyoto University

P7-2. Standard and Low-kVp CT of the Lungs Using Different State-of-the-art Multidetector-row CT Systems: A Comparative Analysis of Image Quality and Radiation Dose

Wolfram Stiller
University Hospital Heidelberg

P7-3. Proposal of New Method: Single Breath Xenon Ventilation CT

Norinari Honda
Saitama Medical Center, Saitama Medical University

P7-4. Relationship between Lung Morphologic and Functional Abnormality Assessed by Breath-Hold Perfusion SPECT-CT Fusion images

Kazuyoshi Suga
St. Hill Hospital

P7-5. Diagnostic Value of Initial Computed Tomography in Critically Ill Patients with Pulmonary Edema

Kosaku Komiya
Oita University Faculty of Medicine

P7-6. Pulmonary Lymphatic Drainage to the Mediastinum Based on CT Observations of Primary Complex of Pulmonary Histoplasmosis

Koji Takahashi
Asahikawa Medical University

P7-7. Evaluation of Cross-bridging Structures in Pneumothorax Patients and Correlation with Aging and Pulmonary Inflammation

Tomoaki Sasaki
Asahikawa Medical University

17:40-18:25 Poster Session 8

Case Report 1

Moderator **Shuichi Ono** Hirosaki University
Yoshihiro Nishimura Kobe University

P8-1. A Case of Thromboembolism in Peripheral Pulmonary Artery, Diagnosed by Dual-energy Multi-detector CT

Takahiko Kanokogi
Nara Medical University

P8-2. CT-guided Pericardiocentesis for Recurrent Cardiac Tamponade due to Carcinomatous Pericarditis in a Patient with Adenocarcinoma of the Lung

Yoshihiro Kanemitsu
Takatsuki Red Cross Hospital

P8-3. A Case of Pleomorphic Carcinoma of the Lung Producing Multiple Cytokines and Forming Rapidly Progressive Mass-like Opacity

Masataka Matsumoto
Kitano Hospital

P8-4. A Case of Malignant Mesothelioma with Diffuse Swelling Mediastinum Lacking of Apparent Pleural and Pericardial Lesion

Hiroki Kimura
The University of Tokyo

P8-5. A Case of Pulmonary Tumor Thrombotic Microangiopathy Presenting Progressive Pulmonary Hypertension

Hiromi Tomioka
Kobe City Medical Center West Hospital

Program

January 29, 2011[Sat]

Room A
Main Hall (2F)

9:00-10:50 **Core session3**

Chronic Obstructive Pulmonary Diseaes

Moderator **Toyohiro Hirai** Kyoto University
Kiminori Fujimoto Kurume University School of Medicine
Discusser **Hans-Ulrich Kauczor** Heidelberg University

Invited Speaker

9:00-9:20
1. Etiology and Pathophysiology of COPD

Kazutetsu Aoshiba
Tokyo Women's Medical University

9:20-9:35
2. PET Assessment for COPD: Changes in Pulmonary Perfusion Distribution

José G. Venegas
Harvard Medical School, Massachusetts General Hospital

9:35-9:50
3. CT Assessment for COPD-Phenotype on CT in COPD

Keisaku Fujimoto
Shinshu University School of Health Sciences

9:50-10:05
4. Proton MR Assessment of COPD

Yoshiharu Ohno
Kobe University

10:05-10:20
5. Hyperpolarized Noble Gas MRI for COPD

Edwin J.R. van Beek
University of Edinburgh

Scientific Presentation

10:20-10:30
1. Hyperpolarized Noble Gases and COPD: The Frontier

James P. Butler
Brigham and Women's Hospital, Harvard Medical School

10:30-10:40
2. Regional Quantification of Hyperpolarized Helium-3 Magnetic Resonance Imaging Apparent Diffusion Coefficients: What Dose Bronchodilator Administration in COPD Accomplish?

Miranda Kirby
The University of Western Ontario

10:40-10:50
3. Airway Disease, Emphysema, and Airflow Limitation in Patients with Chronic Obstructive Lung Disease

Hironi Makita
Hokkaido University Hospital

13:20-14:20 **Special Lecture 2** Sponsored by **PHILIPS**

Basics and Future Direction for Quantitative Functional CT Assessment

Moderator **Michiaki Mishima** Kyoto University
Kenya Murase Osaka University
James P. Butler Harvard Medical School

13:20-13:50
1. Architecture of Lung Parenchyma ~Basics of Interpretation of HRCT of the Lung~
Harumi Itoh
University of Fukui

13:50-14:20
2. Current Status and Future Direction of Quantitative Analysis for Functional CT
Eric A. Hoffman
University of Iowa Carver College of Medicine

14:30-16:15 **Core session 4**

Interstitial Lung Disease

Moderator **Yukihiko Sugiyama** Jichi Medical University
Masashi Takahashi Shiga University of Medical Science
Discusser **Kyung Soo Lee** Samsung Medical Center, Sungkyunkwan University school of Medicine

Invited Speaker

14:30-14:55
1. Update for Diagnosis of IIP
Takeshi Johkoh
Kinki Central Hospital of Mutual Aid Association of Public School Teachers

14:55-15:15
2. Update for Treatment of Idiopathic Interstitial Pneumonias (IIPs)
Kingo Chida
Hamamatsu University School of Medicine

15:15-15:30
3. Smoking-related Interstitial Pneumonia Associated with Emphysema
Minoru Kanazawa
Saitama Medical University

15:30-15:45
4. Hyperpolarlized Noble Gas MRI for ILD
Hiroto Hatabu
Brigham and Women's Hospital, Harvard Medical School

Scientific Presentation

15:45-15:55
1. Prognostic Significance of High-Resolution Computed Tomography in Nonspecific Interstitial Pneumonia
Hironao Hozumi
Hamamatsu University School of Medicine

15:55-16:05
2. Automatic Classification of Regional Disease Pattern of Diffuse Lung Disease at HRCT: Cross-Vendor Study
Kim, Namkug
Ulsan Uinversity College of Medicine, Asan Medical Center

16:05-16:15
3. FDG Positron Emission Tomography Imaging of Drug-induced Pneumonitis
Miwa Morikawa
University of Fukui

Room B
Event Hall (B1)

12:00-13:00 **Luncheon Lecture 2** Sponsored by Astellas Pharma Inc. / AstraZeneca K.K.

Imaging for Asthmatics and COPD

Moderator **Shoji Kudoh** Double-Barred Cross Hospital

12:00-12:30
1. CT Assessment of Asthma

Gregory G. King
The Woolcock Institute of Medical Research

12:30-13:00
2. Hyperpolarized Noble Gas MRI for Asthma and COPD

Mitchell S. Albert
University of Massachusetts Medical School

16:30-17:30 **Evening Lecture 2** Sponsored by Eisai Co., Ltd.

New Techniques for Pulmonary Vascular Disease

Moderator **Kazuro Sugimura** Kobe University

16:30-17:00
1. Dual-Energy CT Application for Pulmonary Vascular Disease

Joon Beom Seo
Uinversity of Ulsan College of Medicine, Asan Medical Center

17:00-17:30
2. Quantitative MR Assessment for Pulmonary Vascular Disease

David L. Levin
Mayo Clinic

Poster Session

Event Hall Lobby (B1)

17:40-18:43 **Poster Session 9**

Pulmonary Circulation 2

Moderator **Christian Fink** University Medical Center Mannheim

Minoru Kanazawa Saitama Medical University

P9-1. Changes in Regional Pulmonary Perfusion and Morphology as a Result of Lung Volume Assessed by Technetium-99m Macroaggregated Albumin SPECT and MinIP with MDCT

Hiroko Tomita
National Defense Medical College

P9-2. Estimation of Pulmonary Arterial Pressure in Pulmonary Hypertension Based on Interventricular Septal Configuration Obtained by Electrocardiogram-gated 320 Slice CT

Toshihiko Sugiura
Chiba University

P9-3. Right Ventricle to Left Ventricular Volume Ratio by Electrocardiogram-gated 320 Slice CT is a Predictor of Right Ventricular Pressure Load in Pulmonary Hypertension

Toshihiko Sugiura
Chiba University

P9-4. Correlation of Right Ventricular Ejection Fraction with Tricuspid Annular Plane Systolic Excursion by Electrocardiogram-gated 320 Slice CT in Pulmonary Hypertension

Toshihiko Sugiura
Chiba University

P9-5. Evaluation of Hemodynamic Changes in Pulmonary and Systemic Arterial Circulation in Patients with Pulmonary Fibrosis in Relation to Breathing Methods Using Phase Contrast MRI

Nanae Tsuchiya
University of the Ryukyus Hospital

P9-6. Alteration of Pulmonary Perfusion after CT Density-Based Non-uniform Attenuation Correction on DIBrH SPECT-CT Fusion Images

Kazuyoshi Suga
St. Hill Hospital

P9-7. Comparative Study of Tc-99m MAA Lung Perfusion SPECT and Multidetector CT Pulmonary Angiography in Patients with Chronic Pulmonary Embolism-Multicenter Trial

Shigeru Kosuda
National Defense Medical College

17:40-18:52 Poster Session 10

Thoracic Malignancy

Moderator **Hidetake Yabuuchi** Kyushu University
Yoshinobu Iwasaki Kyoto Prefectural University of Medicine

P10-1. CT Diagnosis of Recurrence of Lung Cancer

Fumiyasu Tsushima
Hirosaki University

P10-2. Comparison of Quantitative Diagnostic Capability of Lymph Node Metastasis in Non-small Cell Lung Cancer Patients between STIR Turbo SE Imaging, Diffusion-Weighted Imaging and FDG-PET/CT

Daisuke Takenaka
Kobe University

P10-3. Capability for Quantitative Differentiation of Small Cell Lung Cancer from Non-Small Cell Lung Cancer by Diffusion-Weighted Imaging and STIR Turbo SE Imaging

Hisanobu Koyama
Kobe University

P10-4. Comparison of Capability for Pulmonary Nodule Detection ; 1.5T vs 3.0T Systems

Keiko Matsumoto
Yamanashi Hospital of Social Insurance

P10-5. Utility of Nodule Type Assessment for Improving Diagnostic Capability in Patients with Solitary Pulmonary Lung Nodules on Low-Dose CT at FDG-PET/CT

Yumiko Onishi
Kobe University

P10-6. Estimation of Increase of Pulmonary Ground-Glass Opacity:
Integrated evaluation of detected GGOs using early indicator of growth

Shuji Yamamoto
LISIT, Co., Ltd.

P10-7. How Much Can the Radiation Dose be Reduced in Automated Volumetry of Pulmonary Nodules? A Comparison of 16 cm Volume Scans and 64-row Helical Scans with 320-row MDCT.

Ayano Kamiya
University of the Ryukyus

P10-8. Prediction of Postoperative Lung Function in Patients with Lung Cancer: Comparison of Dual-energy Perfusion CT and Perfusion Scintigraphy

Eun Jin Chae
Ulsan College of Medicine, Asan Medical Center

17:40-18:43 Poster Session 11

Chronic Obstructive Pulmonary Disease and Others

Moderator **Osamu Honda** Osaka University
Masaharu Nishimura Hokkaido University

P11-1. Quantitative Analysis of Pulmonary Cysts and Emphysema on Computed Tomography: Lymphangioleiomyomatosis, Birt-Hogg-Dubé Syndrome and Chronic Obstructive Lung Disease

Kazunori Tobino
Juntendo University

P11-2. In Vivo Monitoring of Cystic Fibrosis-like Lung Disease in Mice by Volumetric Computed Tomography

Mark. O. Wielpuetz
University Hospital Heidelberg

P11-3. Using Hyperpolarized 3He MRI for Treatment Evaluation in Cystic Fibrosis

Yanping Sun
University of Massachusetts Medical School

P11-4. Assessment of Paraseptal Emphysema in the Inner Lung Field by Using Inflated-Fixed Lung Specimens

Katashi Satoh
Kagawa Prefectural College of Health Scineces

P11-5. I-123-MIBG Lung Kinetic Abnormality in Pulmonary Emphysema

Kazuyoshi Suga
St. Hill Hospital

P11-6. The Epithelial-Mesenchymal Transition of Progenitor Cells Lead to Low Attenuation Areas of the Pulmonary Parenchyma: An Autopoietic Model Analysis of Alveolar Epithelial Maintenance

Kyongyob Min
Itami City Hospital

P11-7. Oscillatory Mechanics within Respiratory Cycles Related to COPD Severity

Junichi Ohishi
Tohoku University School of Medicine

17:40-18:34 Poster Session 12

Asthma, Airway Disease and Others

Moderator **Jin Mo Goo** Seoul National University Hospital, Seoul National University College of Medicine
Shigeo Muro Kyoto University

P12-1. Hyperpolarized 3He MRI Apparent Diffusion Coefficients as a Probe of Airway Function in Asthma After Methacholine Challenge and Recovery

Stephen E. Costella
Robarts Research Institute

P12-2. 4-Dimentional Imaging of the Central Airway Using a Low Dose Technique: Initial Experience with 320-row Multidetector CT

Ryo Sakamoto
Kyoto University

P12-3. Dynamic Property of Central Airway Walls as Assessed by Computed Tomography: Correlation with Asthma Pathophysiology

Masafumi Yamaguchi
Shiga University of Medical Science

P12-4. Comparison of 3-D-Visualized Respiratory Impedance Patterns and Structural Change Detected by CT in Smokers

Haruko Shinke
Kobe University

P12-5. Usefulness of SD-101, a Non-restrictive Device Developed for Screening Sleep Apnea-hypopnea Syndrome

Keisaku Fujimoto
Shinshu University School of Health Sciences

P12-6. Vibration Response Imaging (VRI) in the Detection of Asynchrony between Left and Right Lung for Main Bronchial Stenosis

Hirotaka Kida
St. Marianna University School of Medicine

17:40-18:34 **Poster Session 13**

Respiratory Motion 2

Moderator **Hideaki Haneishi** Chiba University
Koji Chihara Shizuoka City Shizuoka Hospital

P13-1. Analysis of Lung Motion Due to Respiration and Its Application to PET Images

Hideaki Haneishi
Research Center for Frontier Medical Engineering

P13-2. A 4D Model Generator of the Human Lung: Lung CataChiCaraCure-er, Alias Lung4Cer

Hiroko Kitaoka
JSOL Corporation

P13-3. Alveolar Recruitment Analysis in Acute Respiratory Distress Syndrome (ARDS) Using End-inspiratory and End-expiratory Breath-hold 3D-CT Images

Hiroko Kitaoka
JSOL Corporation

P13-4. Velocity Vector Imaging in Assessing the Regional Diaphragmatic Movement of Patients with Chronic Diaphragmatic Hernia- Preliminary Results

Teng-Fu Tsao
Chung Shan Medical University Hospital

P13-5. Usefulness of Ultrasonography in Preoperative Diagnosis of Solitary Fibrous Tumor of the Pleura

Mitsuaki Sekiya
Juntendo University School of Medicine

P13-6. A Method for Reduction of Subtraction Artifacts on Temporal Subtraction Images by Use of Generalized Gradient Vector Flow Technique

Hyoungseop Kim
Kyushu Institute of Technology

17:40-18:34 Poster Session 14

Basic Study 2

Moderator **Takatoshi Aoki** University of Occupational and Environmental Health School
Gregory G. King The Woolcock Institute of Medical Research

P14-1. Towards a Research Software Platform for Diagnosis and Therapy Monitoring for COPD and Asthma with Pulmonary Magnetic Resonance Images
Peter Kohlmann
Fraunhofer MEVIS

P14-2. Clinical Chest CAD System for Lung Cancer, COPD, and Osteoporosis Based on MDCT Images
Shinsuke Saita
The University of Tokushima

P14-3. Developments of Thrombosis Detection Algorithm using the Contrast Enhanced CT Images
Jun Oya
The University of Tokushima

P14-4. Segmentation of Thoracic Organs from Multi-slice CT Images
Mikio Matsuhiro
The University of Tokushima

P14-5. Iterative Algorithm for Airway Segmentation in CT Images Using a Region-based Active Contour Model
Sumiaki Matsumoto
Kobe University

P14-6. A Comparative Study of HRCT Image Metrics and PFT Values for Characterization of ILD and COPD
Gang Song
University of Pennsylvania School of Medicine

17:40-18:16 Poster Session 15

Case Report 2

Moderator **Fumito Okada** Oita University
Kazuya Fukuoka Hyogo College of Medicine

P15-1. Unexplained Desaturation in the Sitting Position with Stroke
Shigeki Nanjo
Kobe City Medical Center General Hospital

P15-2. Acute-onset Sarcoidosis with Polyarthralgia and Hilar Lymphadenopathy
Hiroshi Santo
Kinki University

P15-3. Pulmonary Function and Computer Tomography of a Relapsing Polychondritis with Bronchial Lesion
Takahiro Tsuji
Tenri Hospital

P15-4. A Case of Toxocariasis Who Presented Abnormal Tubular Structures in Lung Fields
Yuko Nakase
Teikyo University School of Medicine

Program

January 30, 2011[Sun]

Room A
Main Hall (2F)

8:30-10:20 **Core session 5**

Asthma and Airway Disease

Moderator **Yuji Tohda** Kinki University
Shigeru Kosuda National Defense Medical College
Discusser **Shu Hashimoto** Nihon University

Invited Speaker

8:30-8:50
1. Pathophysiology of Asthma

Hiromasa Inoue
Kagoshima University

8:50-9:05
2. Evaluation of Airway Obstruction and Altered Pulmonary Permeability with Lung Scintigraphy in Young Patients

Mayuki Uchiyama
The Jikei University School of Medicine

9:05-9:20
3. CT Assessment for Asthma

Hiroshi Tanaka
Sapporo Medical University School of Medicine

9:20-9:35
4. MR Assessment of Asthma; Hyperpolarized ^{3}He Magnetic Resonance Imaging to Probe Temporal and Spatial Airway Functional Changes

Grace Parraga
The University of Western Ontario

9:35-9:50
5. Update for Treatment of Asthma

Kazuto Hirata
Osaka City University

Scientific Presentation

9:50-10:00
1. The Effect of Methacholine Challenge on Ventilation Heterogeneity in Asthma Measured by SPECT

Gregory G. King
The Woolcock Institute of Medical Research

10:00-10:10
2. Surface Irregularity of Airway Walls as Assessed by MDCT in Asthmatic Patients

Tsuyoshi Oguma
Kyoto University

10:10-10:20
3. Intrathoracic Tracheal Volume and Collapsibility on Inspiratory and End-expiratory CT Scans: Correlations with Lung Volume and Pulmonary Function in 85 Smokers

Tsuneo Yamashiro
University of the Ryukyus

10:30-12:15 **Core session 6**

Respiratory Motion Analysis

Moderator **Ichiro Kuwahira** Tokai University Tokyo Hospital
Shuji Sakai Tokyo Women's Medical University
Discusser **James Gee** University of Pennsylvania

Invited Speaker

10:30-10:45
1. Aims of Respiratory Motion Assessment for Anesthesiology

Klaus Markstaller
Medical University of Vienna

10:45-11:00
2. MR Assessment of Respiratory Motion

Tae Iwasawa
Kanagawa Cardiovascular and Respiratory Center

11:00-11:15
3. Nuclear Medicine Assessment for Respiratory Lung Motion

Kazuyoshi Suga
Yamaguchi University School of Medicine

11:15-11:30
4. Dynamic Volume Scan Using 320-row ADCT for the Assessment of Respiratory Motion

Hiroshi Moriya
Sendai Kosei Hospital

11:30-11:45
5. Respiratory Motion Assessment to Increase the Accuracy of Non-contact Screening System to Prevent the Spread of Infectious Diseases

Takemi Matsui
Tokyo Metropolitan University

Scientific Presentation

11:45-11:55
1. Temporal Stability of the 4D-CT Pulmonary Ventilation Imaging Method

Tokihiro Yamamoto
Stanford University

11:55-12:05
2. Analysis of Respiratory Movement Using 4-Dimensional Chest CT image

Seiji Tani
The University of Tokushima

12:05-12:15
3. Asymmetry of the Mechanical Property in the Human Respiratory System Causes the Asymmetry of the Lingual Center in the Brain: Diaphragmatic Motion Analysis with Dynamic MR Images

Hiroko Kitaoka
JSOL Corporation

13:50-15:05 **Special Lecture 3** Sponsored by TOSHIBA MEDICAL SYSTEMS CORPORATION

Future Direction for Pulmonary Functional and Molecular Imaging

Moderator **Yasutaka Nakano** Shiga University of Medical Science
Yoshiharu Ohno Kobe University
Hiroto Hatabu Brigham and Women's Hospital, Harvard Medical School

13:50-14:15
1. From Basic Science Side

Hisataka Kobayashi
National Institute of Health

14:15-14:40
2. From Radiology Side

Hans-Ulrich Kauczor
Heidelberg University Medical Center

14:40-15:05
3. From Pulmonology Side -Terminal Air Space of X-ray CT Images in COPD-

Michiaki Mishima
Kyoto University

15:05-15:15 **Closing Remark**

Room B

Event Hall (B1)

12:30-13:30 **Luncheon Lecture 3** Sponsored by DAIICHI SANKYO COMPANY, LIMITED

Hyperpolarized Noble Gas MRI

Moderator **Toshihiro Nukiwa** Tohoku University

12:30-13:00

1. Development of Polarizer for Future Clinical Works

F. William Hersman
University of New Hampshire, Xemed LLC

13:00-13:30

2. Hyperpolarized Noble Gas MRI: Clinical Applications

Hiroto Hatabu
Brigham and Women's Hospital, Harvard Medical School

Abstract

Special Lecture

Special Lecture 1-1

Interaction between Functional and Morphological Imaging: 3D Airway Analysis in Chronic Obstructive Pulmonary Disease

Masaharu Nishimura, M.D., Ph.D.
Division of Pulmonary Medicine, Department of Internal Medicine,
Hokkaido University Graduate School of Medicine, Japan

Chronic obstructive pulmonary disease (COPD) is a disease characterized by airflow limitations that are not fully reversible and consists of small airways disease (obstructive bronchiolitis) and parenchymal destruction (emphysema), the relative contributions of which vary among patients. Thin-section computed tomography (CT) has been used to quantify emphysema by detecting low-attenuation areas (LAAs), and the role of CT in diagnosing emphysema is well established. However, airflow limitations as evaluated by forced expiratory volume in 1 s (FEV_1) do not necessarily correlate well with severity of emphysema as evaluated by CT, since small airways disease appears to contribute more significantly to airflow limitations in COPD.

Recent progress in CT technology has enabled the detection and quantification of airway dimensions, including airway wall thickness and airway luminal area. The use of CT to evaluate airway dimensions in a variety of diseases has thus been suggested. However, only a few studies had attempted to measure airway dimensions in patients with COPD until 2006, when our study was first published in Amer J Respir Crit Care Med in 2006. Most previous reports had, unfortunately, suffered from inherent technological problems with respect to the measurement of airway dimensions. First, accurate cross-sectional images could not always be obtained using conventional two-dimensional images, since airways run in various directions in the lung. Second, since investigators did not obtain longitudinal airway images, which generation of the bronchus was actually being measured, could not be recognized. The idea of three-dimensional airway analysis was not entirely new, but had not previously been applied to measuring airway dimensions in patients with COPD.

In this presentation, I would like to show you how we validated our original software using phantoms, and how we applied this software to a series of clinical studies in COPD. Firstly, we have demonstrated, in a relatively large patients with COPD, that the percentage of predicted forced expiratory volume in 1 s (% FEV_1), an airflow limitation index, correlated highly with airway luminal area (Ai) and, to a lesser extent, with percentage wall thickening (WA%) from the 3rd to the 6th generation of both the apical upper bronchus (B1) and the anterior lower bronchus (B8). More interestingly and importantly, we showed that correlation coefficients improved with decreasing airway size in both airways. We then examined the relationship between airway dimensions and emphysema severity at the upper lung and the lower lung separately and how these pathological processes contributed to overall pulmonary function. Secondly, we attempted to determine the relationship between improved pulmonary function and changes in airway caliber at various sites among the airways in response to inhaled anticholinergics in patients with COPD. We performed CT at deep inspiration and detailed pulmonary function tests before and 1 week after daily inhalations of tiotropium bromide in 15 patients with clinically stable COPD. We analyzed the airway luminal area at the 3rd (segmental) to the 6th generations of 8 bronchi in the right lung. Bronchodilation was demonstrated as an overall average of a 39% increase in the inner luminal area, and the mean forced expiratory volume in 1 sec (FEV_1) increased from 1.23 $\pm$ 0.11 to 1.47 $\pm$ 0.13 (SE). The magnitude of bronchodilation closely correlated with improved pulmonary function, particularly with that of FEV_1 ($r = 0.843$, $p < 0.001$). Such correlations were significant at the 4th to the 6th, but not at the 3rd generation of bronchi, and the slope of regression lines became steeper from the 3rd to the 6th generation. In conclusion, inhaled anticholinergics induce overall bronchodilation in proportion to improvements in FEV_1 in patients with COPD, and bronchodilation at distal, rather than proximal airways is the determinant of functional improvement.

These studies clearly demonstrated functional importance of the smaller airways among the 3rd to the 6th generation of airways in COPD. Although we are not in a stage where we can visualize and measure "small airways" which are physiologically defined as those whose inner diameter is less than 2 mm, we have come close to those areas. In this presentation, I will also present potential differences in airway remodeling which might exist between COPD and bronchial asthma. In short, airway remodelling was more prominent in asthma compared with age- and sex-matched COPD subjects at the 3rd- to the 6th-generation airways when airflow limitations as assessed by FEV_1/FVC and % FEV_1 were mild to moderate to similar extent under stable clinical conditions.

In the near future, with further advances in both CT technology and software, this kind of approach will become even more attractive. However, at the same time, we must be cautious about potential problems in the application of three-dimensional airway analysis to longitudinal follow-up studies and/or large-scale multi-center studies, which will be also discussed in this presentation.

Special Lecture 1 - 2

Interaction between Metabolic and Morphological Imaging

Kyung Soo Lee, M.D.
Department of Radiology
Samsung Medical Center, Sungkyunkwan University School of Medicine, Korea

In the era of fusion (*e.g.*, PET-CT or MR-PET) imaging, the representative morphologic imaging tools are CT and MRI, whereas PET and SPECT may be the representative of metabolic imaging. By integrating morphologic and metabolic imaging, synergistic effect of both modalities can be acquired.

The substantial and expected effect of combining metabolic and morphologic imaging devices includes 1) precise localization of lesions detected on metabolic imaging scans within the anatomic frame provided by morphologic imaging tool (seeking a lesion of morphologic changes that matches with a metabolic-imaging lesion), thus increasing specificity of the examination, 2) a supply of morphologic information of target lesions (*e.g.*, attenuation value including calcification at CT and signal intensity of target lesions at MRI) by morphologic imaging and thus preventing observers from making false positive interpretations, 3) an insight on the necessity of additional morphologic information acquisition in organs where normal metabolism of radioisotopes do occur (like brain, myocardium, liver and the kidneys) at FDG PET, and 4) information of a need for development of various radiopharmaceuticals other than FDG and for anatomically-guided partial volume correction in metabolic imaging.

In this talk, the speaker will elaborate on above-mentioned problems by showing illustrative cases.

Special Lecture 2-1

Architecture of Lung Parenchyma ~Basics of Interpretation of HRCT of the Lung~

Harumi Itoh, M.D.
University of Fukui, Japan

1. Introduction

This special lecture will describe three basic structures of the lung. The first is three dimensional features of alveoli and alveolar ducts. The second is a respiratory bronchiole and its relation to adjacent parenchyma. The third is small pulmonary vasculatures and lymphatic vessels. These topics are based on the results of radiologic-anatomic-pathologic correlations on lung specimens obtained from surgery and autopsy. Contact radiography and stereomicroscopic observations were especially useful to study detailed anatomy of peripheral portions of the lung.

2. Normal morphologic features of lung periphery

(1)Spatial configuration of alveoli and alveolar ducts

【Macroscopic observation】

Lung parenchyma is known to occupy 90% of total lung volume, however it looks empty or zero in normal radiological images (chest radiograph, HRCT) because of remarkable radiolucent nature of the normal lung parenchyma. Macroscopically normal lung parenchyma seen in lung specimens looks compact like a liver or brain. These facts implies that radiologic zero-looking lung parenchyma is packed with air and specially designed real tissue which forms lung parenchyma. Contact radiograph and HRCT of normal lung specimen shows the lung parenchyma has weak radio-opacity which is definitely greater than air.

【Stereomicroscopic and histological correlations】

Stereomicroscope is useful to observe lung parenchyma on the cut surface of inflated and fixed lung specimens. With weak magnification the lung parenchyma resembles a sponge. The numerous small holes correspond to alveolar ducts, not the alveoli. With high power magnification, the alveolus appears polyhedral in shape, and two types of alveolar wall are identified, that is, lateral wall and dome of alveolus. Each alveolar entrance is polygonal in shape and is packed like a honeycomb which surrounds the lumen of alveolar ducts.

One set of alveoli facing the adjacent two alveolar ducts shows a back to back arrangement. This back to back arrangement of the alveoli is recognized both in profile and from front under the stereomicroscope. The zigzag pathway of alveolar dome seen in histological section corresponds to this arrangement seen in profile. The superimposed back to back alveoli show fine reticular pattern in a contact radiograph of lung specimens.

Stereomicroscope is also useful to observe the bronchioles in post mortem bronchograph. It shows the diameter of terminal and respiratory bronchioles is smaller than that of more peripheral air passages. Since cross section of such peripheral air passages consists of an alveolar duct and marginal alveoli, its whole diameter becomes bigger than that of the central bronchioles. This change of diameter gives a tree-in-bud pattern made by a contrast medium or by pathologic lesions filling those portions of the lung.

(2)Double and single faced alveolar walls

Each alveolar wall included in the back to back alveoli is called double faced alveolar wall, because gas exchange is performed in both sides of the alveolar wall. In contrast the alveolar walls attaching to the airways, pulmonary vessels, interlobular septum and pleura are single faced alveolar walls, since gas exchange is limited to one direction. Ninety percent of total alveolar walls are the double faced alveolar wall.

(3)Respiratory bronchiole

Respiratory bronchiole is characterized by scattered alveoli opening from the bronchiolar wall. The important point is how the alveoli of the respiratory bronchiole are related to those of surrounding pulmonary parenchyma. Histological study shows the alveolar domes of both sides of alveoli are hold in common, therefore, respiratory bronchiole and adjacent parenchyma are connected by the back to back to alveoli. Instead the alveolar dome surrounding the bronchiolar wall is the single faced alveolar wall and separated from the bronchial lumen.

The back to back to alveoli extending from the wall of the respiratory bronchiole may be responsible for producing centriacinar or centrilobular inflammatory nodules seen in pulmonary infectious diseases.

(4)Arterioles and venules

Pulmonary vessels are one of the non parenchymatous structures of the lung, and occupy less than 10% of total lung volume. However, we tend to overestimate the volume of the pulmonary vessels in HRCT, angiogram, and even in chest radiograph, because the lung parenchyma superimposed to those vessels may not be recognized correctly.

Small pulmonary vessels whose diameter is below 70 microns are called arterioles and venules. Within

the secondary lobule of the lung, the arterioles divide from muscular arteries which run with bronchioles, and distribute along the alveolar domes.

An interesting feature of the arterioles is a peculiar branching pattern which is demonstrated by post mortem angiograph. A number of arterioles divide directly from the axial muscular artery like a twig. Such a small lateral branch provides blood flow to the lung parenchyma adjacent to the respiratory bronchioles.

Arterioles and venules are equipped with lymphatic vessels in the perivascular interstitial space. These lymphatics are related to the pulmonary vessels and do not exist in the alveolar wall.

(5)Alveolar capillaries

The double faced alveolar wall is equipped with denser network of capillaries than that of single faced alveolar wall. A post mortem micro-angiograph shows alveolar capillaries appearing like a polygonal network. However, the microphotograph of the same specimen shows alveolar capillaries are not distributed in a smooth plane but undulated within the alveolar wall, which may contribute to increase alveolar surface area for gas exchange.

(6) Lymphatic vessels

Lymphatic vessels are distributed along non-parenchymatous structures such as airways, pulmonary vessels, interlobular septa and pleura. The lymphatic vessels are usually observed by histological sections, however, those of visceral pleura are able to observe with a naked eye. Three dimensional images of the pleural lymphatic vessels are obtained from HRCT of lung specimens inflated with air. The pleural lymphatics form variously sized polygonal net work. The large network borders the secondary pulmonary lobule with interlobular septum and pulmonary vein.

3. Disease patterns of lung parenchyma

Typical disease patterns are mentioned here, which is suitable for establishing morphological concepts specified to lung parenchyma and related structures.

(1) Disease of alveolar wall

Radiologic-pathologic correlations done in case of adenocarcinoma prove thickening of alveolar walls is responsible for ground glass attenuation in HRCT. Histological studies showed all alveolar walls within the tumor are thickened by cancer invasion and interstitial reaction, and the tumor is surrounded by normal back to back alveoli. These observations suggest that adenocarcinoma may extend continuously along the back to back alveoli.

Usual interstitial pneumonia involves primarily the alveolar walls of back to back alveoli. Histological studies show that in addition to honeycomb lung isolated fibrotic lesions are surrounded by normal back to back alveoli.

(2) Disease of alveoli and alveolar duct

A tree-in-bud pattern seen in HRCT of pulmonary tuberculosis is formed by compact caseous materials filling sequentially the respiratory bronchiole, alveolar ducts and alveoli, while accompanying arteries and arterioles are kept in normal. In HRCT these lesions observed in pulmonary tuberculosis may mimic to those of pulmonary sarcoidosis. In sarcoidosis the disease tends to be localized around the pulmonary vessels.

(3) Centriacinar (Centrilobular) disease

Centriacinar disease involves respiratory bronchioles, peribronchiolar interstitial tissue and adjacent pulmonary parenchyma simultaneously. The back to back alveoli anchored to the wall of respiratory bronchiole may provide bypass route of disease extending to adjacent lung parenchyma. Centriacinar inflammatory nodules are bigger than the diameter of respiratory bronchiole and such lesions are seen typically in diffuse panbronchiolitis, pneumoconiosis and pulmonary infection.

(4) Perivascular disease

Perivascular disease pattern is derived from pathologic lesions distributing along lymphatic vessels related to pulmonary vasculatures. Since pathologic lesions surround pre-existing pulmonary vessels, the vascular images in HRCT become thickened and irregular in contour. Typical images are shown in case of pulmonary sarcoidosis, lymphangiosis carcinomatosa and lymphoma.

4. Summaries

The key structure of the lung parenchyma is the alveolar wall. Most of the alveolar walls are intervened by air both in the alveoli and alveolar ducts except the alveolar walls attaching to the non parenchymatous pulmonary structures. The lateral walls and domes of alveoli are connected to form back to back alveoli and distribute among adjacent alveolar ducts. The superimposed alveolar walls show fine reticular patterns in contact radiograph of sliced lung specimens. The arterioles and venules do not accompany the bronchial trees and are laid within interstitial space of alveolar domes. The respiratory bronchioles are equipped with a bypass route for some diseases extending from the bronchial wall to adjacent lung parenchyma through the back to back alveoli.

Special Lecture 2-2

Current Status and Future Direction of Quantitative Analysis for Functional CT

Eric A. Hoffman, Ph.D.
Professor of Radiology, Medicine and Biomedical Engineering
University of Iowa Carver College of Medicine, Iowa City, Iowa, USA

Imaging-based metrics are playing a central role in the quest to identify COPD phenotypes, serving to establish homogeneous sub-populations to: 1) aid in the search for genotypes; 2) provide targets for the development of new therapeutic interventions; and 3) serve as outcomes measures for the evaluation of therapeutic interventions. CT has emerged as a tool of choice for assessing structural-based changes in the lung associated with COPD including measures of lung density distributions at full inspiration as an index of emphysema, lung hyperlucency at expiration as an index of air trapping together with measures of airway wall remodeling. While measures of lung destruction and airway remodeling are providing metrics which are more sensitive than standard pulmonary function tests, *CT phenotypes of lung disease must move towards providing insights into the etiology of the disease, not just road maps of destruction.*

Recent findings have lead us to believe that CT derived perfusion (PBF) and mean transit time (MTT) measures within inflamed lung parenchyma provide for a functional phenotype of emphysema which may be directly tied to the etiology of the pathologic process leading to emphysema in a subset of the smoking population susceptible to centrilobular emphysema. *Our central hypothesis is that smokers prone to emphysema have abnormal vasoregulation in that regional hypoxic pulmonary vasoconstriction (HPV) continues despite inflammation. This failure to block vasoconstriction alters the repair response and leads to tissue injury and eventually smoking-associated centrilobular (and paraseptal) emphysema in those smokers with abnormal vasoregulation.* The normal response to regional hypoxia in the lung is to shunt blood towards better-ventilated regions. However, if small, regional infiltrates associated with a heterogeneous smoking-associated process induces local hypoxia, HPV in regions of smoking-induced infiltrates will interfere with defense mechanisms serving to clear the irritant and will interfere with mechanisms of repair. We (1) have recently demonstrated that smokers with normal pulmonary function tests (PFTs) but subtle visual CT evidence of smoking-associated centrilobular emphysema (SCE) have increased heterogeneity (coefficient of variation: CV) of CT-derived measures of PBF and MTT as compared with smokers with normal PFTs and normal CT images (SNI). This is consistent with reduced perfusion in hypoxic (alveolar flooded) regions. A corollary to the above hypothesis is that the enhanced CV of perfusion in SCE subjects will appear throughout the lung (smoking is associated with increased parenchymal density on CT) while the destructive effects resultant from HPV will be magnified at the lung apices where gravitational forces resisting flow are the greatest, compounding effects of increased vascular resistance. We thus provide what has been an elusive explanation for the apical distribution of centrilobular emphysema.

While increased heterogeneity of perfusion in SCE subjects is consistent with our above hypothesis, further supportive evidence is required. Additionally, to translate our laboratory research into multi-center studies, we have demonstrated the equivalence of perfused blood volume (PBV) vs. PBF/MTT CV. Using dual energy CT, a PBV protocol avoids placement of a central contrast line and significantly reduces radiation dose. In addition to the use of PBV as an index of regional perfusion, we are seeking to evaluate the equivalency of a single breath / dual energy Xenon CT scan as an alternative to a washin protocol for the assessment of regional ventilation to derive matched PBV / Ventilation images.

Special Lecture 3-1

Future Direction for Functional and Molecular Imaging in the Lung. ~From Basic Science Side~

Hisataka Kobayashi, M.D., Ph.D.
Chief scientist, Molecular Imaging Program, NCI/NIH, USA

The development of imaging technologies that have sufficient specificity and sensitivity to enable early and accurate detection of cancer as well as offer the ability to monitor early tumor response to therapy has long been a goal of oncologic research. Numerous radiological techniques have been used for the diagnosis of diseases including cancer as well as for the surveillance of recurrence. These include: x-ray (plain film and computed tomography [CT]), magnetic resonance imaging (MRI), radionuclide imaging (single photon emission computed tomography (SPECT)/ positron emission tomography (PET), and ultrasonography (US). It is evident that imaging has revolutionized various fields including in the lung diseases. However, despite the widespread use of these technologies, the ability of currently available modalities to facilitate the early detection, precise characterization, and accurate localization of diseases remains suboptimal. For example, the current detection threshold for imaging solid tumors of $1cm^3$ or approximately 10^9 cancer cells exemplifies this, as achieving early and accurate diagnosis clearly requires detecting cancer far earlier in the course of disease. Multiplexed imaging offers great potential for improving cancer detection and treatment. In a broad sense, multiplexed imaging refers to techniques that yield multiple distinct data sets from a single imaging session, however, few primitive methods have recently been used in the clinic. Four general strategies for multiplexed imaging have been proposed.

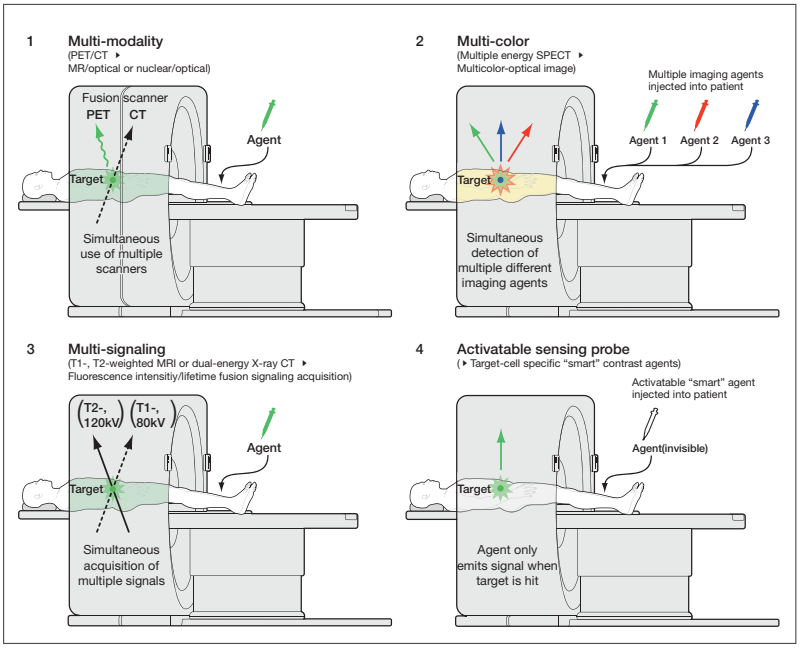

1) *Multimodality* in which two (or more) distinct imaging modalities are simultaneously or consecutively employed; PET/CT is an example that is currently in clinical use. 2) *Multicolor contrast agents* in which multiple different agents, with distinct energies (colors) are simultaneously imaged using a single modality; SPECT has been used in this manner and can simultaneously detect two imaging agents, *i.e.* Tc-99m and Tl-201, by utilizing the differences in energy emission of distinct radioisotopes. 3) *Multiple signal collection* in which a single modality can detect and interpret multiple signals obtained with distinct signaling technologies; MRI techniques such as T1/T2 and diffusion-weighted imaging as well as dual-energy X-ray CT are examples of multiple signal imaging currently used in clinic. 4) And finally, *activatable "smart" reagents*, which generate data regarding both tumor location and molecular profile using targeted probes that emit signal in target tissue only after cellular internalization or other triggering events. These imaging methods based on the multiplexed strategies would overcome the limitation of each one of conventional modalities, which can be broadly categorized into primarily anatomical and primarily molecular imaging techniques, generally with an inverse relationship between spatial resolution and their sensitivity to detect small changes of disease. Primarily anatomic imaging technologies include CT, MRI, and ultrasound. These modalities are limited by their ability to detect disease only after tumor size or associated structural changes are significant enough to be detected grossly. At the other end of the spectrum are primarily molecular imaging modalities, which offer the ability to detect molecular and cellular changes of disease before disease can be detected grossly. Although extremely promising, currently available molecular modalities are often limited by depth of signal penetration as well as poor spatial resolution. Within current clinic, the most widely used functional modalities include PET and SPECT, which can provide information regarding tissue activity at the expense of the anatomic detail due to poor spatial resolution.

Of the desired improvements in clinical imaging, earlier detection of disease, more accurate molecular characterization of tumors and the tumor microenvironment, earlier detection of response to therapy, are the most highly sought after advances. In order to achieve these important imaging objectives, the limitations of individual technologies must be minimized and new innovations developed with these endpoints in mind. Towards this end, the simultaneous use of two or more modalities, contrast reagents, signaling methods, or the coupling of agent and tissue properties, to achieve so called "multiplexed imaging," is a promising approach. For example, combining PET with CT simultaneously yields data regarding tissue metabolism and structural anatomy. A parallel example in molecular imaging is the smart probe, which utilizes both molecular targeting and intracellular probe processing to provide information about the surface molecular profile of a tumor, thus improving sensitivity and specificity compared to conventional "always on" imaging agents. In this lecture, I will provide a broad overview of multiplexed imaging technologies ranging from those currently available to those still under development especially for oncologic imaging.

References:

1. H. Kobayashi, *et al., Lancet Oncol* **11**, 589 (Jun, 2010).
2. H. Kobayashi, *et al., Chem Rev* **110**, 2620 (May 12, 2010).
3. Y. Hama *et al., Cancer Res* **67**, 2791 (Mar 15, 2007).
4. H. Kobayashi *et al., ACS Nano* **1**, 258 (Nov, 2007).
5. M. Ogawa *et al., Bioconjug Chem* **20**, 2177 (Nov, 2009).
6. Y. Urano *et al., Nat Med* **15**, 104 (Jan, 2009).

Special Lecture 3-2

Future Direction for Pulmonary Functional and Molecular Imaging

Hans-Ulrich Kauczor
Heidelberg University Medical Center, Germany

Lung imaging has shown a series of groundbreaking technological developments in recent years. They involve the major radiological imaging techniques such as computed tomography (CT), magnetic resonance imaging (MRI), positron emission tomography (PET) and to some degree single photon emission computed tomography (SPECT) and ultrasonography. They are mainly related to high imaging speed; gating techniques, either respiratory, cardiac or intrinsic; signal enhancement technologies including new contrast agents and mechanisms, as well as new probes and targets. These modalities are available for clinical studies, but also for translational and preclinical research. The complexity increases even more with so-called hybrid imaging systems, such as PET/CT, SPECT/CT, MRI/PET but also combinations with optical imaging systems. For small animal imaging additional approaches such as high-speed video microscopy, multiphoton microscopy, darkfield and (auto-)fluorescence microscopy, as well as molecular confocal live-cell imaging and other techniques of optical imaging are also available or under investigation.

Some years ago, MRI paved the way for comprehensive imaging of structure and function in lung disease. Such protocols include perfusion, ventilation, V/Q ratio and match; gas exchange, vascular permeability, blood flow, shunt; hemodynamics, heart function, lung volumes, respiratory motion, and mechanics. Recent developments, such as "Interpolated volume imaging" with high spatial resolution; contrast enhancement; single and multiphasic MR angiography; diffusion-weighted and diffusion tensor MRI sequences; multidirectional blood flow measurements; angiogenesis imaging and high-resolution ventilation imaging with hyperpolarized ^{129}Xenon gas are the main drivers for broader translational and clinical implementation.

This comprehensive imaging assessment is an asset when compared to CT, which is further complemented by the fact that MRI does not carry any exposure to ionizing radiation which makes it especially advantageous in children, young adults and for follow-up examinations either in disease surveillance or therapy monitoring.

In the meantime, CT has demonstrated a surprising development towards a complex quantitative imaging technology with a substantial increase of measureable variables. Progress in iterative image reconstruction, post-processing, registration algorithms as well as multi-energy, spectral CT and potentially photon counting CT are the current examples. Especially spectral and photo-counting CT will also induce a renaissance of research for CT contrast agents. The most obvious for pulmonary CT being inhaled Xenon gas for imaging of ventilation distribution and trapped air.

Clinical PET/CT of the lung is still mainly based on FDG as an indicator of increased glucose metabolism, especially in malignant disease. Current developments, however, focus more on specific probes targeting dedicated functions or receptors, e.g. in pulmonary inflammation.

Beyond the modality-driven radiological view onto the future direction of pulmonary functional and molecular imaging, the objectives and endpoints of imaging have to be revisited. It is no longer mainly on morphology, e.g. size, volume, shape and a single descriptor of tissue composition, but on function, metabolism and molecular interactions as well as on multilevel analysis of tissue composition.

Thus, future endpoints of pulmonary imaging might be:

1) Inflammation

Infectious inflammatory pulmonary diseases pose a major challenge to public health and healthcare systems worldwide. Although imaging is currently not in a pivotal role for the detection, characterization and treatment decision making, there is a clear unmet clinical need to improve these aspects, especially within the scope of new micro-organisms, pandemias, resistant strains, such as in mycobacteriosis, and opportunistic infections. Besides, the incidence of non-infectious inflammatory diseases is increasing and detection and characterization as well as quantitative disease surveillance and treatment monitoring are becoming increasingly important. Potential future directions will be:

- Differentiation between infectious and non-infectious inflammation
- Estimation of inflammatory activity in pneumonitis, such as pulmonary fibrosis, granulomatosis and pulmonary manifestations of collagen vascular disease
- Airway inflammation in chronic bronchitis, chronic obstructive pulmonary disease (COPD) and asthma
- Imaging cell trafficking
- Imaging pulmonary immune responses and inflammatory signaling events

2) Homeostasis and energy balance

Imaging of water and salt represents a potential novel field for imaging. It will focus on ions such as sodium, potassium, chlorine by dedicated MRI or even MRS techniques at ultrahigh fields. Another important aspect will be the definition of a methodology for measurements of transepithelial transport mechanisms, e.g. gas exchange, but also transport of liquid and mucus along the airway surfaces.

Energy balance imaging also comprises the visualization of the respiratory muscles during breathing, e.g. respiratory mechanics, and their metabolism.

3) Real-time visualization of lung function: "Watch the lungs work"

The concept from structural to functional imaging opens the new field of real-time imaging of lung function, such gas exchange, cell trafficking and airway clearance. These developments are on the way for preclinical applications especially using live cell imaging, optical imaging and video-microscopy, but also in the clinical arena as 4D CT and MRI of pulmonary motion become widely available. Among other techniques, these will include spectral CT and MRI approaches to measure ventilation distribution and ventilation/perfusion ratios using inhaled contrast agents, such as xenon gas; or multidirectional measurements of air and blood flow. Such investigations might be extended to imaging of the lung during pharmacological stress or exercise (treadmill).

4) Imaging tumor biology

Different features of tumor biology may be visualized by imaging. Fluorescent imaging of the airways and early detection of dysplastic and neoplastic cells are important tools for early detection as are different morphologic features of early cancers at CT: solid, semi-solid, non-solid. Characterization of tumor biology will also comprise imaging of tumor angiogenesis as currently available and apoptosis in the future.

5) Phenotyping and genotype correlation

In the future, radiology will be increasingly used for phenotyping disease subtypes, e.g. in airway disease such as COPD. Phenotyping will be an essential counterpart of genotyping and other read-outs from molecular medicine. These activities will pave the way for individualized therapies and concepts for active surveillance in the future.

Special Lecture 3-3

Future Direction of Respiratory Functional Imaging from Pulmonology Side -Terminal Air Space of X-ray CT Images in COPD-

Michiaki Mishima, M.D., Ph.D.
Department of Respiratory Medicine, Graduate School of Medicine, Kyoto University, Japan

1. Introduction

We have been engaged in the digital analysis of X-ray CT image. Nakano et al. reported that LAA% (percent ratio of low attenuation area to whole airway area) and WA% (percent ratio of airway wall area to whole airway area of rt. B1) could complementally explain the obstructive disorders of ventilation in COPD [1].

We now focus on the importance of the analysis of the terminal airspace detected by CT image. The role of "Distribution of terminal airspace" and "Comorbidity of emphysema" will be presented.

2. Distribution of terminal airspace.

Mishima et al. examined the statistical properties of LAA clusters in COPD patients and in healthy subjects [2]. In COPD patients, the percentage of the lung field occupied by LAAs (LAA%) ranged from 2.6 to 67.6. In contrast, LAA% was always <30% in healthy subjects. The cumulative size distribution of the LAA clusters followed a power law characterized by an exponent D (fractal dimension). They show that D is a measure of the complexity of the terminal airspace geometry. The COPD patients with normal LAA% had significantly smaller D values than the healthy subjects, and the D values did not correlate with pulmonary function tests except for the diffusing capacity of the lung. We interpret these results by using a large elastic spring network model and find that the neighboring smaller LAA clusters tend to coalesce and form larger clusters as the weak elastic fibers separating them break under tension. This process leaves LAA% unchanged whereas it decreases the number of small clusters and increases the number of large clusters, which results in a reduction in D similar to that observed in early emphysema patients. These findings suggest that D is a sensitive and powerful parameter for the detection of the terminal airspace enlargement that occurs in early emphysema.Seyama et al. found that the LAA distribution of LAM had poor fractal properties, and the mechanism of low attenuation formation in LAM may be quite different from that in emphysema.

Sato et al. applied the concept of fractal geometry to investigate the structural mechanism of the development of pulmonary emphysema in the klotho mouse, which, after milk feeding, exhibits characteristics resembling aging and develops emphysema [3]. They calculated the relationships between perimeter and size characterizing shape and between cumulative frequency and size of the terminal air spaces identified from histologic slides and found that both relations followed a power law with fractal properties. However, the fractal dimensions related to the shape and size (Dsn) in the klotho mice were significantly lower than in controls. Additionally, in the klotho mice, Dsn decreased with age without significant change in mean linear intercept. These abnormal morphological changes were restored when the klotho mice were fed with a vitamin D-deficient diet. Previously undescribed morphological model simulations showed that a random destruction, in which the destruction process occurs homogeneously in the lungs, was more consistent with the data than a correlated destruction that is usually seen in smoking-related human emphysema. These results suggest that the pathological changes in the lungs of the klotho mice are derived not from localized causes, but from systemic causes that are related to abnormal activation of vitamin D. The morphogenesis of emphysema in the klotho mice and morphological analyses using fractal geometry may contribute to the understanding of the progressive nature and cause of parenchymal destruction in human emphysema.

3. Comorbidity of emphysema:

COPD has recently been announced to be "a systemic disease". It is clinically important that COPD and comorbid diseases influence together on the condition and prognosis of the patients.

Emaciation has been known to be associated with COPD. Ogawa et al. evaluated emphysema using percentage of LAA% and airway by percentage wall area (WA%) [4]. Body mass index (BMI) was significantly lower in the higher LAA% phenotype. BMI correlated with LAA% but not with WA%. BMI was significantly lower in the emphysema dominant phenotype than in the airway dominant phenotype, while there was no difference in forced expiratory volume in 1 s %predicted between the two. These results support the concept of different COPD phenotypes and suggest that there may be different systemic manifestations of these phenotypes.

Osteoporosis is one of the important systemic features of COPD. However, the relationship between the extent of emphysema and reduced bone density has been unclear. Using CT images, the CT scan density of the thoracic and lumbar vertebrae (T4, T7, T10, and L1) and the LAA% were measured quantitatively, and their correlations were analyzed. Linear regression analyses revealed that LAA% had a significant negative correlation with bone mineral density (BMD). In addition, multiple regression analysis showed

that only LAA% and body mass index (BMI) were predictive of BMD among age, BMI, smoking index, FEV(1), arterial blood gas, and LAA%. These results suggested that COPD itself could be a risk factor for osteoporosis [5].

Haruna et al. analyzed the relationship between CT scan assessment and COPD mortality in patients with various stages of COPD [6]. Univariate Cox analysis revealed that emphysematous change as assessed by CT scan, lung function, age, or BMI were significantly correlated with mortality. Multivariate analysis revealed that emphysematous change as assessed by CT scan had the best association with mortality. They concluded that the emphysematous change as assessed by CT scan predicts respiratory mortality in outpatients with various stages of COPD.

4. Conclusion

Analysis of the distribution of terminal airspace using fractal analysis offers the information about the cause and process of the diseases. The emphysema has a tight relationship with the comorbidity. It is a key pathological change which prescribes the prognosis of COPD. "respiratory CT imaging" is always "respiratory functional imaging", and it plays an important role in the development of respiratory medicine.

References:

[1] Nakano Y, Sakai H, Muro S, Hirai T, et al. Computer tomographic measurements of airway dimensions and emphysema in smokers: Correlation with lung functions. Am J Respir Crit Care Med 102: 1052-1057, 2000.
[2] Mishima M, Hirai T, Itoh H, et al. Complexity of terminal airspace assessed by lung CT in normal subjects and patients with chronic obstructive pulmonary disease. Proc Natl Acad Sci USA 96: 8829-8834, 1999.
[3] Sato A, Hirai T, Imura A, Kita N, Iwano A, Muro S, Nabeshima Y, Suki B, Mishima M. Morphological mechanism of the development of pulmonary emphysema in klotho mice. Proc Natl Acad Sci USA 104(7):2361-5, 2007.
[4] Ogawa E, Nakano Y, Ohara T, et al. Body mass index in male patients with COPD: correlation with low attenuation areas on CT. Thorax 64(1):20-5, 2009.
[5] Ohara T, Hirai T, Muro S, et al. Relationship between pulmonary emphysema and osteoporosis assessed by CT in patients with COPD. Chest 134(6): 1244-9, 2008.
[6] Haruna A, Muro S, Nakano Y, et al. CT scan findings of emphysema predict mortality in COPD. Chest 138(3):635-40, 2010.

Abstract

Luncheon Lecture

Luncheon Lecture 1 - 1

Functional Thoracic CT for Pediatric Patients

Hyun Woo Goo, M.D.
Department of Radiology and Research Institute of Radiology
Asan Medical Center, University of Ulsan College of Medicine, Korea

Recent technical developments of multi-slice CT characterized by faster speed and longer coverage facilitate functional thoracic CT evaluation in children by reducing motion artifacts. Changes in lung density and airway caliber throughout the respiratory cycle have been used for the detection of air trapping and tracheobronchomalacia, respectively. Paired end-inspiratory and end-expiratory CT is used for cooperative patients, whereas free-breathing cine-CT that needs only sedation without any respiratory maneuvers or general anesthesia is a useful alternative for uncooperative patients. Dynamic expiratory CT increases sensitivity in detecting tracheobronchomalacia in cooperative patients. Because of longer coverage, 4D analysis of airways puts to our clinical practice. New respiratory-triggered CT acquisition of the whole lung with non-rigid 3D registration enables us to produce density difference map and perform quantitative analysis. Dual-energy CT opens up a new horizon for the qualitative and quantitative evaluation of lung perfusion and lung ventilation. Of interest, collateral ventilation can be visualized and quantified with dynamic xenon-enhanced dual-energy lung ventilation CT. This experience paradoxically underscores the importance of lung anatomy by recognizing that the incomplete and accessory fissures substantially influence regional lung ventilation. In addition to the separate use of lung perfusion or lung ventilation CT, these two emerging methods can be used together like V/Q scan. This combined evaluation is particularly useful for the evaluation of pulmonary embolism. We, pediatric imagers, should keep in mind that clinical benefits should outweigh radiation risks of functional thoracic CT. Therefore, we should try every effort to minimize CT radiation dose.

Luncheon Lecture 1 - 2

Pediatric Applications of Lung MRI

Talissa A. Altes, M.D.
Associate Professor, Section Head Pediatric Radiology, and Vice Chair of Research
Department of Radiology, University of Virginia Medical Center, USA

Lung disease, including asthma, cystic fibrosis and bronchopulmonary dysplasia, is the most common chronic disorder of childhood. However, the assessment of the severity of lung disease can be difficult in the pediatric population. Young children are typically unable to perform the breathing maneuvers required to perform spirometry, the most commonly used method to assess lung function in adults. CT, which provides detailed images of lung structure, exposes the patient to relatively high doses of ionizing radiation. Children are at greater risk of developing a radiation induced malignancy than adults because children are inherently more radiation sensitive (more rapidly dividing cells) and typically have a long life expectancy following the exposure in which to develop a radiation induced malignancy. Thus the role of CT in pediatric lung disease is limited. MRI, which is thought to be very low risk, has the potential to have an important role in the assessment of pediatric lung disease.

Conventional proton MRI in the absence of inhaled or intravenous contrast currently has a limited role in the assessment of lung disease due to the relatively low proton density of the lung. There have been a few studies assessing the utility of proton MRI in cystic fibrosis (CF), essentially as a substitute for CT, to detect lung structural changes such as bronchiectasis, mucus plugging, and consolidation. Not surprisingly, CT has better image quality but important structural alterations can be detected with MRI. Further, there are techniques under development, such as ultra-short TE and Fourier decomposition, which have the potential to greatly increase the type of information about the lung that can be obtained with proton MRI.

Hyperpolarized noble gases (helium-3 and xenon-129) are used as inhaled gaseous contrast agents for MRI, and provide high temporal and spatial resolution images of the lungs. Most of the human imaging with hyperpolarized gas has employed helium-3 as the contrast agent. In the past few years, the available supply of helium-3 has decreased dramatically due to a spike in demand for helium-3 for use in neutron detectors. This coupled with recent advances in xenon polarization technology makes xenon-129 an attractive alternative to helium-3. Since little work has been done in pediatric lungs diseases with xenon-129, the following discussion will be focused on results obtained with helium-3. However, there is every reason to believe similar results could be obtained with xenon-129.

Images of lung ventilation can be obtained by performing spin density imaging during a breath hold following the inhalation of hyperpolarized gas. Areas of the lung that are well ventilated appear bright on the MR images and those that are poorly ventilated appear dark. Asthmatics have more ventilation defects, that is more poorly ventilated regions with their lungs, than healthy subjects. Further there is a moderate correlation between the number of ventilation defects and asthma severity as measured by spirometry or the frequency of symptoms. However the correlation is imperfect with some asthmatics having many ventilation defects but few symptoms and vise versa. Hyperpolarized helium-3 MRI gas has yielded a new insight into the pathophysiology of asthma, that the distribution of ventilation abnormalities in the lung is not random as would be expected if the whole lung was equally affected. Instead, some regions of the lung are more likely to appear abnormal on ventilation imaging than others, suggesting the severity of asthma within the lung varies regionally. This may have important implications for regional treatments such as bronchial thermoplasty in which the airway wall smooth muscle is RF ablated during bronchoscopy. Since asthma is not randomly distributed throughout the lung, it is possible that better results with this treatment will be obtained if imaging is used to guide the procedure.

Hyperpolarized helium-3 MR ventilation defects are also found in patients with CF, even those with normal spirometry. Similar to the results in asthma, there is some correlation between the number of ventilation defects and CF disease severity on spirometry. The number of ventilation defects has been shown to change with treatment including mechanical airway clearance, bronchodilator, and intensive antibiotic treatment. However, both mechanical airway clearance and intensive antibiotic treatment have been shown to increase rather than decrease the number of ventilation defects is some CF patients. The reason for this somewhat paradoxical response is not yet known but is certainly an interesting avenue for further research.

Diffusion imaging with hyperpolarized gas MRI provides information about the size and connectedness of the alveoli. In adults with COPD and in animal models of emphysema, the hyperpolarized gas apparent

diffusion coefficient (ADC) has been shown to correlate with disease severity in humans and alveolar size in animals. Bronchopulmonary dysplasia is a chronic lung disease that occurs in children with a history of premature birth and is also known as chronic lung disease of prematurity. Initially, this lung disease was thought to be the result of lung damage from the oxygen concentrations and high pressure ventilation used in the perinatal period to achieve adequate oxygenation in infants with very immature lungs. Improvements in the treatment of premature infants have decreased the mortality from lung disease but have not decreased the incidence of BPD. Most of alveolar development occurs during 25 to 40 weeks post conception and during the first few years of life. It is now thought that in addition to direct lung injury, in some premature infants something occurs that alters the development of the alveoli resulting in lung with too few alveoli that are too large in size. This has been confirmed in a study with hyperpolarized helium-3 diffusion imaging in which children with a history of BPD had an elevated ADC but similar to smaller lung volumes as compared with age matched healthy children.

In conclusion, MRI of the lung is already yielding new insights into pediatric lung diseases and has the potential to be a clinically useful tool in the assessment and treatment of children with lung disease.

Luncheon Lecture 2-1

CT Assessment of Asthma

Gregory G. King, MB chB, FRACP, Ph.D.
The Woolcock Institute of Medical Research, Australia

Asthma is a common disease that comprises a large burden of disease in many countries. In Australia, it occurs in 10% of adults and 20% of children, a prevalence that has been stable for approximately 15 years[1]. Asthma is a highly heterogeneous disease and may in fact be a cluster of distinct pathophysiogical entities, which may be the basis of the so-called asthma 'phenotypes'. The difficulty in better characterising asthma is that there are few tools that can distinguish clinically important differences in pathophysiology. However, Computed Tomography (CT) is a tool that has been able provide useful information with which to characterise the pathophysiology of asthma and as such, has provided a large amount of important information with which asthma can be characterised[2-11].

Computed Tomography provides structural information of the airways and lung parenchyma. The majority of CT studies have involved measurement of airway dimensions and of airway narrowing. Airway wall dimensions are difficult technically because of the thinness of the airway walls in relation to CT resolution and the variability of measurements is a limitation. Therefore, high-resolution technique is required to enable detection of the wall boundaries. To this end, both axial scanning and thin-slice helical scanning have been used. Despite the limitations of the measurements, results of studies have clearly and consistently shown asthmatic airway walls to be thicker compared with the wall thickness in COPD and with controls. This is in keeping with the findings from morphometric studies of post mortem lungs which show that asthma is characterised by marked airway wall thickening of small and large airways. Furthermore, wall thickening has been related directly to asthma severity[12], airway hyperresponsiveness[6] and response to inhaled steroid treatment[5].

Acute airway narrowing induced by bronchial challenge has also been measured using thin-slice CT[13-16]. Since subjects are required to move between the baseline scans and post-challenge scans to allow the challenge test to be done, the added technical complexity is an added source of measurement variation. Nevertheless, important insights can be gained from knowledge of the distribution of airway narrowing which has implications for the understanding of the pathophysiologic basis of airway hyperresponsiveness.

The combination of CT with functional measures has been used and will likely be the way forward in the study of asthma[17-19]. Functional imaging provides data on regional ventilation in asthma. The pattern of ventilation disruption is relevant because it is apparent that both airway closure and heterogeneity of ventilation are relevant to asthma, potentially from both mechanistic and clinical expression points of view. CT does have the ability to provide some functional information, i.e. on ventilation and gas trapping. How functional information from different modalities compare with CT and to what extent they are complementary are still to be undetermined.

References:

1. Monitoring ACfA. Asthma in Australia 2008. AIHW Asthma Series. Canberra: AIHW, 2008.
2. Jain N, Covar RA, Gleason MC, Newell JD, Jr., Gelfand EW, Spahn JD. Quantitative computed tomography detects peripheral airway disease in asthmatic children. Pediatric Pulmonology 2005; 40:211-8.
3. Kasahara K, Shiba K, Ozawa T, Okuda K, Adachi M. Correlation between the bronchial subepithelial layer and whole airway wall thickness in patients with asthma. Thorax 2002; 57:242-6.
4. Niimi A, Matsumoto H, Amitani R, Nakano Y, Mishima M, Minakuchi M, et al. Airway Wall Thickness in Asthma Assessed by Computed Tomography . Relation to Clinical Indices. Am. J. Respir. Crit. Care Med. 2000; 162:1518-23.
5. Niimi A, Matsumoto H, Amitani R, Nakano Y, Sakai H, Takemura M, et al. Effect of short-term treatment with inhaled corticosteroid on airway wall thickening in asthma. The American Journal of Medicine 2004; 116:725-31.
6. Niimi A, Matsumoto H, Takemura M, Ueda T, Chin K, Mishima M. Relationship of Airway Wall Thickness to Airway Sensitivity and Airway Reactivity in Asthma. Am. J. Respir. Crit. Care Med. 2003; 168:983-8.
7. King G, Müller N, Paré P. Evaluation of airways in obstructive lung disease using High-Resolution CT. Am J Respir Crit Care Med 1999; 159:992-1004.
8. Lee Y-M, Park J-S, Hwang J-H, Park S-W, Uh S-t, Kim Y-H, et al. High-Resolution CT Findings in Patients With Near-Fatal Asthma: Comparison of Patients With Mild-to-Severe Asthma and Normal

Control Subjects and Changes in Airway Abnormalities Following Steroid Treatment. Chest 2004; 126:1840-8.
9. Matsumoto H, Niimi A, Takemura M, Ueda T, Minakuchi M, Tabuena R, et al. Relationship of airway wall thickening to an imbalance between matrix metalloproteinase-9 and its inhibitor in asthma. Thorax 2005; 60:277-81.
10. Aysola RS, Hoffman EA, Gierada D, Wenzel S, Cook-Granroth J, Tarsi J, et al. Airway Remodeling Measured by Multidetector CT Is Increased in Severe Asthma and Correlates With Pathology. Chest 2008; 134:1183-91.
11. Coxson HO, Quiney B, Sin DD, Xing L, McWilliams AM, Mayo JR, et al. Airway Wall Thickness Assessed Using Computed Tomography and Optical Coherence Tomography. Am. J. Respir. Crit. Care Med. 2008; 177:1201-6.
12. Awadh N, Müller NL, Park CS, Abboud RT, Fitzgerald JM. Airway wall thickness in patients with near fatal asthma and control groups: assessment with high resolution computed tomographic scanning. Thorax 1998; 53:248-53.
13. Brown RH, Scichilone N, Mudge B, Diemer FB, Permutt S, Togias A. High-Resolution Computed Tomographic Evaluation of Airway Distensibility and the Effects of Lung Inflation on Airway Caliber in Healthy Subjects and Individuals with Asthma. Am. J. Respir. Crit. Care Med. 2001; 163:994-1001.
14. Okazawa M, Müller NL, McNamara AE, Child S, Verburgt L, Paré PD. Human airway narrowing measured using high resolution computed tomography. Am J Respir Crit Care Med 1996; 154:1557-62.
15. King GG, Carroll JD, Muller NL, Whittall KP, Gao M, Nakano Y, et al. Heterogeneity of narrowing in normal and asthmatic airways measured by HRCT. Eur Respir J 2004; 24:211-8.
16. Brown RH, Croisille P, Mudge B, Diemer FB, Permutt S, Togias A. Airway Narrowing in Healthy Humans Inhaling Methacholine without Deep Inspirations Demonstrated by HRCT. Am J Resp Crit Care Med 2000; 161:1256-63.
17. Fain SB, Gonzalez-Fernandez G, Peterson ET, Evans MD, Sorkness RL, Jarjour NN, et al. Evaluation of Structure-Function Relationships in Asthma using Multidetector CT and Hyperpolarized He-3 MRI. Academic Radiology 2008; 15:753-62.
18. Fain SB, Peterson ET, Sorkness RL, Wenzel S, Castro M, Busse WW. Severe Asthma Research Program - Phenotyping and Quantification of Severe Asthma. Imaging Decisions MRI 2009; 13:24-7.
19. Walsh C, Harris B, Bailey D, Salome C, Berend N, Downie S, et al. Ventilation heterogeneity measured by single photon emission computed tomography/Computed Tomography (SPECT/CT) and multiple breath nitrogen washout (MBNW) in asthma. TSANZ: Respirology, 2008:A20.

Luncheon Lecture 2-2

Hyperpolarized Noble Gas MRI for Asthma and COPD

Mitchell S. Albert
Department of Radiology, University of Massachusetts Medical School, USA

Introduction

Lung diseases, including asthma and COPD, cause high morbidity and mortality, and immense economic expenditures. A component of effective diagnosis and management of chronic lung diseases is testing pulmonary structure and function. However, existing clinical tests—including radiography and high resolution CT, which both utilize ionizing radiation; conventional MRI, which sometimes employs chemical contrast agents; and global spirometry measurements taken at the mouth, which provide no regional information on lung function—all have serous limitations. An innovative MRI technology for lung imaging, hyperpolarized (HP) gas MRI, overcomes many of the limitations of these other modalities, and it offers an extremely promising complimentary tool for diagnosis, disease staging, and treatment evaluation for asthma and COPD.

HP gas MRI, which was pioneered in the 1990s (Albert et al. 1994), can elucidate structure and function previously undetectable with radiography or conventional MRI, and it uses no ionizing radiation or chemical contrasts agents, making it non-invasive and safe. This safety is particularly important for imaging asthmatics, because asthma disproportionately affects children, in whom exposure to radiation should be minimized. HP gas MRI also allows physicians to safely monitor how defects in ventilation progress over time, and how effectively specific treatments work over time.

Conventional MRI detects protons in water in tissues; HP gas MRI, on the other hand, detects atoms of ^{3}He or ^{129}Xe gas that are inhaled by the subject. Protons are rare in the airways and alveoli of the lungs, and thus conventional MRI of pulmonary ventilation is not viable. Although ^{3}He and ^{129}Xe are normally below the detection threshold for MRI, when these atoms are hyperpolarized through spin exchange with rubidium that has been optically excited by a diode laser, their detection increases about 100,000 times! With inhalation of HP ^{3}He or ^{129}Xe, high-resolution HP MR imaging of the lung airways and periphery is possible, providing a complete picture of lung ventilation with spectacular detail.

HP ^{3}He MRI provides images of the lungs far superior to conventional MRI. Figure 1 compares conventional MRI with HP ^{3}He MRI. Note the high level of detail in the ^{3}He MR images. Also note that the ^{3}He MR images clearly show differences in ventilation between the healthy (top right) and asthmatic (bottom right) subjects. Areas where gas is not reaching (known as ventilation defects) can be seen as dark areas in the image of the asthmatic subject on bottom right. This technique precisely pinpoints where gas is reaching and where it is not reaching, something other measurement modalities cannot do.

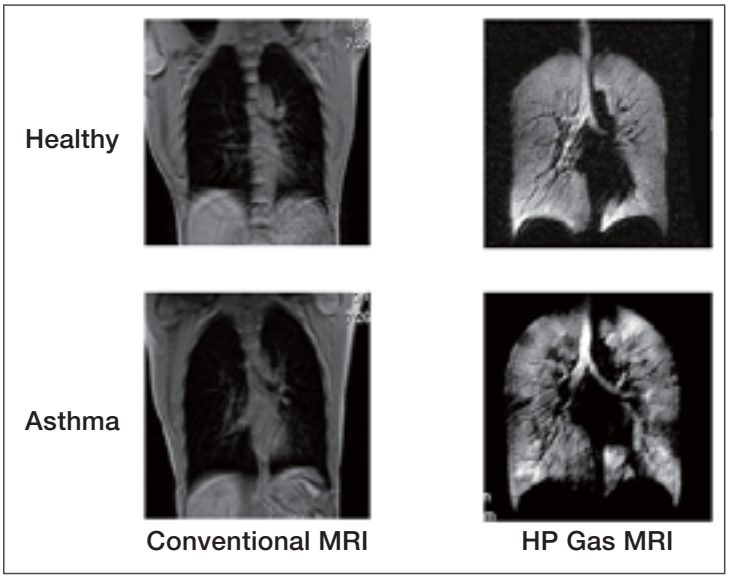

Figure 1. Conventional proton MRI compared with HP ^{3}He MRI.

HP Gas MR Imaging of Asthma

The most commonly employed tools to assess lung function in patients with asthma are spirometry measures of global airflow and resistance. Because of its sensitivity, HP gas MRI can detect asthma at earlier stages, allowing treatment to be provided earlier, thus reducing the loss of lung function from which many asthmatics suffer (Altes et al. 2001). HP gas MRI is also totally changing the way we view asthma. The existing paradigm has been that some asthmatics have reversible obstruction, while others go on to develop fixed obstruction. However, HP ^{3}He MRI studies suggest that asthmatics may have fixed obstruction in some lung regions much earlier in the course of their disease than earlier believed, and that disruption of airflow in asthmatics is regional, not diffuse.

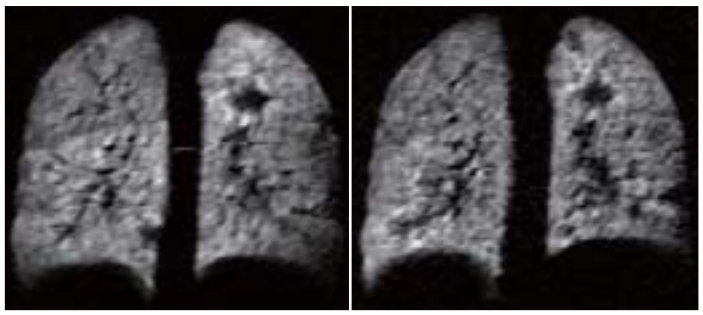

Figure 2. HP ^{3}He MRI images of a mild-moderate asthmatic subject. Ventilation defects can be seen as dark spots.

HP gas MRI investigations have established that ventilation defects in asthmatics can persist for long periods in the same location. Figure 2 illustrates data from our group showing defects that persisted for over two months at baseline in a mild-moderate asthmatic. Note that pronounced defects (dark areas) persist between the scans. de Lange et al. (2007) gave 10 asthmatics a methacholine challenge to create bronchoconstriction, and then gave a second methacholine challenge a mean of 185 days later. Sixty nine percent of ventilation defects were in the same locations during both challenges. de Lange et al. (2009) found, in a study of 43 asthmatics, that 67% of defects persisted from the first baseline measurement to the second over a median interval of 41 days, and 38% of defects persisted from the first baseline measurement to the third over a median interval of 85 days.

Similarly, we looked at the number of defects that remained in the same location, and how they changed in size, over about 45 days at baseline and following administration of methacholine (Sun et al. 2010). We found that the total number of ventilation defects increased post-methacholine, as predicted, and that defects were found to be much more consistent in location during methacholine challenges than at baseline. (Post-methacholine, 96% remained in the same location between Day 1 and Day 2, whereas at baseline, only 75% of ventilation defects remained in the same location.) Data from all of these studies support the hypothesis that respiratory dysfunction in asthma has an important localized component.

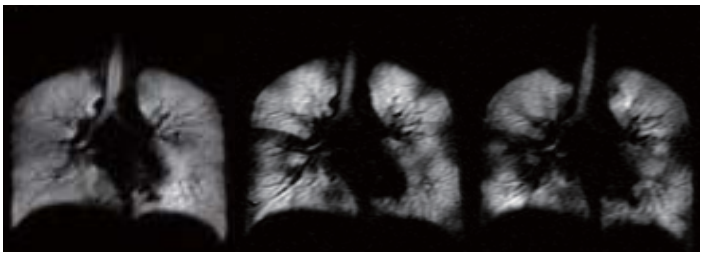

Figure 3. HP ^{3}He MR images of a mild-moderate asthmatic subject at baseline and following methacholine (Mch) challenges.

Several studies have also shown that HP gas MRI measures positively correlate with asthma severity. Altes et al. (2001) found that defect number generally correlated with severity of asthma symptoms. We observed that HP gas MRI ventilation heterogeneity and ventilation defect volume correlated with asthma severity (Sun et al. 2009). Similarly, de Lange et al. (2006) observed that the number of defects was greater in patients with moderate and severe asthma than in patients with mild asthma. de Lange et al. (2006) also reported that many asthmatics with ventilation defects had normal spirometry readings (except for forced expiratory flow between 25% and 75% from the beginning of forced vital capacity); this provides dramatic evidence that HP gas MRI can detect ventilation impairment undetectable with traditional measurements, an invaluable clinical capability.

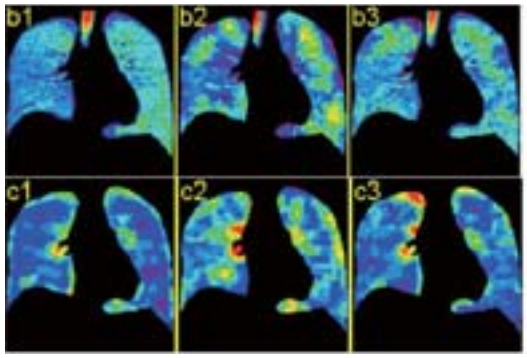

Figure 4. Ventilation maps (b1–b3) and heterogeneity maps (c1–c3) in a healthy subject. b1 & c1 = pre-methacholine challenge; b2 & c2 = post-methacholine challenge; and b3 & c3 = post deep inhalations.

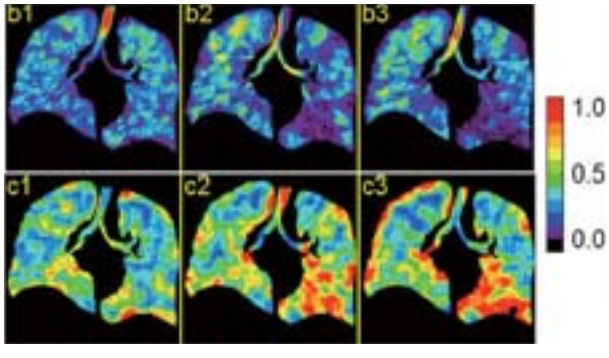

Figure 5. Ventilation maps (b1–b3) and heterogeneity maps (c1–c3) in an asthmatic subject. b1 & c1 = pre-methacholine challenge; b2 & c2 = post-methacholine challenge; and b3 & c3 = post deep inhalations.

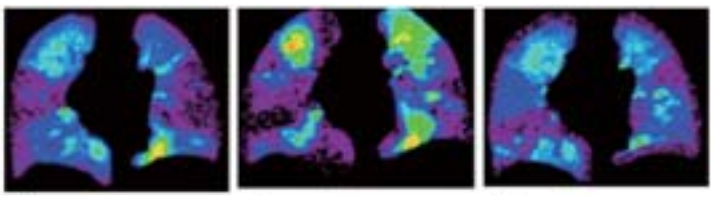

Figure 6. ^{3}He MRI color-coded ventilation maps from a subject with severe asthma. A = pre-methacholine challenge; B = post-methacholine challenge; C = post-albuterol administration.

An important area of ongoing improvement in HP gas MR imaging is increasing quantification of signal characteristics. We have developed advanced techniques to quantify ventilation distribution and heterogeneity throughout ^{3}He MR images (Tzeng et al. 2009). Figures 4 and 5 show ventilation maps and heterogeneity maps pre-methacholine, post-methacholine, and post-deep inhalations. In ventilation maps, colors represent ventilation levels relative to the maximum ^{3}He per pixel (1.0) as seen in the trachea; in heterogeneity maps, the color represents an index associated with the coefficient of variation in ventilation levels for a region of interest around a given pixel. We found that in healthy subjects (Figure 4), ventilation heterogeneity appeared after the methacholine challenge, but was resolved by deep inhalations. In asthmatic subjects (Figure 5), ventilation heterogeneity appeared after the methacholine challenge, but was not resolved by deep inhalations.

Another important quantitative advance we reported was providing information about the percent ventilation in specific regions (Tzeng et al. 2009). Previous studies used only visual inspection to classify regions as defects, assuming that ventilation in a given region was either 100% ventilated or 100% unventilated. We now know that ventilation is not an either-or phenomenon—it varies along a continuum, and thus it is essential to provide spatial quantification of ventilation. Our group developed a technique to estimate the percentage volume occupied by fresh gas in each voxel of the lungs, providing greatly improved accuracy in estimating ventilation.

We also used dynamic ^{3}He MRI to differentiate small ventilation defects (closure of only one terminal airway) from clustered defects (closure of two or more terminal airways). We measured 751 ventilation defects and found that 390 were small and 361 were clustered (Mullally et al. 2009). In addition, whereas previous studies used only visual inspection to classify defect location, we developed a technique to quantify ventilation defect location, a significant advance for the field of HP gas MRI.

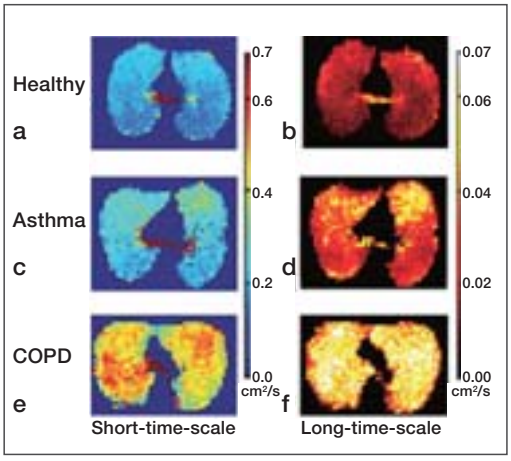

Figure 7. ^{3}He apparent diffusion coefficient (ADC) images (from Wang et al. 2008). Note the dramatic differences between the ADC images of healthy and COPD subjects at both short and long time scales.

A significant new direction in pulmonary imaging is using HP gas MRI to assess the physiological effects of pulmonary therapeutics. We have investigated the efficacy of several medicines for treating patients with lung disease. Figure 6 illustrates the power of HP gas MRI in detecting improvement in ventilation following administration of albuterol, a short-acting, beta$_2$ adrenergic agonist commonly used for treatment of asthma and COPD. This figure shows ^{3}He MRI color-coded ventilation scans of a severe asthmatic at baseline (A), following bronchoconstriction induced by methacholine (B), and following administration of albuterol (C). Ventilation defects were increased by methacholine, and then reversed by albuterol.

HP Gas MR Imaging of COPD

Because it supplies high-resolution functional imaging, HP gas MRI has also been productively applied to the study of COPD. A lot of recent HP gas MRI work on COPD is using apparent diffusion coefficient (ADC) measures (see Fain et al. 2007; Hopkins et al. 2007). Examples of ADC images of healthy, asthmatic, and COPD subjects are shown in Figure 7. The ADC in COPD patients is higher than normal because of the destruction of the alveolar walls that has created larger airspaces. HP gas MRI ADC measures of pulmonary function in COPD patients has been observed to be reproducible (Salerno et al. 2002; Altes et al. 2004; Morbach et al. 2005), to be very sensitive in detecting micro-structural changes (Saam et al. 2000; Salerno et al. 2002), and to be possibly more sensitive than high resolution CT (Salerno et al. 2003; Fain et al. 2006).

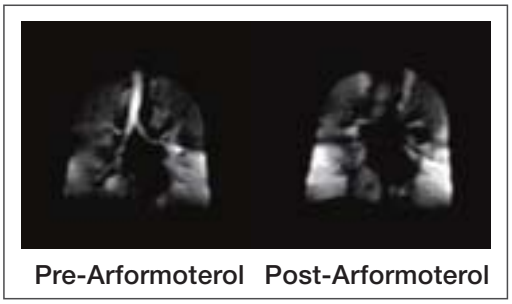

Figure 8. HP ^{3}He MR images of a subject before (left) and after (right) receiving arformoterol.

As with asthma, one of HP gas MRI's most valuable capabilities is the information it provides on lung function before and after therapy. We performed HP ^{3}He MR imaging on patients with COPD to assess the effects of arformoterol tartrate on ventilation function. Arformoterol is a long-acting, beta2 adrenergic agonist bronchodilator. We observed qualitative increases in ventilation in the lower half of the lungs in some subjects receiving arformoterol (see Figure 8). This illustrates how useful HP gas MRI can be in assessing the effect of drug administration on regional lung ventilation function.

Future Directions in HP gas MR Imaging

The future for HP gas MRI is exciting, with the prospect of wide adoption and increased translation to clinical applications. One new direction in HP gas MRI is further development of low-field MR scanners, which could have wide applications in instances where portability and/or low cost are essential. Another noteworthy new direction is a transition from ^{3}He to ^{129}Xe. Xenon offers many advantages over helium: (1) it is cheaper and more widely available; (2) it can measure lung ventilation like helium, but because it readily dissolves in the blood, it can also be used as a perfusion tracer; (3) it is lipid soluble, making it ideal for imaging lipid-rich organs like the brain. Xenon is also heavier than helium, so it has a lower diffusion value. We look forward to seeing HP gas MRI help improve the lives of countless people with chronic pulmonary diseases.

References:

- Albert MS, Cates GD, Driehuys B, Happer W, Saam B, Springer CS Jr, Wishnia A. Biological magnetic resonance imaging using laser-polarized ^{129}Xe. Nature. 1994 Jul 21;370(6486):199-201.
- Altes TA, Powers PL, Knight-Scott J, Rakes G, Platts-Mills TA, de Lange EE, Alford BA, Mugler JP 3rd, Brookeman JR. Hyperpolarized ^{3}He MR lung ventilation imaging in asthmatics: preliminary findings. J Magn Reson Imaging. 2001 13(3): 378–84.
- Altes T, Zhang H, Salerno M, Brookeman J, de Lange EE, Mugler JP 3rd. Repeatability of the hyperpolarized helium-3 apparent diffusion coefficient. In: Proceedings of the 90th Scientific Assembly and Annual Meeting of the Radiological Society of North America (RSNA), Chicago, IL, USA, 2004. p 515.
- de Lange EE, Altes TA, Patrie JT, Gaare JD, Knake JJ, Mugler JP 3rd, Platts-Mills TA. Evaluation of asthma with hyperpolarized helium-3 MRI: correlation with clinical severity and spirometry. Chest. 2006 130(4): 1055–62.
- de Lange EE, Altes TA, Patrie JT, Parmar J, Brookeman JR, Mugler JP 3rd, Platts-Mills TA. The variability of regional airflow obstruction within the lungs of patients with asthma: assessment with hyperpolarized helium-3 magnetic resonance imaging. J Allergy Clin Immunol. 2007 119(5): 1072–8.
- de Lange EE, Altes TA, Patrie JT, Battiston JJ, Juersivich AP, Mugler JP 3rd, Platts-Mills TA.Changes in regional airflow obstruction over time in the lungs of patients with asthma: evaluation with ^{3}He MR imaging. Radiology. 2009 Feb;250(2):567-75.
- Fain SB, Panth SR, Evans MD, et al. ^{3}He MRI detects early emphysematous changes in asymptomatic smokers. Radiology 2006;239:875-883.
- Fain SB, Korosec FR, Holmes JH, O'Halloran R, Sorkness RL, Grist TM. Functional lung imaging using hyperpolarized gas MRI. J Magn Reson Imaging. 2007 May;25(5):910-23.
- Hopkins SR, Levin DL, Emami K, Kadlecek S, Yu J, Ishii M, Rizi RR. Advances in magnetic resonance imaging of lung physiology. J Appl Physiol. 2007 Mar;102(3):1244-54. Epub 2006 Dec 7.
- Morbach AE, Gast KK, Schmiedeskamp J, et al. Diffusionweighted MRI of the lung with hyperpolarized helium-3: a study of reproducibility. J Magn Reson Imaging 2005;21:765-774.
- Mullally W, Betke M, Albert M, Lutchen K. Explaining clustered ventilation defects via a minimal number of airway closure locations. Ann Biomed Eng. 2009 Feb;37(2):286-300.
- Saam B, Yablonskiy D, Kodibagkar V, et al. MR imaging of diffusion of ^{3}He gas in healthy and diseased lungs. Magn Reson Med 2000;44:174-179.
- Salerno M, de Lange EE, Altes T, Truwit J, Brookeman J, Mugler. JP 3rd. Emphysema: hyperpolarized helium-3 diffusion MR imaging of the lungs compared with spirometric indexes—initial experience. Radiology 2002;222:252–260.
- Salerno M, Mugler JP 3rd, de Lange EE, Brookeman J, Altes T. Detection of early smoking related lung diseases with diffusion-weighted hyperpolarized helium-3 MR lung imaging. In: Proceedings of the 89th Scientific Assembly and Annual Meeting of the Radiological Society of North America (RSNA), Chicago, IL, USA, 2003. p. 526.
- Sun Y, Tan T, Zhalehdoust-Sani S, Tzeng YS, Lutchen K, and Albert MS, Hyperpolarized ^{3}He MRI Heterogeneity and Ventilation Defect Volume Correlates with Asthma Severity, The Seventeenth Annual Meeting of the International Society of Magnetic Resonance in Medicine, Honolulu, Hawaii, 2009.
- Sun Y, Shi L, Jin G, Reno A, Zhalehdoust-Sani S, Krinzman SJ, Liu J, Lutchen KR, Madison JM, Albert MS, Assessing the Persistence of Ventilation Defects in Asthmatics at Baseline and Following Methacholine Challenge Using Hyperpolarized ^{3}He MRI, Proceedings of the Eighteenth Annual Meeting of the International Society of Magnetic Resonance in Medicine, Stockholm, Sweden, 2010.
- Tzeng YS, Lutchen K, Albert M. The difference in ventilation heterogeneity between asthmatic and healthy subjects quantified using hyperpolarized ^{3}He MRI. J Appl Physiol. 2009 Mar;106(3):813-22.
- Wang C, Altes TA, Mugler JP 3rd, Miller GW, Ruppert K, Mata JF, Cates GD Jr, Borish L, de Lange EE. Assessment of the lung microstructure in patients with asthma using hyperpolarized ^{3}He diffusion MRI at two time scales: comparison with healthy subjects and patients with COPD. J Magn Reson Imaging. 2008 Jul;28(1):80-8.

Luncheon Lecture 3-1

Development of Polarizer for Future Clinical Works

F. William Hersman[1,2], Iulian C. Ruset[2,1], Jan Distelbrink[2], Isabel Dregely[1], Steve Ketel[2], Jeff Ketel[2], David Watt[2], Talissa A. Altes[3], G. Wilson Miller[3], Jaime Mata[3], John P. Mugler Ⅲ[3], Kai Ruppert[3]

1. Department of Physics, University of New Hampshire, Durham, USA
2. Xemed LLC, Durham, USA
3. Department of Radiology, University of Virginia, Charlottesville, USA

Over a period of fourteen years, the University of New Hampshire hyperpolarized gas academic group has been dedicated to improving technologies and methodologies for producing hyperpolarized 129-Xenon (HXe) [1-8] and acquiring high-quality images of pulmonary function [9-20]. Several technical obstacles to producing large quantities of highly polarized xenon were overcome with innovative developments. Our initial contribution was to recognize that significant improvement can be realized by pre-saturating the xenon and buffer gases with alkali vapor, then flowing the mixed gases through a long polarization cell opposite to the direction of laser propagation, and finally extracting the alkali vapor on a cold surface in the same cell in the presence of the laser. This three step process allowed beneficial utilization of the full polarizing power of the laser while simultaneously avoiding destructive non-linear thermal runaways. Our second contribution was devising a rising-dewar method for distributing the cryogenic extraction of polarized xenon from the gas mixture and subsequent thawing without losing polarization. Our third contribution was a stepped-mirror optical system to create multi-kilowatt, highly directional, spectrally narrowed laser beams for optical pumping. Our fourth contribution was demonstrating a finned-channel copper enclosure to efficiently polarize xenon in the presence of such intense laser beams while efficiently extracting the deposited heat. These four innovations combined to allow assembly and operation of xenon polarizers with productivity that exceeded earlier technologies by a factor of one hundred.

The first of our xenon polarizer prototypes, completed in 2004 at UNH, incorporated the first two of these innovations [2]. This prototype yielded a liter of 50% polarized xenon, sufficient to initiate human studies. At that time in 2004 we also founded a spin-off company Xemed to undertake development of additional polarizer prototypes. A second polarizer prototype built by UNH and Xemed together integrated the capability we had already demonstrated into a compact, partially automated package [1].

The third generation, "Einstein", was implemented with two 12 bar stacks of 100W diodes and a copper polarizing column [3]. Although capable of free-running power of 2400W, we designed the laser for spectrally narrowed operation at 1400W. An afocal telescope with two converging lenses and magnification of four produces an image of the emitter bars on a grating in Littrow configuration [4]. Path lengths between off-axis bars and the angled grating are corrected using the step-mirror, allowing a perfect focus for all emitters [7]. The zeroth order beam is transported to the polarizing cell via another afocal pair, with cylindrical lenses providing different horizontal and vertical magnifications. The collimated beam is reconfigured using periscopes to match the square format of the polarizing cell. Flow of gases undergoing kilowatt heating will not be stable without effective heat removal. Cylindrical glass cells are insufficient for the task. We implemented a copper polarization cell with an internal finned structure to provide a factor four increase in heat removal surface area [8]. Because the directionality of the lasers is very high, the polarization can be performed in sixteen narrow long channels. The polarization cell is configured with two thermal zones along its length. As the gas flows through the warmer section, it interacts with the laser and increases its polarization. After reaching a polarization maximum, the gas moves into the cooler region where it loses its rubidium. With a high power laser and finned copper polarization cell, Einstein is capable of producing several liters of hyperpolarized xenon in twenty minutes.

During four months in the fall of 2009, we tested the clinical utility of this third generation xenon polarizer prototype at the University of Virginia. For these measurements we assembled a 32-element parallel receive coil and mated it to a highly-uniform birdcage transmit coil with an asymmetric shape to fit into the 3T Siemens scanner [9]. Six hundred measurements were performed on 64 subjects, including healthy volunteers and patients with COPD, asthma, and cystic fibrosis. Roughly a dozen imaging protocols were demonstrated, some for the first time. We acquired ventilation images with resolution in the range 2mm to 3mm within a ten second breath hold using GRAPPA acceleration [10, 11]. We studied diffusion weighted imaging at short and long distance scales in lungs of COPD patents [12]. Image sets with a breath hold were used to determine xenon T1 longitudinal relaxation in order to map regional variations in alveolar oxygen partial pressure [13]. In addition to these gas-phase protocols, a

versatile suite of imaging protocols was developed to interrogate the xenon dissolved phase [14-18]. The Xenon magnetization Transfer Contrast (XTC) protocol senses xenon exchange between the gas and dissolved phase by repeatedly quenching the dissolved phase and imaging the changes in the gas phase polarization [21]. We studied the XTC protocol for various choices of frequency range of the dissolved xenon, allowing us to isolate xenon exchanging between alveolar gas and red blood cells [14, 15]. We also acquired sets of images using the XTC protocol for a range of choices of the exchange time, extracting the rate of saturation of the xenon compartments [16, 17]. Finally, we also performed imaging of the gas and dissolved phase directly, together in a single pulse sequence [18]. A region of hyperintensity on the dissolved-phase image of the lung of a healthy volunteer, which corresponded to hypointensity on the xenon ventilation image, was later attributed to an inflammatory lesion, confirmed by proton MRI.

Over the past year (2010) we assembled our fourth generation prototype, "Hawking," improving on operational methodology and incorporating new technology. The sixteen channel finned copper column remains unchanged, however heating and cooling systems are implemented with improvements in stability and robustness. The 1400W spectrally narrowed laser is redesigned, with a new optical layout and a mechanically stabilized step mirror. We also incorporated deflection and focusing corrective optics for each of the 1440 emitters. The cryogenic separation system incorporates larger volume helixes, a diaphragm pump to scavenge polarized xenon from the freeze-out volume and deliver it into the bag, and a four-port bagging system.

In addition to these technical improvements, the fourth generation polarizer offers improvements in operation, safety, stability, and reproducibility. All processes are fully automated including the production sequence, polarization measurement, warm-up, cool-down, and self-check. Quality control is incorporated throughout. Each bolus bag is bar-coded and labeled with its Investigational Drug status, its quantity of hyperpolarized xenon, the polarization, and a time-stamp. On-board diagnostics are incorporated into every subsystem and data are logged and stored archivally. The polarizer can be controlled locally or remotely. The laser path is fully enclosed and interlocked, permitting Class 1 designation. The frame is designed to be aesthetic, robust, easily transportable on its wheels, or able to be packed for shipping. Operator training will no longer require advanced degree in physics. The technician simply pushes a soft button on the polarizer's touch screen or schedules a bag of gas with the polarizer online.

Xemed is expanding partnerships with research sites for validating clinical indications towards regulatory approval of hyperpolarized xenon and seeking funding mechanisms to support those activities. In the US, the National Institutes of Health is continuing its support to Xemed for refinement of polarization and imaging infrastructure, development of new pulse sequences, and investigations of clinical indications. A recently approved grant will add a clinical site to the network of Xemed's academic partners. Xemed is pursuing joint development agreements with pharmaceutical and medical device companies. One such project recently funded will develop quantitative hyperpolarized xenon imaging biomarkers for lung disease and compare with other metrics. With the recent completion of our latest polarizer, we now have a new resource for pursuing future clinical work and advancing the regulatory status of hyperpolarized xenon worldwide.

References:

1. F.W. Hersman, I.C. Ruset, S. Ketel, et al. "Large Production System for Hyperpolarized 129Xe for Human Lung Imaging" *Academic Radiology* 15(6): 683-692 (2008). PMCID: 18486005
2. I.C. Ruset, S. Ketel, F.W. Hersman, "Optical pumping system design for large production of hyperpolarized ^{129}Xe" Phys. Rev. Lett. 96: 053002 (2006) PMCID: 16486926
3. J. Distelbrink, J. Ketel, D. Watt, et al. "Hyperpolarized xenon at 10 liters per hour for diagnostic MRI" *Proceedings of the 16th ISMRM,* p1776 (2008).
4. H. Zhu, I.C. Ruset, F.W. Hersman. "Spectrally-narrowed external-cavity high power diode laser arrays" *Opt. Lett*. 30 (11): 1342-1344 (2005). PMCID: 15981527
5. F. W. Hersman, M.B. Leuschner, J.A. Carberry, "Method and Apparatus for Polarizing Polarizable Nuclear Species" US Patent #6,949,169 awarded 9/27/05
6. F. W. Hersman and I. Ruset, "Method and Apparatus for Accumulating Hyperpolarized Xenon" US Patent #7281393 awarded 10/16/2007
7. F. W. Hersman, J. H. Distelbrink, and H. Zhu "High Brightness Spectral-Narrowing Diode Laser Array System" US Patent #7769068 awarded 8/3/2010
8. F. W. Hersman, "Xenon Polarization in Multiple Heat-exchanger Channels" US Patent pending
9. Dregely, I. M.; Wiggins, G. C.; Ruset, et al. "A 32 Channel Phased Array Lung Coil for Parallel Imaging with Hyperpolarized Xenon 129 at 3T" *Proceedings 17th Scientific Meeting ISMRM, Honolulu,* p.4918 (2009).
10. F.W. Hersman, J. Ketel, I.C. Ruset, et al. "First results from clinical sitings of a high production prototype xenon polarizer" *Proceedings of the 18th ISMRM,* p4598 (2010)
11. T.A. Altes, J.P. Mugler Ⅲ, I.M. Dregely, et al. "Hyperpolarized xenon-129 ventilation MRI: preliminary results in normal subjects and patients with lung disease" *Proceedings of the 18th ISMRM,* p2529 (2010)
12. C. Wang, J.P. Mugler Ⅲ, E.E. de Lange, et al. "Measurements of the diffusion of hyperpolarized 129Xe in human lung over short and long time scales during one breath hold". *Proceedings of the 18th ISMRM*, p2543 (2010).
13. G.W. Miller, J.P. Mugler Ⅲ, T.A. Altes, et al. "Motion-corrected pO2 mapping in human lungs using hyperpolarized Xe-129 MRI" *Proceedings of the 18th ISMRM,* p2558 (2010).

14. K. Ruppert, J.F. Mata, I.M. Dregely, et al. "Hyperpolarized xenon-129 dissolved-phase signal dependence on flip angle and TR" *Proceedings of the 18th ISMRM*, p2551 (2010)
15. K. Ruppert, J.F. Mata, I.M. Dregely, et al. "Hyperpolarized xenon-129 dissolved-phase signal dependence on the echo time" *Proceedings of the 18th ISMRM*, p2552 (2010)
16. Dregely, I. M.; Ruppert, K.; Mata, et al. "Lung Microstructure Changes in a Rabbit After Elastase Instillation as Detected with Multiple Exchange Time XTC (MXTC)" *Proc18th Scientific Meeting ISMRM, Stockholm,* p.2554. (2010)
17. Dregely, I. M.; Ruset, I. C.; Ketel, J.; et al. "The Structural Response of the Compliant Lung to Different Ventilation Volumes Assessed by Multiple Exchange Time Xenon Transfer Contrast (MXTC)" *Proc 18th Scientific Meeting ISMRM, Stockholm,* p. 2555 (2010)
18. J.P. Mugler Ⅲ, T.A. Altes, I.C. Ruset, et al. "Simultaneous imaging of ventilation distribution and gas exchange in the human lung using hyperpolarized Xe129 MRI" *Proceedings of the 18th ISMRM,* p197 (2010).
19. S. Patz, F.W. Hersman, I. Muradian, et al. "Hyperpolarized ^{129}Xe MRI: A Viable Functional Lung Imaging Modality?" *European Journal of Radiology* 64: 335-344 (2007). PMCID: 17890035
20. S. Patz, I. Muradian, M.I. Hrovat, et al. "Human Pulmonary Imaging and Spectroscopy with Hyperpolarized ^{129}Xe at 0.2T Initial Experience" *Academic Radiology* 15(6): 713-727 (2008). PMCID: 18486008
21. K. Ruppert, J.R. Brookeman, K.D. Hagspiel, J.P. Mugler Ⅲ *Magn. Reson. Med.* 44: 349 (2000); 51: 676 (2000).

Luncheon Lecture 3-2

Hyperpolarlized Noble Gas MRI: Clinical Applications

Hiroto Hatabu, M.D., Ph.D.
Clinical Director, MRI Program, Medical Director, Center for Pulmonary Functional Imaging
Department of Radiology, Brigham and Women's Hospital Associate Professor of Radiology,
Harvard Medical School, USA

Hyperpolarized noble gas magnetic resonance imaging has been explored extensively as a promising tool for the quantitative evaluation of regional pulmonary pathophysiology. This noninvasive technique is capable of providing both structural information down to the level of the alveolar microstructure and functional information, such as dynamic ventilation, intrapulmonary partial pressure of oxygen, and alveolar surface area. In this lecture, the role of hyperpolarized 3-helium and 129-xenon magnetic resonance imaging for clinical applications, current and in the future, will be reviewed.

Abstract

Evening Lecture

Evening Lecture 1 - 1

Animal Studies for Functional Imaging at High-Field System: Ultra-short TE (UTE) MRI of the Lung

Masaya Takahashi, Ph.D.
Advanced Imaging Research Center, University of Texas Southwestern Medical Center at Dallas, USA

Understanding how the mammalian respiratory system works and how it changes in disease states and under the influence of drugs is frequently pursued in model systems such as small rodents. Indeed, the field of lesion modeling is progressing at an accelerated pace and creating mouse models that accurately reproduce the genetic and histopathological alterations present in human diseases. Animal models of human pulmonary disorders have been very valuable tools for proof of concept studies, for investigating respiratory biology and for increasing our knowledge about disease mechanisms. Given the heterogeneity of disease and the slow progression of chronic obstructive pulmonary disease and interstitial lung disease, a pilot clinical study would be difficult to design and costly to carry out. More importantly, histopathological correlation is requisite for development of new technologies to test the sensitivity and specificity of the methods. For those reasons, animal study is important particularly in this field of research. Hence, one needs the ability to assess morphology and function in *in vivo* systems.

High-resolution computed tomography (HR-CT) is the standard for assessing pulmonary disorders, which yields in detailed anatomical information but incurs radiation exposure. It has been identified that an important challenge in pulmonary disorders is the development of more powerful, multi-variate methods for predicting regional outcome and individual responsiveness to particular therapies on the basis of clinical and laboratory characteristics.

One of our major research focuses is to exploit the recent advances in magnetic resonance imaging (MRI) to image the lung *in vivo*. MR imaging of the lung is extremely challenging due to multiple inherent difficulties associated with the properties of the lung. These challenges, including low proton density, severe magnetic field susceptibility, and respiratory and cardiac motion artifact, have resulted in the delay in refining lung imaging as compared to MRI progress with other major organs. However, the recent development of fast MR imaging techniques along with more powerful hardware has made possible detailed, non-invasive imaging of pulmonary parenchyma, and pulmonary MRI is currently an active area of research. We have during the past years been dedicated to the development of new acquisition and processing methods by means of MRI in animals and humans, permitting quantitative characterization of the pathophysiological change in pulmonary disorders, including lung cancer.

The utility of ultra-short TE (UTE) MRI in conjunction with projection acquisition of the free inducting decay (FID) allows us to reduce TE to less than 100 μsec to minimize signal decay caused by short transverse relaxation time (T2*). It brings higher MR signals from tissues which have short T2* and thus are unobservable in conventional methods with short TE (c.a. 2 msec). On the subtraction image between the images with an UTE (c.a. ~500 μsec) and a conventional range of TEs, the biological materials/ tissues, such as tendon, bone or periostea are enhanced. In early 90s, it was demonstrated that UTE imaging with projection reconstruction provided much higher signal intensity (SI) in the lung parenchyma and finer pulmonary structures in human. Using cardiac and respiratory gating, it was showed excellent UTE images of the lung in normal rats using a small animal imaging system. It was also reported the ultra-high quality UTE images of the normal rat lung *in vivo* that resolve the thin membranes that separate lung lobes. Another study using a single point imaging method that could achieve an ultra-short TE (200 μs) demonstrated lower MR signal and shorter T2* in a mouse model of emphysema than those in the control. However, utilization of UTE MRI for lung imaging is still sparse in these days.

In this lecture, we will first discuss the principal of UTE MRI. Subsequently, our systemic approach to use UTE MRI for pulmonary imaging will be introduced. Using an UTE sequence, we have demonstrated in normal and a transgenic murine model that the parenchyma with airspace enlargement exhibits reduced SI and T2* that closely relate to lung tissue density. Further, the capability to acquire endogenous MR signal of the lung parenchyma also enables us to assess change in SI due to inhalation of molecular oxygen (O_2) or intravenous injection of Gd, which demonstrates regional ventilation and perfusion, respectively. The method could detect the regions with ventilation/perfusion mismatch in a model of pulmonary embolism. The method can be implemented in a standard clinical system and does not require any special equipment and is directly translatable to clinical use. The requisite image processing is simpler compared with currently existed methods. The UTE MRI has the new potential to assist in the diagnosis of early lung disease and in monitoring of response to treatment without incurring the risks of radiation exposure.

Evening Lecture 1 - 2

Clinical Functional Imaging at High-Field MRI

Christian Fink, M.D.
Vice Chair and Associate Professor of Radiology Section Chief Cardiothoracic Imaging
Department of Clinical Radiology and Nuclear Medicine University Medical Center Mannheim
Medical Faculty Mannheim - Heidelberg University, Germany

Magnetic resonance imaging (MRI) of the lung has been considered experimental for many years. With ongoing technical improvements such as multichannel MRI, systems with powerful gradients as well as the development of innovative pulse sequence techniques e.g. implementing parallel imaging, MRI of the lungs was finally clinically implemented. Nowadays MRI is routinely used for lung imaging in clinical practice as a radiation-free alternative to computed tomography (CT), e.g. in children with lung disease. In addition to a morphologic assessment, MRI offers the great potential of functional lung imaging. In clinical medicine this may help in the differential diagnosis of pulmonary disorders, improve disease stratification – and thus improving therapy selection, and finally giving insights into pathophysiology. Several functional MRI techniques have been developed, among which contrast-enhanced perfusion imaging, diffusion weighted imaging (DWI), and dynamic MRI of respiratory mechanics can be clinically implemented on almost every modern MR system. Less commonly used or more complex MR techniques are oxygen-enhanced MRI and hyperpolarized noble gas imaging.

For a long time imaging of lung perfusion was the domain of nuclear medicine. With the development of time-resolved MR angiography (MRA) techniques perfusion imaging of the lung became clinically feasible. Perfusion imaging has been used for the visualization of regional pulmonary perfusion in patients with different lung diseases such as lung cancer, airway disease or pulmonary vascular disease. In combination with morphologic MRI perfusion imaging allows a comprehensive assessment of those lung diseases thereby improving differential diagnosis (e.g. the differentiation between chronic obstructive pulmonary hypertension and other forms of pulmonary hypertension). Using perfusion as a surrogate parameter of lung function perfusion MRI can be used to objectively quantify the functional impairment in pediatric lung disease.

After two decades of diffusion-weighted imaging for the evaluation of intracranial diseases, DWI of the thorax has become feasible by implementation of MRI techniques with significantly reduced acquisition times, thus minimizing artifacts from respiratory and cardiac motion. In chest imaging, DWI has been mainly suggested for the characterization of lung cancer, lymph nodes and pulmonary nodules.

DWI visualizes the microscopic movement of water molecules within tissues which is highly influenced by the cellular environment of water, intracellular organelles and macromolecules. As water molecules move within tissues, they encounter various restrictions and hindrances. Thus, DWI allows for a functional assessment of microstructure in relation to gross anatomy. The movement of the spinning water molecules causes phase dispersion, which results in a signal intensity loss. This signal intensity loss can be quantified by calculating the apparent diffusion coefficient (ADC). Malignant tumors are characterized by increased cellularity, larger nuclei with more abundant macromolecular proteins, a larger nuclear/cytoplasmic ratio and less extracellular space relative to normal tissue. Because of these characteristics, the diffusion of water molecules in malignant tumors is restricted, resulting in decreased ADC. DWI has been used to differentiate lung cancer from benign lesions as well as for the subcharacterization of different histologic subtypes of lung cancer. Moreover, DWI has been used to differentiate central tumor from the surrounding lung consolidation, and as alternative imaging test for the detection of nodal and distant metastasis.

Dynamic CINE MRI techniques have traditionally been used for the assessment of cardiac function. By applying these techniques to the entire chest respiratory mechanics can be visualized in vivo. Several applications of dynamic MRI in pulmonary imaging have been described such as radiotherapy planning, cancer staging or assessment of airway and lung motion in airway disease.

Compared to standard field strength (i.e. 1.5 Tesla) high field MRI (e.g. 3 Tesla) has the advantage of an improved SNR, since the signal scales linearly with field strength. Moreover, for contrast-enhanced applications, the sensitivity to injected Gd agents is heightened since the longitudinal relaxation time (T1) of unenhanced blood increases with field strength. At MR angiography shortening of T2* causes a reduction of background noise, thus resulting in a better discrimination of enhancing blood vessels. In the lungs, however, the higher magnetic susceptibility gradients associated with high magnetic field can be limiting, resulting in signal loss and potentially lower image quality when compared to standard field strength MRI. The increasing number of installation of high field MR systems necessitates functional MRI of the lungs to be implemented at high field. This lecture will give an overview of the current status of functional MRI of the lungs at high field and present some clinical examples.

Evening Lecture 2-1

Dual-Energy CT Application for Pulmonary Vascular Disease

Joon Beom Seo, M.D., Ph.D.
Associate Professor, Department of Radiology,
University of Ulsan College of Medicine, Asan Medical Center, Korea

Dual-energy CT (DECT) is a new, emerging, imaging technique which can differentiate such materials as iodine, xenon, bone, and air, based on their specific attenuation differences at high and low x-ray energies. Dual-source CT (DSCT) allows acquisition of both high-energy CT data and low-energy CT data during a single scanning by applying two different tube voltage settings, typically 140 kVp and 80 kVp. Clinical DECT application using first generation of DSCT was somewhat limited due to several technical factors including limited field-of-view and energy differentiation. These limitations have been significantly improved by the introduction of second generation dual source CT with larger field-of-view and better dual-energy contrast. Recently, alternative approach of DECT has been introduced by different manufactures, which is based on rapid kV switching method using single x-ray tube. Although this new technique is somewhat different from dual-source approach in image processing and evaluation algorithm, this approach will also allow the similar clinical applications.

For the past few years, there have been several studies on the thoracic applications of this interesting technique. One of typical applications is perfusion or blood volume imaging, which is based on the ability of extraction of iodine content from contrast enhanced CT images. With application of the material decomposition theory, dual-energy CT can be used to differentiate the iodine component from lung parenchyma enhanced with iodine contrast material. Materials can be differentiated by analysis of changes in attenuation coefficients in materials at two energies. Owing to the photoelectric effect, the material decomposition theory is especially applicable to materials with large atomic numbers, such as iodine, and iodine is generally known to have stronger enhancement at low tube voltage settings. At dual-energy CT, pulmonary CTA and the iodine enhancement representing lung perfusion can be performed simultaneously in a single acquisition after contrast injection.

Studies have shown that perfusion images obtained at dual-energy CT may be useful adjunct in diagnosing acute pulmonary embolism. The perfusion defect was found in the corresponding area of the occluded vessel, and visualization of the perfusion defect with dual-energy CT had good agreement the findings at perfusion scintigraphy. In addition, Chae et al, reported that the degree and extent of perfusion defects can be sued in severity assessment of acute pulmonary embolism (AJR 2010). In segment-based analysis in their study, they found interesting mismatch between the vascular occlusion and perfusion defect. Perfusion was preserved in the segments in which there was partial occlusion above the segmental artery. Therefore, these segments may represent partial occlusion with normal perfusion. Conversely, there were segments having perfusion defects more severe than the degree of vascular obstruction. One assumption that may explain the mismatched areas is that they represented areas of microcirculation disturbance.

Another way to use DECT in assessment of acute pulmonary embolism is so called 'lung vessel' application, allowing differentiation of small thrombosed small vessels from contrast-filled non-thrombosed vessels even with the presence of partial volume effects. Despite the presence of partial volume effects, the ratio of the respective low and high kV CT-values relative to air (negative 1000 HU) is only a function of the iodine content but not of the vessel diameter. Using this concept, the 'Lung Vessels' application software can divide the pixels of lung vessels into those with iodine and those without iodine by means of a straight line in the CT-value diagram. Lee, et al has recently reported that the diagnostic performance of pulmonary CTA in diagnosing acute PE can be improved by applying this interesting application (Eur Radiol 2010). This effect was more pronounced in detecting small, peripheral emboli.

DECT pulmonary perfusion map can also allow for the depiction of perfusion defects in patients with chronic thrombembolic pulmonary hypertension. Perfusion imaging is also useful in the assessment of other vascular diseases including congenital vascular anomalies, vasculitis and so on. This technique also may replace perfusion scintigraphy for preoperative assessment of lung cancer patient, because perfusion CT was comparable to perfusion scintigraphy in the prediction of postoperative lung function.

In addition, perfusion imaging can be also applied in assessing the perfusion status of various diffuse lung diseases including COPD, smoker's lung, interstitial lung diseases, and so on. More importantly, xenon ventilation DECT imaging for the simultaneous assessment of anatomy and ventilation has been introduced (Chae et al, Radiology 2008 / Invest. Radiol 2010). Possible clinical indications of this new

approach include the assessment of COPD, asthma, and other diffuse airway and vascular disease. Simultaneous assessment of anatomy, perfusion and ventilation using DECT technique may open new fields of functional CT imaging of various pulmonary diseases.

In this talk, firstly, the basic principles and theory of dual energy CT imaging will be introduced. Early experiences in using dual energy CT in various pulmonary vascular diseases will be discussed.

Evening Lecture 2-2

Quantitative MR Assessment for Pulmonary Vascular Disease

David L. Levin, M.D., Ph.D.
Department of Radiology Mayo Clinic, USA

Quantitative assessment of pulmonary blood flow may be able to provide tremendous insight into the mechanisms of pulmonary vascular disease. In this presentation, we will discuss aspects of normal pulmonary physiology that affect the quantitative assessment of pulmonary blood flow, including respiration and gravitational affects on lung structure and blood flow. We will then examine both contrast and non-contrast methods that can be used to quantify the various parameters that define pulmonary perfusion. Lastly, we will examine the application of these methods to the study of pulmonary vascular disease using the study of high-altitude pulmonary edema (HAPE) as a model that has been investigated using both contrast and non-contrast techniques.

Abstract

Core Session

Core Session 1 - Invited Speaker 1 -

Etiology and Pathophysiology of Pulmonary Hypertension

Koichiro Tatsumi
Department of Respirology, Graduate School of Medicine, Chiba University, Japan

Pulmonary hypertension (PH) has been defined as a resting mean pulmonary arterial pressure > 25 mm Hg. The subgroup of PH known as pulmonary arterial hypertension (PAH) adds the criterion that the pulmonary arterial wedge pressure (PAWP) is ≤ 15 mm Hg. The prevalence of PH varies substantially depending on the type, etiology and underlying condition, such as idiopathic PAH (IAPH), scleroderma, portal hypertension, pulmonary embolism and so on. Right heart catheterization with the measurement of pulmonary arterial pressure (PAP), cardiac output (CO), right arterial pressure (RAP) and PAWP remains the gold standard for the diagnosis of PAH.

Although the tools used to diagnose and assess patients with PAH have improved, the number and complexity of therapeutic interventions have increased, making it even more challenging to accurately predict prognosis. With the introduction of Doppler echocardiography, approximate evaluation of PAP became feasible. Although this method is helpful in detecting or excluding significant PH, its intrinsic and operator-dependent limitations make early PH diagnosis and screening challenging. In addition, the sensitivity and specificity of echocardiography for the detection of PH remain undefined.

The usual cause of death in PAH is right ventricular (RV) failure. Both diastolic and systolic dysfunction are likely contributors to RV failure. Diastolic RV dysfunction is thought to be related to RV hypertrophy and chronic pressure overload, with prolonged isovolumetric relaxation time. With systolic RV dysfunction, isovolumetric contraction time is prolonged and ejection time is shortened. Magnetic resonance imaging is useful in the noninvasive assessment of the right heart in PH, although it cannot be used as a screening test.

Core Session 1 - Invited Speaker 2 -

Nuclear Medicine Assessment for Pulmonary Hypertension

Takayuki Shinkai
Department of Radiation Oncology, Nara Medical University, Japan

CTEPH should be considered for all patients with unexplained PH because there are many treatment strategies for it. Pulmonary perfusion and ventilation scintigraphy has been used for the differential diagnosis of chronic pulmonary thromboembolism from other variable diseases which cause PH. Ventilation-Perfusion (V/Q) lung scan of patients with CTEPH generally show multiple segmental-sized or larger mismatched perfusion defects. SPECT acquisition is recommended to detect a small perfusion defect. Perfusion scan for CTEPH have a tendency to underestimate the severity, although negative scan results are highly specific for absence of thromboembolism. A normal V/Q scan means that CTEPH is unlikely cause of PH.

In Japan, latest and advanced CT scanners have been widely used across the country, and most of them are available 24 hours. This accessibility made SPECT unnecessary in the APTE diagnosis. Ventilation scan are recently often left out in the diagnostic procedure. However, the diagnosis on perfusion SPECT without ventilation SPECT may cause false positive results of other all pathological conditions which cause regional alveolar hypoxemia –COPD, for example. In such cases, comparison with CT for each perfusion defect is requisite to avoid such misdiagnosis. Simultaneous evaluation using SPECT/CT is considered desirable.

V/Q SPECT has advantages over CTPA in terms of free complications induced by contrast medium or an excessive radiation exposure to the breast. Diagnosis in accordance with proper plans should be made; V/Q scanning must be performed in all patients with unexplained PH to rule out CTEPH. If V/Q scan reveals suggestion of CTEPH, pulmonary angiography or CTPA is required for an accurate diagnosis.

Core Session 1 - Invited Speaker 3 -

CT Assessment of Pulmonary Hypertension

Joon Beom Seo, M.D.. Ph.D.
Associate Professor,
Department of Radiology, University of Ulsan College of Medicine, Asan Medical Center, Korea

Pulmonary hypertension may be idiopathic or arise in association with chronic pulmonary embolism, parenchymal lung disease, liver disease, vasculitis, congenital left-to-right cardiac shunt, pulmonary veno-occlusive disease, left-sided cardiac disease and others. With the advance of multi-detector technology, CT has become one of essential test to evaluate pulmonary hypertension. One of the key roles of CT pulmonary angiography is to differentiate the causes of pulmonary hypertension because each disease has somewhat different imaging features. CT also can be used to assess the severity of the diseases. In addition, CT can be used in to predict the effect of vasodilators in treating idiopathic pulmonary hypertension. CT angiography also can be used in selecting candidates for thromboendarterectomy in treating chronic thromboembolic pulmonary hypertension. In this talk, I will be focusing on the technical aspects of CT imaging for assessing pulmonary hypertension and the typical and atypical CT features of various causes of pulmonary hypertension. In addition, recommendations for clinical use will be given. Lastly, recently introduced pulmonary perfusion CT imaging with dual energy CT technique will be introduced and early experience in using dual energy CT in pulmonary hypertension will be discussed.

Core Session 1 - Invited Speaker 4 -

MR Assessment for Pulmonary Hypertension

David L. Levin, M.D., Ph.D.
Department of Radiology, Mayo Clinic, USA

In this presentation, we will discuss various methods that have been used in the evaluation of pulmonary arterial hypertension (PAH). These methods can be divided into those that evaluate the proximal pulmonary arteries and those that examine the peripheral circulation. Within the proximal pulmonary arteries, correlations have been made between patterns of arterial blood flow and pulmonary artery pressure. In addition, the mechanical properties of the pulmonary artery have also been shown to correlate with pulmonary arterial pressures. Quantitative evaluation of the peripheral pulmonary circulation may identify differences in pulmonary blood flow, blood volume, or mean transit time between normal subjects and patients with PAH. Qualitative evaluation of the peripheral pulmonary circulation has been shown to be useful in distinguishing chronic thromboembolic PAH from non-thrombotic causes.

Core Session 1 - Invited Speaker 5 -

Update of Treatment for Pulmonary Hypertension

David G. Kiely
Pulmonary Vascular Disease Unit and NIHR Cardiovascular Biomedical Research Unit,
Royal Hallamshire Hospital, UK

Pulmonary hypertension (PH), is defined at cardiac catheterisation as a mean pulmonary artery pressure of ≥ 25 mmHg. It has a variety of mechanisms and causes which are classified into 5 major clinical groups (Dana Point). In patients with pulmonary arterial hypertension (PAH) and chronic thromboembolic pulmonary hypertension (CTEPH) life expectancy is significantly reduced. Since the first randomised controlled trial in 1996 in idiopathic PAH approximately 30 RCT's have been published. Currently licensed therapies for PAH include drugs that target prostanoid, nitric oxide and endothelin pathways. For a selected group of patients with CTEPH, pulmonary endarterectomy can offer the prospect of cure. Drug therapies for PAH are expensive and although they have been shown to improve exercise capacity, quality of life and slow progression of disease there remains no cure. Long term data is emerging from various registries and suggest that these therapies also improve survival. A number of therapies targeting other important pathways are currently under development / trial. In the 3 other forms of PH such as that owing to, lung disease / hypoxia (PH-Lung) to left heart disease (PH-LHD) and that with unclear / multifactorial mechanisms (PH-Multifactorial) although PH is associated with a worse outcome and functional status there is lack of efficacy and safety data. Therapies suitable for PAH are not recommended in these patients. Radiological assessment is crucial in the systematic evaluation of patients with unexplained PH, in the accurate classification of PH and therefore in defining patients most likely to benefit form specific interventions.

Core Session 1 - Scientific Presentation 1 -

Optimized Flowchart of Multi-technical MR Protocol for Pulmonary Circulation and Right Heart Function on the Busy Clinical Schedule

Shu-Hui Peng[1,2], Teng-Fu Tsao[1,2,3], Ruei-Jin Kang[4], Fong-Lin Chen[5], Chun-Hung Su[6], Gwo-Shen Chen[1,2], Chien-Yi Chiu[1,2], Szu-Yin Wu[1,2], Yung-Chang Lin[3], Yeu-Sheng Tyan[1,2]

1. Department of Medical Imaging, Chung Shan Medical University Hospital, Taiwan
2. School of Medical Imaging and Radiological Sciences, Chung Shan Medical University, Taiwan
3. Department of Veterinary Medicine, National Chung Hsing Univerity, Taiwan
4. National Chi Nan University, Taiwan
5. Division of Pediatric Cardiology, Chung Shan Medical University Hospital, Taiwan
6. Division of Cardiology, Chung Shan Medical University Hospital, Taiwan

Purpose:

There are various techniques of current MR imaging to noninvasively evaluate the pulmonary circulation and right heart function. The evaluation for this specific purpose based on electively one or two techniques may be difficult in clinical practice because of the lack of full information available. The combination of multiple scanning techniques without an adequately designed flowchart, however, may expand the scan time for the overloaded MR schedule. The purpose of our study was to evaluate the feasibility of a multi-technical full set MR protocol for clinical usage.

Material and Methods:

To resolve various clinical problems about pulmonary circulation and right heart function, we designed a MR protocol with multiple techniques using the 1.5 Tesla MR scanner. This set included (1) tissue characteristics study using steady-state precession (true FISP) and black-blood fast low angle shot gradient echo (FLASH) (2) dynamic gadolinium-enhanced MR pulmonary perfusion evaluation using FLASH (3) right heart function evaluation using serial short-axis cine true FISP (4) gadolinium-enhanced 3D MR angiography, and (5) phase contrast MR pulmonary flow measurement. The expected scanning time to cooperative patients was established by four experienced MR technicians after inspecting the protocol.

Results:

The expected scanning time from four technicians was 30 minutes, 30 minutes, 35 minutes, and 40 minutes respectively. All of them were within the default setting (40 minutes per MR case) in our hospital.

Conclusion:

Our optimized multi-technical full set MR protocol for the evaluation of pulmonary circulation and right heart function is feasible with acceptable scanning time.

Core Session 1 - Scientific Presentation 2 -

V-Q Imbalance in Primary/Passive Pulmonary Hypertension on V/Q SPECT

Kazuyoshi Suga[1], Osamu Tokuda[2], Munemasa Okada[2], Masahiro Koike[2], Hideyuki Iwanaga[2], Naofumi Matsunaga[2]

1. Department of Radiology, St. Hill Hospital, Japan
2. Department of Radiology, Yamaguchi University School of Medicine, Japan

Cross-sectional lung ventilation (V)-perfusion (Q) imbalance in primary pulmonary arterial hypertension (PAH) and passive pulmonary hypertension (PH) was characterized by automated V/Q SPECT.

Technegas/MAA SPECT-derived V/Q SPECT and V/Q profile were automatically built to characterize cross-sectional lung V-Q imbalance in 12 patients with primary (idiopathic or familial) PAH and 15 patients with passive PH associated with left ventricular dysfunction or failure. The abnormality ofV/Q distribution in these patients was correlated with PaO2 and pulmonary arterial pressure and with lung morphologic changes on CT.

Markedly low V/Q ratios (reverse V-Q mismatch) in the background lungs with heterogeneous V/Q distribution was seen in 12/12 (100%) patients with primary PAH and in 10/15 (66%) patients with passive PH, which were predominantly seen in upper lung zone. Including these regions with reverse V-Q mismatch, V/Q profile frequently showed flattened peaks with asymmetric and broadened V/Q distribution in all patients, with significant correlation between the standard deviation (SD) of V/Q ratios in the entire lungs and PaO2 and mean pulmonary arterial pressure (both; $P < 0.01$). At the lung regions with reverse V-Q mismatch, bronchial lumens compressed by dilated pulmonary arteries and heterogeneous lung attenuations were frequently seen on CT.

Patients with primary PAH and passive PH appear to characteristically have a high prevalence of reverse V-Q mismatch indicative of an inadequate hypoxic vasoconstriction reflex on V/Q SPECT, frequently accompanied with heterogeneous lung attenuations and compressed airways on CT.

Core Session 1 - Scientific Presentation 3 -

Estimation of Pulmonary Vascular Resistance by the Calculation of Contrast Transit Time from Gadolinium Contrast Enhanced Pulmonary MRI

Adam G Telfer[1], Judith Hurdman[3], David Capener[1], Helen Marshall[1], Robin Condliffe[3], Charlie Elliot[3], Christine Davies[2], Smitha Rajaram[1], Jim Wild[1], David Kiely[3], Catherine Hill[2]
1. Academic Radiology Unit, University of Sheffield, UK
2. Department of Radiology, Royal Hallamshire Hospital, UK
3. Pulmonary Vascular Diseases Unit, Royal Hallamshire Hospital, UK

Cardiac Output (CO), Pulmonary Artery Pressures (PAP) and Pulmonary Vascular Resistance (PVR) are key diagnostic variables in Pulmonary Hypertension (PH). The current gold standard technique for the measurement of these variables is Right Heart Catheterisation (RHC). Well validated non-invasive alternative techniques using Echocardiography or MRI exist for estimating both CO and PAP, however at the present time no validated method exists for the non invasive estimation of PVR.

In this study 21 patients with CTEPH, IPAH or Systemic Sclerosis with or without PH were selected who had undergone RHC and Gadolinium Contrast Enhanced Pulmonary MR imaging within a 72 hour period. Using each patients MRI data functional maps were created showing the passage of contrast through each pixel and Regions of Interest drawn outlining the complete lung field on three sample coronal slices. The Contrast Transit Time (CTT) from the contrast bolus being detected in the Superior Vena Cava (SVC), Right Atrium (RA), Right Ventricle (RV) and Pulmonary Artery (PA) to the time of peak MR signal in each sample slice was recorded and compared with the PVR using a Pearson's Rank Correlation.

Correlation Coefficients were highest in the most posterior sample slice (level of the Descending Aorta) with a correlation coefficient between PVR and CTT from the SVC of $r=0.922$, $p<0.001$, no correlation coefficients of less than 0.801 were recorded in any sample.

CTT appears to correlate strongly with PVR and may serve as a non-invasive measurement of this clinically important physiological variable in patients with PH.

Core Session 2 - Invited Speaker 1 -

Newest Evidences of Drug Therapy for Lung Cancer

Yoichi Nakanishi
Research Institute for Diseases of the Chest, Graduate School of Medical Sciences, Kyushu University, Japan

Lung cancer is the number one cause of cancer death. Most cases are found after distant metastasis, and outcome of drug therapy for these patients used to be disappointing. However, we have faced a new paradigm shift, i.e., the molecular targeted therapy and the individualized therapy. Many promising data have reported from not only western countries but also Asian countries such as the efficacy of EGFR TKI to tumors with mutated EGFR, that of ALK inhibitor to tumor with EML4-ALK fusion protein, and that of pemetrexed to non-small non-squamous cell lung cancers. New questions have emerged from these new evidences derived from some important clinical trials. Among them, questions regarding with ethnic difference would be one of the most important issues. Are survival data same between Asian and Caucasian? (Data from Japan Lung Cancer Registry Study as well as some global trials have shown survival of Asian patients with lung cancer appears to be obviously better than that of Caucasian.) Why EGFR mutation is frequent in Asian patients? Is only EGFR gene status related with prognosis of lung cancer? Is the criteria of pathological diagnosis for lung cancer same between Asian countries and western countries?

Here, newest evidences for treatment of lung cancer will be presented, and importance of ethnic difference and Asian trials will be discussed.

Core Session 2 - Invited Speaker 2 -

Update for New Molecular Targeted Therapy for Lung Cancer

Kazuhisa Takahashi, M.D., Ph.D.
Department of Respiratory Medicine, Juntendo University School of Medicine, Japan

Lung cancer is the leading cause of cancer death worldwide. Despite progress of platinum-based chemotherapy, the median survival time of patients with inoperable non-small cell lung cancer (NSCLC) still remains poor. The median survival time is approximately 14 months, and has improved only marginally over the last few decades. A recent advance in the treatment of inoperable lung cancer is the development of molecular-targeting drugs including gefitinib and erlotinib targeting the epidermal growth factor receptor (EGFR). Anti-angiogenetic drug, such as bevacizumab, in a combination with chemotherapy has become clinical use in the treatment for NSCLC. Moreover, discovery of EML4-ALK made the great progress in cancer research in NSCLC. In this lecture, the development of molecular-targeting drugs, such as EGFR-TKI, anti-angiogenetic drug, and EMLA-ALK inhibitors will be reviewed.

Core Session 2 - Invited Speaker 3 -

Molecular Imaging for Lung Cancer Treatment

Koji Murakami, M.D.
Division of Nuclear Medicine, Department of Radiology, School of Medicine, Keio University, Japan

The role of the diagnostic imaging for lung cancer diverges into many fields. As for staging before starting therapy, CT is the best and indispensable tool for detection, differential diagnosis, and local extension. On the other hand, CT is known to have limitation and insufficient ability to estimate lymph node metastases, distant metastases, and recurrence.

"Molecular imaging" is a promising modality not only to improve diagnostic ability in addition to CT, but also to provide entirely new information such as metabolic activity, receptor distribution, etc. FDG-PET is the most popular and widely performed modality that is categorized in molecular imaging. There are a lot of literature which describe the efficacy of FDG-PET for lung cancer though poor specificity and low spatial resolution causes many false positive, false negative cases. One of the solutions to improve spatial resolution is PET/CT that is combined CT and PET systems. Recently, radiation field planning using PET/CT is introduced in some institutions. According to the literature using PET/CT for setting radiation field, approximately 10-80% of cases were changed its target volume compared to set the field using CT alone. PET/CT can allow to delineate more correct margin of radiation field than using CT data alone.

Many non-FDG radiopharmaceuticals are now under research, and some of them are in stage of clinical experience. 18F-FLT(fluorothymidine) is an analogue of nuclear acid which reflects cell proliferation. It is expected as the promising radiopharmaceutical that can estimate therapeutic effect of cancers faster. Another promising method is a hypoxic imaging. 18F-FMISO, 62Cu-ATSM, etc. are popular radiopharmaceuticals to be used in this fields. I would like to present the outline of current status of molecular imaging for lung cancer.

Core Session 2 - Invited Speaker 4 -

MR Imaging for Lung Cancer Treatment

Juergen Biederer
Department of Diagnostic Radiology, University Hospital Schleswig-Holstein, Campus Kiel, Germany

In current practice, staging and follow-up of lung cancer is based on MDCT (morphology), PET (metabolism), scintigraphy (ventilation/perfusion/bone metastases) and MRI (brain).

This arsenal of modalities is challenged by MRI. It offers superior soft tissue contrast for differentiation of tumour/atelectasis, mediastinal involvement or chest wall invasion. MRI is superior to X-ray and matches CT in detection of nodular and infiltrative lung disease. In whole-body staging, the diagnostic accuracy of MRI matches even PET-CT - plus comprehensive functional imaging capacities without radiation exposure to patients or hospital personnel.

Functional MRI of the lung presently comprises tumour - and lung contrast-enhanced perfusion studies, diffusion-weighted imaging and analysis of respiration dynamics. Non-contrast enhanced, motion-corrected V/Q-MRI and arterial spin labelling are under development. Their value for monitoring tumour viability and metabolism in response to treatment is subject to current investigation. In radiotherapy, refinements of target definition and dose delivery based on regional lung tissue characterization with ventilation/perfusion MRI are being discussed. Furthermore, concepts for radiotherapy of organs with respiratory motion have raised the need for dynamic volume lung imaging. The CT-approach, so-called 4D-CT in helical or cine mode, either with prospective acquisition or retrospective reconstruction, leads to long exposure times and high radiation dose. It is therefore limited to very few indications. Instead, 4D-MRI with parallel imaging and echo sharing allows for repeated and prolonged measurements of lung motion and tumour displacement without radiation exposure, which makes it the future tool for patient selection in motion adapted radiotherapy and for scientific work in the field.

Core Session 2 - Invited Speaker 5 -

CAD for Lung Cancer Treatment – Evaluation of Tumor Response to Treatment

Jin Mo Goo, M.D.
Department of Radiology, Seoul National University Hospital, Korea

Oncologic imaging has made tremendous progress over the past decades and targeted treatment strategies have been suggested to improve patients' outcome. Objective criteria defining treatment responses are essential to evaluate the treatment effect of anticancer drugs.

Currently imaging biomarkers approved for drug development are based on measurements of size in one dimension. Volume-based size change using the volumetric imaging with MDCT and the application of computerized segmentation of tumors might provide more reproducible measurements and a more sensitive scale for change assessment compared with unidimensional measurements.

Tracer kinetic modeling of dynamic imaging data enables estimates of blood volume, blood flow, and capillary endothelial permeability. With the development of new targeted therapy, selection of eligible patients for these targeted drugs and patient monitoring during the treatment require the availability of noninvasive tools that are capable of assessing tumoral neovascularization. Studies have shown significant changes in perfusion parameters after treatment and have suggested that early prediction for the treatment response may be possible. The availability of rapid imaging with MDCT and commercial analysis software has made perfusion imaging with CT feasible. Perfusion imaging can be performed as an adjunct to a conventional CT examination and is therefore particularly appropriate when a conventional CT is part of routine clinical protocols.

These new techniques need to be validated for their reproducibility and should be standardized for multicenter trials.

Core Session 2 - Scientific Presentation 1 -

Comparative Reading System for Lung Cancer CT Screening

Hidenobu Suzuki[1], Yoshiki Kawata[1], Noboru Niki[1], Hironobu Ohmatsu[2], Takaaki Tsuchida[3], Kenji Eguchi[4], Masahiro Kaneko[3], Noriyuki Moriyama[5]

1. Institute of Technology and Science, The University of Tokushima Graduate School, Japan
2. National Cancer Center Hospital East, Japan
3. National Cancer Center Hospital, Japan
4. Teikyo University, School of Medicine, Japan
5. National Cancer Research Center for Cancer Prevention and Screening, Japan

Lung cancer kills more people than any other cancer worldwide. Lung cancer screening using low-dose CT have been performed in many countries. Comparative reading of current and past CT images is important for evaluation of pulmonary nodules in lung cancer CT screening. However, primary problem in comparative reading is the mismatch of slice and nodule positions caused by lung variation. It is hard for physicians to manually match slice positions, nodule positions, and evaluate the nodule's degree of change. A system to assist smooth comparative reading is necessary. We proposed a comparative reading system for lung cancer CT screening. It's distinctive feature is a highly accurate matching method of region of interest based on thoracic organs registration. Pulmonary blood vessels registration using analysis of the tree structure is performed . The system is evaluated using 1mm and 2mm slice thickness CT images obtained from lung cacer CT screening. We show its usefulness for lung cancer CT screening.

Core Session 2 - Scientific Presentation 2 -

The Evaluation of Lung Perfusion in a Radiation Field Through the Radiation Therapy for Lung cancer - Using Lung Perfused Blood Volume Imaging with Dual Energy CT -

Sachiko Miura[1], Hiroshi Okada[2], Shigeto Hontsu[2], Masatoshi Hasegawa[2], Kimihiko Kichikawa[1], Toshihide Itoh[3]

1. Department of Radiology, Nara Medical University, Japan
2. Department of Radiation Oncology, Nara Medical University, Japan

Purpose

To evaluate the changes of lung perfusion in a radiation therapy (RT) field using lung perfused blood volume (PBV) imaging with dual-energy CT (DECT).

Materials and methods

19 patients receiving RT for primary lung cancers underwent dual-source DECT (SOMATOM Definition Flash). Lung PBV images were generated at 4 points, before, during, 1 week after and 1 month after RT. Follow-up periods was 3-11 months (median 7 months). Radiation dose was 60-70Gy/30-35 fraction. Normalized lung PBV (nPBV) images were created by considering heterogeneous structure of lung parenchyma. The changes of nPBV were analyzed:1) inside and outside of RT-field, 2) in patients with radiation pneumonitis within 1 month after RT and in patients without pneumonitis.

Results

Radiation pneumonitis was observed in 12/19 patients (63%) within 1 month after RT and in 3/19 (16%) later, and no radiation pneumonitis in 4/19 (21%) in all periods. 1) nPBV decreased 1 month after RT compared with before RT ($p=0.0002$) inside of RT-field, but didn't change outside in all periods. 2) For patients with early radiation pneumonitis, nPBV increased 1 week after RT compared with before RT ($p=0.034$) and decreased 1 month after RT compared with during RT ($p=0.02$) or 1 week after RT ($p=0.002$). For patients without radiation pneumonitis, no relation was found.

Conclusion

The changes of nPBV decreased 1 month after RT for all patients, and increased 1 week after RT for early radiation pneumonitis patients. nPBV has the potential to detect radiation pneumonitis earlier than other methods described in previous reports.

Core Session 2 - Scientific Presentation 3 -

Therapy Response Assessment in Neoadjuvant Chemotherapy for Esophageal Cancer: Comparison of PET Response Criteria in Solid Tumors (PERCIST) and Response Evaluation Criteria in Solid Tumors (RECIST)

Masahiro Yanagawa[1], Mitsuaki Tatsumi[2], Tadashi Watabe[2], Kayoko Isohashi[2], Hiroki Kato[2], Mitsuhiro Koyama[1], Osamu Honda[1], Eku Shimosegawa[2], Jun Hatazawa[2], Noriyuki Tomiyama[1]

1. Department of Radiology, Osaka University Graduate School of Medicine, Japan
2. Department of Nuclear Medicine, Osaka University Graduate School of Medicine, Japan

Purpose:

To evaluate therapeutic response to neoadjuvant chemotherapy for esophageal cancer, compared PERCIST to RECIST.

Materials and Method:

Thirty-one patients with esophageal cancers were scanned by 18F-FDG PET/CT before and after chemotherapy. Tumor size was measured in the longest diameter on CT. Standardized uptake value on PET was normalized to lean body mass (SUL). SULpeak was measured using maximal 1.2-cm diameter volume region of interest placed on the hottest lesion of tumor on PET. Objective therapeutic responses were decided according to the RECIST [complete response(CR), partial response(PR), stable disease(SD), and progressive disease(PD)] and the PERCIST [complete metabolic response(CMR), partial metabolic response(PMR), stable metabolic disease(SMD), and progressive metabolic disease(PMD)].

Results:

The reduction ratio of tumor sizes was 30.3±23.9%: tumor size before chemotherapy, 7.0±2.4cm; after, 5.1±2.9cm. Objective therapeutic response on the RECIST was as follows: CR(n=0), PR(n=13), SD(n=18), and PD(n=0). The reduction ratio of SULpeak was 53.9±24.3%: SULpeak before chemotherapy, 8.9±2.9; after, 4.1±2.6. Objective therapeutic response on the PERCIST was as follows: CMR(n=8), PMR(n=17), SMD(n=6), and PMD(n=0). The results between the RECIST and PERCIST criteria were significantly different in all 31 patients (Mann-Whitney's U-test, p=0.0002). Twenty-one of 31 patients were finally judged as clinical complete responders because of no recurrence in the progress after an operation. In these 21 patients, the results of PERCIST [CMR(n=6), PMR(n=11), SMD(n=4), and PMD(n=0)] were more accurate than those of RECIST [CR(n=0), PR(n=9), SD(n=12), and PD(n=0)] (p=0.002).

Conclusion:

PERCIST criteria were more suitable for the evaluation of chemotherapy response to esophageal cancer than RECIST criteria.

Core Session 3 - Invited Speaker 1 -

Etiology and Pathophysiology of COPD

Kazutetsu Aoshiba
Pulmonary Division, Graduate School Medical Science, Tokyo Women's Medical University, Japan

COPD is an inflammatory disease of the lungs that is caused by long-term inhalation exposure to noxious substances including tobacco smoke, indoor and outdoor air pollution, and occupational dusts. The lungs of COPD patients exhibit specific changes in the architecture of their central airways, peripheral airways, alveoli, and pulmonary vessels, secondary to increased inflammatory responses to noxious substances by the airways and lungs. The increased inflammatory response leads to a protease/antiprotease imbalance and oxidant/antioxidant imbalance, and, in turn, damage to the airways and lungs. Other hypotheses regarding its pathogenesis of COPD include increased apoptosis, cellular senescence, and DNA damage responses. Clinically COPD is characterized by not fully reversible airflow obstruction, which is progressive and attributable to the complex effects of the peripheral airway lesions and emphysematous lesions. Airflow obstruction and dynamic pulmonary hyperinflation are the basic pathologic conditions that lead to exertional dyspnea in COPD. Hypersecretion of airway mucus causes chronic cough and sputum production, and uneven distribution of ventilation-perfusion ratios leads to hypoxemia. Severe cases are complicated by pulmonary hypertension, whose progression leads to cor pulmonale. COPD is associated with systemic inflammation that causes systemic comobidities including body weight loss, decreased muscle mass and muscle strength, cardiovascular diseases, osteoporosis, depression, diabetes mellitus, sleep disorders, and anemia. Therefore, COPD should be considered as a systemic disorder. It is also important to pay attention to pulmonary complications such as lung cancer and pneumothorax.

Core Session 3 - Invited Speaker 2 -

PET Assessment for COPD: Changes in Pulmonary Perfusion Distribution

José G. Venegas
Department of Anesthesia, Harvard Medical School, Massachusetts General Hospital, USA

The progression of COPD involves changes in vasculature and parenchyma. Changes in parenchyma tissue are well characterized by HRCT and MR images of apparent diffusion of hyperpolarized gases are sensitive to early alterations in distal lung structures. However, not much is known about the changes in regional perfusion (Qr) in COPD, particularly in early disease stages. Studies using HRCT and PET suggest that the pattern of distribution of Qr may be altered early in the disease. Here I will discuss those studies and present the PET imaging methodology used to compare patients with mild-to-moderate COPD against healthy controls. The ^{13}NN-labeled saline injection method was used to generate images of Qr and ventilation (Vr), while tissue density was estimated from the PET transmission scans. The mean-normalized variance was used to characterize the heterogeneity of Qr, and to quantify the contributions to heterogeneity caused by regions ranging from less than 12 mm to more than 108 mm. Compared with healthy subjects, COPD subjects had larger heterogeneity in Qr, and in Qr normalized by tissue density, with higher contribution from large length scales, and lower contribution from small length scales. Healthy subjects showed higher Vr in dependent regions, whereas no gradients in Vr were sown by COPD. CONCLUSION: Qr heterogeneity was greater in COPD than in healthy subjects and this was caused by changes in relatively large lung regions not explained by changes in tissue density or Vr. The redistribution pattern of Qr in COPD may be an early biomarker of the disease.

Core Session 3 - Invited Speaker 3 -

CT Assessment for COPD -Phenotype on CT in COPD

Keisaku Fujimoto, M.D., Ph.D.
Department of Biomedical Laboratory Sciences, Shinshu University School of Health Sciences, Japan

We have compared the clinical characteristics of COPD patients visually classified according to the dominancy of emphysema or the presence of bronchial wall thickening (BWT), and also examined combined pulmonary fibrosis and emphysema (CPFE). Little-emphysema phenotype showed a higher prevalence of patients who had never smoked, maintained body mass index, milder decreases in DLco and SpO_2 during exercise as compared with the emphysema-dominant phenotype. COPD with BWT showed a higher prevalence of patients complaining of a large amount of sputum, productive cough, and wheezing, and higher rate of exacerbation or hospitalization, and higher rate of patients having sputum eosinophilia who showed greater reversibility of airflow limitation responsive to the treatment with inhaled corticosteroids as compared with the COPD without BWT. The prevalence of CPFE was low at 0.96% in health screening study. We have compared clinical characteristics with CPFE and emphysema-dominant COPD without fibrosis. Forty-six of the 47 CPFE were male. Paraseptal emphysema was particularly common in the CPFE. Honeycombing, ground-glass opacities and reticular opacities were present in 75.6% and 84.4% of CPFE, respectively. Twenty-two patients (46.8%) were complicated with lung cancer. Pulmonary function tests showed that the CPFE had milder airflow limitation and lower diffusing capacity. Desaturation during exercise was more severe than those in emphysema-dominant COPD without fibrosis. It has been demonstrated the patients with CPFE having pulmonary hypertension is poor prognosis. These findings suggest that the morphological phenotypes of COPD show several clinical characteristics. It should be noteworthy that the prevalence of lung cancer might be high in CPFE phenotype.

Core Session 3 - Invited Speaker 4 -

Proton MR Assessment of COPD

Yoshiharu Ohno, M.D., Ph.D.
Division of Functional and Diagnostic Imaging Research, Department of Radiology,
Kobe University Graduate School of Medicine, Japan

According to the American Thoracic Society/ European Respiratory Society consensus and the Global Initiative for Chronic Obstructive Lung Disease guidelines, chronic obstructive pulmonary disease (COPD) is described as a slowly progressive disease characterized by airflow limitation, cough, sputum production, and, at later stages, dyspnea. Currently, computed tomography (CT) is most widely used for radiological disease severity assessment in COPD in clinical and academic practice. Although CT provides morphological information with high spatial resolution, increased iodinated radiation exposure and no direct assessment of pulmonary function are major its' drawback in routine clinical practice. To overcome these drawbacks, several investigators have been suggested the potential advantages of magnetic resonance imaging (MRI) from the results of basic and clinical researches in 1990' s.

In the last decade, hyperpolarized noble gas MRI, oxygen-enhanced MRI (O_2-enhanced MRI) and contrast-enhanced or non-contrast-enhanced perfusion MRI (CE or non-CE perfusion MRI) have also been suggested as useful for assessment of regional morphological and functional changes in COPD patients. Although hyperpolarized noble gas MRI is warranted several special equipments such as laser polarizer, specialized transmitter and receiver coils etc, CE and non-CE perfusion MRIs and O2-enhanced MRI are able to perform by using conventional proton MR scanners.

In this lecture, I will talk about 1) the basics of CE and non-CE perfusion MRIs and O_2-enhanced MRI; 2) summaries of clinical studies by using these MR techniques in COPD subjects; and 3) advantages and disadvantages of these MR technique for clinical setting. We hope this lecture will encourage to clinical setting of proton MR techniques for COPD in clinical and academic practices.

Core Session 3 - Invited Speaker 5 -

Hyperpolarized Noble Gas MRI for COPD

Edwin J.R. van Beek, M.D., Ph.D., MEd FRCR
Clinical Research Imaging Centre, University of Edinburgh, UK

Chronic obstructive pulmonary diseases are a group of lung diseases that are intimately linked to smoking and other types of exposures. The prevalence is increasing, and as a result there is a need to increase the understanding of the disease process, its natural progression and the way in which we can quantify it appropriately. Regional information is heavily reliant on imaging methods, including CT and MRI. This information is hopefully going to be transformed into novel treatment modalities, such as improved delivery methods, interventional methods to decrease hyperinflation and methods which will result in anti-inflammatory effects - all these treatments are aimed at preservation of lung function.

Hyperpolarized noble gas MRI has been shown to hold great promise to probe both the extent of functional impairment in COPD, its underlying physiological and morphological properties and the possible quantification of these measures. Thus far, mainly due to restrictions in availability of methodology and also due to a lack of a reliable 3-Helium gas supply, the work has not propagated into main stream clinical practice. However, with the resurgence of 129-Xenon gas imaging and the improvements in polarizer equipment, there is a new opportunity to apply the technology into a wider community. Whether the technology will become main stream practice remains to be seen (MDCT is also increasingly being developed and has wider availability), but it is quite likely that hyperpolarized noble gas MRI will result in improved understanding of the disease and may be helpful in the development of new treatment opportunities.

Core Session 3 - Scientific Presentation 1 -

Hyperpolarized Noble Gases and COPD: The Frontier

James P. Butler, Ph.D.
Department of Medicine and Radiology,
Brigham and Women's Hospital, Harvard Medical School, USA

Structure and function are two sides of the same pulmonary coin of physiology and pathophysiology. Structure exists to service the lung's function, and the lung's function is dictated by its structure. Hyperpolarized noble gases have the unique capability of probing both, in a non-invasive manner, with imaging to obtain regional information, and without ionizing radiation.

Specific to structure, the use of 3He or 129Xe, through the apparent diffusion coefficient (ADC), probes lung structure at various length scales, depending on the times between dephasing and rephasing MR pulses. This provides a direct measure of the mean squared diffusive displacement of gas molecules. Restrictions due to parenchymal septal tissue, specifically alveolar and ductal architecture, lead to systematic changes in ADC, from which length scales can be assessed. Loss of septal surface for gas exchange, a hallmark of emphysema in COPD can be measured through this approach.

Specific to function, the solubility of 129Xe, together with its NMR chemical shift in tissue, makes 129Xe an ideal surrogate for oxygen transport. Saturation pulses kill the tissue polarization, and recovery measured. Uptake dynamics can be directly related to structural parameters with immediate functional consequences: (1) alveolar surface area loss, (2) septal thickening and remodelling, and (3) capillary transit time and links to vascular co-morbidities; all three biomarkers of COPD.

This, then, is the frontier - hyperpolarized noble gases have the potential for broadening our understanding of basic physiology and its derangements in COPD, and represent novel tools for diagnosis, patient management, and follow-up care.

Core Session 3 - Scientific Presentation 2 -

Regional Quantification of Hyperpolarized Helium-3 Magnetic Resonance Imaging Apparent Diffusion Coefficients: What Does Bronchodilator Administration in COPD Accomplish?

Miranda Kirby[1], Andrew Wheatly[2], Roya Etemad-Rezai[3,6], Peter D Pare[2,4], Harvey O Coxson[4], Jim C Hogg[4], David G McCormack[5], Grace Parraga[1,2,6]

1. Department of Medical Biophysics, The University of Western Ontario, Canada
2. Imaging Research Laboratories, Robarts Research Institute, Canada
3. Department of Medical Imaging, The University of Western Ontario, Canada
4. Division of Respiratory Medicine and the James Hogg iCAPTURE Centre for Cardiovascular and Pulmonary Research, University of British Columbia, St.Paul's Hospital, Vancouver, Canada
5. Division of Respirology, Department of Medicine, The University of Western Ontario, Canada
6. Graduate Program in Biomedical Engineering, The University of Western Ontario, Canada

Hyperpolarized helium-3 (3He) magnetic resonance imaging (MRI) apparent diffusion coefficients (ADC) enable direct quantification of lung microstructure based on the 3He signal in gas ventilated regions. In serial or acute interventional studies there exists the potential for functional lung changes that might allow for different microstructural environments to be probed, leading to altered ADC values. Here we evaluated ten GOLD stage Ⅱ - Ⅳ COPD subjects before and after administration of a bronchodilator (salbutamol) and interrogated the ADC signal in regions of interest that were newly ventilated. 3He ADC was calculated from MRI diffusion-weighted imaging, and ADC maps were generated for the five center slices, using in-house software, for calculation of ADC in the whole lung (WL), the regions of pre/post overlap (RO), and the regions of pre/post non-overlap (RNO) using two-dimensional landmark-based registration. The subsets of pre/post overlap were identified and mean ADC were calculated in the RO and then used as a mask on pre/post images to calculate mean ADC in RNO. 3He ADC was not significantly different pre - and post-salbutamol for the WL (pre=0.51 cm2/s, post=0.51 cm2/s, p=.35) or the RO (pre=0.51

cm2/s, post=0.51 cm2/s, p=.21). However in five subjects post-salbutamol, 3He ADC for the RNO was statistically significantly higher than the RO (RO=0.46 cm2/s, RNO=0.51 cm2/s, p<.0001). In conclusion, although mean 3He ADC did not significantly change following bronchodilation, comparison of ADC in RO and RNO post-salbutamol indicated that for a subset of COPD subjects, newly ventilated lung regions following salbutamol administration have more emphysematous destruction.

Core Session 3 - Scientific Presentation 3 -

Airway Disease, Emphysema, and Airflow Limitation in Patients with Chronic Obstructive Lung Disease

Hironi Makita, Masaru Hasegawa, Kaoruko Shimizu, Yasuyuki Nasuhara, Satoshi Konno, Katsura Nagai, Tomoko Betsuyaku, Masaharu Nishimura
First Department of Internal Medicine, Hokkaido University Hospital, Japan

Rationale: Understanding of the relative contributions of airway disease and emphysema to airflow limitation in chronic obstructive lung disease (COPD) has been a subject of interest for many years.

Objectives: To examine the relationships between airway dimensions and emphysema severity in the upper and lower parts of the right lung separately using 3D computed tomography, and then to explore the relationships of both pathologic processes to airflow limitation indices on a regional basis.

Methods: Seventy male patients with clinically stable COPD and 10 male smokers at risk served as subjects who underwent pulmonary function tests and computed tomography at full inspiration. Wall area % (WA%) was measured at the 3rd (segmental bronchus) to 6th generation of the two bronchi as a marker of airway disease, and low attenuation volume (LAV%) was measured as a marker of emphysema severity.

Measurements and main results: The relationship between airway dimensions and LAV% was not significant in the upper lung and was weakly significant in the lower lung. The significant correlations observed between WA% and FEV1 (% predicted) were better at the more distal generations of both airways. LAV% correlated significantly with FEV1 (%predicted) only for the lower lung($r=0.621$, $p<0.001$) but not for the upper lung($r=-0.178$, $p= 0.127$).

Conclusions: Relationship of airway disease and emphysema may be different in the upper lung and the lower lung and thus relative contribution of both pathologic processes to airflow limitation may be different according to region of the lung in male patients with smoking-related COPD.

Core Session 4 - Invited Speaker 1 -

Update for Diagnosis of IIP

Takeshi Johkoh, M.D., Ph.D.
Department of Radiology, Kinki Central Hospital of Mutual Aid Association of Public School Teachers, Japan

Idiopathic interstitial pneumonias (IIPs) are a heterogeneous group of diseases characterized histologically by inflammation and fibrosis of the parenchymal interstitial tissue. Their causes are unknown and some degree of airspace disease commonly accompanies the interstitial abnormality in all these conditions. IIPs are a heterogeneous group of diseases characterized histologically by inflammation and fibrosis of the parenchymal interstitial tissue. IIPs are classified acute interstitial pneumonia (AIP), cryptogenic organizing pneumonia (COP), nonspecific interstitial pneumonia (NSIP), usual interstitial pneumonia (UIP), desquamative interstitial pneumonia (DIP), respiratory bronchiolitis-asscociated interstitial pneumonia (RB-ILD) and lymphoid interstitial pneumonia (LIP). Each IIP has characteristic CT findings including extensive areas with ground-glass attenuation, patchy areas of airspace consolidation and architectural distortion in AIP, bilateral peripheral areas of airspace consolidation in COP, areas with ground-glass attenuation with lower and peribronchiolar predominance in NSIP, intralobular reticular opacities and honeycombing distributing mainly in the subpleural regions and lung bases in UIP etc. However, there are several overlaps of their characteristic CT findings. Characteristic CT findings of LIP diagnosed by recent criteria have been unclear. Some cases show lower lobe predominance and areas with ground-glass attenuation. In this lecture, imaging finding of each IIP will be presented paying special attention to its characteristic CT findings and pathologic backgrounds. Moreover, the recent diagnostic criteria of IPF/UIP by ATS-ERS-JRS will be mentioned paying special attention to the drawbacks.

Core Session 4 - Invited Speaker 2 -

Update for Treatment of Idiopathic Interstitial Pneumonias (IIPs)

Kingo Chida
Second Division, Internal Medicine, Hamamatsu University School of Medicine, Japan

The ATS/ERS proposal approaches the classification of IIPs by identifying the pathologic patterns seen on lung biopsy in addition to clinico-radiologic findings, thereby dividing into 7 categories. According to corticosteroid (CS) resposivity, the IIPs are broadly divided into two groups: cases such as NSIP, COP and DIP that respond to CS, and cases with IPF and AIP that poorly respond to CS. Among IIPs, IPF is the most common type of IIPs, and the underlying concept that IPF is primarily an epithelial-fibroblastic disease explains the failure of anti-inflammatory therapy, and consequently, introduction of antifibrotic agents has been expected to improve survival rates of IPF. In this session new treatments for IPF are summarized, including interferon-γ, pirfenidone, antioxidants, anti-TNF-α antibody, endothelin receptor antagonist and BIBF 1120 (triple kinase inhibitor).

Abbreviations:
NSIP: nonspecific interstitial pneumonia
COP: cryptogenic organizing pneumonia
DIP: desquamative interstitial pneumonia
IPF: idiopathic pulmonary fibrosis
AIP: acute interstitial pneumonia

Core Session 4 - Invited Speaker 3 -

Smoking-related Interstitial Pneumonia Associated with Emphysema

Minoru Kanazawa[1], Akiko Kaga[1], Shohei Minezaki[1], Yutaka Usui[1], Fumikazu Sakai[2]
1. Department of Respiratory Medicine, Saitama Medical University, Japan
2. Department of Diagnostic Radiology, Saitama Medical University, Japan

Cigarette smoking affects many diseases such as chronic obstructive pulmonary disease, lung cancer and cardiovascular diseases. Cigarette smoking may also prime the lung toward a fibrotic response and participates in the etiology of a spectrum of fibrosing lung diseases, including idiopathic interstitial pneumonias (IIPs). The purpose of the presentation is to clarify clinical and radiographic features of chronic fibrosing IIPs, especially in view of the influence of smoking history. One hundred and eight consecutive patients with chronic IIPs were studied. They were devided into three groups according to smoking history and presence of centrilobular emphysema (CLE) on HRCT. The three groups were: fibrosing IIP with CLE and smoking history (IPE, n=54), fibrosing IIP without CLE but with smoking history (IPS, n=33) and fibrosing IIP without smoking (IPNS, n=21). Forty two out of 54 patients with IPE showed thick-walled large cysts (TWLC) more than 2cm in diameters. Ten out of 33 showed TWLC in IPS group and none demonstrated TWLC in the IPNS group. The mean %VC was 90% in IPE, 89% in the IPS, 59% in the IPNS, and was decreased in IPNS. The mean FEV1% was 77%, 83%, 88%, and was decreased in the IPE. The mean %DLCO was 56%, 73%, 67%, respectively, and was decreased in the IPE. TWLC is characteristic of chronic fibrosing IIPs with smoking history. UIP pattern may be highly associated with the progression as well as the development of TWLC in subjects with smoking history.

Core Session 4 - Invited Speaker 4 -

Hyperpolarlized Noble Gas MRI for ILD

Hiroto Hatabu, Iga Muradyan, Mirko I. Horvat, Mikayel Debaghyan, George R. Washko, James P. Butler, Samuel Patz
Center for Pulmonary Functional Imaging, Department of Radiology, Brigham and Women's Hospital and Harvard Medical School, USA

Hyperpolarized $_{129}$Xe NMR was utilized to measure pulmonary alveolar surface area per unit gas volume S_A/V_{gas}, alveolar septal thickness h, and capillary transit time. The global S_A/V_{gas}, h, and capillary transit time were measured in normal subjects and subjects with mild interstitial lung disease. These are the first noninvasive, non-radiation based, quantitative measurements of alveolar septal thickness and capillary transit time in patients with pulmonary disease. This new approach may open a new window to monitor disease progression and treatment response in patients with interstitial lung disease.

Core Session 4 - Scientific Presentation 1 -

Prognostic Significance of High-Resolution Computed Tomography in Nonspecific Interstitial Pneumonia

Hironao Hozumi[1], Yutaro Nakamura[1], Takeshi Johkoh[1,2], Hiromitsu Sumikawa[3], Hiroshi Hayakawa[1], Koushi Yokomura[1], Kazumasa Yasuda[1], Toshihiro Shirai[1], Takafumi Suda[1], Kingo Chida[1]

1. The Second Division, Department of Internal Medicine, Hamamatsu University School of Medicine, Japan
2. Department of Radiology, Kinki Central Hospital of Mutual Aid Association of Public Teachers, Japan
3. Department of Radiology, Osaka University Graduate School of Medicine, Japan

Purpose: To assess the prognostic implications of high-resolution computed tomography (HRCT) findings for patients with biopsy-proven nonspecific interstitial pneumonia (NSIP).

Materials and Methods: 59 patients with biopsy-proven NSIP (25 idiopathic NSIP, 34 collagen-vascular disease-associated NSIP) were included in this retrospective study. Data and HRCT images were obtained before surgical lung biopsy and treatment. Two chest radiologists independently evaluated the extent, presence and distribution of various HRCT findings of NSIP patients. Cox proportional hazards regression analysis was used to assess the relationship between HRCT findings and survival outcome.

Results: The median observation period was 1477 days, ranging from 289 to 4526. Among all patients, the 5-year survival rate was 83% and the 10-year survival rate was 66%. Univariate analysis revealed that the extent of GGO without bronchi-bronchiolectasis (hazard ratio = 0.78, $P < 0.01$) and total consolidation (hazard ratio = 0.83, $P = 0.04$) were associated with favorable outcome whereas the extent of intralobular reticular opacity (hazard ratio = 1.23, $P < 0.01$) was associated with worse prognosis. Multivariate analysis revealed that the extent of total consolidation was an independent prognostic factor of favorable outcome (hazard ratio = 0.59, $P = 0.03$).

Conclusion: In patients with biopsy-proven NSIP, detailed analysis of HRCT is useful for predicting outcome.

Core Session 4 - Scientific Presentation 2 -

Automatic Classification of Regional Disease Pattern of Diffuse Lung Disease at HRCT: Cross-Vendor Study

Kim, Namkug[1], Youngjoo Lee[1], Joon Beom Seo[1], David A Lynch[2]

1. Department of Radiology, Ulsan Unversity College of Medicine, Asan Medical Center, Korea
2. Division of Radiology, National Jewish, University of Colorado Denver, USA

To investigate the effect of HRCT images from different vendors on classification accuracy for regional disease pattern analysis of diffuse lung disease (DLD).

Using HRCT images from vendor A and B, two sets of 600 rectangular regions of interest (ROIs) with 20x20 pixels, comprising of each 100 ROIs representing six regional disease patterns (normal, GGO, reticular opacity, honeycombing, emphysema, and consolidation) were marked by two experienced radiologists with consensus at HRCT images of various DLDs. Each ROI image, then, was represented by 28 features (histogram, gradient, run-length, GLCM, LAA cluster, and top-hat transform). For automatic classification, support vector machine was employed to generate a classification model. Firstly, classification accuracies using each vendor's data were estimated by a 10-folding cross validation with 20 repetitions (internal-vendor study). Secondly, A and B data were used for training and testing, respectively, and vice versa (cross-vendor study). Finally, all ROI data were integrated, trained and tested by 2-folding cross validation with 20 repetitions (integrated data study).

On internal-vendor study, the accuracies of vendor A and B were $89.4 \pm 0.98\%$ and $89.8 \pm 0.79\%$,

respectively. The classification accuracies of cross-vendor study were 45.8 ± 0.85% when training vendor A data and testing vendor B data, and 42.7 ± 0.81% vice versa (t-test, p=0.000). On integrated data study, accuracy was 88.3 ± 1.48%. Selected features were different among the studies.

It is recommended to train automatic classifiers for each vendor separately or to build an automatic classifier with integrated data set if needed.

Core Session 4 - Scientific Presentation 3 -

FDG Positron Emission Tomography Imaging of Drug-induced Pneumonitis

Miwa Morikawa[1], Yoshiki Demura[2], Yukihiro Umeda[1], Shingo Ameshima[1], Takeshi Ishizaki[1], Hidehiko Okazawa[3]

1. Department of Respiratory Medicine, University of Fukui, Japan
2. Department of Respiratory Medicine, Ishikawa Prefectural Central Hospital, Japan
3. Biomedical Imaging Research Center, University of Fukui, Japan

Fluorine-18-labeled fuluoro-2-deoxy-D-glucose positron emission tomography (FDG-PET) is increasingly used for diagnosing lung cancer, but FDG accumulation is not specific to malignancy. There are numerous causes of FDG uptake in benign processes, such as inflammatory lung disease. However, 67Ga scintigraphy has been widely used for the evaluation of interstitial pneumonitis. Several studies have reported the findings of FDG-PET in benign lung disease with diffuse pulmonary injury, but the characteristics and effectiveness of FDG-PET imaging for interstitial pneumonitis have not been substantiated. We report two cases of drug-induced pneumonitis in two patients treated for breast cancer who were diagnosed by FDG-PET examination.

Both of these cases showed diffuse interstitial infiltration in the bilateral lungs on CT, but the degree of FDG accumulation was different. It is probable that the degree of FDG accumulation reflected the activity of the drug-induced pneumonitis. The present cases show very interesting FDG-PET imaging findings of diffuse lung disease.

Core Session 5 - Invited Speaker 1 -

Pathophysiology of Asthma

Hiromasa Inoue, M.D.
Department of Pulmonary Medicine, Graduate School of Medical and Dental Sciences,
Kagoshima University, Japan

Bronchial asthma is characterized by chronic inflammation, eosinophilic infiltration, reversible airway narrowing, airway hyperresponsiveness (AHR) to non-specific stimuli, hyperplasia/metaplasia of goblet cells, hypertrophy/hyperplasia of airway smooth muscle cells and subepithelial fibrosis. It is now considered that airway inflammation and structural changes of the airways are important features. T helper 2 (Th2) cells are the predominant lymphocyte population that infiltrates the airways of asthmatics, and Th2 cytokines, such as IL-4, IL-5, and IL-13, play essential roles in airway eosinophilia, AHR, and serum IgE in animal models. These cytokines bind to receptors at the cell surface to activate complex signal transduction pathways, including JAK-STAT and Ras-ERK signaling pathways. This presentation will cover the function of cytokine signaling pathway in pathophysiology of asthma and discuss new therapeutic targets. The suppressor of cytokine signaling (SOCS) family proteins has been shown to regulate JAK-STAT, and the Sprouty-related EVH1-domain-containing protein (SPRED) family proteins regulate the Ras-ERK pathway. In the inflammatory/immune cells, SOCSs contribute to helper T cell differentiation during immune responses, and SPRED-1 negatively controls the eosinophil numbers and functions by modulating IL-5 signaling. In the airway structural cells, SOCS1 induction by IL-13 is critical to negatively control asthma. Airway cells from asthmatics had impaired in upregulation of SOCS1 after IL-13 stimulation. Therefore, modulators of Th2 responses including the negative regulators of cytokine signals may improve our understanding of these processes to asthma and hold therapeutic potential in asthma.

Core Session 5 - Invited Speaker 2 -

Evaluation of Airway Obstruction and Altered Pulmonary Permeability with Lung Scintigraphy in Young Patients

Mayuki Uchiyama, M.D.
Department of Radiology, The Jikei University School of Medicine, Japan

The ^{133}Xe ventilation scan shows three distinct phases. The initial phase is the wash-in or ventilation phase. The second phase is the equilibrium phase representing the gas volume. Finally, the wash-out phase, when the ^{133}Xe has been disconnected, gives information about the possibility of any gas trapping, which may occur in obstructive airways disease. In addition to imaging with ^{99m}Tc-DTPA aerosol of the disappearance rate of tracer from regions of the lung can provide further information about lung permeability and may degrade the ventilation images very rapidly.

In contrast to the adult form of rheumatoid disease, follicular bronchiolitis appears to be the most common manifestation of pulmonary involvement in the juvenile form. Bronchiolitis obliterans appears in patients with chronic graft-versus-host disease. The ^{133}Xe ventilation scan and the ^{99m}Tc-DTPA aerosol inhalation scan can be performed in young patients with bronchiolitis obliterans safety and evaluated in quantitative analysis. These lung scans are considered useful as a method for diagnosing in early stage and a follow-up to bronchiolitis and interstitial pneumonitis, provided that pulmonary function tests and CT show normal patterns and images.

Metered dose inhalation therapy of beta agonist or steroid is gaining popularity in the treatment of bronchial asthma, and the spacer is applied to distribute the drug to the lung stably and diffusely. The inhalation scan is useful to assess the effect of spacer on deposition rate and distribution of the medicine in the lung, besides response to the therapy.

Core Session 5 - Invited Speaker 3 -

CT Assessment for Asthma

Hiroshi Tanaka, M.D.
Third Department of Internal Medicine, Sapporo Medical University School of Medicine, Japan

Bronchial wall thickening, air-trapping, and mosaic pattern at deep inspiration are characteristic CT findings of stable asthma. Thickened central bronchial wall is excellently correlated with predicted FEV1, and low attenuation area without destruction of inter lobular septa is correlated with RV/TLC. Central airway diseases are almost even, however peripheral airway diseases are uneven and ventilation heterogeneity is apparent during asthma exacerbation. Previous reports have provided evidence that area of peripheral airway diseases move in each exacerbation using radioisotope or CT scans. In general, heterogeneity of peripheral airway disease is measured by closing volume, slope of phase Ⅲ of single N2 washout test. Pathological findings of open lung biopsy specimens during asthma exacerbation demonstrate that 1) peripheral airways are filled with sputum, 2) peripheral airways are dilated by accumulated sputum, and 3) the degrees of these diseases are uneven in the lung. Pathological-radiological correlation shows that ground glass opacities are peripheral airway disease under the diameter of 500 micrometer, centrilobular nodules are dilated peripheral airways filling with sputum. And all findings disappear after asthma treatment. However, severe persistent asthma remains centrilobular nodules for a long time, which may contribute to persistent severe obstructive change. CT scans of patients with aspirin induced asthma during asthma exacerbation reveal that thickening of inter lobular septa and pleural effusion in addition to ordinary asthma exacerbation, suggesting edema of pulmonary parenchyma. In this session, I focus on heterogeneity of peripheral airway disease, using pulmonary function test, CT finding and pathological features.

Core Session 5 - Invited Speaker 4 -

MR Assessment of Asthma; Hyperpolarized ^{3}He Magnetic Resonance Imaging to Probe Temporal and Spatial Airway Functional Changes

Grace Parraga
Imaging Research Laboratories, The University of Western Ontario, Canada

Asthma is diagnosed in an estimated 300 million people worldwide and it claims the lives of 250,000 people annually. Clinical diagnosis is typically achieved using methods that report global lung function such as spirometry measurements of the forced expiratory volume in 1 s (FEV1) during a methacholine challenge. Recently, pulmonary functional imaging with hyperpolarized ^{3}He magnetic resonance imaging (MRI) has identified the spatial and temporal heterogeneity of asthma and the apparent persistence of ^{3}He MRI ventilation abnormalities or defects over time in asthma subjects. These ventilation defects are believed to be related to airway functional changes in asthma due to airway collapse/constriction or increased time constants for filling lung tissue due to other reasons. We present and summarize recent results of hyperpolarized ^{3}He MRI for the quantitative evaluation of asthma over time, before, and immediately after both exercise and methacholine challenge and then after recovery. We also present evidence of the utility of both ^{3}He ventilation and apparent diffusion coefficients for understanding regional differences between the normal and asthmatic lung. We also review current methods for generating and evaluating airway functional changes that appear to be "persistent" over time (ventilation probability maps) and evaluate the potential for ^{3}He MRI ventilation probability maps for therapy guidance and for predicting asthma changes over time.

Core Session 5 - Invited Speaker 5 -

Update for Treatment of Asthma

Kazuto Hirata, M.D., Ph.D.
Department of Respiratory Medicine, Graduate School of Medicine, Osaka City University, Japan

Medication plans should be selected on the basis of the severity of asthma, availability of antiasthma medications, conditions of health care system, and individual patient circumstances to achieve best control. Therapeutic strategy for asthma, the basically standard medication is inhaled corticosteroids (ICS). ICS reduces the risk of hospitalization or mortality in elderly asthmatic patients as same as in younger adult asthmatic patients. The addition of a long-acting beta-agonist (LABA) including combination LABA and ICS or the addition of a leukotriene modifier improves symptoms in patients with inadequately controlled asthma by ICS. Recently, It is reported that the addition a long-acting anticholinergic agent, tiotropium improved symptoms and lung function in these patients. But a careful treatment is required in some asthmatic patients who cannot inhale drugs or cannot adhere to their treatment regimens well.

Smoking, obesity, elderly asthma and comorbidity with chronic sinusitis are well known risk factors of uncontrolled asthma by ICS. Especially smoking is a risk factor for accelerated lung function deterioration, impaired corticosteroid response, and increased mortality, so smoking cessation is strongly recommended. Diet modification and weight loss intervention are also recommended for obesity. For severe asthma with fixed airway obstruction, an anti-IgE therapy is recommended in the patients with persistent eosinophilic airway inflammation, and macrolids antibiotics and PDE4 inhibitor may improve non eosinophilic inflammation, particularly neutrophilic inflammation.

Core Session 5 - Scientific Presentation 1 -

The Effect of Methacholine Challenge on Ventilation Heterogeneity in Asthma Measured by SPECT

Gregory G. King[1], Catherine Walsh[1,3,4], Dale Bailey[1,2,3], Cheryl Salome[1,3,4]

1. The Woolcock Institute of Medical Research, Australia
2. Department of Nuclear Medicine, Royal North Shore Hospital, Australia
3. Central and Northern Clinical Schools, Sydney Medical School, Sydney University 2006, Australia
4. Cooperative Research Centre for Asthma, Australia

Introduction: In asthma ventilation is heterogeneous and airway closure is increased, both being associated with greater asthma severity and airway hyperresponsiveness. Heterogeneous ventilation has been demonstrated by various imaging techniques but the changes in spatial distribution during bronchoconstriction, and the predictors of that change are unknown.
Hypothesis: that the spatial heterogeneity of ventilation in Technegas SPECT correlates with global measures of ventilation distribution and that it increases with methacholine challenge.
Methods: 14 Asthmatic subjects underwent Technegas SPECT/CT before and after bronchial challenge. 1L breaths of Technegas were inhaled from FRC, in upright posture before SPECT and CT acquisition in supine posture. Technegas distribution was measured by plotting the ventilated volume determined from 3 different thresholds vs those thresholds, in log-log space (TechnegasDIST). Ventilation distribution was also measured by multiple breath nitrogen washout (MBNW) from which Sacin and Scond were calculated, as indices of heterogeneity in diffusion dependent airways and in small, conducting airways, respectively.
Results: FEV1 was 87.5 ± 15.8 % predicted and 7 subjects had AHR. Methacholine challenge decreased FEV1 by 23 ± 5% of baseline. TechnegasDIST increased from -0.35 ± 0.03 to -0.47 ± 0.15 (p=0.008). TechnegasDIST at baseline was unrelated to spirometry or MBNW indices. However, the post-methacholine TechnegasDIST and the change from baseline, correlated with baseline Sacin (r=-0.62, p0.17 and r=-0.64, p=0.013, respectively).
Conclusions: The spatial distribution of ventilation measured by Technegas SPECT increases with methacholine challenge which in turn, is predicted by baseline heterogeneity in diffusion dependent airways. The anatomical basis of ventilation distribution requires further study.

Core Session 5 - Scientific Presentation 2 -

Surface Irregularity of Airway Walls as Assessed by MDCT in Asthmatic Patients

Tsuyoshi Oguma, Akio Niimi, Hisako Matsumoto, Isao Ito, Hitoshi Nakaji, Hideki Inoue, Toshiyuki Iwata, Tomoko Tajiri, Tadao Nagasaki, Michiaki Mishima

Department of Respiratory Medicine, Graduate School of Medicine, Kyoto University, Japan

[Backgrounds] In asthmatic patients, airway wall remodeling is observed both at large and small airways. Injury to the epithelium is a common finding in asthma, and loss of alveolar attachments at small airways was reported in severe fatal asthma. But few reports have described structural changes in outer layer of large airways.
[Objectives] To analyze inner and outer surface irregularity of central airways using multi-detector row CT (MDCT) and examine its correlations with clinical variables.
[Methods] CT scans were performed in treatment-naive asthmatic patients. Then, inner radius and wall thickness of all segmental bronchi were calculated by using three-dimensional reconstruction, and coefficient of variation (CV) of distance from center line to inner and outer walls at each bronchus were calculated. Finally, correlations between clinical variables and averaged CV of all right segmental bronchi were calculated.
[Results] Averaged CV of both inner and outer wall showed negative correlation with FEV1, FEF25-75 of spirometory and airway hyperresponsiveness estimated by Dmin of acetylcholine using Astograph, and positive correlation with R5 R20 R5-R20 and AX of impulse oscillometry. They showed no significant correlation with exhaled NO or sputum eosinophils.
[Conclusions] Surface irregularity of airway walls may have some relations with disease severity of asthma, although its pathological mechanism is not unclear.

Core Session 5 - Scientific Presentation 3 -

Intrathoracic Tracheal Volume and Collapsibility on Inspiratory and End-expiratory CT Scans: Correlations with Lung Volume and Pulmonary Function in 85 Smokers

Tsuneo Yamashiro[1], Raul San Jose Estepar[2], Shin Matsuoka[3], Brian J. Bartholmai[4], James C. Ross[2], Alejandro Diaz[5], Sadayuki Murayama[4], Edwin K. Silverman[5], Hiroto Hatabu[2], George R. Washko[5]

1. Department of Radiology, Graduate School of Medical Science, University of the Ryukyus, Japan
2. Department of Radiology, Brigham and Women's Hospital, USA
3. Department of Radiology, St. Marianna University School of Medicine, Japan
4. Department of Radiology, Mayo Clinic, USA
5. Pulmonary and Critical Care Division, Brigham and Women's Hospital, USA

Objectives: To evaluate the correlations of tracheal volume and collapsibility on inspiratory and end-expiratory computed tomography (CT) with lung volume and with lung function in smokers.

Materials and Methods: An institutional review board approved this study at each institution. 85 smokers (age range 45-87 years), enrolled in the Lung Tissue Research Consortium, underwent pulmonary function tests and chest CT at full inspiration and end-expiration. On both inspiratory and end-expiratory scans, intrathoracic tracheal volume (from the apex to the carina) and lung volume were measured by open-source software. Collapsibility of the trachea and the lung was expressed as expiratory/inspiratory (E/I) ratios of these volumes. Correlations of the tracheal measurements with the lung measurements and with lung function were evaluated by the linear regression analysis.

Results: Tracheal volume correlated with lung volume on both inspiratory ($r=0.661$, $p<0.0001$) and end-expiratory ($r=0.749$, $p<0.0001$) scans. The E/I ratio of tracheal volume also correlated with the E/I ratio of lung volume ($r=0.711$, $p<0.0001$). The E/I ratio of tracheal volume negatively correlated with the ratio of forced expiratory volume in the first second to forced vital capacity (FEV1/FVC) ($r=-0.436$, $p<0.0001$). A weak, positive correlation was observed between the E/I ratio of tracheal volume and the ratio of residual volume to total lung capacity (RV/TLC) ($r=0.253$, $p=0.02$).

Conclusions: Tracheal volume and collapsibility, measured by inspiratory and end-expiratory CT scans, is related to lung volume and collapsibility. The highly collapsed trachea on end-expiratory CT does not indicate more severe airflow limitation or air-trapping in smokers.

Core Session 6 - Invited Speaker 1 -

Aims of Respiratory Motion Assessment for Anesthesiology

Klaus Markstaller
Chair, Division of General Anesthesia and Intensive Care
Medical University of Vienna / AKH Vienna

From time immemorial, lung physiology has been explained in concepts assuming staedy state conditions. Within the last decade clear evidence has been found, that lung ventilation and perfusion are highly dynamic processes, with regional inhomogeneities in their kinetics. This holds specifically true in the injured lung.

Cyclic recruitment of atelectasis ("atelectotrauma"), and regional lung overdistention due to high airway pressures ("barotrauma") or high tidal volumes ("volutrauma") have been shown to lead to an inflammatory response of lung tissue ("biotrauma"). These iatrogenic mechanisms during mechanical ventilation are summarized in the definition of "ventilator associated lung injury".

Thus, novel therpeutic strategies require dynamic and regional information of lung ventilation and perfusion. Dynamic computed tomography and magetic resonance imaging with inhalative contrast agents have brought new insights and became an emerging research field. However, up to this point, these imaging modalities are not routinely applied in the treatment of patients with acute lung injury. Non-invasive and bedside imaging technologies like electrical impedance tomography or vibration response imaging could serve as a bridge to bring the imaging information from the bench to the bedside.

Core Session 6 - Invited Speaker 2 -

MR Assessment of Respiratory Motion

Tae Iwasawa
Department of Radiology, Kanagawa Cardiovascular and Respiratory Center, Japan

MR is a suitable tool for observing respiratory motion noninvasively. From 1980s dynamic images applies to assess the chest wall motion. Recent advances in MR allow to visualize internal motion of the lung. Voorhees A, et al applied 3D tagging method and showed the lung internal motion in tidal breathing [1]. Plathow C et al. measured the motion of the lung tumor in 3D-dynamic MRI [2]. We developed a system to trace the pulmonary vessels on 2D dynamic MRI [3]. In this presentation I will introduce recent results using this system. Shibata H et al. showed the motion of the pulmonary vessels was restricted in the patients with chronic obstructive lung disease (COPD), and movement of the vessels on MR significantly correlated with airflow limitation evaluated by spirometry [4]. Shinohara T et al. evaluated the COPD patients using 2D dynamic MRI before and after rehabilitation [5]. After rehabilitation, the movement pattern of the pulmonary vessels changed to similar pattern observed in normal volunteers. These results suggest that motion of the pulmonary vessels reflects the expansion and deflation of the lung parenchyma. This method will be a tool to investigate the respiratory mechanics.

1. Voorhees A, et al. Magn Reson Med 2005; 54: 1146-1154
2. Plathow C, et al. Radiology. 2006, 240: 537-45
3. Gotoh T, et al. 18th IFAC world Congress.
4. Shibata H, et al. 5th IWPFI
5. Shinohara T, et al. 5th IWPFI

Core Session 6 - Invited Speaker 3 -

Nuclear Medicine Assessment for Respiratory Lung Motion

Kazuyoshi Suga, M.D.[1], Ue Hideaki, Ph.D.[2], Hideaki Haneishi, Ph.D.[2], Hideyuki Iwanaga, Ph.D.[1], Naofumi Matsunaga, M.D.[1]

1. Department of Radiology, Yamaguchi University School of Medicine, Japan
2. Research Center for Frontier Medical Engineering, Chiba University, Japan

Purpose: Regional respiratory lung motion was analyzed by 3D displacement vector images obtained from a nonlinear motion correction technique for inspiratory and expiratory perfusion SPECT.
Methods: 21 patients with COPD, 10 patients with pulmonary thromboembolism and 6 healthy controls underwent respiratory-gated perfusion SPECT. In a process of nonlinear motion correction between expiratory and inspiratory SPECT, the direction and magnitude of the displacement of each voxel were imaged as 3D displacement vector images, which were used for qualitative and quantitative analysis of respiratory regional lung motion. The findings were correlated with Tc-99m Technegas ventilation study.
Results: In controls, 3D displacement vector images showed regular, symmetric respiratory lung expansion towards caudal direction, with the largest motion in the lower dorsal portion. In COPD patients, these images showed focally irregular and decreased lung motion, with occasional paradoxical lung motion. In 23 (95%) of these patients, the lung areas with the worst or paradoxical motion were consistent with the most severely disturbed ventilation sites assessed on Technegas ventilation study. All PTE patients except for one patient with pleural effusion showed regular, symmetrical lung motion, similar to healthy controls. Quantitatively, the normalized cranio-caudal lung motion index in the entire lungs of COPD patients was significantly less compared with that of the control values (0.25 ± 0.01 vs 0.43 ± 0.08; $P < 0.01$).
Conclusion: 3D displacement vector images obtained from gated perfusion SPECT are useful for assessment of impaired regional respiratory lung motion in COPD patients.

Core Session 6 - Invited Speaker 4 -

Dynamic Volume Scan Using 320-row ADCT for the Assessment of Respiratory Motion

Hiroshi Moriya
Sendai Kousei Hospital Department of Radiology, Japan

The development of 320-row area detector CT (ADCT) has made it possible to perform dynamic volume scanning. A range of 160 mm can be scanned in a single rotation in a short time of 0.35s. ADCT provides superior performance in terms of both temporal resolution and spatial resolution. The acquired data can be obtained in the same time phase regardless of the position in the axial direction. Using dynamic volume scanning, temporal uniformity and four-dimensional data can be acquired.

In the chest region, dynamic volume scanning is a simple method to evaluate the various respiratory mechanics. For example, diaphragm motion, chest wall motion, intrathoracic tumor mobility, deformity of trachea, bronchus and lung tissue during the respiration cycle.

Controlling the exposure dose is one of the main issues that must be addressed. Thus, mainly 3 types of scanning protocols (intermittent scan, respiration-gated scan, and continuous scan) with low-dose exposure have been used. By adjusting the number of scan, tube voltage, tube current, and noise-reduction reconstruction method, we have to try to obtain the four-dimensional data without compromising image quality.

Core Session 6 - Invited Speaker 5 -

Respiratory Motion Assessment to Increase the Accuracy of Non-contact Screening System to Prevent the Spread of Infectious Diseases

Takemi Matsui
Faculty of System Design, Tokyo Metropolitan University, Japan

Pandemic influenza A(H1N1) virus emerged worldwide in 2009. WHO provided guidance on public health measures, including entry screening at airports to reduce the risk of transmission. A number of countries have already applied thermography at international airports in order to detect infected passengers. However, the effectiveness of the conventional screening system using thermography is limited in detecting asymptomatic or sub-clinical infections. In order to conduct more accurate and fast screening, we have developed a non-contact screening system that can perform human medical inspections within ten seconds. The system monitors not only temperature but also heart and respiratory rates, which leads to an increase in accuracy in detecting infected individuals. The system is operated by a screening program via a linear discriminant analysis using non-contact derived variables, i.e., palmar pulse derived from a laser Doppler blood-flow meter, respiration rate determined by a 10-GHz microwave radar, and average facial temperature measured by thermography. In our case control study, the discriminant function of this system is found to be effective in distinguishing influenza patients regardless of their temperatures. This can be attributed to the fact that even in the cases of influenza patients with normal temperatures, their heart and respiratory rates are relatively high compared with normal subjects. The system enables PPV rate of 93%, which is much higher than the conventional method using only thermography. It can be improved for future applications to reduce the risk of transmission of infectious diseases.

Matsui T, Hakozaki Y, Abe S. et.al. A novel screening method for influenza patients using a newly developed non-contact screening system. J Infect. 2010;60(4):271-7.

Core Session 6 - Scientific Presentation 1 -

Temporal Stability of the 4D-CT Pulmonary Ventilation Imaging Method

Tokihiro Yamamoto[1], Sven Kabus[2], Jens von Berg[2], Cristian Lorenz[2], Billy W. Loo, Jr.[1], Paul J. Keall[1]

1. Department of Radiation Oncology, Stanford University, USA
2. Department of Digital Imaging, Philips Research Europe, Hamburg, Germany

Purpose: A novel pulmonary ventilation imaging method based on four-dimensional (4D) computed tomography (CT) has advantages over existing methods and could be used for functional avoidance in lung cancer radiotherapy as 'free' information. The purpose of the present study was to quantify the temporal stability of the 4D-CT ventilation imaging method from repeat scans.

Methods: Two 4D-CT ventilation images from repeat scans (interval range, 9-13 days) in the absence of therapeutic intervention were created for three radiotherapy patients with lung cancer. Both the Hounsfield-unit (HU) change-based metric (V_HU) and Jacobian-based metric (V_Jac) were used to create the ventilation images from the displacement vector fields. The second 4D-CT ventilation image was deformed into the domain of the first ventilation image for the analysis. The voxel-based Spearman's rank correlation coefficients between two ventilation images were quantified.

Results: From visual inspection, repeat 4D-CT ventilation images showed regions of agreement and disagreement for both V_HU and V_Jac. The correlation coefficients ranged from 0.30 to 0.47 for V_HU, which were consistently lower than those for V_Jac ranging from 0.38 to 0.66. It was found that the large differences between two ventilation images mainly manifested around the interfaces between two adjacent 4D-CT data segments, and also around the 4D-CT artifacts (especially diaphragm).

Conclusions: The temporal stability of 4D-CT pulmonary ventilation imaging was weak to moderate and varied between patients and ventilation metrics. Future work will investigate the spatial characteristics of the stability of 4D-CT ventilation images for more patients.

Core Session 6 - Scientific Presentation 2 -

Analysis of Respiratory Movement Using 4-Dimensional Chest CT image

Seiji Tani[1], Kazuo Noma[1], Hidenobu Suzuki[2], Shinsuke Saita[2], Yoshiki Kawata[2], Noboru Niki[2], Masayoshi Miyazaki[3], Yasutaka Nakano[4]

1. Graduate School of Advanced Technology and Science, The University of Tokushima, Japan
2. Institute of Technology and Science, The University of Tokushima Graadute School, Japan
3. Osaka Medical Center for Cancer and Cardiovascular Disease, Japan
4. Shiga University of Medical Science, Japan

Recent improvements in radiotherapy technology have enabled the respiratory gating system. The system tracks patient's respiratory cycle using camera and reflective marker. In this study, we quantitatively analyze respiratory movement of pulmonary organs and nodules using 4-dimensional chest Computed Tomography images, aim for the therapeutic application.

Firstly, we apply automatic segmentation of pulmonary organs, lung, pulmonary blood vessel, trachea, bronchus, interlobar fissure, lung lobe, rib, and spine. Secondly, lung nodules are segmented. Thirdly, volumetric variation and locational motion of the organs and nodules with respiration are visualized and quantified.

Core Session 6 - Scientific Presentation 3 -

Asymmetry of the Mechanical Property in the Human Respiratory System Causes the Asymmetry of the Lingual Center in the Brain: Diaphragmatic Motion Analysis with Dynamic MR Images

Hiroko Kitaoka[1], Koji Chihara[2]
1. Division of Engineering Technology, JSOL Corporation, Japan
2. Division of Thoracic Surgery, Shizuoka City Shizuoka Hospital, Japan

The reason why the lingual center is located in the left hemisphere has been unknown. Here, we propose a hypothesis that asymmetric diaphragmatic motion during vocalization leads the motor lingual center to the left side. Recent comparative neurophysiologic research strongly suggests that animal vocalization is the origin of the language. Meaningful vocalization is performed not only by acoustic source organs such as vocal cords, but also by the respiratory system which generates and controls expiratory airflow. During vocalization, abdominal muscles work so as to control diaphragmatic motion and to control expiratory airflow rate. There is an extreme difference in organs located beneath the diaphragm between the right and the left sides. The solid liver is expected to convert horizontal force generated by the abdominal muscles into vertical force much more precisely than the air-containing stomach. Consequently, the information from the right pleura is expected to be used for control of vocalization. In order to validate the hypothesis, we acquired dynamic 2D MR images for a normal volunteer on the frontal section at the center of the thorax at supine posture, and measured diaphragmatic motions both at rest and during singing. The result indicated that there was significant difference between right and left diaphragmatic motions only during singing. The right diaphragmatic motions were completely coherent to vocalization but the left diaphragmatic motions were often paradoxical. The importance of abdominal breathing should be investigated more intensively in relation to the lingual function as well as the respiratory physiology.

Abstract

Poster Session

Poster Session 1 - 1

Follow-up Cases with Perfusion Scintigraphy in Patients with Pulmonary Thromboembolism

Shigeru Tominaga, Shinichi Sasaki, Yasuko Yosioka, Masayosi Yosioka, Kengo Koike, Yoko Katura, Yukiko Nanba
Department of Respiratory Medicine, Juntendo University Urayasu Hospital, Japan

We investigated the recovery course of pulmonary perfusion on Tc-99m-MAA pulmonary perfusion scintigraphy in nineteen patients with pulmonary thromboembolism. We classified 19 patients into 2 groups in whom the onset day was evident (Group A) and those in whom the onset day was not evident (Groupe B). Group A consisted of 10 patients in which 7 patients had underlying disease, such as malignant and autoimmune diseases, and thrombolytic and anticoagulant therapies were performed in 3 and all patients, respectively. Perfusion defects on scintigraphy were completely and partially recoovered within 2 weeks of therapy in 3 and 5 patients, respectively. Since responses to therapy were good, re-examination for course observation should be performed within 12weeks in cases meeting the group A conditions. Group B consisted of 9 patients in which 6 patients had underlying diseases, and thrombolytic and anticoagulant therapies were performed in 1 and all patients, Only 1 and 2 cases were completely and partially recovered within 2 weeks after the initiation of therapy, respectively, showing low response. This group included cases with delayed discovery and diagnosis due to the slow progression of symptoms. No improvement of pulmonary perfusion was noted in 3cases of chronic pulmonary thromboembolism. One case completely recoverd after 4 years, showing that long term follow-up by perfusion scintigraphy is necessary to investigate whether partial recovery case meeting the condition of 2 groups completely recover or enter chronic state.

Poster Session 1 - 2

Most Optimum Display Condition(Width,Center) of Dual Energy Perfusion CT for Diagnosing Pulmonary Embolism

Tomohiro Suzuki, Masaki Hara, Motoo Nakagawa, Yoshiyuki Ozawa, Keita Sakurai, Yuta Shibamoto
Department Radiology, Nagoya City University Graduate School of Medical Sciences, Japan

PURPOSE: Recently computed tomography pulmonary angiography (CTPA) becomes an alternative to conventional perfusion scintigraphy for diagnosing pulmonary embolism (PE). Using dual energy (DE) technique of dual source CT (DSCT) it becomes possible to visualize the information of pulmonary perfusion in addition to thrombus in pulmonary arteries. Although dual energy iodine value (DEIV) calculated on DECT is an absolute value, the perfusion images using color scale might be affected by window settings. In this study we investigated the optimum display settings of DECT using DSCT for diagnosing PE.

MATERIAL AND METHOD: Thirty-one lesions diagnosed with pulmonary artery embolism by perfusion scintigraphy and 66 regions evaluated as normal in 13 patients were enrolled. Scanners were SOMATOM Definition (SIEMENS) using DE mode (80 and 140 kVp), pitch: 0.5 and rotation time: 0.33 seconds and E. CAM (SIEMENS) using 185 MBq of 99mTc-MAA.

RESULT: DEIVs (average ± SD) of lesions and normal areas were 12.3 ± 10.6 and 34.9 ± 6.9, respectively. The optimum display settings to separate the both groups would be expected as window center of 20-25 and window width of 15-20. The results of CT and SPECT were correlated well in all cases except for one location that showed normal on CT with a defect on scintigraphy.

CONCLUSION: The appropriate display settings to differentiate the areas with perfusion defect from those with normal blood flow were determined on DE mode of DSCT. DECT might replace perfusion scintigraphy.

Poster Session 1 - 3

Pulmonary CT Perfusion Imaging in Assessment of Pulmonary Vascular Disease- First Experience Using 320-MDCT.

Edwin J.R. van Beek, John H Reid, John T Murchison
Clinical Research Imaging Centre, University of Edinburgh, UK

Introduction: There is increasing evidence that pulmonary embolism may lead to significant vascular bed alterations, including the development of pulmonary hypertension in 5-7% of patients. MDCT using 320-slice system can provide volumetric perfusion data in a single rotation at acceptably low-dose radiation to make this a possible clinically useful application.

Materials and Methods: We studied 5 subjects with suspected pulmonary hypertension (one with liver cirrhosis and four following large pulmonary emboli). Patients underwent expiratory breath-hold CT following 70 ml Iomeron 400 mg I/ml (Bracco) and 30 ml saline flush at 9 ml/s i.v..

Scan parameters: 100 kv, 100 mA, a dynamic field-of-view of 400L and a rotation time of 0.5s. Scans were obtained from 5 s to 20 s after start of injection at 2 s intervals with 160 mm z-axis coverage.

Initial Results: We demonstrated expected gravity dependent perfusion as expected in a normal distribution pattern in 2 subjects, minor peripheral defects in 1 subject and significant peripheral defects in a further 2 subjects.

Conclusion: Large z-axis, low-dose CT perfusion may be a useful method to study physiological effects of lung and pulmonary vascular diseases. This work is to be expanded in the near future.

References: Alford SK, van Beek EJR, McLennan G, Hoffman EA. Heterogeneity of pulmonary perfusion as a mechanistic image-based phenotyps in emphysema susceptible smokers. Proc Nat Acad Sciences (NY) 2010;107:7485-7490.

Poster Session 1 - 4

Reevaluation of the Tc-99m MAA Whole Body Imaging for Detecting Right-to-left Shunt

Takayuki Shinkai[1], Teruhiko Imai[2], Masatoshi Hasegawa[1]
1. Department of Radiation Oncology, Nara Medical University School of Medicine, Japan
2. Department of Internal Medicine, Saiseikai Nara Hospital, Japan

We retrospectively evaluated examinations for R/L shunt index measurement by Tc-99m MAA whole body imaging.

Subjects & Methods: 26 cases with suspicious of R/L shunt performed a whole body perfusion scan. 4 of 26 perfusion scans were performed with Xe ventilation scan (group-Xe), 8 with Tc-99m Technegas inhalation scan (group-TcG).Remaining 14 cases were performed perfusion scan only; whole body scan was performed directly after injection of Tc-99m MAA (group-Dir). The site of extrapulmonary accumulation and the shunt index were analyzed and compared among the 3 groups.

Results: 13 scans showed the brain accumulation. 11of 13 cases were diagnosed as having R/L shunt. All of 4 cases in group-Xe showed brain accumulation. Group-TcG showed higher rate of the shunt index than other groups. 7cases of group-Dir were diagnosed as having R/L shunt, and uptake for muscle or intestine were considered characteristic. Remaining 7cases of group-Dir diagnosed as having no shunt, but these cases showed extrapulmonary accumulations for thyroid, stomach or urinary bladder.

Conclusion: R/L shunt index measurement by Tc-99m MAA whole body imaging has many pitfalls. For precise evaluation of the shunt, whole body perfusion scan is recommended to perform separately from ventilation scan. The evaluation of extrapulmonary accumulations is important for the diagnosis of R/L shunt.

Poster Session 1 - 5

Nonembolic Causes of Perfusion Defect on Contrast-enhanced Dual-Energy CT: Review of 85 Consecutive Cases

Chae-Hun Lim, Joon Beon Seo, Bohyun Kim, Eun Jin Chae, Hye Jeon Hwang, Hyun Joo Lee, Jae-Woo Song, Jin Seong Lee, Koun Sik Song
Department of Radiology, University of Ulsan College of Medicine, Asan Medical Center, Korea

PURPOSE
To identify nonembolic causes of perfusion defects on contrast enhanced dual-energy pulmonary CT angiography (DECTPA) and to analyze the defect pattern for each cause.

METHOD AND MATERIALS
152 consecutive patients underwent DECTPA for clinical suspicion of embolism (PE). Consequently, 85 patients with 510 lobes were included in the study (M:F=42:43; mean age, 60.64 yr). DECTPA scanning (Somatom Definition, Siemens) was performed at 140 kV and 80 kV. Color-coded perfusion images were obtained with the workstation software (Syngo Dual Energy). The presence, and pattern of perfusion defects (PD) in each lobe were evaluated and their causes were assessed by two radiologists.

RESULTS
Out of 510 lobes, 37 lobes demonstrated artifacts accounted for more than 30% of the each lobe area. With the right middle lobes being the most common sites (27%), these lobes were waived from further evaluation. PDs were seen in 114 out of 510 lobes in total (22%). Nonembolic vascular causes of PDs were as follows; extrinsic occlusion/stenosis of PA at hilum by fibrosing inflammation, congenital PA hypoplasia, venous occlusion, and pulmonary angiosarcoma. PD areas were matched with vascular territory in most cases. Nonvascular causes include: mosaic lung attenuation, bronchitis, emphysema, bronchiectasis, cellular bronchiolitis, bronchial obstruction by mucus and bronchopneumonia. PDs was geographic and mismatched with anatomic extent in cases with bronchitis, bronchiectasis and bronchopneumonia, whereas PDs by cellular bronchiolitis, mosaic attenuation and emphysema were well matched with anatomic extent.

CONCLUSION
PDs without is not uncommon. Various nonembolic vascular and nonvascular diseases can develop PDs in different pattern.

Poster Session 2-1

Correlation between Airwary Dimensions and Emphysema Scores in Patients with Chronic Obstructive Pulmonary Disease: Patient-based versus Lobe-based Analysus

Ji-Young Ko, Jin Mo Goo, Chang Hyun Lee, Chang Min Park, Hyun Ju Lee
Department of Radiology, Seoul National University Hospital, Korea

PURPOSE
The purpose of this study was to correlate airway dimension and emphysema score (ES) using patient-based and lobe-based analysis.

METHODS AND MATERIALS
Forty-one patients with COPD (39 men, 2 women; mean age, 66.75 years; range, 51-78 years) were included in this study. ES (relative area under the threshold of -950 HU), airway dimensions (wall area, WA; total airway area, TAA) at the level of segmental bronchi, and lobe segmentation were obtained with a commercial software package (Thoracic VCAR, General Electric Medical System). For each patient and lobe, summation of WA to summation of TAA (WA/ TAA) was calculated. Correlation analysis was performed between software measurements and pulmonary function test results, and between airway dimensions and ES. The correlation coefficients within subjects were also calculated using ANCOVA.

RESULTS
ES showed significant correlations with FEV1 (%predicted) ($r=-0.523$, $p<0.01$) and GOLD stage ($r=0.497$, $p<0.01$), whereas airway dimensions did not. On patient-based analysis, WA/ TAA did not show a significant correlation with ES. On lobe-based analysis, however, a significant correlation between WA/ TAA and ES was observed ($r=-0.251$, $p<0.01$). On ANCOVA, there was a significant effect of WA/ TAA on ES ($p=0.048$) after controlling for the effect of subjects and a significant correlation between WA/ TAA and ES ($r=-0.154$, $p<0.01$)

CONCLUSION
Our results suggest that regional changes in airways at the level of segmental bronchi have a significant correlation with parenchymal destruction in patients with COPD.

Poster Session 2-2

Comparison of Airway Remodelling Assessed by Three-dimensional Computed Tomography between Bronchial Asthma and Chronic Obstructive Pulmonary Disease

Kaoruko Shimizu, Masaru Hasegawa, Hironi Makita, Yasuyuki Nasuhara, Satoshi Konno, Masaharu Nishimura
First Department of Medicine, Hokkaido University School of Medicine, Japan

Objective: There are few studies of direct comparison between asthma and COPD on airway remodelling assessed by computed tomography (CT). We hypothesized that differences might exist in airway dimensions between them showing similar levels of airflow limitation, under clinically stable condition.

Methods: We recruited 19 older asthmatic patients showing FEV1/FVC<70% with no or 5 pack-year of smoking history, randomly selected 28 age-matched COPD patients demonstrating similar airflow limitation from participants to Hokkaido COPD cohort study. 13 age and sex-matched healthy never-smokers were enrolled. Using our software, we selected 8 airways in the right lung, and measured wall area percent (WA%) and airway luminal area (Ai) at the mid-portion of the 3rd to the 6th generation of each airway. For comparison, we took the average of 8 measurements per generation.

Results: Both FEV1%predicted and FEV1/FVC were similar between asthma and COPD (82.3 ± 3.3%SE vs. 77.6 ± 1.8% and 57.7 ± 1.6% vs. 57.9 ± 1.4%). At any generation, WA% was larger and Ai/BSA was smaller in asthma, followed by COPD, then by controls. Significant differences were observed only between asthma and controls in WA% of the 3rd to the 5th generation and Ai/BSA of any generation, but not in either variable between COPD and controls. There were significant differences in Ai/BSA of any generation between two diseases.

Conclusions: Airway remodelling assessed by CT may be more prominent in older asthmatic patients compared with age-matched COPD patients at the airways of the 3rd to the 6th generation showing similar levels of airflow limitation, in clinically stable condition.

Poster Session 2-3

Airway Wall Remodeling in Different Anatomic Locations Assessed by Computed Tomography in Patients with Stable Asthma and COPD

Tsuyoshi Oguma, Toyohiro Hirai, Akio Niimi, Shigeo Muro, Hisako matsumoto, Yuuma Hoshino, Isao Ito, Michiaki Mishima

Department of Respiratory Medicine, Graduate School of Medicine, Kyoto University, Japan

[Backgrounds] In obstructive airway diseases such as asthma and COPD, it has been reported that percentage wall area of airway (WA%) measured on CT images was related with pulmonary function and disease severity. Although recently multi-detector row CT (MDCT) allowed to measure airway dimensions of multiple bronchi, heterogeneity in remodeling of plural bronchi remains unclear.

[Objectives] To investigate airway wall remodeling in different anatomic locations on CT images.

[Methods] CT scans using MDCT scanner and pulmonary function test were performed in patients with stable asthma and COPD. WA% values of all segmental bronchi were calculated using in-house software, and their relations with pulmonary function were examined. To assess the anatomic heterogeneity in airway wall remodeling, coefficient of variation (CV) and ratio of upper lobe to lower lobe (U/L ratio) of WA% were obtained in each subject.

[Results] Average values of WA% in all segmental bronchi and all right bronchi showed significant correlations with %FEV1, whereas WA% of upper apical bronchus did not show significant correlation in both asthma and COPD groups. U/L ratio and CV of WA% showed no differences between asthma and COPD, and had no correlation with pulmonary function and disease severity in both groups.

[Conclusions] Measurements of airway dimensions in multi bronchi could improve relationship with pulmonary function compared with measurement in one airway. There were no specific segmental bronchi with more progressive remodeling in stable asthma and COPD.

Poster Session 2-4

Quantitative Assessment of Chronic Obstructive Pulmonary Disease (COPD) with Multi-detector row CT (MDCT): Comparison with Lung Structure and Pulmonary Function Test

Jun Sato[1], Masahahiro Uehara[1], Masaki Ikeda[1], Shinya Sagisaka[1], Hiroshi Uchiyama[1], Shiro Imokawa[1], Kazumasa Yasuda[1], Masaki Kamiya[2], Masaki Terada[2], Sadatoshi Kuwahara[3], Yasuo Takehara[4], Takafumi Suda[5], Kingo Chida[5]

1. Department of Respiratory Medicine, Iwata City Hospital, Japan
2. Department of Radiological Technology, Iwata City Hospital, Japan
3. Philips Electronics, Japan
4. Department of Radiology, Hamamatsu University School of Medicine, Japan
5. The Second Division, Department of Internal Medicine, Hamamatsu University School of Medicine, Japan

PURPOSE: To test severity indices derived from three-dimensional reconstruction images of lungs using multi-detector row CT (MDCT) are correlated with the data of pulmonary function tests in chronic obstructive pulmonary disease (COPD).
MATERIAL AND METHODS: This study included 23 patients (23 men; mean age, 71.8 years; age range; 51 to 85 years) who were diagnosed as COPD, and examined by MDCT (Brilliance iCT, Philips) in our hospital. Their values for predicted forced expiratory volume in 1 second (FEV1.0) ranged from 24.9 to 103.6% (mean, 64.1%). The lungs were reconstructed as 3D volume model, and were assessed with the application (Lung Emphysema, Philips). Relative volumes of lungs with attenuation coefficients lower than -950 HU as the threshold were calculated, and the value was defined as low attenuation volume (LAV)%. Also, the mean CT attenuation value of whole lungs was measured as an index of the severity of emphysema.
RESULTS: The mean LAV% in these patients was 11.8% (range; 0.35 to 38.89%), and the mean CT attenuation value was -871.23 HU (range; -919.39 to -814.85 HU). Significant correlations were observed between LAV% and FEV1.0 (%predicted) ($r=-0.622$, $p<0.01$), as well as between the mean CT attenuation value and FEV1.0 (%predicted) ($r=0.539$, $p<0.01$).
CONCLUSIONS: Relative lung volume with attenuation coefficients lower than -950 HU and the mean CT attenuation value of the whole lungs measured with MDCT may be useful quantitative indicators reflecting the severity of the pulmonary emphysema.

Poster Session 2-5

Quantitative Assessment of Low Attenuation Volume Percentage(LAV%) and Mean Lung Density(MLD) in Chronic Obstructive Pulmonary Disease Using Inspiratory and Expiratory MDCT

Naoko Kawata[1], Noriyuki Yanagawa[1], Masako Suzuki[2], Hiromune Sato[2], Toshihiko Sugiura[1], Masao Shinohara[1], Yukiko Matsuura[1], Ken Iesato[1], Yuji Tada[1], Koichiro Tatsumi[1]

1. Department of Respirology, Graduate School of Medicine, Chiba University, Japan
2. Department of Radiology, Chiba University Medical Hospital, Japan

Purpose: To quantify low attenuation volume percentage (LAV%) and mean lung density (MLD) in chronic obstructive pulmonary disease (COPD) using inspiratory and expiratory multi-detecter row CT (MDCT) scans and analyze the relationship between airflow limitation and these parameters.

Materials and Methods: Forty-two consecutive patients with COPD were underwent 64-MDCT (Aquilion ONE, Toshiba) and pulmonary function tests (PFTs). Images were obtained using 120kV and 200mA (CT-AEC) and 0.35sec/rotation. CT images were reconstructed with 0.5mm slice thickness using standard and bone algorithm. Using commercial software (Virtual Place, Aze), the whole lung volume was segmented with attenuation between 1024 and 740 HU. Low attenuation volume percentage (LAV%) was segmented with attenuation less than 960HU, and we also quantified mean lung density (MLD). Then, we assessed the relationship between these parameters and PFTs.

Results: LAV% in inspiratory and expiratory CT scan had a inverse correlation with FEV1/FVC and FEV1 (%predicted). The correlation coefficients of LAV% in inspiratory CT with FEV1/FVC and FEV1 (%predicted) were -0.66 ($p < 0.001$) and -0.60 ($p < 0.001$), respectively. The correlation coefficients of MLD ratio with FEV1/FVC and FEV1 (%predicted) were -0.58 ($p < 0.001$) and -0.68 ($p < 0.001$), respectively.

Conclusion: This study suggests that LAV% and MLD ratio can be useful for the evaluation of the severity of COPD.

Poster Session 2-6

Relationship between Low Attenuation Areas Evaluated by Thurlbeck Panel Method and Body Weight in Patients with Stable COPD

Takanobu Shioya[1], Masahiro Satake[1], Keiyu Sugawara[2], Hitomi Takahashi[2],Mitsunobu Homma[3], Yoshinori Hirano[4], Manabu Hashimoto[5], Ryo Morita[6], Kazuhiro Sato[6], Masa-aki Sano[6]

1. Deparment of Physical Therapy, Akita University Graduate School of Health Sciences, Japan
2. Department of Rehabilitation, Akita City General Hospital, Japan
3. Department of Respiratory Medicine, Akita City General Hospital, Japan
4. Department of Radiology Department, Akita City General Hospital, Japan
5. Department of Radiology Departmnet, Akita Graduate School of Medicine, Japan
6. Department of Respiratory Medicine, Akita Graduate School of Medicine, Japan

Purpose The purpose of this study was to verify the effectiveness of Thurlbeck panal method in the evaluation of emphysema in COPD patients. The second purpose of this study was to clarify the relationship between low attenuation areas (LAA) and body weight, exercise capacity and HRQOL in these patients.
Methods Emphysema was evaluated in 32 COPD patients (30 males, 2 females, mean age 76.6yrs, BMI: 21.4kg/m2, FEV1/FVC: 46.0%, FEV1pred: 55.5%). These patients were divided into three groups; under body weight group (%IBW < 90%), normal body weight group (90% < %IBW < 110%) and over weight body weight group (%IBW > 110%). High resolution CT was used to quantify LAA with -960 HU at the cut-off level. CT sections were analyzed at bilateral upper, middle and lower lung fields. LAA was scored using Goddard method and Thurlbeck panel method by two pulmonologists and one radiologist independently. Kruskal-Wallis rank test was used to compare groups. Spearman's rank correlation was used to evaluate relationship among LAA, IBW and exercise capacity.
Results CT scores evaluated by Goddard method and Thurlbeck panel method were significantly correlated ($r=0.83$, $p<0.0001$). There was a significant negative correlation between CT scores and %IBW ($r=-0.505$, $p<0.01$). CT scores in low body weight group were smallest in three groups.
Conclusions A low IBW is associated with the presence of emphysema suggesting the concept of different COPD phenotype. Our dada also suggest effectiveness of Thurlbeck panel method in evaluation of LAA in COPD.

Poster Session 2-7

Effects of Chronic Obstructive Pulmonary Disease on Thoracic Vascular Calcifications

Bertram J Jobst[1], Michael Owsijewitsch[1], Kauczor Hans-Ulrich[1], Stefan Delorme[3], Nikolaus Becker[2], Claus Peter Heussel[4], Sebastian Ley[1], Julia Ley-Zaporozhan[1]

1. Department of Radiology, University of Heidelberg, Germany
2. Department of Epidemiology, DKFZ Heidelberg, Germany
3. Department of Radiology, DKFZ Heidelberg, Germany
4. Department of Radiology, Thoraxklinik Heidelberg, Germany

Background: Although some of the associations between COPD and atherosclerosis may be the result of common risk factors such as smoking, recent epidemiological evidence suggest that impaired lung function and emphysema are risk factors for cardiovascular disease due to systemic inflammation. We tested the hypothesis that COPD is a risk factor for cardiovascular calcifications, independent of tobacco use.
Subjects: 72 patients referred for MDCT lung cancer screening were included and grouped according to the severity of pulmonary disease. 25 subjects without pulmonary disease (mean age 58 ± 5 years), 25 subjects with mild COPD (GOLD Ⅰ/Ⅱ) (mean age 59 ± 4 years), and 22 subjects with severe COPD (GOLD Ⅲ/Ⅳ) (mean age 62 ± 6 years). Overall volume of thoracic vascular calcifications (thoracic aorta, coronary arteries, supraaortic branches, and aortic valve) was determined by applying a volume score on low dose ungated MDCT scans. Effects of FEV1%, smoking status, gender, age, BMI, emphysema index and 15th percentile point on vascular calcifications were determined by stepwise multiple linear regression analysis.
Results: There was no difference in age between the different severity groups. Median values of overall calcium in severe COPD were 1875 ± 2577 mm3, in mild COPD 721 ± 1082 mm3 and in patients without COPD 880 ± 1793 mm3. Multiple linear regression analysis revealed that only age was linked to the overall volume of calcifications ($R2=0.162$; $p \leq 0.05$).
Conclusion: In our cohort, pulmonary disease with concomitant systemic inflammation was not independently associated with thoracic vascular calcifications. Only age could be considered as a significant contributor to vascular disease.
Funding Acknowledgement: The work was supported by the Competence Network Asthma/COPD funded by the German Federal Ministry of Education and Research (FKZ 01GI0884).

Poster Session 2-8

Analysis of Ventilation Abnormalities in Patients with Obstructive Lung Diseases on Xenon-enhanced CT According to Lung Lesion Patterns: Multicenter Study

Eun Jin Chae[1], Joon Beom Seo[1], Yeon-Mok Oh[2], Gladys Lo[3], Wing Hang Yeung[3], Seung Won Ra[2], Bing Lam[3], Sang Do Lee[2]

1. Department of Radiology, Ulsan College of Medicine, Asan Medical Center, Korea
2. Department of Pulmonary and Critical care Medicine, Ulsan College of Medicine, Asan Medical Center, Korea
3. Department of Radiology, Sanatorium Hospital, Hongkong

PURPOSE
To analyze ventilation abnormalities on xenon-enhanced CT in patients with obstructive lung diseases according to lung lesion patterns.
METHOD AND MATERIALS
Forty-seven subjects(M:F=35:12, mean age, 61.8 yrs) with obstructive PFT abnormality were enrolled from two centers. Patients' diagnoses were COPD(32), asthma(4), bronchiolitis obliterans syndrome(3), diffuse panbronchiolitis(2), bronchitis(2), bronchiectasis(2), bronchopneumonia(1), and anthracofibrosis(1). All subjects underwent single phase, thoracic dual-energy CT using dual-source CT (Definition and FLASH, Siemens) when they inhaled 30% xenon for 90 seconds. Lung lesion pattern was evaluated on weighted average image and ventilation defect (VD) was evaluated on color-coded xenon map. In each lobe, lung lesion pattern in point of both airway and parenchyma, extent of ventilation defect per lesion(VD/lesion, %), and extent of ventilation defect per lobe(VD/lobe, %) were evaluated.
RESULTS
There was no noticeable change in monitored parameters in all subjects. Among 235 lobes of 47 patients, 231 lobes were evaluated and 4 lobes were excluded due to total collapse. Mean VD/lobe was 37.2%. In point of parenchyma, lesion patterns included centrilobular emphysema(CLE, n=82), panlobular emphysema(PLE, 8), hypoattenuation(78), bullous emphysema(1), ground glass opacity(1), and normal(61). In point of airway, lesion patterns included diffuse bronchial wall thickening(n=135), cellular bronchiolitis(56), large airway obstruction(6), bronchiectasis(4) and normal(30). The results of VD/lesion in point of parenchyma were: mild CLE, 34.6%; moderate CLE, 71.2%; severe CLE, 80.9%; moderate PLE, 90.0%; severe PLE, 100%; hypoattenuation, 96.4%. The results of VD/lesion in point of airway were: bronchial wall thickening, 35.3%; cellular bronchiolitis, 80.4%; large airway obstruction, lobar, 85%; segmental/subsegmental, 100%; bronchiectasis, 25.0%.
CONCLUSION
Areas of hypoattenuation, cellular bronchiolitis, segmental/subsegmental airway obstruction, and PLE showed relatively matched areas of ventilation defect, whereas areas of CLE, bronchial wall thickening, and bronchiectasis showed smaller extent of ventilation defect than anatomical extent.

Poster Session 3-1

Evaluation of the Extent of Ground-glass Opacity on High-Resolution CT in Patients with Interstitial Pneumonia: Comparison between Quantitative and Qualitative Analysis

Hidetake Yabuuchi[1], Masamitsu Hatakenaka[2], Hiroshi Tsukamoto[3], Yoshio Matsuo[2], Shunya Sunami[2], Takeshi Kamitani[2], Mikako Jinnouchi[2], Kyoko Suzuki[4], Koichi Akashi[3], Hiroshi Honda[2]

1. Department of Health Sciences, Kyushu University Graduate School of Medical Sciences, Japan
2. Department of Clinical Radiology, Kyushu University Graduate School of Medical Sciences, Japan
3. Department of Medicine and Biosystemic Science, Kyushu University Graduate School of Medical Sciences, Japan
4. Fuji Film Medical Co. Ltd., Japan

PURPOSE:
To compare quantitative and qualitative analysis in the evaluation of the extent of ground-glass opacity on high-resolution CT (HRCT) in patients with interstitial pneumonia (IP) with systemic sclerosis (SSc).
METHOD AND MATERIALS:
Fifteen patients with refractory IP associated with SSc received peripheral blood stem cell transplantation, and HRCT was performed before and 12 months after treatment. We evaluated the activity of the IP by monitoring serum KL-6 and %VC. Five readers analyzed the extent of GGO (%GGO) on HRCT obtained before and 12 months after treatment using qualitative analysis (estimated to the nearest 10% of parenchymal involvement). Quantitative analysis of the %GGO was also performed using a commercially available workstation. We also assessed the therapeutic effect by calculating KL-6 and %VC during one year after treatment. Pearson's correlation coefficients were used to examine the relationship between pretreatment %GGO, %GGO, and KL-6 and %VC. Thereafter, we compared the correlation coefficient value ( ) between quantitative and qualitative analysis.
RESULTS:
The %GGO was correlated negatively with KL-6 and correlated positively with %VC on both quantitative and qualitative analysis. However, evaluation with quantitative analysis showed stronger correlation than the qualitative analysis.
CONCLUSION:
Quantitative analysis of the extent of ground-glass opacity (GGO) on high-resolution CT (HRCT) using a work station could aid in making a correct decision in predicting or monitoring the therapeutic response of interstitial pneumonia (IP) compared with qualitative analysis.

Poster Session 3-2

Correlation between Pirfenidone Effect and the Initial CT Findings in the Patients with Idiopathic Pulmonary Fibrosis

Tae Iwasawa[1], Takashi Ogura[2], Takahiro Endo[2], Tomohisa Baba[2], Akira Asakura[3], Toshiyuki Gotoh[3], Tomio Inoue[4]

1. Department of Radiology, Kanagawa Cardiovascular and Respiratory Center, Japan
2. Department of Respiratory Medicine, Kanagawa Cardiovascular and Respiratory Center, Japan
3. Graduate School of Environment and Information Sciences, Yokohama National University, Japan
4. Department of Radiology, Yokohama City University, School of Medicine, Japan

Objectives: Pirfenidone is a new anti-fibrotic drug for idiopathic pulmonary fibrosis (IPF). We evaluated the prognostic value of CT image for the response to pirfenidone.
Materials and Methods: In this retrospective cohort study, written informed consent was waved. The subjects were 51 consecutive patients (37 males, 14 females; mean age, 69.9 ± 8.3, ± SD) with IPF. The pattern of usual interstitial pneumonia was confirmed histopathologically using surgical biopsy in 33 patients. About a half of patients were receiving the combination therapy with corticosteroid (n=20) and immune-suppressants (n=11). We checked side effects and pulmonary function test (PFTs). In PFTs after 12 months, 10% or greater decline of VC in predicted value was defined deterioration. We also analyzed initial CT quantitatively using originally-developed computed-assisted system. This system can divide the lungs into normal (N-pattern) and each lesion pattern.
Results: Twelve patients discontinued pirfenidone because of adverse effects; sever appetite loss (n=7), rash (photosensitivity) (n=3), liver dysfunction (n=1) and others (n=1). In 39 patients who were continuing pirfenidone, 7 patients died and 8 patients deteriorated (non-responder). Other 24 patients were stable in PFTs (responder). Initial vital capacity (VC) %predicted was significantly smaller in non-responder (63.6 ± 20.4% vs 75.5 ± 14.0%, p=0.037). In quantitative CT results, initial N-pattern volume was significantly smaller in non-responder (25.2 ± 13.9 vs 37.6 ± 12.3%predTLC, p=0.006), and Consolidation-pattern volume was larger in non-responder (1.1 ± 0.8 vs 0.6 ± 0.5%predTLC, p=0.021).
Discussion and conclusion: Pirfenidone clinically stabilized disease in 62% of patients for one-year follow-up. The initial CT findings were correlated with response to pirfenidone.

Poster Session 3-3

Relation between Radiological Abnormalities and Functional Impairment Assessed from Distributional Analysis on Ventilation and Diffusing Capacity to Perfusion in Idiopathic Interstitial Pneumonias

Kazuhiro Yamaguchi[1], Masaaki Mori[2], Akira Kawai[2], Tomoaki Takasugi[2], Yoshitake Oyamada[2], Eiichi Kohda[3], Atsushi Nagai[4]

1. Department of Comprehensive and Internal Medicine, Tokyo Women's Medical University Medical Center East, Japan
2. Department of Medicine, School of Medicine, Keio University, Japan
3. Department of Radiology, Ohashi Medical Center Toho University, Japan
4. Department of the 1st Internal Medicine, Tokyo Women's Medical University, Japan

We attempted to clarify the simultaneous distributions of VA/Q and diffusing capacity to perfusion (D/Q) in patients with idiopathic interstitial pneumonias (IIP) with varied pathological abnormalities. We categorized the patients with IIP into three groups based on HRCT findings; group Ⅰ (n=6): ground-glass with no obvious reticular pattern, group Ⅱ (n=9): reticular pattern associated with honeycombing cysts but without distinct ground-glass opacities, and group Ⅲ (n=12): a mixture of ground-glass and reticular patterns. To assess functional abnormalities in their lungs, we determined VA/Q and D/Q distributions by using O2, CO2 and CO together with six foreign inert gases as indicator gases. We transformed the measured data on indicator gases in arterial blood into a continuous distribution of Q in the VA/Q-D/Q field. Group Ⅰ subjects exhibited bimodal Q distributions along the D/Q axis but fairly homogeneous Q distributions along the VA/Q axis. Group Ⅱ subjects showed markedly abnormal VA/Q distributions but unimodal Q distributions along the D/Q axis. Group Ⅲ subjects showed broad but unimodal Q distributions along the D/Q axis. Q distributions along the VA/Q axis in group Ⅲ were qualitatively similar to those observed in group Ⅱ. In IIP, active alveolitis or acinitis played a major role in producing low D/Q regions impeding gas exchange by a diffusion limitation, while extensive fibrosis with minimal inflammation accounted for low D/Q as well as low VA/Q regions. These findings suggest that hypoxemia in IIP patients may be caused by inhomogeneous distributions of D/Q in combination with those of VA/Q.

Poster Session 3-4

Clinical Considerations of Postoperative Acute Exacerbation in Patients with Interstitial Pneumonia Combined with Lung Cancer

Takahiro Omori[1], Joji Samejima[1], Ko Takahashi[1], Michihiko Tajiri[1], Takashi Ogura[2], Tae Iwasawa[3]

1. Department of Thoracic Surgery, Kanagawa Cardiovascular and Respiratory Center, Japan
2. Department of Respiratory Medicine, Kanagawa Cardiovascular and Respiratory Center, Japan
3. Department of Radiology, Kanagawa Cardiovascular and Respiratory Center, Japan

Objective

The purpose of this study was to examine the predictive factors of postoperative acute exacerbation of interstitial pneumonia(IP) combined with lung cancer.

Methods

Subjects were 530 patients who received operation in our hospital. We reviewed CT images obtained before surgery to evaluate presence of IP. We classified IP into three patterns; UIP pattern, NSIP pattern and combined pulmonary fibrosis and emphysema(CPFE) pattern. We also analyzed other clinical data such as background, hematological examinations, respiratory function tests and operation- related factors.

Results

We found 87 patients with IP in total 530 patients. The 15 patients had UIP pattern, 13 patients had NSIP pattern and 59 patients had CPFE pattern. The postoperative acute exacerbation of IP was observed 5 of 87 patients(5.7%); 4 out of 15 patients with UIP pattern(26.7%), 1 out of 13 patient with NSIP pattern(7.7%). Non of patients with CPFE pattern developed acute exacerbation. In background and hematological examination, Hugh-Jones score, preoperative oxygen use, preoperative steroid use and WBC were significantly higher in the patients developed acute exacerbation(AE group) than in the patients did not developed acute exacerbation(NAE group). In respiratory function test and operation- related factors, %FVC and tidal volume during one lung ventilation were significantly lower in the AE group than in the NAE group.

Conclusion

The UIP pattern on preoperative CT was a risk factor of postoperative acute exacerbation.

Poster Session 3-5

Thoracic and Abdomino-pelvic Radiologic Findings of Japanese Patients with Lymphangioleiomyomatosis

Kuniaki Seyama[1], Kazunori Tobino[1], Takeshi Johkoh[2], Kiminori Fujimoto[3], Hiroaki Arakawa[4], Fumikazu Sakai[5], Yoshihito Hosika[1], Katunori Ando[1], Kazuhisa Takahashi[1]

1. Department of Respiratory Medicine, Juntendo University School of Medicine, Japan
2. Department of Radiology, Kinki Central Hospital of Mutual Aid Association of Public School Teachers, Japan
3. Department of Radiology, Kurume University School of Medicine and Center for Diagnostic Imaging, Kurume University Hospital, Japan
4. Department of Radiology, Dokkyo Medical University School of Medicine, Japan
5. Department of Diagnostic Radiology, Saitama International Medical Center, Saitama Medical University, Japan

Aim: To analyze thoracic and abdomino-pelvic radiologic findings of Japanese patients with lymphangioleiomyomatosis.

Subjects and methods: The chest CT images of 138 patients with LAM (125 sporadic LAM and 13 TSC-associated LAM) and also abdomino-pelvic CT images of 76 patients (70 sporadic and 6 TSC) among them were studied by 4 radiologists. All were female. Although this is a cross-sectional study, the frequency of "lymphatic lesion" in each part of the body may answer to the question.

Results: Pulmonary cysts were demonstrated in all patients and its mean extent in the lung fied was 39%. Small nodules in the lung field (4%), dilatation of thoracic duct (4%), and pleural effusion (11%) were identified with the similar frequency with those reported by NIH group. In abdomino-pelvic scan, renal angiomyolipomas (AMLs) (26%), AMLs in liver (24%), ascites (12%), lymphangioleiomyomas (46%), and lymph node enlargement (20%) were identified. Lymphatic involvement was more frequently demonstrated pelvic cavity than thoracic cavity.

Conclusion: Radiologic findings and their frequencies in the pulmonary manifestation was similar to that of NIH group, but this may not be the case in the extrapulmonary manifestations: lower incidence of renal AML, increased detection of liver AML, and frequent lymphatic involvement in the pelvic cavity in Japanese LAM patients.

Poster Session 3-6

Clinical and Radiographic Features of Pulmonary Aspergillosis in Patients with Chronic Fibrosing Interstitial Pneumonia

Akiko Kaga[1], Yutaka Usui[1], Fumikazu Sakai[2], Makoto Nagata[1], Koichi Hagiwara[1], Minoru Kanazawa[1]

1. Department of Respiratory Medicine, Saitama Medical University, Japan
2. Department of Radiology, International Medical Center, Saitama Medical University, Japan

(Background)
Pulmonary aspergillosis has been regarded as an important complication of patients with chronic fibrosing interstitial pneumonia (CFIP) with or without immunosuppressive treatment, however, their clinicoradiographical features have not been fully described.

(Objective)
To clarify the clinical and radiographic features of pulmonary aspergillosis in patient with CFIP of unknown etiologies, we retrospectively analyzed medical records of 196 patients with CFIP who visited our department between September 2007 and May 2010.

(Results)
Out of 196 patients with CFIP, 6 cases of pulmonary aspergilloma and 6 cases of chronic necrotizing pulmonary aspergillosis were found. Each lesion of aspergillosis developed in the pulmonary lesions of airspace enlargement, such as honeycombing, emphysema, or thick-walled large cyst. In patients with pulmonary aspergillosis, the mean smoking index was high, pulmonary emphysematous changes were highly prevalent, and the mean diffusion capacity for gas exchange was markedly decreased. Ever-smokers with combined pulmonary fibrosis and emphysema were more likely to be complicated with pulmonary aspergillosis, compared to ever-smokers without emphysema as well as never-smokers.

(Conclusion)
Patients with smoking-related interstitial pneumonia with emphysema was likely to be suffered from pulmonary aspergillosis. Airspace enlargement of the lung was the site of infection, possibly due to insufficiency in local innate immunity.

Poster Session 3-7

Clinical and Radiographic Features of Pneumothorax and Pneumomediastinum in Patients with Chronic Fibrosing Interstitial Pneumonia

Ayako Shiono, Yutaka Usui, Akiko Kaga, Ken-ichiro Komiyama, Makoto Nagata, Koichi Hagiwara, Minoru Kanazawa

Department of Respiratory Medicine, Saitama Medical University, Japan

(Background)

Pneumomediastinum as well as pneumothorax has been regarded as a distressing problem in patients with chronic fibrosing interstitial pneumonia (CFIP). Some are intractable and they are sometimes life-threatening. However, their clinicoradiographical features have not been fully described.

(Objective)

To clarify the clinical and radiographic features of pneumothorax and pneumomediastinum developed in patients with CFIP, we retrospectively analyzed medical records of patients with CFIP who visited our department between January 2007 and May 2010.

(Results)

Out of 498 subjects with CFIP, 37 were found to have pneumothorax, pneumomediastinum or both. Each number of cases was 12, 8, and 17, respectively. The overall mean smoking index was 24 pack years. By high-resolution computed tomography, 21 subjects demonstrated the usual interstitial pneumonia pattern of interstitial pneumonia, 21 demonstrated emphysema or thick-walled large cyst, and 9 subjects demonstrated bilateral pneumothorax. 14 out of 16 subjects, who could be estimated the severity of CFIP by SpO2, %FVC, and %DLco, showed moderate to severe CFIP. The severity of pneumothorax was usually up to the second degree. The development of pneumomediastinum was associated with glucocorticosteroid administration.

(Conclusion)

Pneumothorax and pneumomediastinum were clinically significant complications during the course of CFIP.

Poster Session 4-1

Effect of Pulmonary Rehabilitation on Parenchymal Lung Motion Evaluated with Dynamic MRI in COPD Patients

Takeshi Shinohara[1], Tae Iwasawa[2], Toshiyuki Gotoh[3], Kaori Tsuruta[4], Takuma Sasaki[4], Takahiro Endo[1], Takashi Ogura[1], Hiroshi Takahashi[1]

1. Division of Pulmonary Medicine, Kanagawa Cardiovascular and Respiratory Center, Japan
2. Department of Radiology, Kanagawa Cardiovascular and Respiratory Center, Japan
3. Graduate School of Environment and Information Sciences, Yokohama National University, Japan
4. Department of Rehabilitation, Kanagawa Cardiovascular and Respiratory Center, Japan

Background:
Pulmonary rehabilitation does not improve lung function, but it increases exercise tolerance and improves quality of life; the underlying mechanism is uncertain. Recently, parenchymal lung motion in COPD patients is recognized to be different from it in healthy subjects evaluated with dynamic MRI.
Purpose:
To analyze parenchymal lung motion evaluated with dynamic MRI before and after pulmonary rehabilitation in COPD patients.
Methods:
A total of 12 subjects were examined, including 7 COPD patients and 5 control individuals. Rehabilitation programs feature 2 sessions per week, each lasting 1 hour for 12 weeks. Dynamic MRI and clinical assessments including lung function test, 6-minute walk test and QOL test were performed before and after rehabilitation. MRI was performed using 10 sample points for motion analysis during deep slow breathing. The directional ratio of the sample points (the ratio of the cranio-caudal change to the dorsal-ventral change) was calculated as parenchymal lung motion.
Results:
In patients with COPD, the directional ratio increased compared with that in control (1.98 ± 0.58 vs 1.33 ± 0.35, respectively). After pulmonary rehabilitation, the directional ratio decreased (1.98 ± 1.33 vs 1.31 ± 0.40, respectively).
Conclusions:
The parenchymal lung motion was altered from cranio-caudal to dorsal-ventral direction after pulmonary rehabilitation in patients with COPD and was suggested to become similar to that in control individuals.

Poster Session 4-2

Diaphragmatic Motion before and after Plication of Central Tendon in Patients with Diaphragmatic Eventration

Koji Chihara, Shigeyuki Tamari, Masayuki Hirano, Hideki Motoyama, Kenji Okita
Division of Thoracic Surgery, Shizuoka City Shizuoka Hospital, Japan

As diaphragmatic eventration is a chronic disorder, it is rather difficult for both a patient and a surgeon to select operative treatment with few evidences. There are few reports on the diaphragmatic motion before and after surgery. We performed plication of a thin and extended central tendon of the left diaphragm in two elder patients with symptoms such as palpitation, or exertional dyspnea during daily activities. Dynamic MRI during deep breathing of the chest and the upper abdomen in the mid-coronal and sagittal slices were obtained with a 1.5T MR instrument using fast spoiled GRASS method. In coronal slice, the central part of the left diaphragm was pulled down to the right side during inspiration while the lateral part did not move like a piston but did like a hinge. In sagittal slice, the posterior part of the left diaphragm moved a little resulting smaller excurtion than the anterior part. These impairment were basically same but lesser after operation. Although the dome shape of the left floppy diaphragm could be fairly corrected, tention yielded by the healthy right diaphragm during contraction might be transffered through the central tendon, and affect strongly the left diaphragmatic motion due to strength difference between the two hemidiaphragms.

Poster Session 4-3

Dynamic MRI Measured Respiratory Motion of the Internal Structures of the Lung. Differences between Healthy Subjects and COPD Patients.

Hirofumi Shibata[1], Tae Iwasawa[2], Toshiyuki Gotoh[3], Seiichiro Kagei[3], Takeshi Shinohara[4], Takashi Ogura[4], Ukihide Tateishi[1], Tomio Inoue[1]

1. Department of Radiology, Yokohama City University School of Medicine, Japan
2. Department of Radiology, Kanagawa Cardiovascular and Respiratory Center, Japan
3. Graduate School of Environment and Information Science, Yokohama National University, Japan
4. Department of Respiratory medicine, Kanagawa Cardiovascular and Respiratory Center, Japan

Objective

The aim of this study was to evaluate respiratory motion of the internal structure of the lung using dynamic MRI in healthy subjects and patients with chronic obstructive pulmonary disease (COPD).

Methods

The subjects were 5 normal volunteers and 21 patients diagnosed cigarette smoking-related COPD. Imaging sequence of the dynamic MRI was a balanced fast field echo (BFFE). We sequentially captured 80 frames of the mid sagittal portion of the right lung while repeating forced deep breathing. We set 15 tracking points for pulmonary vessels, 5 tracking points in the upper lobe and 10 tracking points in the middle and lower lobes and measured maximal motion distance of each tracking point for ventrodorsal direction (X-axis) and craniocaudal direction (Y-axis). We compared these parameters with spirometric data and evaluated the correlation between airflow limitation and the respiratory motion of the internal structure of the lung.

Results

Respiratory motion distance (X and Y-axis of middle and lower lobe) and spirometric data such as forced expiratory volume (FEV) 1/forced vital capacity (FVC), FEV1 and %FEV1 showed a highly significant positive correlation. %residual volume (RV) showed a highly significant negative correlation.

Conclusion

Dynamic MRI using BFFE sequences is a highly precise technique to directly and noninvasively visualize dynamic respiratory motions of the internal pulmonary structures. Respiratory motions of the internal structure of the lung correlate spirometric data which express airflow limitation in normal volunteers and patients with COPD.

Poster Session 4-4

Respiratory Motion Analysis with Correlation Function and Frequency Decomposition from MR Image Sequences of COPD Patients and Normal Subjects

Yew Kurabayashi[1], Takuya Kubo[2], Hiroki Matsumoto[2], Toshihiro Furukawa[3], Tae Iwasawa[4]

1. Faculty of Commercial Science, Takasaki University of Commerce, Japan
2. Undergraduate Department of Industry, Maebashi Institute of Technology, Japan
3. Faculty of Engineering Division I, Tokyo University of Science, Japan
4. Department of Radiology, Kanagawa Cardiovascular & Respiratory Center, Japan

We examine motions of some points on a diaphragm with their correlation and frequency analysis. We expect that the information of correlation and frequency can be used to measure quality of respiratory motion of a lung and for image diagnosis on COPD and so on.

Each part of a lung of normal subject, especially his or her diaphragm, extends toward outside and shrinks toward inside together, while that of a patient sometimes moves unevenly. Recording positions of some points on a diaphragm, we can get sequences of each of them. Frequency analysis involved with correlation is performed to these sequences and the spectrum is used to obtain features of a respiratory motion of a subject. These features are used as measures of quality of respiratory motion.

Bispectrum is a Fourier transformation of correlation function of three sequences. We got three sequences of different positions of points on diaphragms and calculated bispectrum of them in our previous study. There was a difference between the phases of bispectrum of patients and ones of normal subjects. It suggests that the phase of bispectrum can be used as a measure of respiratory motion.

We verify that the difference shows up again by using points of positions different from previous study on each diaphragm in this time. In addition, we present results from correlation analysis with wavelet transform for sequences of points on diaphragms.

Poster Session 4-5

Evaluation of Airway Dimension During Respiration

Hiroshi Wada[1], Gen Masuda[1], Yasushi Ryujin[1], Tetsuya Oguma[1], Hideto Yamada[1], Taishi Nagao[1], Hidenobu Suzuki[2], Yoshiki Kawata[2], Noboru Niki[2], Yasutaka Nakano[1]

1. Division of Respiratory Medicine, Department of Internal Medicine, Shiga University of Medical Science, Japan
2. Institute of Technology and Science, The University of Tokushima, Japan

Introduction
It is widely known that the lung volume changes during respiration. However, it is unknown how the airway dimensions change during normal respiration.
Objectives
We hypothesized that, in normal subjects, airway length and luminal area extend from expiration to inspiration. To investigate this hypothesis, we used inspiratory and expiratory CT of normal subjects.
Methods
We recruited 13 normal and healthy subjects and they underwent both inspiratory and expiratory CT. We analyzed volumetric CT data and measured the airway length, luminal area, wall thickness, wall area, and WA% (percentage of wall area to total airway area) of right apical bronchus (the fourth generation) at inspiration and expiration.
Results
The airway length was longer at inspiration than expiratory (mean (SD) 12 (1.83) vs 10 (1.35) mm, respectively; $p<0.001$). The airway luminal area at inspiration was greater than expiration (mean (SD) 21.2 (5.53) vs 16.1 (4.77) mm2, respectively; $p<0.001$). There was no difference in the wall thickness between inspiration and expiration. The airway wall area was greater at inspiration than expiration (mean (SD) 34.1 (5.20) vs 32.1 (5.38) mm2, respectively; $p=0.03$). WA% was smaller at inspiration than expiration (mean (SD) 62.6 (3.46) vs 67.1 (3.18) %, respectively; $p<0.001$).
Conclusion
The airway length of right apical bronchus in normal healthy subjects extended from expiration to inspiration. Luminal area and airway wall area increased but WA% decreased from expiration to inspiration.

Poster Session 4-6

New Method for Ventilation Function Using Dynamic Chest x-ray Examination: Evaluation of Regional Changes in Inspiratory / Expiratory Flow Rate Ratio

Norihisa Motohashi[1], Hideo Ogata[1], Naoyuki Yoshida[1], Takashi Yoshiyama[1], Takashi Uchiyama[1], Hiroyuki Kokuto[1], Kozo Morimoto[1], Misako Aoki[1], Yuji Shiraishi[2], Syoji Kudoh[1]

1. Respiratory Medicine Division, Respiratory Diseased Center, Fukujuji Hospital, JATA, Japan
2. Chest Surgery Division, Respiratory Diseased Center, Fukujuji Hospital, JATA, Japan

Purpose: Evaluation of a regional ventilation function with use of dynamic chest X-ray. The differential value of density between expiratory and inspiratory phases has possibilities to reflect the regional ventilation function on dynamic chest X-ray.

Subjects: Dynamic chest X-ray from 11 ventilation impairment patients with COPD and 5 normal volunteers were obtained in the upright position in about 10 seconds of tidal breathing at rest. Image data captured at 7.5 frames per second was synchronized with the pulsed X-ray.

Methods: We developed an automatic analyzing software for a regional ventilation function, which includes:
1) Lung fields extraction from dynamic chest X-ray.
2) Identification of small local areas.
3) Calculation of the maximal differential values in each ventilation phase at the corresponding small local area in the series of dynamic chest X-ray.
4) Calculation of the regional relative flow rate ratio as the ratio of peak inspiratory phase to peak expiratory phase.
5) Display a color map for the ratio on a representative chest image from the dynamic chest X-ray.

Results: The regional changes in inspiratory / expiratory flow rate ratio had larger values and broader distribution in patients with COPD compared to those of normal volunteers. The average of the ratio in patients and in normal volunteers was 1.26 ± 0.25 and 1.03 ± 0.07 (mean $\pm$ SD, $P = 0.013$), respectively.

Conclusion: The newly proposed method using dynamic chest X-ray examination enabled us to noninvasively analyze the regional flow rate.

Poster Session 5-1

Hyperpolarized 3He Magnetic Resonance Imaging Biomarkers of Bronchoscopic Airway Bypass in COPD

Lindsay Mathew[1], Miranda Kirby[1,2], Donald Farquhar[4], Chris Licskai[4], Roya Etemad-Rezai[1,3], David McCormack[4], Grace Parraga[1,2,3]

1. Imaging Research Laboratories, Robarts Research Institute, Canada
2. Department of Medical Biophysics, The University of Western Ontario, Canada
3. Department of Medical Imaging, The University of Western Ontario, Canada
4. Division of Respirology, Department of Medicine, The University of Western Ontario, Canada

We explored and examined hyperpolarized 3He magnetic resonance imaging (MRI) acquired longitudinally, both pre- and post- airway bypass and compared these to measurements of pulmonary function, the six-minute walk distance (6MWD), St. George's respiratory questionnaire (SGRQ) and modified medical research council (mMRC) score. A single subject underwent pulmonary function tests, 3He MRI diffusion-weighted, static ventilation, and proton MRI at 3.0T. 3He MRI apparent diffusion coefficients were calculated and as well 3He MRI ventilation and ventilation defect measurements using two-dimensional landmark-based registration of 3He and 1H pulmonary images, and subsequent application of an automated K-means cluster algorithm to generate 3He ventilation defect volume (VDV), and 3He ventilation volume (VV).

Four days prior to bronchoscopic introduction of the airway bypass (Exhale Drug Eluting Stent, Broncus Technologies, Mountainview CA) and six months post-stent, the subject reported mMRC scores of 2 and 1, 6MWD of 288m and 366m and SGRQ scores of 65 and 27 respectively. At eight months pre-stent, whole lung 3He MRI VV was 1.7L and at six months post-stent VV was 4.0L- an increase of 2.3L, whereas the RV/TLC ratio was 57% and 56%. FEV1 was 1.09L and 1.11L, and FVC was 3.15L and 3.51L, pre- and six months post-stent respectively. In conclusion, for a single COPD subject, the high sensitivity of 3He MRI provided a way to detect regional functional ventilation changes that were suggestive of ventilation improvements and that were in accordance with improvements in mMRC score and 6MWD and were not detected by established pulmonary function tests.

Poster Session 5-2

Line-Narrowed Diode Lasers for High-Efficiency Continuous Production of Hyperpolarized Xe-129 using Optimized Cell for High Concentration of Optically Pumped Rubidum

Mineyuki Hattori[1], Takashi Hiraga[1], Naohiro Kaga[2], Takashi Nakajima[2], Kazunori Tsunoda[2], Norio Ohtake[3]

1. Photonics Research Institute, National Institute of Advanced Industrial Science and Technology, Japan
2. L.C.S. Inc., Japan
3. Toyoko Kagaku, Co. Ltd., Japan

A flow-through-type apparatus for the polarization of Xe-129 using four line-narrowed high-power InGaAsP diode laser arrays, with fast and slow axis collimation lenses (Ingeneric) and a volume holographic grating (Ondax PowerLocker™, PLR794.5-22.5-13-1.75-1.5) (794.73 ± 0.15 nm, 40 W 4 = 160 W) was constructed. The obtained maximum polarization of Xe-129 for the natural abundance of Xe gas was 20 ± 5 % when the temperature of the cell was ~ 220 oC and the flow rate of the mixture gas was 40-100 sccm. We have developed a flow-through-type apparatus with a cell structure that is optimized for the hyperpolarization of Xe-129. In this equipment, to increase the laser adsorption coefficient, heating temperatures in the polarization cell are set at 180 to 300 oC. Heating causes the vapor pressure of Rb to increase, and the irradiation cell gap is set at 1 mm, resulting in a polarization rate of ~ 20% and a high rate of polarization of Xe-129 per unit of time at a flow rate of 40-100 sccm. The newly developed equipment makes it possible to realize the continuous production of hyperpolarized Xe-129 with high productivity.

Poster Session 5-3

Development of a Novel Method for Evaluating Pulmonary Disease Using Hyperpolarized Xe-129 Ultrashort Echo-time MRI

Hirohiko Imai, Satoshi Iguchi, Hideaki Fujiwara, Atsuomi Kimura
Division of Health Sciences, Graduate School of Medicine, Osaka University, Japan

Hyperpolarized (HP) Xe-129 is capable of wide application in lung MRI by the use of both gas- (air space) and dissolved-phase (tissue and blood) signals, offering a powerful tool for the physiological evaluation. However, it is still difficult to obtain the dissolved-phase image due to the extremely short T2* and the low spin density. In the present study, we intended to apply ultrashort echo-time (UTE) sequence in acquiring the dissolved-phase image and to develop a novel method to visualize and evaluate the pulmonary function.

HP Xe-129 gas was produced by a home-built polarizer and continuously supplied to the mouse, which breathed the gas spontaneously. Measurements were performed with a 9.4-T MRI system (Varian). Gas- and dissolved-phase images were acquired using the UTE sequence with frequency selective excitation. We proposed the novel marker, xenon distribution ratio, which is the ratio of magnetization of the dissolved-phase Xe-129 relative to that of the gas-phase Xe-129. The distribution ratio maps were compared between healthy mice and elastase-induced mouse models of emphysema.

The application of the UTE sequence enabled to obtain the dissolved-phase Xe-129 lung image as well as the gas-phase one with relatively high spatial resolution. As a result, we could evaluate the local xenon distribution ratio in the mouse lung by combining these images. It was found that the distribution ratio in elastase-treated mice was reduced and widely distributed compared to that of healthy mice, reflecting impaired diffusing capacity caused by emphysema.

This work was supported in part by JST (a210017 and AS2124004F).

Poster Session 5-4

Non-contrast Enhanced MR Angiography Using Volumetric T2-weighted Imaging Technique on 3T

Mitsutomi Ishiyama, Masaki Matsusako, Katsunori Oikado, Akari Makidono, Minobu Kamo, Takahumi Haraguchi, Yukihisa Saida
St.Luke's International hospital, Japan

Purpose.
To investigate the clinical potential of volumetric T2-weighted MR imaging technique in depicting pulmonary arteries on 3T.

Materials and Methods.
Six healthy volunteers who underwent lung MRI were enrolled in this retrospective study. MR protocol included volumetric T2-weighted imaging (TR/TE 4300-6500/49) with ECG and respiratory gating. To depict pulmonary arteries as bright, MR data acquisition was performed during diastolic phase which was determined by cardiac cine study using a steady state free precession sequence. Two radiologists performed a consensus evaluation of reformatted axial and coronal images on a per-vessel basis (main pulmonary artery (PA), lobar PA, segmental PA, and subsegmental PA). The image quality was graded into three categories (poor, fair, and good).

Results.
In six subjects, the image quality on a per-vessel basis was good in 11 of 12 main arteries (91.7%), 30 of 36 lobar arteries (83.3%), 96 of 108 segmental arteries (88.9%), and 216 of 252 subsegmental arteries (85.7%), respectively.

Conclusion.
MR angiography using volumetric T2-weighted imaging technique appears to be feasible in depicting pulmonary arteries. It may be applicable to patients with renal impairment or allergy to contrast media.

Poster Session 5-5

Non-Contrast-Enhanced Pulmonary MR Angiography Using Electrocardiography-triggered Three-Dimensional Half-Fourier FSE with a Swap Phase Encode Extended Data (SPEED) Acquisition and Image Processing

Norio Yoshizaki[1], Atsushi Ono[1,2], Kenya Murase[2], Katsuyoshi Ito[3], Atsushi Higaki[3], Kazuo Sanou[4], Satoru Takata[1], Mitsue Miyazaki[5,6]

1. Department of Medical Technology, Kousei Hospital, Japan
2. Department of Medical Physics and Engineering, Graduate School of Medicine, Osaka University, Japan
3. Department of Diagnostic Radiology, Kawasaki Medical School, Japan
4. Department of Surgery, Kousei Hospital, Japan
5. MR Department, Toshiba Medical Research Institute USA, USA
6. MR Department, Toshiba Medical Systems Corp., Japan

Three variations of a non-contrast-enhanced MR angiography technique using electrocardiography (ECG)-triggered three-dimensional (3D) half-Fourier FSE fresh blood imaging sequences were acquired to visualize the pulmonary arterial vasculature. Systolic and diastolic images with the phase encode directions swapped between the first and second acquisitions were obtained in ten consecutive healthy volunteers. Prior to the 3D acquisition, an ECG preparation scan was acquired to determine the appropriate diastolic and systolic ECG delay times. For the pulmonary arterial imaging, automatic subtraction of the systolic images from the diastolic images is performed for all of the paired acquisitions to produce arterial images. The two sets of arterial images are then added together to produce the swap phase encode extended-data (SPEED) acquisition data. The subtracted arterial images and the SPEED calculated images then undergo maximum intensity projection (MIP) processing.

The image quality of the pulmonary arterial segments in the three MR angiography techniques were assessed quantitatively by measurements of signal-to-noise ratio (SNR) and contrast-to-noise ratio (CNR). For all pulmonary arterial segments, the MR angiography using SPEED acquisition and image processing technique produced significantly higher SNR and CNR values compared with the MR angiography techniques acquired in the right-left or superior-inferior RO direction alone. Our proposed non-contrast-enhanced MR angiographic technique allows depiction of the pulmonary arteries without dephasing signals due to the relationship of the RO direction and the vessel orientation.

Poster Session 5-6

Quantitative Analysis of the Lung using Hyperpolarized Helium-3 Imaging

James C. Gee[1], Nicholas J. Tustison[2], Brian B. Avants[1], Talissa A. Altes[2], Gang Song[1], Eduard E. Delange[2], John P. Mugler[2]

1. Department of Radiology, University of Pennsylvania, USA
2. Univercity of Virginia, USA

A computational framework was developed for quantitative analysis of hyperpolarized helium-3 MR lung ventilation image data. Application to a cohort of 55 subjects (47 asthmatic and eight normal) included the generation of multiple image features comprised of first and second-order statistical measures calculated both regionally and globally. A mutual information feature subset selection algorithm was used to determine which imaging features best characterized clinical diagnosis. The performance of these imaging features were compared with spirometry features. It was found that the top image features perform much better compared with the current clinical gold-standard spirometric values when considered individually. Interestingly, it was also found that spirometric values are relatively orthogonal to these image feature values in terms of informational content.

Related was the development of a segmentation algorithm designed to quantify ventilation defects specifically in these lung image data. Comparative assessment was performed using 43 subjects (8 normal and 35 asthmatic) in which the poorly ventilated regions identified by the computational algorithm were compared to two independent human readers (R1 and R2) who were blinded to all clinical information. Inter-rater agreement between our algorithm and R1/R2 was characterized using Bland-Altman test plotting and calculation of the intra-class correlation coefficient (ICC) between pairings (ICC(R1,R2) = 0.97, ICC(R1,AP) = 0.86, and ICC(R2,AP) = 0.85). The findings indicate the proposed approach may be a potentially useful method for further lung research.

Poster Session 6-1

The Phantom Study for Analyzing the Small Airway Disease

Noriyuki Yanagawa[1], Naoko Kawata[1], Masako Suzuki[2], Ryosuke Irie[2], Yasuaki Namihira [2], Koichi Sawada[2], Hirotaka Sato[2], Toshihiko Sugiura[1], Yukiko Matsuura[1], Koichiro Tatsumi[1]

1. Department of Respirology, Graduate School of Medicine, Chiba University, Japan
2. Department of Radiology, Chiba University Medical Hospital, Japan

Purpose: To obtain most acceptable algorithm for quantifying the small air way disease, and to analyze the inner diameter and the wall thickness, using phantom, with mutidetecter-row computed tomography scans (MDCT).

Methods: CT scans of 2 types of phantom were performed using 3 types of multidetector-row helical-CT(MDCT) with 16(Activion16), 64(Aquilion64), 64(AquilionONE) detector arrays. CT scans were acquired with the following.

parameters: 120kv, 270 mA(CT-AEC), 0.35sec/rot, pitch:0.567,0.5mm slice thickness. All CT data were reconstructed using FC3(for soft tissue imaging), FC30(for bone imaging), and FC52(for high-contrast lung imaging) algorithms. We obtained multi-planner-reconstruction (MPR) images of each phantom with workstation (AZE, Co, Ltd,). Then, we evaluated the inner diameter of the phantom using the full width at half maximum principle (FWHM).

Results: Using the ladder phamtom, FC52 algorithm was most acceptable for reconstructing the images obtained with 3 types of CT scanners. The difference was not observed for evaluating axial resolution between 3 types of CT scanners. AqullionONE (64 detector arrays) was most acceptable for evaluating Z axis resolution. The measurement of the inner diameter was strongly influenced by the wall thickness, in addition to the length of the inner diameter and other parameters.

Conclusion: Our results indicates FC52 algorithm is most acceptable for reconstructing the iamges, and the measurement of the inner diameter may be strongly influenced by the wall thickness, in addition to the length of the inner diameter and other parameters.

Poster Session 6-2

Integral-based Half-Band Method in Measuring Airway Wall Thickness on CT: Comparison with Conventional Full-Width Half Maximum Method in Actual and Simulated Phantoms

Kim, Namkug[1], Jeongjin Lee[2], Joon Beom Seo[1], Eun Jin Chae[1]

1. Department of Radiology, Ulsan Unversity College of Medicine, Asan Medical Center, Korea
2. Department of Digital Media, The Catholic University of Korea, Korea

To compare accuracy and robustness of a new integral-based half-band method with them of a conventional full-width half maximum method (cFWHM) in measuring airway wall thickness on CT using actual and simulated phantoms.

Images were magnified ten-times and boundary of segmented lumen was used as an initial band. The band enlarged outward to the peak of density profile. The integrals of average density was accumulated and doubled for final measurement. Physical phantom, consists of various 11 poly-acryl tubes, were used for validation. The measured densities of the wall and airspace filled with poly-urethane foam were 150HU and -900HU, respectively. The phantom was scanned in 0.75mm collimation with a 16-multi detector row CT scanner (Siemens Sensation 16). CT images were reconstructed by various reconstruction kernels. To mimic complex anatomy of bronchi, simulated phantoms of attached vessel and incomplete airway wall were generated. Measured wall thickness was compared with real thickness and that of cFWHM method using Bland-Altman and paired t-test.

Measured wall thickness on phantom CT images with soft and standard kernels using a new method showed better agreement with actual thickness than cFWHM method (Bland-Altman 95% CI: -0.17~-0.01, -0.12~0.14, -0.32~0.18mm, vs. -1.03~0.32, -0.67~0.37, -0.28~0.44mm, respectively). Using the new method, the accuracy was higher in measuring wall thinner than 1.2mm (all $p<0.05$). However, on images reconstructed with sharp kernels (B70f, B80f), the measurement errors were larger (all $p<0.05$). In measuring simulated airway phantoms of attached vessel and incomplete wall, the new method was more accurate (all $p<0.001$).

Poster Session 6-3

Enhancement of Computerized Differentiation Accuracy of Region Pattern of Diffuse Infiltrative Lung Disease Using Local Context Sensitive SVM Classifier

Kim, Namkug[1], Jonghyuk Lim[2], Joon Beom Seo[1]

1. Department of Radiology, Ulsan Unversity College of Medicine, Asan Medical Center, Korea
2. Department of Industrial Engineering, Seoul National University, Korea

PURPOSE

To propose a novel local context sensitive SVM classifier (CSSVM) to improve differentiation of regional disease patterns of diffuse infiltrative lung disease (DILD) at HRCT : Comparison with that of radiologist's decision.

METHOD AND MATERIALS

900 rectangular regions of interest (ROIs) with 20x20 pixels, consisting of each 150 ROIs representing six regional disease patterns (normal, NL; ground-glass opacity, GGO; reticular opacity, RO; honeycombing, HC; emphysema, EMPH; and consolidation, CONS) were marked by two experienced radiologists with consensus at HRCT images of various DILD. 21 textual and shape features (textural features: histogram, gradient, run-length, co-occurrence matrix and shape features: cluster, top-hat) were calculated and employed to characterize the ROIs. A proposed CSSVM classified the center ROI by using probability (SVM's decision value) of each class and feature distance and class difference from eight neighborhood ROIs to the current ROI, simultaneously. Sequential forward selection was used for feature selection method. In addition, five folding cross validation with twenty repetitions were performed for cross validation. To validate the results, 900 ROIs and only consensus region of 67 slices drawn by two radiologists were compared, independently.

RESULTS

The accuracy of the proposed method of ROIs and whole lung region (89.88 ± 0.02, and 62.18 ± 0.15, respectively) was higher than that of the conventional SVM classifier (87.39 ± 0.02, and 59.72 ± 0.12, respectively) (paired t test, $p = 0.000$, and $p=0.000$, respectively).

CONCLUSION

The proposed local context sensitive SVM classifier showed more accurate differentiation of regional patterns of DILD.

Poster Session 6-4

Newly Developed Denoising Technique: Utility for Quantitative Assessment of Pulmonary Emphysema on Low-Dose CT Examination

Mizuho Nishio, Sumiaki Matsumoto[1], Yoshiharu Ohno[1], Naoki Sugihara[2], Takeshi Yoshikawa[1], Daisuke Takenaka[1], Kazuro Sugimura[1]

1. Department of Radiology, Kobe University Graduate School of Medicine, Japan
2. Toshiba Medical Systems Corporation, Japan

PURPOSE: To evaluate the utility of a new denoising technique for quantitative assessment of emphysema on low-dose CT (LDCT) as compared with the assessment on standard-dose CT (SDCT).

MATERIALS AND METHODS: Twenty-six patients (20 men, 6 women; age, 57-84; smoking history, 0-180 pack-years) underwent standard-dose (150 mAs) and low-dose (25 mAs) CT examinations using a 16-detector-row CT scanner. We utilized a new denoising technique, called adaptive iterative dose reduction (AIDR), for LDCT and reconstructed thin-section images with and without AIDR. As quantitative indices of emphysema, we calculated emphysema index and numbers of four emphysema clusters (cluster 1, 2-8 mm3; cluster 2, 8-65 mm3; cluster 3, 65-120 mm3; cluster 4, >120 mm3) on LDCT without AIDR, LDCT with AIDR, and SDCT. To evaluate the effect of AIDR, we compared Bland-Altman 95% limits of agreement (LOA) between SDCT and LDCT without AIDR as well as SDCT and LDCT with AIDR.

RESULTS: The LOA of emphysema index was -0.084 to 0.055 between SDCT and LDCT without AIDR and -0.046 to 0.076 between SDCT and LDCT with AIDR. The bias of emphysema index on LDCT was slightly improved by using AIDR. The LOA of four emphysema clusters was also improved by using AIDR, especially in small clusters. The LOA of clusters 1-2 were: -36200.6 to 5395.9 and -8974.5 to 1754.0 between SDCT and LDCT without AIDR; -7242.1 to 4224.5 and -1787.4 to 1471.1 between SDCT and LDCT with AIDR.

CONCLUSION: The new denoising technique can be useful for quantitative assessment of emphysema on LDCT.

Poster Session 6-5

Comparative Study of Respiratory Function for Pulmonary Lobectomy Based on Computer Simulation

Yasushi Hirano[1], Rui Xu[1], Shoji Kido[1], Xian Chen[1], Katsuya Ishii[2]
1. Graduate School of Medicine, Yamaguchi University, Japan
2. Information Technology Center, Nagoya University, Japan

The authors propose a method for quantitative evaluation of respiratory function for pulmonary lobectomy. This method is based on the computer simulation of air flow in bronchus regions extracted from clinical chest CT images. Pulmonary lobectomy is a general operative procedure for lung cancer surgery. In this procedure, surgeons cut off entire pulmonary lobes in which lung cancers exist. Therefore this procedure has high effectiveness for treatment of lung cancers. While there is a risk of causing respiratory dysfunction because bronchi transform unnaturally during the process that rest of lung lobe(s) expand to fill the space of the thoracic cavity.

The proposed method of computer simulation to estimate a respiratory function for quantitative evaluation is as follows ; (1) extraction of a bronchus region including an air region from a chest CT image, (2) division of the bronchus region into polyhedral meshes and (3) the hydrodynamic simulation using appropriate boundary conditions of an inlet and outlets for inspiration.

The computer simulations based on the above procedure were performed using chest CT images after pulmonary lobectomy, which contain two cases with good respiratory function and two cases with poor respiratory function. A quantitative evaluation was performed by comparing cases with good and poor respiratory function. Furthermore, the results of the computer simulation were evaluated by a medical doctor.

Poster Session 6-6

Lung CT Image Registration Using Diffeomorphic Transformation Models

Gang Song, Nicholas Tustison, Brian Avants, James C. Gee
Penn Image Computing and Science Laboratory (PICSL), Department of Radiology, University of Pennsylvania School of Medicine, USA

Given the importance of quantifying kinematics in the lung and segmenting its complex structure, various algorithms have been proposed in the literature for inter-subject and intra-subject lung registration. in this work, we describe the use of our open source Advanced Normalization Tools (ANTS) software package in the EMPIRE10 challenge. Specifically, we describe the results of applying a subset of possible algorithmic configurations focusing on two ANTS diffeomorphic transformation models: greedy Symmetric Normalization (picsl-gsyn) and exponential mappings (picsl-exp), which placed 1st and 10th respectively in the EMPIRE10 challenge evaluating 24 total algorithms. The registration pipeline begins with an affine alignment using lung masks. which precedes each of the two diffeomorphic models for deformable registration using normalized cross correlation integrated over local windows. The results show that our general image registration algorithm is able to achieve the state-of-the-art performance and is reproducible by using the same set of parameters in a fully automatic and open source pipeline.

Poster Session 6-7

Airway Tree Segmentation by Removing Paths of Leakage

Gang Song, Nicholas Tustison, James C. Gee
Department of Radiology, University of Pennsylvania, School of Medicine, USA

This paper describes a new method for airway segmentation from CT images. We propose a form of adjusted image gradients for thin airways segmentation and apply it in multi-stencil fast marching. A graph of airway path segments is constructed from the arrival time function of fast marching. Instead of detecting leakage during segmentation, our method verifies each path segment in a separate step, using a novel leakage cost function defined on the whole path. Our scheme of path removal can be viewed as complementary post-processing for existing region growing methods. Experiments show that the proposed method can remove leakage regions while keeping most thin airways.

Poster Session 7-1

A Low Dose CT Lung Screening Method for Smoking-related Thoracic Abnormalities Using 3D Automatic Exposure Control: Diagnostic Capability and Effectiveness in Radiation Dose Reduction (iLEAD Study)

Takeshi Kubo[1], Yoshiharu Ohno[2], Daisuke Takenaka[2], Mizuki Nishino[3], Hans-Ulrich Kauczor[4], Hiroto Hatabu[5]

1. Department of Diagnostic Imaging and Nuclear Medicine, Kyoto University Graduate School of Medicine, Japan
2. Department of Radiology, Kobe University Graduate School of Medicine, Japan
3. Department of Radiology, Dana-Farber Cancer Institute, USA
4. Diagnostic and Interventional Radiology, University Clinic Heidelberg, Germany
5. Department of Radiology, Brigham and Women's Hospital, USA

PURPOSE: To determine the utility of 3D automatic exposure control system of 64-detector row CT system for low-dose chest CT screening examination of smoking-related thoracic diseases.
METHOD AND MATERIALS: 75 consecutive enrollees (40 male, 35 female) underwent a chest non-contrast MDCT examination consisting of two scans; (1) 3D AEC (automatic exposure control) scan and (2) non-AEC scan (fixed tube current).
A target standard deviation value of 160 (on lung images) was set for 3D AEC scan and current time product of 150 mAs was used for non-AEC scan. All reconstructed images were 2mm-thick. Three chest radiologists independently reviewed the 150 CT examinations (2 x 75 patients) in random order. Reviewers assessed the likelihood of smoking related chest abnormality including aortic aneurysm, calcification of coronary arteries, emphysema, ground-glass opacity, honeycombing and nodules, using a 5-point score (1, definitely absent; 2, probably absent; 3, equivocal; 4, probably present; 5, definitely present). The kappa values and the score agreement rates (the rate of a reviewer assigning the same scores to the two scans of a patient) between AEC and non-AEC scans were calculated for three reviewers. The mean values of kappa values and agreement rate were calculated.
RESULTS: The mean kappa values were 0.70, 0.81, 0.72, 0.43, 0.63 and 0.67 for aortic aneurysm, coronary calcification, emphysema, ground-glass opacity, honeycombing and nodules, respectively and mean agreement rates were 0.93, 0.83, 0.80, 0.88, 0.94 and 0.83, respectively.
CONCLUSION: 3D AEC-assisted low dose CT protocol can produce the screening results consistent with standard dose CT protocol.

Poster Session 7-2

Standard and Low-kVp CT of the Lungs Using Different State-of-the-art Multidetector-row CT Systems: A Comparative Analysis of Image Quality and Radiation Dose

Wolfram Stiller, Gregor Pahn, Stella Veloza, Sebastian Ley, Julia Ley-Zaporozhan, Hans-Ulrich Kauczor

Department of Diagnostic & Interventional Radiology, University Hospital Heidelberg, Germany

Objectives: To quantitatively assess image quality relative to radiation dose for standard and low-kVp CT of the lungs with different state-of-the-art MDCT systems, and relate these findings to qualitative evaluation of lung structures and tissues.
Materials and Methods: For three MDCT systems, a 32- and a 64-row detector dual-source CT (Somatom© Definition DS/Flash, Siemens Medical Solutions, Forchheim, Germany), and a 128-row detector CT (Brilliance iCT, Philips Medizin Systeme GmbH, Hamburg, Germany) image data of a cylindrical water (Ø =40cm), a low-contrast, and a spatial resolution phantom (Siemens Cone-Beam Phantom, QRM GmbH, Moehrendorf, Germany) as well as a formalin-fixated porcine lung explant have been acquired using standard (120kVp/150mAs) and low-kVp (80kVp/300mAs) protocols. Primary collimation varied from 256, 128, 64, 32, and 8x0.5/0.6mm, reconstructed slice thicknesses were 0.5, 1.0, and 2.0mm.
Other scanning parameters (fixed): 300/600mA tube current, 0.5s rotation time, helical pitch 1, 10cm scan length, 500mm FOV. Apart from qualitative evaluation of image quality in the lung explant, image noise, homogeneity, low-contrast as well as spatial resolution have been determined from geometric phantom image data. For each dataset, CTDIvol and DLP have been determined and compared to console prediction and scan summary values.
Results and Conclusions: For lung CT imaging, state-of-the-art MDCT systems differ in the efficiency of their radiation dose usage with regard to achievable image quality. Independent of the systems' dose efficiency, low-kVp protocols at elevated tube current-time products show potential to allow for future radiation dose savings, although spatial and low-contrast resolution are affected by increasing image noise.
Acknowledgements: This research project is funded by the German Federal Ministry of Education and Research (BMBF) within the collaboration project: "Innovative Methods for the Optimization of Radiological Applications in Biomedical Imaging", grant numbers 02NUK008G/B.

Poster Session 7-3

Proposal of New Method: Single Breath Xenon Ventilation CT

Norinari Honda[1], Wataru Watanabe[1], Keiichiro Nishimura[1], Hisato Osada[1], Hitoshi Ohno[1], Takemichi Okada[1], Kei Nakada[1], Hisami Yanagida[1], Mitsuo Nakayama[2]

1. Department of Radiology, Saitama Medical Center, Saitama Medical University, Japan
2. Department of Thoracic Surgery, Saitama Medical Center, Saitama Medical University, Japan

[Purpose] CT ventilation images in clinical studies have been acquired by re-breathing of stable xenon (Xe) exclusively. Though the method is suitable for quantitative assessment of ventilation in normal tidal breathing, it requires relatively large amount of Xe leading to side effect of anesthesia. The method is not suited for some diseased lung where the analytic model does not fit. We propose a new method to obtain Xe concentration (Xe-C) images by a single breath of Xe.

[Materials and Methods] A phantom of an acryl cylinder of 4 L capacity inserted with six small cylinders of variable apertures of 1 - 12 mm diameter was created (Anzai Medical). The phantom was pictured by a dual energy, dual source CT (SOMATOM Definition flash, Siemens) after aspirating 3 L of 35%Xe-65%O2 mixture prepared by Xe control system (AZ-726, Anzai Medical) into the phantom. Four volunteers underwent dual energy CT by the dual source CT during a breath hold after a single vital capacity breath of 35%Xe-65%O2 mixture. Three-material decomposition was used to obtain Xe-C images.

[Results] The Xe-C images showed expected Xe distribution in the phantom and in the volunteers: Xe concentrations were parallel with the aperture sizes of the inserted cylinders. In healthy volunteers, Xe concentration was higher in the anterior parts of the lung. In one smoking volunteer with emphysema, the emphysematous portion has lower Xe concentration.

[Conclusion] Single vital capacity breath of Xe followed by dual energy CT and three-material decomposition can create ventilation image.

Poster Session 7-4

Relationship between Lung Morphologic and Functional Abnormality Assessed by Breath-Hold Perfusion SPECT-CT Fusion images

Kazuyoshi Suga[1], Hideyuki Iwanag[2], Okada Munemasa[2], Mitsue Kunihiro[2], Naofumi Matsunaga[2]

1. Department of Radiology, St. Hill Hospital, Japan
2. Department of Radiology, Yamaguchi University School of Medicine, Japan

Automated deep-inspiratory breath-hold (DIBrH) perfusion and ventilation SPECT-CT fusion images were used to objectively assess relationship between lung CT morphologic and functional abnormality in various lung diseases.

The fusion images showed a good correlation between lung CT attenuation changes and perfusion heterogeneity at CT mosaic attenuation areas, as perfusion was persistently decreased at low CT attenuation areas and preserved at intervening high CT attenuation areas in vascular or airway obstructive diseases and chronic obstructive lung diseases, and as perfusion was persistently decreased at high CT attenuation areas in interstitial lung diseases and bronchial pneumonia. These images frequently showed perfusion defects even in normal lung areas on CT in patients with vascular obstructive diseases, hepatopulmonary syndrome and pulmonary arteriovenous fistulas.

Assessment of relationship between lung CT morphologic and functional abnormality on the fusion images contributes to clarification of mechanisms and pathophysiology of abnormal lung CT appearance in various lung diseases.

Poster Session 7-5

Diagnostic Value of Initial Computed Tomography in Critically Ill Patients with Pulmonary Edema

Kosaku Komiya[1], Hiroshi Ishii[1], Hiroaki Oka[1], Atsuko Iwata[1], Okada Fumito[2], Katashi Satoh[3], Noriyuki Ebi[4], Hidehiko Yamamoto[4], Junji Murakami[5], Jun-ichi Kadota[1]

1. Internal Medicine 2, Oita University Faculty of Medicine, Japan
2. Radiology, Oita University Faculty of Medicine, Oita, Japan
3. Nursing Science, Kagawa Prefectural College of Health Sciences, Kagawa, Japan
4. Respiratory Medicine, Aso Iizuka Hospital, Fukuoka, Japan
5. Radiology, Aso Iizuka Hospital, Fukuoka, Japan

Rationale, Discriminating cardiogenic pulmonary edema (CPE) from non-cardiogenic pulmonary edema caused by acute lung injury (ALI) or acute respiratory distress syndrome (ARDS) is clinically important since the management and prognosis of the two conditions are very different. Previous studies showed limitations in the use of chest radiographs, however, the usefulness of chest CT in the differentiation of pulmonary edema has not been fully elucidated.
Objectives, To determine the diagnostic utility of chest CT in differentiating CPE from ALI/ARDS in critically ill patients with respiratory failure at the emergency department.
Methods, Emergency outpatients with acute respiratory failure presenting bilateral pulmonary infiltrates on chest radiographs were enrolled. The etiology of pulmonary edema (CPE, ALI/ARDS or mixed) was determined by 2 intensive-care specialists based on the clinical course including the findings of right-heart catheterization, but not chest radiographs and CT. The diagnosis of CPE or ALI/ARDS on chest CT was retrospectively and independently assessed by 2 chest radiologists without knowing any clinical information.
Results, Seventy patients (20 with ARDS/ALI, 41 with cardiogenic edema, and 9 with mixed) were evaluated. Increased transverse diameter of superior vena cava ($p<0.0001$), upper and central dominant pulmonary opacities ($p=0.003$), subpleural sparing ($p=0.067$), right-sided dominant pulmonary effusion ($p=0.012$), and peribronchovascular bundle thickening ($p<0.0001$) were significantly more frequent in patients with CPE than in those with ALI/ARDS.
Conclusions, Chest CT in the emergency department appears to be useful in differentiating CPE and ALI/ARDS in patients with acute respiratory failure. Further prospective studies are needed to validate these findings.

Poster Session 7-6

Pulmonary Lymphatic Drainage to the Mediastinum Based on CT Observations of Primary Complex of Pulmonary Histoplasmosis

Koji Takahashi, Tomoaki Sasaki, Tomonori Yamada, Hatsune Hiranuma, Toshihiro Yamaki, Naofumi Watanabe, Nobuhisa Takada, Youko Takada, Eriko Takabayashi, Keigo Kobayashi

Department of Radiology, Asahikawa Medical University, Japan

PURPOSE: To assess mediastinal lymphatic drainage patterns from each pulmonary segment/lobe using computed tomographic (CT) observations of calcified primary complex pulmonary histoplasmosis.

MATERIALS AND METHODS: We assessed 585 CT studies of patients with primary complex histoplasmosis consisting of a pulmonary lesion in single segment and hilar and/or mediastinal nodal disease. We assessed the distribution of hilar and mediastinal nodal involvement depending on pulmonary segment and lobe with focus on the incidence of N1and skip N2 involvement, the mean number of involved mediastinal nodal stations in non-skip N2 and skip N2 group, and preferentially involved mediastinal node stations. Institutional review board approval was obtained without requirement for informed consent for this retrospective study.

RESULTS: Skip involvement was common in apical segment (9/45,20.0%), posterior segment (7/31,22.6%), and medial basal segment (13/20,65.0%) in the right lung and in apical posterior segment (7/55 ,12.7%), lateral basal segment (6/26, 23.1%), and posterior basal segment (16/47, 34.0%) in the left lung. The incidence of skip involvement in each segment of both lungs shows a significant inversed correlation with that of N1 involvement ($r=-0.51$, $P<0.05$). The mean number of involved mediastinal nodal stations in non-skip N2 and skip N2 group in all segments of both lungs were 1.4 (434/301) and 1.2 (93/77) and the former was significantly larger than the latter ($p<0.01$). Preferentially involved mediastinal node was shown in relation to each pulmonary segment and lobe.

CONCLUSION: Our data showed a predictable pattern of segmental and lobar lymphatic drainage to the mediastinum, including skip invasion.

Poster Session 7-7

Evaluation of Cross-bridging Structures in Pneumothorax Patients and Correlation with Aging and Pulmonary Inflammation

Tomoaki Sasaki, Koji Takahashi, Tamio Aburano
Department of Radiology, Asahikawa Medical University, Japan

Objective: In T4 stage of non-small cell lung cancers, specific mediastinal invasion has better prognosis, which presumes direct pathways could be present other than the pulmonary hilum. We evaluated whether cross-bridging structures between each lung lobe and the mediastinum in the pneumothorax patients other than the pulmonary hilum exist and what factor affects these structures.

Material and Methods: The studies were approved by the Ethics Committee. We analyzed multidetector low computed tomographic images of 81 patients with pneumothorax for the incidence and distribution pattern of cross-bridging structures in the pleural cavities.

Result: Cross-bridging structures were observed in 34 of 54 patients (63%) in the right pneumothoraces, in 19 of 32 patients (59%) in the left pneumothoraces. The positive correlation was noted between the number of cross-bridging structures and aging or with pulmonary diseases. The cross-bridging structures were also present in specific distribution patterns, a part of them were common in their locations regardless of pulmonary disease or age.

Conclusion: Cross-bridging structures in pneumothoraces existed more than 50% of patients and were more frequently in older patients and with pulmonary diseases. These structures indicated specific distribution pattern and could play an important role as a direct pathway from each lung to the medistinum.

Poster Session 8-1

A Case of Thromboembolism in Peripheral Pulmonary Artery, Diagnosed by Dual-energy Multi-detector CT

Takahiko Kanokogi, Atsuhiro Nakamura, Masaki Sakurai, Takahiro Ohya, Koichi Tomoda, Masanori Yoshikawa, Kaoru Hamada, Hiroshi Kimura
Second Department of Internal Medicine, Nara Medical University, Japan

Dual energy multi-detector CT (MDCT) can reveal many information, not only pathological change but also lung physiology including perfused blood volume (PBV). At present, it become available to clinical use such as diagnosis of pulmonary thromboembolism.

Here, we report a case with an acute exacerbation on chronic thromboembolism, affected in the peripheral lung, with an obvious contribution of the dual energy MDCT for diagnosis. A 76-year-old female with thromboembolic pulmonary hypertension, was referred to our hospital because of persistent left leg edema. She wore a plastic cast because of patella fracture of her left knee joint. Although she denied having worsening of her respiratory condition, the increasing D-dimer (32ng/ml) indicated newly developed thromboemboli. Contrast enhanced CT did not reveal any thrombus in the lungs. However it showed venous thrombosis in her left leg. In addition, the dual-energy MDCT demonstrated defect of PBV in peripheral area in right upper lobe, indicating acute-on-chronic thromboembolism. No additional parenchymal or interstitial opacities were noted by the lung field view. After the 2-weeks' anticoagulant therapy, the decreased blood perfusion has been improving with normalized laboratory data including D-dimer. Of course, possible mechanism of persistent vascular constriction still remains to be elucidated enough. The case presented here revealed contribution of the dual energy MDCT on the clinical diagnosis of impaired pulmonary circulation including 'peripheral type thromboembolism' which is difficult to be detected by the conventional CE-CT.

Poster Session 8-2

CT-guided Pericardiocentesis for Recurrent Cardiac Tamponade due to Carcinomatous Pericarditis in a Patient with Adenocarcinoma of the Lung

Yoshihiro Kanemitsu, Hideo Kita, Michiharu Suga, Yoshinori Fuseya, Kazuya Tanimura, Yuko Katayama, Shigeto Nishikawa, Wataru Chiba, Mariko Murata, Yumi Nishihara
Department of Respiratory Medicine, Takatsuki Red Cross Hospital, Japan

A 60 year-old man with dyspnea on effort was admitted to our hospital because of an abnormal lesion on Chest X-ray.

The next day of admission, he rapidly developed dyspnea on rest.

Chest-X ray showed cardiomegaly and transthoracic echocardiogram (TTE) indicated massive pericardial effusion (PE).

Ultrasound-guided pericardiocentesis through the subxyphoid approach was performed.

cytology of pericardial effusion and histology of lung specimens from bronchoscopy revealed adenocarcinoma of the lung.

Despite of Erlotinib treatment, the patient developed cardiac tamponade again.

PE at apex was minimum with pericardial adhesion, which was resulted from the previous puncture.

Chest CT demonstrated massive PE located at left and right paraventriclar spaces.

We chose CT-guided pericadiocentesis from the right parasterunum and successfully placed a dorainage catheter.

CT enables to visualize intrathoracic anatomy including intercostal and internal mammary arteries, and thereby allows safe access to the pericardial space in case that subxyphoid or apical approach by TTE is difficult.

Poster Session 8-3

A Case of Pleomorphic Carcinoma of the Lung Producing Multiple Cytokines and Forming Rapidly Progressive Mass-like Opacity

Masataka Matsumoto[1], Ryo Itotani[1], Manabu Ishitoko[1], Shinko Suzuki[1], Minoru Sakuramoto[1], Masaya Takemura[1], Motonari Fukui[1], Yoshiaki Yuba[2], Takashi Nakayama[3], Osamu Yoshie[3]

1. Division of Respiratory Medicine, Kitano Hospital, Japan
2. Department of Pathology, Kitano Hospital, Japan
3. Department of Microbiology, Kinki University School of Medicine, Japan

A case of 52-year-old man who complained of high-grade fever accompanying with a mass-like opacity in the apex of the right lung on chest x-ray film. Lung abscess was suspected since CRP levels and neutrophil counts progressively increased in the blood examination. Despite of the administration of antibiotics, the mass-like opacity rapidly grew, and fluoro-2-deoxyglucose positron emission tomography (FDG-PET) showed FDG uptake was localized to the center of the mass-like lesion as well as to the bone-mallow and the swelling liver and spleen. Although transbronchial biopsy specimen disclosed only infiltration of lymphocytes, malignancies could not rule out. Thus, a right upper lobectomy was performed. Histopathological findings of the excised lung tissue showed a neoplastic lesion as pleomorphic carcinoma surrounded with the intense infiltration of neutrophils and lymphocytes. Serological and immnohistochemical examinations revealed the increased levels of serum IL-6, IL-8 and G-CSF and positive staining for them in the tumor lesion. A possible explanation is that the elevation of IL-6 levels contributed to high-grade fever and increased CRP levels, and increased serum G-CSF levels to the neutrophilia and hematopoietic activation. Additionally, we suggested the production of IL-8 from the cancer recruited neutrophils and lymphocytes around itself resulting in the rapid growing of the bulky mass-like opacity. This case indicated that FDG-PET in addition to conventional radiological approach such as CT scan may detect the immunological responses evoked around the tumor.

Poster Session 8-4

A Case of Malignant Mesothelioma with Diffuse Swelling Mediastinum Lacking of Apparent Pleural and Pericardial Lesion

Hiroki Kimura, Satoshi Noguchi, Yasuhiro Yamauchi, Shin Kawasaki , Tadashi Kohyama, Nobuya Ohishi, Takahide Nagase

Department of Respiratory Medicine, Graduate School of Medicine, The University of Tokyo, Japan

We report a case of malignant mesothelioma with very unusual radiological feature. A 67-year-old man visited our hospital with complaint of exersional dyspnea. This patient was a retired craftsman of fabric items and gave a negative history for both environmental and occupational asbestos exposure. Chest X-ray showed bilateral pleural effusion and swelling of mediastinum. CT scan revealed remarkable swelling of mediastinal soft tissue density, but apparently no pleural or pericardial lesion was detected. The pleural effusion was exudates, and hyaluronic acid of pleural effusion was markedly increased to 302 mcg/ml. The diagnois of malignant mesothelioma was established by histopathological findings from cell block preparation of pleural effusion, including the immunohistochemical profile. So far, a small number of cases of malignant mesothelioma with mediastinal lesion have been reported. However, to our knowledge, this is the first case of malignant mesothelioma with diffuse swelling of mediastinum lacking of apparent pleural and pericardial lesion.

Poster Session 8-5

A Case of Pulmonary Tumor Thrombotic Microangiopathy Presenting Progressive Pulmonary Hypertension

Hiromi Tomioka[1], Shyuji Yamashita[1], Toshihiko Kaneda[1], Yoko Kida[1], Masahiro Kaneko[1], Hiroshi Fujii[1], Masahiko Takeo[2], Eiji Katsuyama[3], Kyousuke Ishihara[1]

1. Department of Respiratory Medicine, Kobe City Medical Center West Hospital, Japan
2. Department of Respiratory Surgery, Kobe City Medical Center West Hospital, Japan
3. Department of Pathology, Kobe City Medical Center West Hospital, Japan

Pulmonary tumor thrombotic microangiopathy (PTTM) is characterized by widespread fibrocellular intimal proliferation of the small pulmonary arteries and arterioles in patients with metastatic carcinoma. Microscopic pulmonary tumor emboli have frequently occurred in patients with malignant tumors, however, few cases of PTTM have been reported. We report a case of PTTM presenting progressive pulmonary hypertension and lethal respiratory failure. A nonsmoking 64-year-old woman visited our hospital because of cough, chest pain and dyspnea on effort. High-resolution CT showed subpleural patchy small consolidation with ground-glass opacity. Right ventricular systolic pressure (RVSP) by echocardiography predicted mild pulmonary hypertension (48mmHg). Tc-99m MAA lung perfusion images showed multiple small defects in both lungs. Sputum cytology revealed adenocarcinoma cells, and FDG-positron emission tomography image showed increased uptake at right lower lobe and vertebral body of the Th7 level. A video-assisted lung biopsy was performed, and histology revealed well differentiated adenocarcinoma combined with PTTM, lymphangitis carcinomatosis and necrosis due to the pulmonary infarction. The patient was diagnosed as having PTTM associated with clinical stage Ⅳ primary lung adenocarcinoma. In spite of chemotherapy with cisplatin and vinorelbine, respiratory failure combined with pulmonary hypertension was progressed (RVSP=150 mmHg) and she died of respiratory failure. Generally it is difficult to diagnose PTTM in patients during life. This was an important case of PTTM associated with lung cancer and diagnosed antemortem by video-assisted lung biopsy.

Poster Session 9-1

Changes in Regional Pulmonary Perfusion and Morphology as a Result of Lung Volume Assessed by Technetium-99m Macroaggregated Albumin SPECT and MinIP with MDCT

Hiroko Tomita[1], Masahiro Horikawa[1], Kaori Ohta[1], Tamotsu Kita[1], Katsumi Hayashi[1], Shigeru Kosuda[1], Naoto Kitamura[2]

1. Department of Radiology, National Defense Medical College, Japan
2. Department of Radiology, Keio University School of Medicine, Japan

Objective: To evaluate the effects of lung volume on regional pulmonary perfusion using techntium-99m macroaggregated albumin (Tc-99m MAA) SPECT and the morphological changes using minimal intensity projection (minIP) with MDCT.

Methods: Four healthy volunteers were enrolled in this study. The subjects were injected with the tracer in the sitting position during the breath-hold at the levels of the functional residual volume (RV) and the total lung capacity (TLV). Regional pulmonary perfusion was assessed using SPECT imaging and profile curves produced by plotting and normalizing the perfusion values from the apex to the bottom of each lung. minIP and conventional images were also obtained during the breath-hold at the levels of RV and TLC using a 64-MDCT.

Results: The gravity-related perfusion decrease was observed in the upper lobes at TLC, but it disappeared and homogeneous perfusion was noted at RV. minIP revealed volume reduction at RV resulted in enlargement of the pulmonary vessels and shrinkage of the bronchi and tracheae, compared with their sizes at TLC (2.9 mm at TLC to 3.4 mm at RV in diameter of the lower lobes, 11.9 mm at TLC to 8.9 mm at RV in diameter of the tracheae, 11.3 mm at TLC to 9.1 mm at RV in diameter of the intermediate bronchi).

Conclusion: Redistribution of perfusion at RV is ascribable not to pulmonary artery stricture, but to hypoxia due to bronchial constriction, which probably overcomes the gravity effect.

Poster Session 9-2

Estimation of Pulmonary Arterial Pressure in Pulmonary Hypertension Based on Interventricular Septal Configuration Obtained by Electrocardiogram-gated 320 Slice CT

Toshihiko Sugiura, Nobuhiro Tanabe, Naoko Kawata, Yukiko Matsuura, Noriyuki Yanagawa, Miyako Saito Kitazono, Ayumi Sekine, Rintaro Nisimura, Takayuki Juzyo, Kouichiro Tatsumi

Department of Respirology, Graduate School of Medicine, Chiba University, Japan

Purpose: To estimate pulmonary artery (PA) pressure in subjects with pulmonary hypertension (PH), we retrospectively evaluated the interventricular septal configuration obtained by ECG-gated conventional scanning with 320-slice computed tomography (CT). The configuration of the interventricular septum was compared with systolic PA pressure (sPAP) and mean PA pressure (mPAP) obtained by right heart catheterization (RHC).

Materials and Methods: 38 subjects (10 male, 56 ± 12 yrs) with proven PH (23 chronic thromboembolic pulmonary hypertension and 15 pulmonary arterial hypertension) underwent enhanced 320-slice CT (Aquilion one) and RHC one month apart with no change in clinical status between the examinations. CT images were reconstructed every 5% from 0-95% of the R-R interval and a series of short-axis images was acquired covering the entire left and right ventricles (Zio Station). We compared the leftward shift of the interventricular septum (LSIVS) and septal bowing expressed as curvature (reciprocal of radius [/cm], a leftward curvature was denoted as a negative value) at end systole (ES) with both sPAP and mPAP.

Results: sPAP and mPAP from RHC were 70.8 ± 20.0 mmHg and 42.0 ± 11.6 mmHg, respectively. LSIVS at ES was detected in 19 subjects. sPAP and mPAP were significantly higher in subjects with LSIVS (84.3 ± 14.0 vs 57.3 ± 15.3 mmHg [sPAP] ($P<0.001$), and 49.4 ± 8.0 vs 34.6 ± 9.7 mmHg [mPAP] ($P<0.001$)). The correlation coefficients of septal curvature with sPAP and mPAP were -0.73 ($P<0.001$) and -0.74 ($P<0.001$), respectively.

Conclusions: Septal curvature based on ECG-gated 320-slice CT can be used to obtain an accurate estimate of sPAP and mPAP in subjects with PH.

Poster Session 9-3

Right Ventricle to Left Ventricular Volume Ratio by Electrocardiogram-gated 320 Slice CT is a Predictor of Right Ventricular Pressure Load in Pulmonary Hypertension

Toshihiko Sugiura, Nobuhiro Tanabe, Naoko Kawata, Yukiko Matsuura, Noriyuki Yanagawa, Miyako Saito Kitazono, Ayumi Sekine, Rintaro Nisimura, Takayuki Juzyo, Kouichiro Tatsumi
Department of Respirology, Graduate School of Medicine, Chiba University, Japan

Purpose: To estimate predictors of right ventricular (RV) pressure in subjects with pulmonary hypertension (PH), we measured right (RV) and left ventricular (LV) volumes by ECG-gated 320-slice CT and compared the RV to LV volume ratio with pulmonary arterial pressure (PAP) and pulmonary vascular resistance (PVR) obtained by right heart catheterization (RHC).

Materials and Methods: 38 subjects (10 male, 56 ± 12 yrs) with PH (23 chronic thromboembolic pulmonary hypertension and 15 pulmonary arterial hypertension) underwent enhanced retrospective ECG-gated conventional 320-slice CT (Aquilion ONE) and RHC 1 month apart between the two examinations. CT images were reconstructed every 5% from 0-95% of the R-R interval. We quantified RV ES (RVESV) and ED volumes (RVEDV), LV ES (LVESV) and ED volumes (LVEDV), the ratios of RVESV/LVESV and RVEDV/LVEDV. These parameters were compared with the results of RHC.

Results: RVESV, RVEDV, LVESV, and LVEDV were 96 ± 47, 164 ± 48, 31 ± 10, and 96 ± 26ml, respectively. In RHC, mean PAP (mPAP), sytolic PAP(sPAP) and PVR were 42 ± 12mmHg, 71 ± 20mmHg and 780 ± 342dyne. sec.cm-5, respectively. The correlation coefficients of RVESV/LVESV with mPAP, sPAP and PVR were 0.60 ($P<0.001$), 0.55 ($P<0.001$) and 0.69 ($P<0.001$), respectively. The correlation coefficients of RVESV/LVESV with mPAP, sPAP and PVR were 0.60($P<0.001$), 0.55($P<0.001$) and 0.69($P<0.001$), respectively. The correlation coefficients of RVEDV/LVEDV with mPAP, sPAP and PVR were 0.51($P=0.001$), 0.44($P=0.005$) and 0.70($P<0.001$), respectively.

Conclusions: The RV to LV volume ratio by ECG-gated 320-slice CT significantly correlated with PVR acquired by RHC in subjects with PH, and it may estimate mPAP, sPAP and PVR acquired by RHC in these subjects.

Poster Session 9-4

Correlation of Right Ventricular Ejection Fraction with Tricuspid Annular Plane Systolic Excursion by Electrocardiogram-gated 320 Slice CT in Pulmonary Hypertension

Toshihiko Sugiura, Nobuhiro Tanabe, Naoko Kawata, Yukiko Matsuura, Noriyuki Yanagawa, Miyako Saito Kitazono, Ayumi Sekine, Rintaro Nisimura, Takayuki Juzyo, Kouichiro Tatsumi
Department of Respirology, Graduate School of Medicine, Chiba University, Japan

Purpose: There is a strong correlation between right ventricular ejection fraction (RVEF) and tricuspid annular plane systolic fraction (TAPSE) determined by echocardiography in subjects with pulmonary hypertension (PH). However, it is unknown whether there a correlation between RVEF and TAPSE determined by 320-slice CT. We tested whether TAPSE measured by ECG-gated 320-slice CT correlates with RVEF, and correlates with pulmonary arterial pressure (PAP) and pulmonary vascular resistance (PVR) obtained by right heart catheterization (RHC) in PH subjects.

Materials and Methods: 38 subjects (10 male, 56 ± 12 yrs) with PH (23 chronic thromboembolic pulmonary hypertension and 15 pulmonary arterial hypertension) underwent enhanced retrospective ECG-gated conventional 320-slice CT (Aquilion ONE) and RHC, with 1 month between the two examinations. CT images were reconstructed every 5% from 0-95% of the R-R interval and a series of apical 4-chanber images. TAPSE was measured from systolic displacement of the RV freewall and tricuspid annular plane junction (Zio Station). RV end-systolic and end-diastolic true volumes were measured from 3-dimensional reconstruction (Virtual Place Fujin, AZE) and used to calculate RVEF.

Results: TAPSE and RVEF were 14.9 ± 3.6 mm and 46.1 ± 12.6%, respectively. In RHC, mean PAP (mPAP) and PVR were 42 ± 12 mmHg and 680 ± 342 dyne sec cm-5, respectively. The correlation coefficient of TAPSE with RVEF was 0.81 ($P<0.001$). The correlation coefficients of TAPSE with mPAP and PVR were 0.67 ($P<0.001$) and 0.62 ($P<0.001$), respectively.

Conclusions: TAPSE by ECG-gated 320-slice CT correlated strongly with RVEF and significantly with mPAP and PVR acquired by RHC in subjects with PH.

Poster Session 9-5

Evaluation of Hemodynamic Changes in Pulmonary and Systemic Arterial Circulation in Patients with Pulmonary Fibrosis in Relation to Breathing Methods Using Phase Contrast MRI

Nanae Tsuchiya, Yuichiro Ayukawa, Sadayuki Murayama
Department of Radiology, University of the Ryukyus Hospital, Japan

PURPOSE: Blood flow volume of the pulmonary and systemic arterial circulation in patients with pulmonary fibrosis is not well understood. The purpose of this study was to evaluate the hemodynamic changes in relation to breathing methods in patients with pulmonary fibrosis using phase-contrast MRI.

METHODS: Eleven patients with pulmonary fibrosis and 15 healthy volunteers were examined by a 1.5T MR apparatus. Phase-contrast flow measurements with free breathing and inspiratory breath-holding were performed in the ascending aorta and pulmonary trunk. Blood flow volume per minute measured from the time-velocity curve was compared. For statistical analysis of each blood flow volume between the patients and the healthy subjects, the Mann-Whitney U test was used. Wilcoxon's signed-ranked test was used to assess significant differences in both the pulmonary and systemic flow volume between free breathing and breath-holding in patients and volunteers.

RESULTS: The pulmonary and systemic blood flow in patients with pulmonary fibrosis was significantly reduced compared with those in healthy subjects during both free breathing and inspiratory breath-holding. However, shunt volume between pulmonary and systemic blood flow in patients with pulmonary fibrosis was maintained during both free breathing and inspiratory breath-holding.

CONCLUSION: Physiological shunt volume was confirmed to be maintained without influence of breathing methods even in patients with low blood flow circulation affected by pulmonary fibrosis.

Poster Session 9-6

Alteration of Pulmonary Perfusion after CT Density-Based Non-uniform Attenuation Correction on DIBrH SPECT-CT Fusion Images

Kazuyoshi Suga[1], Munemasa Okada[2], Hideyuki Iwanaga[2], Mitsue Kunihiro[2], Naofumi Matsunaga[2]
1. Department of Radiology St. Hill Hospital, Japan
2. Department of radiology, Yamaguchi University School of Medicine, Japan

Alteration of pulmonary perfusion after CT density-based, nonuniform photon attenuation correction (AC) on deep-inspiratory breath-hold (DIBrH) SPECT-CT fusion image was evaluated.

Forty patients with pulmonary emphysema, 32 with pulmonary thromboembolism, 23 with lung cancer and 6 normal controls underwent DIBrH Tc-99m-MAA SPECT, using a dual-head SPECT system and a respiratory tracking device. Scatter-corrected DIBrH SPECT with the triple energy window method was automatically coregistered with DIBrH CT. AC of DIBrH SPECT was performed using an attenuation coefficient map of a variable-effective linear coefficient calculated from CT pixel density of the co-registered DIBrH CT. Alteration of pulmonary perfusion after AC was evaluated by comparison with uncorrected DIBrH SPECT.

Compared with non-AC DIBrH SPECT, the maximum pixel counts in normal lungs were predominantly increased at deep lung portions near the mediastinum and vertebrae and at the upper and middle lungs, regardless of systematic increases (145% ± 28), with significant enhancement of physiological gravitational ventral-dorsal gradient of pulmonary perfusion ($P < 0.01$). In the affected lungs of all the lung diseases, perfusion defect clarity and/or heterogeneity were significantly enhanced ($P < 0.001$), without noticeable artifacts. The correlation between perfusion heterogeneity and the lung diffusing capacity for carbon monoxide was significantly improved in patients with emphysema ($P < 0.005$), and postoperative respiratory function (FEV1) could be better predicted in patients with lung cancer ($P < 0.005$).

Alteration of pulmonary perfusion after AC on DIBrH SPECT-CT fusion images appears to better reflect physiologic perfusion in normal lungs and perfusion impairment in the lung diseases.

Poster Session 9-7

Comparative Study of Tc-99m MAA Lung Perfusion SPECT and Multidetector CT Pulmonary Angiography in Patients with Chronic Pulmonary Embolism-Multicenter Trial

Shigeru Kosuda[1], Mayuki Uchiyama[2], Kazuyoshi Suga[3], Noriyuki Tomiyama[4], Ayumu Horikawa[5], Norinari Honda[6], Atsuo Inoue[4], Ryoji Ohno[1], Masami Kawamoto[1], Tsuyoshi Komori[1]

1. National Defense Medical College, Japan
2. Tokyo Jikeikai Medical College, Japan
3. Saint Hill Hospital, Japan
4. Osaka University School of Medicine, Japan
5. South Yokohama Kyosai Hospital, Japan
6. Saitama General Medical Center, Japan

Chronic pulmonary embolism (CPE) leads to pulmonary hypertension that is a progressive disease with a poor prognosis.

Objectives: To retrospectively compare Tc-99m MAA lung perfusion SPECT study with multidetector CT pulmonary angiography (CTPA) regarding the number of affected segmental pulmonary arteries in patients with CPE.
Methods: We retrospectively reviewed the results of Tc-99m MAA SPECT and CTPA in CPE patients at our hospitals between 2001 and 2008. A total of 50 patients (27 males, 23 females; age range, 32-79 y; mean age 65.0 y) were enrolled. The SPECT and CTPA images were interpreted by three NM physicians. The CTPA criteria of PTE were as follows; pouch defect, abrupt narrowing, obstruction, intimal irregularity, webs and bands. Semi-quantification was done by using a scoring system with a maximal sore of 17 segments.
Results: Seven (23%) patients had a final diagnosis of chronic PTE hypertension. Only 4 (13%) patients had a complete improvement of acute PTE, though 18 (60%) patients exhibited a partial improvement of PTE. SPECT showed improvement and aggravation of the disease more accurately than CTPA. However, CTPA provided us with morphological information such as PA dilation, RV enlargement.
Conclusions: Our results demonstrated that SPECT and CTPA were complementary to each other and Tc-99m MAA SPECT was more accurate than CTPA in monitoring PTE patients. SPECT should be performed as a baseline study at the initial diagnosis of acute PTE.

Poster Session 10-1

CT Diagnosis of Recurrence of Lung Cancer

Fumiyasu Tsushima, Shuichi Ono, Shinya Kakehata, Hiroko Seino, Kohei Morimoto, Koichi Shibutani, Hiroyuki Miura, Yoshihiro Takai
Department of Radiology, Graduate School of Medicine Hirosaki University, Japan

The purpose of this study was to determine recurrence of lung cancer predictors based on postoperative CT findings. Among 203 patients with primary lung cancer who underwent thoracotomy since January 2003 until December 2004, 61 patients had recurrence, 46 of them were found to have recurrent tumor, LN swelling or pleural dissemination. In 43 of 46 patients, recurrent tumor, LN swelling, pleural nodules or thickening were detected on postoperative CT.

From these results, we conclude that CT is essential for detecting recurrence of postoperative lung cancer.

Poster Session 10-2

Comparison of Quantitative Diagnostic Capability of Lymph Node Metastasis in Non-small Cell Lung Cancer Patients between STIR Turbo SE Imaging, Diffusion-Weighted Imaging and FDG-PET/CT

Daisuke Takenaka, Yumiko Onish, Hisanobu Koyama, Sumiaki Matsumoto, Takeshi Yoshikawa, Yoshiharu Ohno, Kazuro Sugimura
Department of Radiology, Kobe University Graduate School of Medicine, Japan

Purpose: To prospectively compare quantitative diagnostic capabilities of lymph node metastasis among short inversion time inversion recovery (STIR) turbo spin-echo imaging, diffusion-weighted imaging (DWI), and FDG-PET/CT in non-small cell lung cancer (NSCLC) patients.

Material and Methods: 62 consecutive NSCLC patients underwent STIR-TSE imaging, DWI, integrated FDG-PET/CT and surgical resections. For quantitative differentiation of metastatic from non-metastatic lymph nodes, ratio of signal intensity between lymph node and muscle (LMR) on STIR, apparent diffusion coefficient (ADC) on DWI and SUV on PET/CT at each lymph node were measured by ROI measurement. Then, each index was statistically compared between metastatic and non-metastatic lymph nodes by Student's t-test. To determine the feasible threshold value of each index, ROC-based-positive test was performed on a per node basis. Finally, sensitivity, specificity and accuracy of each index were compared each other on a per node basis and on a per patient basis by McNemar's test.

Results: LMR and SUV had significant difference between metastiatic and non-metastatic lymph nodes. When each feasible threshold value revealed with ROC-positive test was adapted on a per node basis analysis, specificities and accuracies of STIR was significantly higher than those of DWI and PET/CT on a per node basis assessment. When corresponding values were adapted on a per patient analysis, specificity and accuracy of STIR were significantly higher than those of PET/CT.

Conclusions: STIR turbo spin-echo imaging is more accurate method for quantitative diagnosis of metastatic lymph node than PET/CT, and would be better to utilized rather than DWI in NSCLC patients.

Poster Session 10-3

Capability for Quantitative Differentiation of Small Cell Lung Cancer from Non-Small Cell Lung Cancer by Diffusion-Weighted Imaging and STIR Turbo SE Imaging

Hisanobu Koyama[1], Yoshiharu Ohno[1], Nobukazu Aoyama[3], Yoshimasa Maniwa[3], Tomoo Ito[4], Yoshihiro Nishimura[5], Kazuro Sugimura[1]

1. Department of Radiology, Kobe University Graduate School of Medicine, Japan
2. Division of Radiology, Kobe University Hospital, Japan
3. Division of Cardiovascular, Thoracic and Pediatric Surgery, Kobe University Graduate School of Medicine, Japan
4. Division of Diagnostic Pathology, Kobe University Graduate School of Medicine, Japan
5. Division of Cardiovascular and Respiratory Medicine, Department of Internal Medicine, Kobe University Graduate School of Medicine, Japan

Objective: To determine the capability of quantitative differentiation between small cell lung cancer (SCLC) and non SCLC (NSCLC) of diffusion-weighted image (DWI) and short TI inversion recovery turbo spin-echo imaging (STIR).
Materials and Methods: In this study, the pathological diagnoses of all subjects were proved from surgical specimens for purposes of accuracy. Four patients with SCLC (mean age; 66.3 years) and 20 NSCLC patients selected from our database who were matched to SCLC patients in age and in the diameter of cancer were enrolled. All MR examinations were performed on a 1.5 T scanner, and DWI and STIR were acquired. For quantitative assessments of histological classification, apparent diffusion coefficient (ADC) values on DWI and contrast ratios between cancer and muscle (CRs) on STIR were measured. ADC values and CRs were then compared, and diagnostic capabilities were obtained statistically.
Results: There were significant differences between the mean ADC values of SCLC and those of NSCLC ($p<0.05$); however, there were no significant differences between the mean CRs of SCLC and those of NSCLC ($p>0.05$). With adopted threshold values, the specificity and accuracy of DWI were 90.0% (18/20) and 87.5% (21/24), respectively. Those diagnostic capabilities were higher than those of STIR ($p<0.05$). In addition, the combination of both sequences could improve diagnostic accuracy (specificity; 100% [20/20], and accuracy: 95.8% [23/24]).
Conclusion: DWI is a sensitive sequence for the differentiation of SCLC from NSCLC, and the combination of DWI and STIR had a reliable diagnostic indicator of differentiation.

Poster Session 10-4

Comparison of Capability for Pulmonary Nodule Detection ; 1.5T vs 3.0T Systems

Keiko Matsumoto, Yoshiharu Ohno[2], Yumiko Onishi[2], Hisanobu Koyama[2], Daisuke Takenaka[2], Nobukazu Aoyama[3], Hideaki Kawamitsu[3], Kazuro Sugimura[2], Tsutomu Araki[4]

1. Departmenr of Radiology, Yamanashi Hospital of Social Insurance, Japan
2. Department of Radiology, Kobe University Graduate School of Medicine, Japan
3. Division of Radiology, Kobe University Graduate School of Medicine, Japan
4. Division of Radiology, University of Yamanashi, Japan

[PURPOSE] To prospectively and directly compare the detection and differentiation capabilities of non-contrast-enhanced (non-CE) pulmonary MR imaging between 1.5 T and 3T systems.

[MATERIALS AND METHOD] A total of 40 patients (20 male, 20 female; mean age 66.4 years) with 70 pulmonary nodules detected on thin-section MDCT underwent non-CE MR imaging on 1.5T and 3T systems. Black-blood T1WI, T2WI and STIR turbo spin-echo imaging were obtained on both systems. The gold standard was determined from the results of thin-section MDCT. The probabilities of nodule presence were assessed by using 5-point scoring system. To determine for nodule detection on appropriate sequences, ROC analyses were performed to determine the feasible threshold values. Overall nodule detection rates of all sequences were compared by using McNemar's test. For determination of the practical threshold values to differentiate malignant from benign nodules, ROC-based positive tests were performed. Finally, sensitivity, specificity and accuracy were directly compared by McNemar's test.

[RESULTS] Although ROCs of all sequences had no significant difference for qualitative nodule detection ($p>0.05$), overall nodule detection rates of T1WI, T2WI and STIR at 1.5 T MR scanner and STIR at 3.0 T MR scanner were significantly lower than the standard reference ($p<0.05$).

[CONCLUSION] Non-CE MR imaging on 3T system was more useful for detection and diagnosis of pulmonary nodules than that on 1.5T system.

Poster Session 10-5

Utility of Nodule Type Assessment for Improving Diagnostic Capability in Patients with Solitary Pulmonary Lung Nodules on Low-Dose CT at FDG-PET/CT

Yumiko Onishi, Yoshiharu Ohno, Hisanobu Koyama, Mizuho Nishio, Daisuke Takenaka, Sumiaki Matsumoto, Kazuro Sugimura
Department of Radiology, Kobe University Graduate School of Medicine, Japan

PURPOSE: To determine the utility of nodule type assessment on low-dose CT at integrated FDG-PET/CT examination to improve diagnostic capability in patients with solitary pulmonary nodules (SPNs).

METHOD AND MATERIALS: Seventy-five patients (49 males, 26 females; mean age, 69years) with SPNs detected on thin-section MDCT examinations underwent integrated FDG-PET/CT. All SPNs were divided into two groups (malignant vs. benign nodules) according to the final diagnoses. To determine the capability of nodule type assessment on low-dose CT at FDG-PET/CT examination, two radiologists assessed all nodules on low-dose CT for attenuation correction and thin-section CT by using 5-point scoring system. Then, final assessment at each nodule was determined as consensus of two readers. To evaluate the difference of nodule type assessment between both CTs, kai square test was performed. For comparison of diagnostic capabilities between FDG-PET/CT without and with nodule type assessment on LDCT, ROC-based positive tests were performed to determine the feasible threshold values for overall and each type of nodules. Finally, sensitivity, specificity and accuracy were compared by means of McNemar's test.

RESULTS: When compared the results of nodule type assessment between two types of CT, there were no significant difference ($p>0.05$). When feasible threshold values were adopted, accuracy (89.3 [67/75] %) of PET/CT with nodule type assessment on low-dose CT were significantly higher than that of PET/CT without nodule type assessment on low-dose CT (77.3 [58/75]%, $p<0.05$).

CONCLUSION: Nodule type assessment on low-dose CT at integrated FDG-PET/CT examination is useful to improve diagnostic capability in patients with solitary pulmonary nodules.

Poster Session 10-6

Estimation of Increase of Pulmonary Ground-Glass Opacity: Integrated evaluation of detected GGOs using early indicator of growth

Shuji Yamamoto[1], Masahiro Suzuki[2], Shiho Gomi[2], Youichi Yamazaki[3], Ryutaro Kakinuma[2], Kenya Murase[3], Noriyuki Moriyama[2]
1. LISIT,Co.,Ltd, Japan
2. Department of Radiology, National Cancer Center, Cancer Prevention and Screening, Japan
3. Department of Medical Engineering, Division of Allied Health Sciences, Osaka University Medical School, Japan

A GGO is a finding on thin-section CT images of the lung that has been described as a hazy area of increased attenuation with preservation of the bronchial and vascular margins. The major teaching points in our presentations are: 1. To demonstrate a optimal segmentation method of localized Ground Glass Opacity (GGO) both pure GGO and mixed GGO. 2. To present the effective quantitative analysis to evaluate the characteristics of GGOs on original developed 2D and 3D approached application softwere. 3. To understand the limitation of low dose HRCT with simulated control of signal to noise ratio for GGO physically. In this presentation, we suggest the integrated three approaches (clinical, experimental and computational approach) for lung cancer screening.

Poster Session 10-7

How Much Can the Radiation Dose be Reduced in Automated Volumetry of Pulmonary Nodules? A Comparison of 16 cm Volume Scans and 64-row Helical Scans with 320-row MDCT.

Ayano Kamiya, Sadayuki Murayama, Hisashi Kamiya, Tetsuhiro Miyara
Depertment of Radiology, University of the Ryukyus graduate school of Medical science, Japan

Purpose: To determine how much the radiation dose can be reduced in automated volumetry of pulmonary nodules with 16 cm volume scans and 64-row helical scans using a chest phantom with artificial pulmonary nodules.

Material and Methods: A lung phantom containing four nodules of different sizes (5 and 10 mm diameters) and densities (solid and ground glass opacity; GGO) with three different nodule categories (intraparenchymal, attached to blood vessels or the pleura) was scanned using both 16 cm volume scans and 64-row helical scans with a 320-row MDCT scanner . Nodules were imaged using varying tube currents and collimations. Data sets were analyzed with a dedicated workstation using volumetry software . Absolute percentage error of estimated volume to known real volume < 20% was defined as eligible.

Results: Nodules with 10 mm diameter on thinner section CT were evaluated in detail, as measurement eligibility was high. All solid nodules were measured accurately by both scans, even with tube currents as low as 3.5 and 5 mAs. GGO nodules could be accurately measured using 17.5 mAs with a volume scan. Intraparenchymal nodules and those attached to the pleura were not measured accurately with tube current lower than 35 mAs in a helical scan.

Conclusions: Volumetry of 10 mm solid nodule was eligible with a very low tube current when a thin section was applied. For GGO nodules, volumetry with a tube current of 17.5 ms was eligible in a volume scan, which was lower than in a helical scan.

Poster Session 10-8

Prediction of Postoperative Lung Function in Patients with Lung Cancer: Comparison of Dual-energy Perfusion CT and Perfusion Scintigraphy

Eun Jin Chae[1], Joon Beom Seo[1], Jae-Woo Song[1], Namkug Kim[1], Joo-Young Park[1], Hyun Joo Lee[1], Hye Jeon Hwang[1], Chaehun Lim[1], Yong Hee Kim[2]
1. Department of Radiology, Ulsan College of Medicine, Asan Medical Center, Korea
2. Department of Thoracic and Cardiovascular Surgery, Ulsan College of Medicine, Asan Medical Center, Korea

Purpose: To assess the potential of a dual-energy perfusion CT as a substitute for a pulmonary perfusion scintigraphy for predicting postoperative lung function in patients undergoing lung resection.

Materials and Methods: Forty-five patients (M:F = 35:10; mean age, 63.2 years) were prospectively enrolled and they underwent dual-energy perfusion CT, perfusion scintigraphy, and pulmonary function test (PFT) before surgery and 6 months after surgery. Lobectomy in 42, bilobectomy in two, and pneumonectomy was performed in one patient. CT was scanned at 40 seconds after contrast injection using dual-source CT (Definition, Siemens) with dual-energy technique. On dual-energy CT data, each lobe was segmented using in-house software. Regional perfusion of each lobe was measured by multiplying lobe volume and iodine value per voxel. The proportion of perfusion of each lobe per whole lung was obtained from both perfusion CT and scintigraphy. Predicted postoperative FEV1 (po-FEV1) was calculated by multiplying preoperative FEV1 and (1 -proportion of perfusion of lobe(s) to be resected). Agreements between predicted po-FEV1 and real po-FEV1 were assessed with Bland-Altman plot for both modalities. Precision of prediction of two modalities was assessed by comparing percentage errors of predicted po-FEV1 to real po-FEV1.

Results: On Bland-Altman method, the limits of agreement (±2SD) between real po-FEV1 and predicted po-FEV1 in liter, were -0.88 and 0.85 in scintigraphy and -0.88 and 0.56 in CT. The limits of agreement (±2SD) between real po-FEV1% predicted and predicted po-FEV1% predicted, were -30.1 and 27.7 in scintigraphy and -30.0 and 18.0 in CT. Percentage errors of FEV1 in liter and FEV1% predicted by perfusion CT were comparable to those by scintigraphy (15.8% and 16.0% by CT; 18.5% and 18.7% by scintigraphy).

Conclusion: Dual-energy perfusion CT was comparable to perfusion scintigraphy in the prediction of postoperative lung function.

Poster Session 11 - 1

Quantitative Analysis of Pulmonary Cysts and Emphysema on Computed Tomography: Lymphangioleiomyomatosis, Birt-Hogg-Dubé Syndrome and Chronic Obstructive Lung Disease

Kazunori Tobino[1], Toyohiro Hirai[2], Takeshi Johkoh[3], Masatoshi Kurihara[4], Kiminori Fujimoto[5], Kazuhisa Takahashi[1], Kuniaki Seyama[1]

1. Department of Respiratory Medicine, Juntendo University Graduate School of Medicine, Japan
2. Department of Respiratory Medicine, Kyoto University, Graduate School of Medicine, Japan
3. Department of Radiology, Kinki Central Hospital of Mutual Aid Association of Public School Teachers, Japan
4. Pneumothorax Center, Nissan Tamagawa Hospital, Japan
5. Department of Radiology, Kurume University School of Medicine and Center for Diagnostic Imaging, Kurume University Hospital, Japan

Objectives: To characterize the pulmonary cysts in patients with cystic lung diseases (i.e. Lymphangioleiomyoma [LAM] and Birt-Hogg-Dubé syndrome [BHDS]) and emphysema in patients with chronic obstructive lung disease (COPD) by quantification of low attenuation areas (LAAs) on CT and to assess the usefulness of the methods of characterizing fractals of LAAs to analyze the pathophysiology in cystic lung diseases.

Subjects and Methods: This study included 52 LAM patients, 18 BHDS patients and 40 COPD patients who had undergone CT scans at Juntendo University hospital between January 2002 and August 2009. The number and size of discrete continuous low attenuation areas (CLA) on CT were quantitatively assessed by computer software, and then the fractal properties of LAAs were evaluated in these diseases.

Results: The characteristics of LAAs differed between these diseases, and the fractal properties of CLA varied with a value of LAA% in LAM and BHDS, but in COPD. By comparing these results, the way of the development of LAAs in these diseases were suggested.

Conclusion: The computer-assisted, quantitative analysis of LAAs on CT images is useful to elucidate the pathogenesis of cystic lung diseases including LAM, BHDS, and COPD.

Poster Session 11 - 2

In Vivo Monitoring of Cystic Fibrosis-like Lung Disease in Mice by Volumetric Computed Tomography

Mark. O. Wielpuetz[1], Monika Eichinger[2], Karin Leotta[3], Stephanie Hirtz[4], Sönke H. Bartling[3], Wolfhard Semmler[3], Hans-Ulrich Kauczor[1], Marcus A. Mall[4], Michael Puderbach[2]

1. Department of Diagnostic and Interventional Radiology, University Hospital Heidelberg, Germany
2. Department of Radiology, German Cancer Research Center (dkfz), 69120 Heidelberg, Germany
3. Medical Physics in Radiology, German Cancer Research Center (dkfz), 69120 Heidelberg, Germany
4. Division of Pediatric Pulmonology & Allergy and Cystic Fibrosis Center, Department of Pediatrics Ⅲ, University of Heidelberg, 69120 Heidelberg, Germany

Purpose

The onset and spontaneous progression of cystic fibrosis (CF) lung disease is poorly understood. Aim of our study was to longitudinally characterize βENaC-transgenic (βENaC-TG) mice, an established in vivo model of CF lung disease, by flat-panel volumetric computed tomography (VCT) as a new method to identify initial lesions and monitor spontaneous disease progression as compared to wild-type (WT) littermates.

Methods and Materials

Using a VCT scanner prototype (80kV, 50mAs, scan time 19s, spatial resolution 200μm) 20 βENaC-TG and 23WT mice were examined longitudinally at 10 different time points from the age of 3 to 42 days. Studies were performed in inhalative sedation and free breathing. Blinded for the genotype, VCT images were evaluated with respect to qualitative (airway-obstruction [trachea, bronchi], diffuse infiltrates, atelectasis, air-trapping, parenchyma homogeneity), and quantitative parameters (lung density in Hounsfield units [HU]).

Results

The presence of airway-obstruction, diffuse infiltrates, atelectasis, and air-trapping were significant signs for βENaC-TG mice (p-values from <0.05 to <0.001). Obstruction of the trachea occurred exclusively in βENaC-TG mice and proved to be a predictive factor for early mortality. Lung parenchyma showed inhomogeneous texture as well as significantly lower HU in βENaC-TG compared to WT mice at all time-points ($p<0.001$).

Conclusion

We conclude that VCT is a sensitive technique for non-invasive detection of early lesions, and longitudinal intra- and inter-individual monitoring of spontaneous progression of CF-like lung disease in mice. Our data suggest that VCT may provide a useful tool for pre-clinical evaluation of novel treatment strategies for CF and other chronic lung diseases.

Poster Session 11 - 3

Using Hyperpolarized 3He MRI for Treatment Evaluation in Cystic Fibrosis

Yanping Sun[1], Brian P. O'Sullivan[2], Ronn Walvick[1], Austin Reno[1], John P. Roche[1], Linxi Shi[1], Dawn Baker[2], Joey Mansour[1], Mitchell S. Albert[1]

1. Department of Radiology, University of Massachusetts Medical School, USA
2. Department of Pediatrics, University of Massachusetts Medical School, USA

We used hyperpolarized (HP) 3He MR imaging, with addition of an advanced, semi-automated analysis technique, to quantitatively investigate the volume of lung ventilation in three subjects with cystic fibrosis. We conducted HP 3He static ventilation MRI scans on a Philips 3.0T Achieva MRI scanner using a flexible, wrap-around, 3He, radio-frequency (RF) coil. For image analysis, we employed a novel semiautomatic segmentation algorithm that involved statistical noise subtraction, segmentation refinement, automated trachea removal, smoothing and artifact removal, and voxel summation. We imaged subjects at baseline, and then following 11 days of treatment. Treatment consisted of daily administration of intravenous tobramycin and a beta-lactam antibiotic, inhalation of 4 ml of 7% hypertonic saline twice a day, inhalation of 2.5 mg of recombinant human DNase (dornase alpha) once a day, and chest physiotherapy three times a day. Following treatment, HP 3He MR images of one subject displayed a 25% increase in total ventilation volume. The other two subjects showed slight decreases in total ventilation volume (-9% and -10%, respectively). All three subjects showed increases in spirometric measures of FEV1 and FVC following treatment. The increases in FEV1 and FVC were pronouncedly higher in the subject displaying a 25% increase in ventilation volume than in the two subjects showing decreases in ventilation volume. These data provide additional support for the conclusion that HP 3He MRI can be a powerful tool for evaluating lung ventilation in patients with cystic fibrosis, but raise important unresolved questions about the correlation between spirometry and HP gas MRI measurements.

Poster Session 11 - 4

Assessment of Paraseptal Emphysema in the Inner Lung Field by Using Inflated-Fixed Lung Specimens

Katashi Satoh[1], Makiko Murota[2], Hirotoshi Honma[3], Hiroki Takahashi[3], Hiroyuki Koba[4]

1. Department of Nursing, Kagawa Prefectural College of Health Scineces, Japan
2. Department of Radiology, Kagawa University School of Medicine, Japan
3. Department of Internal Medicine (Section 3), Sapporo Medical College, Japan
4. Department of Internal Medicine, Keijinkai Hospital, Japan

Objectives: There are several morphological subtypes of pulmonary emphysema based on their location in the secondary pulmonary lobule. Although morphological features of paraseptal emphysema usually involve abnormalities in the periphery of the pulmonary lobule, typical findings on CT images show them only adjacent to the pleura including along the interlobar fissures. The objective of the present study was to examine paraseptal emphysema in the inner lung field.

Materials and Methods: Emphysematous lesions and anthracosis adjacent to the interlobular septa or large vessels and bronchi and their predominant areas within lung parenchyma were examined in the inflated-fixed lung specimens.

Results: Lesions adjacent to interlobular septa were seen in places ranging from continuous to pleural surfaces to the inner zone of the lung and mild to severe in degree. They were also seen in the areas adjacent to large vessels and bronchi. The lesions existed not only in one pulmonary lobule but also in both lobules adjoining each other. In cases of co-existence of centrilobular and paraseptal types, the former type was more predominant than the latter. However, only few cases were observed where both types were present equally. Similar to centrilobular type, paraseptal emphysema lesions were seen in the upper lobe as well.

Conclusions: The present study suggests that in routine clinical examination, HRCT could depict paraseptal emphysema adjacent to interlobular septa in the inner zone of the lung in some cases. For understanding of pulmonary function, it is important to distinguish emphysema types of different origins.

Poster Session 11-5

Ⅰ-123-MIBG Lung Kinetic Abnormality in Pulmonary Emphysema

Kazuyoshi Suga[1], Mitsue Kunihiro[2], Munemasa Okada[2], Osamu Tokuda[2], Hideyuki Iwanaga[2], Naofumi Matsunaga[2]

1. Department of Radiology, St. Hill Hospital, Japan
2. Department of Radiology, Yamaguchi University School of Medicine, Japan

The aim of this study was to clarify abnormal lung kinetics of Ⅰ-123-metaiodobenzylguanidine (MIBG) in pulmonary emphysema (PE).

MIBG SPECT was obtained at 15 min and 4 hr after intravenous injection of MIBG in 36 PE patients and 31 age-matched non-smokers without PE changes on CT. Lung MIBG distribution was compared with lung morphology on high-resolution CT and perfusion on Tc-99m-MAA perfusion SPECT. Lung MIBG kinetic parameters of early (at 15 min) and delayed (at 4 hr) lung-to-mediastinum (L/M) uptake ratios, and washout rate (%WR) [(Early L/M ratio-delayed L/M ratio)/ early L/M ratio x 100%] were calculated in the whole lungs.

The normal lungs showed fairly uniform MIBG distribution, which was nearly consistent with perfusion distribution. In contrast, PE lungs showed heterogeneously reduced MIBG uptake predominantly in the upper lungs, and MIBG uptake was apparently and widely reduced even in the lung areas without PE changes on CT in 31 (86%) patients. Lung distribution of MIBG and perfusion were also discordant in 16 (44%) PE patients, where apparently reduced MIBG uptake was seen even in the lung areas with preserved perfusion. All the MIBG kinetic parameters in the whole lungs of PE patients were significantly lower than the control values ($P < 0.0001$). %WR was significantly correlated with lung carbon monoxide diffusing capacity in these patients ($R = 0.715$; $P < 0.0001$).

Lung MIBG kinetics in PE can be impaired independently of lung morphology and perfusion abnormalities, and it is a good indicator of pulmonary endothelial impairment.

Poster Session 11-6

The Epithelial-Mesenchymal Transition of Progenitor Cells Lead to Low Attenuation Areas of the Pulmonary Parenchyma: An Autopoietic Model Analysis of Alveolar Epithelial Maintenance

Kyongyob Min, Keita Hosoi, Yoshinori Kinoshita, Hiroyuki Degami, Satoshi Hara, Tetsuo Takada, Takahiko Nakamura

Respiratory Division of Internal Medicine, Itami City Hospital, Japan

BACKGROUND AND PURPOSE: A group of progenitor cells maintains alveolar epithelial integrity in the pulmonary parenchyma. The existence of progenitors which have the ability to differentiate into the alveolar epithelium and the fibroblast (EMT) may be important in the genesis of pulmonary fibrosis. However, no reports refer to the role of EMT in case of pulmonary emphysema. In this paper, we obtained a set of equations to describe the role of EMT in the genesis of pulmonary emphysema.

METHOD: An autopoietic system is a network of processes that produces the components that produce those processes. We defined a network of bronchiolo-alveolar surfaces in the pulmonary lobule as an autopoietic system by using Bourgine and Stewart's mathematical theory (Artificial Life 10:327,2004).

RESULTS: We obtained two equations for emphysema: $dCM/dt = kcCM+kb(C1-CM)Pr(CM)$, and $LAA\% = \{ (a1 [a]) (S/V) d/dt([a] [b])\}/kb[b]$. CM was the number of alveolar type I cells (C). [a] and [b] were densities of stem cells (A) and of progenitor cells (B), respectively. S/V was the density of the alveolar capillary surfaces. ka, kb and kc were kinetic parameters of the transition from A to B, from B to C, and from C to apoptosis, respectively. The was the engrafting ratio of A. Fibroblasts (F) catalyzed A to B. The process of B F was EMT, which could produce a stable attractor of CM=0 in the phase space.

CONCLUSION: Loss of the progenitor cells by EMT would induce emphysematous loss of the bronchiolo-alveolar surfaces.

Poster Session 11 - 7

Oscillatory Mechanics within Respiratory Cycles Related to COPD Severity

Junichi Ohishi[1], Hajime Kurosawa[2], Daisuke Kobayashi[1], Miha Masuda[1], Etsuhiro Nikkuni[1], Masashi Kanezaki[1], Masahiro Kohzuki[1]

1. Department of Internal Medicine and Rehabilitation Science, Tohoku University School of Medicine, Japan
2. Department of Occupational Health, Tohoku University School of Medicine, Japan

Oscillatory properties of respiratory system vary considerably within respiratory cycle (RC) in patients with COPD. As seen in the representative features of airway narrowing at tidal expiration, the oscillatory flow resistance tends to be higher at expiration than inspiration. The relationship between the RC dependency and COPD severity is not fully investigated. We examined the relationship by means of our original 3-D color images.

Oscillatory properties were assessed in patients with COPD (n=39, mean 70-yrs) using Impulse Oscillometry (MS-IOS; Cardinal Health, USA). Impulse Oscillometry was performed in 40 seconds under tidal breathing at sitting position. The oscillatory pressure and flow relationships, resistance (Rrs) and reactance (Xrs), were calculated every 0.2 second between 5 and 35 Hz. All data were evenly divided into 4 sections at inspiration and expiration respectively, and were averaged on 8 respiratory phases. Rrs and Xrs were lined up and assigned color gradients, which resulted in colored 3-D graphs. COPD severity was estimated by %FEV1.

In patients with severe COPD, the main characteristics at lower frequency were the increases in Rrs and the shifts of Xrs curves toward negative on whole respiratory phases, especially during expiration. Those RC dependencies were more remarkably with decrease in %FEV1. The variations of Rrs and Xrs within respiratory phases were not necessarily similar. These physiological features were visualized on 3-D graphs.

The oscillatory flow resistance can be high on whole respiratory phases and have RC dependency with COPD severity. Our 3-D color images can be an effective tool to understand those mechanics.

Poster Session 12-1

Hyperpolarized 3He MRI Apparent Diffusion Coefficients as a Probe of Airway Function in Asthma After Methacholine Challenge and Recovery

Stephen E. Costella[1], Stephen Choy[1], Miranda Kirby[1,3], Andrew Wheatley[1], Roya Etemad-Rezai[4], David McCormack[5], Grace Parraga[1,2,3,4]

1. Imaging Research Laboratories, Robarts Research Institute, London, Canada
2. Graduate Program in Biomedical Engineering, The University of Western Ontario, London, Canada
3. Department of Medical Biophysics, The University of Western Ontario, London, Canada
4. Department of Medicine, Division of Medical Imaging, The University of Western Ontario, London, Canada
5. Department of Medicine, Division of Respirology, The University of Western Ontario, London, Canada

We measured hyperpolarized 3He Apparent Diffusion Coefficients (ADC) to quantitatively evaluate the asthmatic lung before, immediately after methacholine challenge and after recovery from methacholine challenge,30 minutes post bronchodilation with salbutamol. We hypothesized that functional imaging measurements such as 3He MRI ADC that are reflective of airway and airspace microenvironments would be altered after induction of broncho-constriction in a methacholine challenge. Hyperpolarized 3He magnetic resonance imaging (MRI) was performed at 3.0 T to acquire diffusion weighted images (b= 1.6 s/cm2, 14-16 slices at 30mm slice thickness) in the coronal plane using a fast gradient-recalled echo (FGRE) method with centric k-space sampling. Plethysmography and spirometry were also performed with MRI on subjects with a clinical diagnosis of asthma (n=13, age = 32.3 $\pm$ 9.2y) three times within an hour (just prior to methacholine challenge, 5 minutes after achieving PC20 and finally 30 minutes after bronchodilator administration following PC20 dose and MRI). A two-way ANOVA showed significant interactions between mean whole lung ADC and patient/timepoint with significant differences between all patients post-methacholine and after salbutamol recovery. A region of interest (ROI) analysis identified that these significant differences were specific to the posterior slices and posterior ROI ($p < 0.0001$). The increased ADC post-methacholine with significant reversal after salbutamol administration suggests that 3He MRI ADC sensitively reflects the presence of gas-trapping in asthma that is relieved after administration of salbutamol.

Poster Session 12-2

4-Dimentional Imaging of the Central Airway Using a Low Dose Technique: Initial Experience with 320-row Mzultidetector CT

Ryo Sakamoto, Satoshi Noma[2], Takeshi Kubo[1], Hiroyuki Sekiguchi[1], Shigeaki Umeoka[1], Takanori Higashino[3], Yuko Nishimoto[2], Yutaka Emoto[4], Kaori Togashi[1]

1. Department of Diagnostic Imaging and Nuclear Medicine, Kyoto University Graduate School of Medicine, Japan
2. Department of Radiology, Tenri Hospital, Japan
3. Department of Radiology, National Hospital Organization, Himeji Medical Center, Japan
4. Department of Radiological Technology, Faculty of Medical Science, Kyoto College of Medical Science, Japan

BACKGROUND: 320-row multidetector CT (MDCT) provides not only volumetric image acquisition capability but also wide craniocaudal coverage of 160 mm without table movement. Therefore, it has become possible to obtain continuous volumetric images of central airway from trachea to proximal bronchi during a respiratory maneuver, at a cost of higher radiation exposure.
MATERIALS AND METHODS: Five adult patients with suspected central airway disorders were scanned during an exhalation. Scanning area was set to cover intrathoracic trachea to proximal lower lobe bronchi. Low dose technique was used while performing a continuous image acquision of the central airway until full expiration. Consecutive volumentric images were reconstructed at 0.5 second intervals, thus producing 4 dimentional image data of the central airway. In each frame, images were reconstructed in the same plane containing a particular bronchus of interest. The reconstructed images were presented in a cine mode.
RESULTS: With a low dose technique, radiation exposure during 4-D acquisition was reduced nearly to the level of routine whole lung helical CT scan. Production of cine images was possible with acceptable image noise and motion artifacts which allow us to evaluate real-time airway morphology. Cine imaging demonstrated the dynamic deformation of airways, representing pathological changes of each clinical condition.
CONCLUSION: Cine CT using 320-row MDCT with low dose technique provides continuous evaluation of airway motion during respiratory maneuvers. Application of this new diagnostic method to various respiratory diseases is expected to disclose the dynamic change in central airway, thus clarifying pathophysiological mechanism of these diseases.

Poster Session 12-3

Dynamic Property of Central Airway Walls as Assessed by Computed Tomography: Correlation with Asthma Pathophysiology

Masafumi Yamaguchi, Akio Niimi[2], Hisako Matsumoto[2], Isao Ito[2], Toyohiro Hirai[2], Yasutaka Nakano[1], Michiaki Mishima[2]

1. Department of Cardiovascular and Respiratory Medicine, Shiga University of Medical Science, Japan
2. Department of Respiratory Medicine, Kyoto University, Japan

Background: A subset of asthmatic patients suffers from frequent exacerbations despite continuous medication, possibly due to various features of remodeling and associated elastic properties of airway walls.
Objective: To examine the fragility of central airways and sputum biomarkers of airway remodeling in different classes of asthmatics, classified according to disease stability.
Methods: We studied moderate-to-severe asthmatics with ≤ 1 asthma worsening during the previous year requiring beta 2-agonist therapy (stable, n=18), those with ©2 such episodes (unstable, n=11), and 11 healthy controls. Wall thickness and luminal area of a segmental bronchus were measured by computed tomography at full-inspiration. Percentage decrease in luminal area from full-inspiration to full-expiration was calculated as a measure of airway fragility. Sputum biomarkers associated with fibrosis [TGF-beta 1 and matrix metalloproteinase (MMP)-9/tissue inhibitors of metalloproteinase (TIMP)-1 molar ratio] and those associated with angiogenesis/edema [vascular endothelial growth factor (VEGF) and vascular permeability index (sputum/serum ratio of albumin levels)] were examined.
Results: The airway wall was similarly thickened in both asthmatic subgroups as compared with controls. Airway fragility was greater in unstable asthmatics than in stable asthmatics and controls but was similar in the latter two groups. Sputum TGF-beta 1 levels were higher and MMP-9/TIMP-1 molar ratios were lower in stable asthmatics than in controls. Sputum VEGF levels and vascular permeability index were higher in unstable asthmatics than in controls.
Conclusion: Fragility of thickened airway walls, which in turn may depend on whether fibrosis or angiogenesis/edema predominates in the airways, may be associated with stability of asthma.

Poster Session 12-4

Comparison of 3-D-Visualized Respiratory Impedance Patterns and Structural Change Detected by CT in Smokers

Haruko Shinke[1], Masatsugu Yamamoto[1], Nobuko Hazeki[1], Kazuyuki Kobayashi[1], Yasuhiro Funada[1], Yoshikazu Kotani[1], Yoshiharu Ohno[2], Yoshihiro Nishimura[1]

1. Division of Respiratory medicine, Department of internal medicine, Kobe University Graduate School of Medicine, Japan
2. Department of Radiology, Kobe University Graduate School of Medicine, Japan

Background
We previously reported the influence of smoking on respiratory impedance using MostGraph-01 (CHEST, Tokyo), which enables us to evaluate the variance of respiratory resistance and reactance as 3-D graph along time axis. Further studies are needed to clarify the relationship between structural change and impedance change in respiratory system. To examine that, we analyzed the structural changes using CT scan to compare estimated parameters from CT images and 3D image pattern of respiratory impedance.
Methods
We have examined total of 15 smokers who visited the out-patient clinic of respiratory medicine in Kobe University hospital. The subjects were measured pulmonary function test (PFT). Low attenuation area of the lung (LAA) and airway parameters were measured using CT scan. The respiratory impedance patterns were measured under spontaneous tidal breathing by impulse signal using MostGraph-01. The patterns on 3D graph were categorized to compare with other clinical parameters.
Results
Resistance at 5Hz (R5) was 0.27 ± 0.11kPa s/L, Reactance at 5Hz (X5) was -0.726 ± 0.64 kPa s/L, Mean LAA% was 8.056 ± 8.938%. Some smokers with normal PFT showing frequency dependency of resistance or negative shift of reactance showed increase of %LAA as COPD patients. The impedance variances were seen dominantly in expiratory phase.
Conclusion
The variance of respiratory impedance reflects early change of pulmonary airway disorder induced by smoking. Using this method may provide easy screening strategy to detect occult structural changes and flow limitation in smokers. Now we are accumulating clinical data.

Poster Session 12-5

Usefulness of SD-101, a Non-restrictive Device Developed for Screening Sleep Apnea-hypopnea Syndrome

Keisaku Fujimoto[1], Takaya Nishiyama[1], Shigeo Kubota[1,2], Toshihiko Agatsuma[3], Yoshimichi Komatsu[3], Kazuhisa Urushihata[3], Takayuki Honda[4], Teruomi Tsukahara[5], Tetsuo Nomiyama[5], Keishi Kubo[3]

1. Department of Biomedical Laboratory Sciences, Shinshu University School of Health Sciences, Japan
2. Department of New Air-conditioning Business, GAC Corporation, Japan
3. First Department of Internal Medicine, Shinshu University School of Medicine, Japan
4. Department of Laboratory Medicine, Shinshu University School of Medicine, Japan
5. Department of Preventive Medicine and Public Health, Shinshu University School of Medicine, Japan

Background and objective: Kentzmedico in Japan has developed the SD-101 as a nonrestrictive, sheet-like medical device with an array of pressure sensors, to automatically detect sleep-disordered breathing (SDB) by sensing gravitational alterations in the body corresponding to respiratory movements. The purpose of this study was to examine the clinical usefulness of the SD-101 for screening sleep apnea-hypopnea syndrome (SAHS).
Methods: Nocturnal polysomnography (PSG) and SD-101 recordings were run simultaneously and compared for 201 subjects attending our hospital with suspected SAHS (suspected SAHS group) and in all 165 male employees of a transport company (screening group).
Results: PSG revealed apnea-hypopnea index (AHI) < 5, 5 AHI < 15, 15 AHI < 30, 30 AHI < 60, and AHI 60 events/h in 39, 35, 38, 68 and 21 subjects in the suspected SAHS group and 103, 34, 12, 12 and 4 subjects in the screening group, respectively. Central SAHS and obstructive SAHS were subsequently diagnosed in 11 (5.5%) and 135 (67.2%) subjects in the suspected SAHS group and 5 (3.0%) and 39 (23.6%) subjects in the screening group, respectively. Significant correlations were apparent between AHI and respiratory disturbance index (RDI) measured with the SD-101 in both the suspected SAHS group (r = 0.88) and screening group (r = 0.92). Receiver operating characteristic analysis revealed 89.5% sensitivity and 85.8% specificity in identifying SAHS, using an RDI of 14.0 events/h.
Conclusion: These findings suggest that the SD-101 is a useful device for screening SAHS.

Poster Session 12-6

Vibration Response Imaging (VRI) in the Detection of Asynchrony between Left and Right Lung for Main Bronchial Stenosis

Hirotaka Kida, Masamichi Mineshita, Naoki Furuya, Hiroshi Handa, Hiroki Nishine, Seiichi Nobuyama, Taeko Shirakawa, Teruomi Miyazawa

Division of Respiratory and Infectious Diseases, Department of Internal Medicine, St. Marianna University School of Medicine, Japan

INTRODUCTION:
The VRI is an imaging modality that records energy generated by the vibrations of the lungs during respiration cycle and creates an image that can be viewed dynamically or sequentially. The timing of inspiratory and expiratory vibration energy peaks (VEPs) of right versus left lungs can be analyzed. We defined the average of absolute value of the gaps between VEPs of both lungs during 12 sec as VEPgap, and observed left and right lung asynchrony in patients with main-stem bronchial stenosis.
PURPOSE:
In this study we planed to elucidate the threshold level of stenosis that cause left and right lung asynchrony using lung model, then validate this threshold level in patients with main-stem bronchial stenosis.
METHODS:
We created a lung model using a pig lung in a sealed box connected to a ventilator. We measured airway pressure of right and left bronchus at the same time using two catheters to manually narrow the airways. We validated the relation between rate of stenosis and time delay.
The stenosis rate was measured by computed tomography using ZAIO soft and VEPgap in 10 patients with unilateral main-stem bronchial stenosis.
RESULTS:
Time delay increased sharply from 90% in the pig model ($P<0.05$). As in the Pig model, VEPgap increased sharply from 90% in the patients with unilateral main-stem bronchial stenosis.
CONCLUSIONS:
In this study, the VRI was able to identify severe stenoses above 90% in patients. We found VRI was useful in assessing treatment outcomes and decisions on interventional indication.

Poster Session 13-1

Analysis of Lung Motion Due to Respiration and Its Application to PET Images

Hideaki Haneishi[1], Masayuki Kanai[1], Kyoka Kobuna[1],Yoshitaka Tamai[2], Atsushi Sakohira[2], Kazuyoshi Suga[2]

1. Research Center for Frontier Medical Engineering, Japan
2. St. Hill Hospital, Japan

Lung motion due to respiration causes image degradation in medical imaging, especially in nuclear medicine which requires long acquisition time. We have developed a method for image correction between the respiration-gated (RG) PET images in different respiration phases. The method offers the motion field vector of lung from the PET image set and the motion field vector plays a role for image summation of the RGPET images. This technique is applied to a set of breath-hold (BH) PET images in this paper. In the BH method, a patient is asked to hold his/her breath for 10 to 30 s as the image acquisition is performed. This is repeated several times and the obtained images are summed. In practice, however, a patient cannot necessarily hold his/her breath at the same timing of breathing. In such a case, the summed images still has a blur. We propose to apply our image registration method developed before for RG images to BH images. The BH images are nonlinearly motion-corrected so as to match a reference BH image and summed. Through the experiment with nine patient BH image data, we confirmed that the proposed method is effective in obtaining a non-blurred image.

Poster Session 13-2

A 4D Model Generator of the Human Lung: Lung CataChiCaraCure-er, Alias Lung4Cer

Hiroko Kitaoka

Division of Engineering Technology, JSOL Corporation, Japan

We have developed a free software which generates various kinds of 4D lung models for the purpose of studying structure and function of the human broncho-alveolar system. The name of “CataChiCaraCuri-er” is arisen from Japanese words, CataChi (= form,structure) and CaraCuri(= machine, mechanism). The last “er” indicates a doer in English and its pronunciation also means a doer in Japanese (Ya). The alias of “4Cer” means a 4D model generator like a farmer who grows vegetables rapidly. Lung4Cer makes dynamic air pathway models from the trachea to alveoli based on four algorithms published previously. Breathing motion is given by parameters which assign respiratory modes and body postures. Lung4Cer contains a newly developed algorithm which converts geometric models into 4D finite element models which allow airflow simulation by means of computational fluid mechanics. Visualization of generated models is expected to use a free popuular software “ParaView”, which can be easily obtained by internet. Potentially, Lung4Cer can make a whole lung model with 300 million alveoli. However, it costs incredibly huge computer resources.. Instead, suitable model types can be selected according to user's interest and available computer resource, such as (1) airway tree only, (2) airway tree with air-supplyed parenchymal regions, (3) air pathway from the trachea to a subacinus with alveolar structure, and (4) alveolar system only. Lung4Cer also contains Origami models for alveolar ducts nearly equivalent to the computer models so that users may handle them in reality. Lung4Cer will be a powerful basic tool for studying pulmonary functional imaging.

Poster Session 13-3

Alveolar Recruitment Analysis in Acute Respiratory Distress Syndrome (ARDS) Using End-inspiratory and End-expiratory Breath-hold 3D-CT Images

Hiroko Kitaoka[1], Osamu Hirao[2], Yuji Fujino[2], Noriyuki Tomiyama[3]
1. Division of Engineering Technology, JSOL Corporation, Japan
2. Intensive Care Unit, Osaka University Hospital, Japan
3. Department of Radiology, Osaka University Graduate School of Medicine, Japan

Purpose: Open lung strategy for ARDS is an artificial ventilation which intends to increase persistent alveolar recruitment (= recruited through respiratory cycle) and decrease cyclic recruitment (= recruited at end-inspiration but collapsed at end-expiration) without hyperinflation of intact alveoli. We have developed a quantitative image analysis technique for detecting recruited alveolar regions in 3D CT images by the use of nonrigid image registration between expiratory and inspiratory CT images for the purpose of estimating the optimal artificial ventilation mode.

Methods: Five patients of ARDS under artificial ventilation were subjected (approved by the in-hospital ethics committee). A set of iBH-CT and eBH-CT images was obtained under the same settings of mechanical ventilation in ICU. Another set was obtained ten minutes after increasing PEEP by 5cmH2O. Two sets of eBH-CT and iBH-CT at respective PEEP levels and a set of eBH-CTs at different PEEP levels were subjected to nonrigid image registration by which CT value difference between corresponding points in iBH-CT and eBH-CT were computed. The last set was to assess the direct effect of PEEP level. A voxel cluster whose CT values changed more than 400 HU was defined as a recruited region.

Results: Recruitments were detected at dependent zones in all cases. FiO2 deference between different PEEP levels was in strong correlations to volumes of persistent recruitment and volume reduction of cyclic recruitment.

Conclusions: Our method can evaluate alveolar recruitments both visually and quantitatively. It is expected to assist open lung strategy fpr ARDS.

Poster Session 13-4

Velocity Vector Imaging in Assessing the Regional Diaphragmatic Movement of Patients with Chronic Diaphragmatic Hernia- Preliminary Results

Teng-Fu Tsao[1,2,3], Hsin-Hui Huang[1,2], Ming-Chi Wu[1,2], Ruei-Jin Kang[4], Siu-Wan Hung[5], Mein-Kai Gueng[5], Yung-Chang Lin[3], Yi-Hsun Tseng[1,2], Ching-Wen Lin[1,2], Yeu-Sheng Tyan[1,2]
1. Department of Medical Imaging, Chung Shan Medical University Hospital, Taiwan
2. School of Medical Imaging and Radiological Sciences, Chung Shan Medical University, Taiwan
3. Department of Veterinary Medicine, National Chung Hsing Univerity, Taiwan
4. National Chi Nan University, Taiwan
5. Department of Radiology, Taichung Veterans General Hospital, Taiwan

Purpose:
To evaluate the regional diaphragmatic movement in patients with chronic diaphragmatic hernia using the velocity vector imaging (VVI) technique, a two-dimensional angle-independent ultrasound speckle tracking method.
Material and Methods:
Two-dimensional cine-loop ultrasound images of right lateral intercostal view were obtained in 5 patients with chronic right diaphragmatic hernia and 3 healthy volunteers under quiet respiration. The regional movements of right hemi-diaphragm were analyzed with VVI offline software. The diaphragmatic contours were manually identified in a single frame of a cine-loop and the contours in other frames were automatically generated with the ability for the operator to alter any of those contours. After performing calculation process, the velocity vectors superimposed on two-dimensional cine-loop ultrasound images to describe the pattern of diaphragmatic movement.
Results:
Of the 5 cases with chronic right diaphragmatic hernia, 3 (60%) cases were successfully analyzed with VVI software, while another 2 cases were excluded due to poor acoustic window. Among the 3 successfully analyzed cases, 2 cases showed dyssynchronous movement with opposite direction in both inspiratory and expiratory phases at the free edge of diaphragm close to the defect of the hernia. The other case with hernia showed synchronous movement during whole respiration phases that were typically noted in the healthy volunteers.
Conclusion:
VVI could recognize and quantify the regional diaphragmatic movement in cases with adequate acoustic windows. We demonstrate the regional dyssynchronous movement of diaphragm in two cases of chronic diaphragmatic hernia. This is an interesting phenomenon and has not well documented in the previous lecture.

Poster Session 13-5

Usefulness of Ultrasonography in Preoperative Diagnosis of Solitary Fibrous Tumor of the Pleura

Mitsuaki Sekiya, Kaku Yoshimi[1], Keiko Muraki[1], Noriyuki Homma[1], Teruhiko Sato[1], Takashi Dambara[2], Kenji Suzuki[3], Toshimasa Uekusa[4], Kazuhisa Takahashi[1]

1. Department of Respiratory Medicine, Juntendo University School of Medicine, Japan
2. Department of General Medicine, Juntendo University School of Medicine, Japan
3. Department of General Thoracic Surgery, Juntendo University School of Medicine, Japan
4. Department of Pathology, Kanto Rosai Hospital, Japan

Background: Solitary fibrous tumor of the pleura (SFTP) is a rare pleural tumor of mesenchymal origin, accounting for 5% to 10% of primary pleural tumors. Although usefulness of thoracic CT and MRI in the evaluation of SFTP has been well documented, ultrasonographic evaluation has not been reported. We reviewed the ultrasonographic features of three pathologically proven cases of SFTP.

Methods and results: Patients consisted of two men and one female (age 55±19 years old). Thoracic CT demonstrated a well-defined, pleural-based lesion that has obtuse angles and tapering margin with adjacent pleura. The patients underwent thoracic ultrasonography (US) using the commercially available ultrasonic unit (SSA-550A; Toshiba, Tokyo, Japan) with the convex type linear array probe (PLM-805AT 8MHz, Toshiba, Tokyo, Japan). Thoracic US demonstrated solitary, homogeneous, hypo-echoic, hemicycle lesions. All lesions abut on the hemicycler line originating from visceral pleura of the adjacent lung. However, they showed respiratory motion together with adjacent lung. On the basis of the above findings, pedunculated tumors arising from the visceral pleura, especially SFTP, were suspected. We performed surgical resection and confirmed pedunculated tumors of visceral pleura. Then, pathological diagnosis of SFTP was established in all cases.

Conclusion: Preoperative thoracic US could be useful in the evaluation of the patients with SFT

Poster Session 13-6

A Method for Reduction of Subtraction Artifacts on Temporal Subtraction Images by Use of Generalized Gradient Vector Flow Technique

Hyoungseop Kim[1], Noriaki Miyake[1], Joo Kooi Tan[1], Seiji Ishikawa[1], Seiichi Murakami[1,2], Takatoshi Aoki[2],

1. Graduate School of Engineering, Kyushu Institute of Technology, Japan
2. Department of Radiology, University of Occupational & Environment Health, Japan

Introduction: A temporal subtraction (TS) image, which is obtained by subtraction of a previous image from a current one, can be used for enhancing interval changes on images by removing most of the normal structures. In this paper, we propose a registration method for TS using GGVF.

Methods: In the first stage, the vector fields are described using GGVF from the previous and current images, respectively. Next, some VOIs are set up on the CT image pairs. Furthermore, the shift vectors are calculated using nearest neighbor matching of the vector fields in these VOIs. The previous CT voxel which resemble standard the current voxel is detected by voxel value and vector of the GGVF in the kernel. Finally, a TS image is made by subtraction of a warping image from a current one.

Results: We employed 6 databases obtained from different time-series on same patients and evaluate the effect of reducing the subtraction artifacts based on histogram and satisfactory results are obtained. In the experimental results, there was a trend toward a decrease in contrast value on the TS image.

Conclusions: In this paper, we have developed a new image registration method to reduce subtraction artifacts in TS images. Subtraction artifacts on temporal subtraction image were substantially removed. We believe that the TS images can be introduced as a useful tool to analyze an interval changes.

Acknowledgement: This work was supported in part by a research grants from Kitakyshu Foundation for the Advancement of Industry Science and Technology.

Poster Session 14-1

Towards a Research Software Platform for Diagnosis and Therapy Monitoring for COPD and Asthma with Pulmonary Magnetic Resonance Images

Peter Kohlmann, Hendrik Laue, Stefan Krass, Heinz-Otto Peitgen
Fraunhofer MEVIS, Germany

A variety of magnetic resonance (MR) sequences for diagnosis and therapy monitoring of the widespread lung diseases COPD and asthma is available. In addition to conventional proton MRI, helium-3 MRI is performed in clinical research settings. The research software platform (PulmoMR), developed by Fraunhofer MEVIS in close cooperation with clinical partners, provides various computer-assisted methods for the analysis of this heterogeneous pool of image types. Particular effort is invested to improve quantitative accuracy, reproducibility, and robustness of the incorporated methods and algorithms. In addition to basic functionality (data import, image/curve display, selecting regions-of-interest, etc.), a set of advanced components is already integrated. Firstly, PulmoMR provides methods to visualize and to quantify contrast-enhanced perfusion MRI. These include the calculation and simultaneous display of derived images (e.g., subtraction images), time-intensity curves (TICs), and perfusion parameter maps. Descriptive perfusion parameters are derived from the TICs and quantitative perfusion parameters are determined by a singular value decomposition technique. Secondly, PulmoMR allows quantifying longitudinal relaxation time T1 from an inversion recovery snapshot fast low angle shot (FLASH) sequence to enable oxygen-enhanced analysis of pulmonary MR images. Currently methods for the alignment of different MR sequences as well as for longitudinal studies are developed. Additionally, lung segmentation is currently implemented, which will amongst others allow an analysis of breathing motion. Further work-in-progress is the integration of methods for image analysis of helium-3 MRI.

Acknowledgments: The work was supported by the Competence Network Asthma/COPD funded by the German Federal Ministry of Education and Research (FKZ 01GI0881-0888).

Poster Session 14-2

Clinical Chest CAD System for Lung Cancer, COPD, and Osteoporosis Based on MDCT Images

Shinsuke Saita[1], Yoshiki Kawata[1], Noboru Niki[1], Hironobu Ohmatsu[2], Takaaki Tsuchida[3], Kenji Eguchi[4], Masahiro Kaneko[3], Noriyuki Moriyama[5], Yasutaka Nakano[6], Michiaki Mishima[7]
1. Institute of Technology and Science The University of Tokushima, Japan
2. National Cancer Centre Hospital East, Japan
3. National Cancer Centre Hospital, Japan
4. Teikyo University, Japan
5. National Cancer Center Reseach Center for Cancer Prevention and Screening, Japan
6. Shiga University of Medical Science, Japan
7. Graduate School of Medicine, Kyoto University, Japan

Cancer is the leading cause of death with lung cancer as the number one cause. Since the survival rates of those with lung cancer are low, earlier detection and early treatment are important. In addition, chronic obstructive pulmonary disease (COPD) appears to be in the top ten cause of death in 2000, and more than 5.3 million Japanese older than 40 years old have this disease. Specifically, treatment for pulmonary emphysema is difficultly, therefore early detection of the disease at an early stage is important. The patients of osteoporosis comprised of about 10 million people in Japan and it is one of the problems the aging society has. We developed clinical chest CAD system for lung cancer, COPD, and osteoporosis based on MDCT images.

Clinical chest CAD system could quantitatively detect lung cancers of many size, type, and texture variations. In addition, our CAD system could detect lung cancers, COPD, and osteoporosis at early stage.

Poster Session 14-3

Developments of Thrombosis Detection Algorithm using the Contrast Enhanced CT Images

Jun Oya[1], Yoshiki Kawata[2], Noboru Niki[2], Toshihiko Sugiura[3], Nobuhiro Tanabe[3], Yuichi Takiguchi[3], Koichiro Tatsumi[3]

1. Graduate School of Advanced Technology and Science, The University of Tokushima, Japan
2. Institute of Technology and Science The University of Tokushima, Japan
3. Department of Respirology Graduate School of Medicine, Chiba University, Japan

In the diagnosis of thrombosis with no specific clinic symptoms, diagnostic imaging plays a greater role. Particularly, contrast Enhanced CT is low invasive diagnostics, and the thrombus in the pulmonary artery can be detected as a low density without the contrast effect. Moreover, because describing the change of concentration in lung field and the decline in lung blood vessel shadow is also possible, it is indispensable to diagnose of thrombosis. As the image diagnosis support, it is necessary to classify the pulmonary artery and vein that relate to the thrombosis, and to analyze the lung blood vessel quantitatively. The technique for detecting the thrombosis by detecting the position of the thrombus has been proposed so far. In this study, it aims to focusing on the dilation of the main pulmonary artery and to detect the thrombosis. The effectiveness of the method is shown by measuring the pulmonary trunk diameter by using the extracted pulmonary artery from contrast Enhanced CT through semi-automated method, and comparing it with a normal case.

Poster Session 14-4

Segmentation of Thoracic Organs from Multi-slice CT Images

Mikio Matsuhiro[1], Shinsuke Saita[1], Yoshiki Kawata[1], Noboru Niki[1], Yasutaka Nakano[2], Michiaki Mishima[3], Hironobu Ohmatsu[4], Kenji Eguchi[5], Masahiro Kaneko[6], Noriyuki Moriyama[7]

1. Institute of Technology and Science The University of Tokushima, Japan
2. Dept.of Respiratory Medicine, Shiga University of Medical Science, Japan
3. Department of Respiratory Medicine, Graduate School of Medicine, Kyoto University, Japan
4. National Cancer Hospital East, Japan
5. Faculty of Medicine, Teikyo University, Japan
6. National Cancer Center Hospital, Japan
7. National Cancer Research Center for Cancer Prevention and Screening, Japan

With the development of multi-slice CT technology, obtaining an accurate 3D image of lung field in a short time becomes possible. To support that, a lot of image processing methods need to be developed. To diagnose lung cancer in the clinical field, it is important to study and analyse lung structure. Therefore, classification of lung lobe and classification of lung segment provide useful information for lung cancer analysis. In this report, we describe algorithms which segment thoracic organ, classify lungs into lung lobes and lung segments from multi-slice CT images. The classification algorithm of lung lobes is efficiently carried out using information of lung blood vessel, bronchus, and interlobar fissure. On the other hand, the classification algorithm of lung segments is carried out using information of bronchus and pulmonary artery.

Poster Session 14-5

Iterative Algorithm for Airway Segmentation in CT Images Using a Region-based Active Contour Model

Sumiaki Matsumoto, Mizuho Nishio, Yoshiharu Ohno, Kazuro Sugimura
Department of Radiology, Kobe University Graduate School of Medicine, Japan

Purpose: To develop and evaluate a new algorithm for airway segmentation in CT images using a region-based active contour model.

Materials and methods: Being based on level sets, the region-based active contour model requires no intrinsic parameter concerning gray levels. The new algorithm gradually executes airway segmentation though the iterative use of the active contour model. Initially, a central trunk of airway leading from the right (or left) main bronchus to the ipsilateral lower lobe bronchus is extracted. In this trunk, regions near the origins of its branches are identified. On the other hand, a FIFO queue of seed regions is set up and initialized with these regions. Subsequently, a seed region retrieved from the queue is elongated distally along airways according to the evolution of the active contour model; this elongation is stopped when new candidate seed regions are identified. Each candidate seed region, if not rejected as a leak outside airways by a classifier, is then put into the queue. The above process is repeated until the queue becomes empty. Using 15 thin-section standard-dose CT datasets, the results of airway segmentation obtained with this algorithm were compared with those obtained with a benchmark (recently-proposed centricity-based region growing algorithm).

Results: The number of extracted airway branches was 103 ± 19 and 65 ± 13 when using the new algorithm and the centricity-based algorithm, respectively. The difference between these numbers was significant ($P<0.01$, paired t-test).

Conclusion: The new algorithm for airway segmentation in CT images was superior to the benchmark algorithm.

Poster Session 14-6

A Comparative Study of HRCT Image Metrics and PFT Values for Characterization of ILD and COPD

Gang Song, Eduardo Mortani Barbosa Jr, Nicholas Tustison, Warren B. Gefter, Maryl Kreider, James C. Gee, Drew A. Torigian
1. Penn Image Computing and Science Laboratory (PICSL), Department of Radiology, University of Pennsylvania School of Medicine, USA
2. Department. of Radiology, University of Pennsylvania School of Medicine, USA
3. Department of Medicine, University of Pennsylvania School of Medicine, USA

Several image metrics have been proposed in the literature for pulmonary assessment via thoracic high-resolution computed tomography for various diseases. This article describes a systematic analysis of the utility of such metrics for characterizing interstitial lung disease and chronic obstructive pulmonary disease in comparison to data from pulmonary function testing. 14 patients with ILD and 11 with COPD were retrospectively identified who had undergone both HRCT and PFT within 3 days of each other. Using a custom-made computational pipeline, 93 different image-based features were computed for each patient.

The relationships between these image metrics and the 21 clinically-used PFT parameters were analyzed using a minimalredundancy-maximal-relevance statistical framework. The results showed that not only are some image metrics good discriminators for characterization of ILD and COPD compared with PFT, but also that image metrics are not redundant for differentiation between ILD and COPD groups when PFT values are provided. Image metrics of the attenuation histogram statistics and of more sophisticated texture descriptions are both selected, which suggests that both types of image metrics may be valuable for further investigation in computer assisted diagnosis.

Poster Session 15-1

Unexplained Desaturation in the Sitting Position with Stroke

Shigeki Nanjo[1], Tsuyoshi Kitai[2], Norifumi Sugo[3], Ryo Tachikawa[1], Kojiro Otsuka[1], Michio Hayashi[1], Nobuyuki Katakami[1], Keisuke Tomii[1]

1. Department of Respiratory Medicine, Kobe City Medical Center General Hospital, Japan
2. Department of Cardiology Medicine, Kobe City Medical Center General Hospital, Japan
3. Department of Neurology Medicine, Kobe City Medical Center General Hospital, Japan

A 87 year old woman admitted to our hospital with speech disturbance was found to have unexplained desaturation in the sitting position. Her brain MRI showed multiple infarctions in bilateral cerebellum, left occipital lobe, and right thalamus. Oxygen saturation at O2 4L/min fell precipitously from 93% in the supine position to 70% in the sitting position. Chest enhanced CT revealed no findings suggestive of thromboembolism. Micro bubble test in the sitting position was positive, and pulmonary perfusion scintigraphy suggested 23% right-to-left shunt. A transesophageal echocardiogram was taken in the supine and sitting positions. The images taken in the supine position showed patent foramen ovale with atrial septal aneurysm, and mainly left-to-right shunt. However, the images taken in the sitting position showed further opening of foramen ovale with massive right-to-left shunt across the defect. We diagnosed her with platypnea-orthodeoxia syndrome, which was characterized by dyspnea and hypoxemia induced by orthostatism and relieved by supine position. Multiple infarctions were thought to be caused by paradoxical embolism due to this shunting. Anatomical and functional components are necessary to cause platypnea-orthdeoxia. In this case, foramen ovale was open anatomically, and a dilated aortic root functionally changed the blood flow to right-to-left shunt through the foramen in the sitting position.

Poster Session 15-2

Acute-onset Sarcoidosis with Polyarthralgia and Hilar Lymphadenopathy

Hiroshi Santo[1], Ryuji Sato[1], Nanase Watatani[1], Shu Inbe[1], Yasushi Makino[1], Hirokazu Nakajima[1], Katuyki Tomita[1], Hroaki Kume[1], Kenichi Omori[2], Yuji Toda[1]

1. Department of Respiratory Medicine and Allergology, Kinki University, Faculty of Medicine, Japan
2. Department of Respiratory surgery, National Hospital Organization Kinki-Chuo Chest Medical Center, Japan

A 33 years old woman was adomitted because of high grade of fever, polyarthralgia and coughing. Chest Computed tomography showed multiple lymphadenopathy of the mediastinum,hilra and left collarbone fossa, and also showed nodele with the cavity in the left S6 domain.Bronchial alveolar lavage showed a slightly high number of lymphocyte and a high CD4/CD8 cell ratio. Although transbronchial lung biopsy of the lung nodule did not show noncaseating granuloma.Gallium scintigraphy showed Accumulation to hilar lymph nodes, eye sockets,and parotoids. Video-assisted thoracic surgery and lymph node biomicroscopy were performed for diagnosis. In the pathology organization, both lymph node and lungs organization accepted a noncaseating granuloma.Fever up and the arthralgia were improved from preoperation, but those symptoms comes out again from postoperative the sixth day. Gallium scintigraphy showed accumulation to the same part as the last time and an and both knees, an ankle. We diagnosed as an Löfgren syndrome without the erythema nodosum. Oral administration of prednisolone(20mg/day) was initiated. A symptom was improved afterward and became the discharge.

The Löfgren syndrome is one model of the acute sarcoidosis to assume 3 the main sign,erythema nodosum, polyarthralgia, and bilateral hilar lymphadenopathy. It is reported that a ratio with the erythema nodosum is high with a woman in comparison with the man. We add it and report consideration from literatures about relations with this case.

Poster Session 15-3

Pulmonary Function and Computer Tomography of a Relapsing Polychondritis with Bronchial Lesion

Takahiro Tsuji[1], Ikezoe Kouhei[1], Kaji Yusuke[1], Yasuda Takehiro[1], Seishu Hashimoto[1], Kunihiko Terada[1], Takashi Hajiro[1], Eisaku Tanaka[1], Keisuke Noma[2], Yoshio Taguchi[1]

1. Department of Respiratory Medicine, Tenri Hospital, Japan
2. Department of Radiology, Tenri Hospital, Japan

A 69-year-old man with stable asthma was admitted to our department because of frequent cough and persitent positive CRP. He had a history of conjunctivitis. The flow-volume curve illustrated constrictive upper airway flow pattern and CT scan showed that the trachea was deformed with its wall thickened.

He was diagnosed as having relapsing polychondritis based on Damiani's criteria. Then he was treated with oral prednisolone, which alleviated cough, decreased CRP, and improved upper airway constriction. CT scans after two-week steroids demonstrated significant improvement of both deformity and thickness of the tracheal wall.

CT findings of the trachea was helpful to evaluate tracheal involvement of relapsing polychondritis.

Poster Session 15-4

A Case of Toxocariasis Who Presented Abnormal Tubular Structures in Lung Fields

Yuko Nakase[1], Naoya Sugimoto[1], Takako Toda[1], Michio Kuramochi[1], Hiroyuki Tashimo[1], Hiroyuki Nagase[1], Asako Yamamoto[2], Koji Takeshita[2], Masao Yamaguchi[1], Ken Ohta[1]

1. Division of Respiratory Medicine and Allergology, Department of Medicine, Teikyo University School of Medicine, Japan
2. Department of Radiology, Teikyo University School of Medicine, Japan

Helminthic infections are relatively rare in respiratory medicine, but we must keep in mind the possibility of parasitic disorders when there are pulmonary infiltrations or distinctive abnormal structures whose diagnosis is not obvious. Here, we report a 65-year-old male with toxocariasis who presented with unusual tubular structures in both lung fields in CT images. His chief complaint was transient hemosputa, but no fever or eruptions were noted. Chest plain radiograph showed ground glass opacity in his right lower lung. Axial and multiplanar reconstructed CT images showed irregularly curving tubular structures, approximately ~10 cm long, that passed along the subpleural area of bilateral lower lobes beyond the segments. The tubular structures connected to lower lobe bronchioles and consolidations on the diaphragm. Based on these radiographic findings, we speculated that the distinctive images might be due to migration scars of some parasite. Although there was no blood eosinophilia or elevation of serum IgE levels, IgG ELISA demonstrated the presence of serum antibodies against Toxocara canis ES antigen. Raw foods such as beef liver were suspected sources. Three months after 4-week administration of albendazole, the specific IgG level declined, indicating that the toxocariasis became inactive. Although the radiographic findings do not necessarily equate with toxocariasis and may be evidence of some other previously migrated parasites, the observed patterns are strongly suggestive of scars of helminth migration. We believe that curved multiplanar reconstruction technique of CT scan is a powerful tool for clear depiction of the full-length scars left by migrated parasites.

MEMO